

U. S. Department of Commerce
National Oceanic and Atmospheric Administration
National Weather Service
National Centers for Environmental Prediction
5830 University Research Court
College Park, MD 20740

Technical Note

User manual and system documentation of
WAVEWATCH III[®] version 5.16[†]

WAVEWATCH III[®] Development Group[‡]

Environmental Modeling Center
Marine Modeling and Analysis Branch

October 2016

[†] MMAB Contribution No. 329.

[‡] Code manager e-mail: jessica.meixner@noaa.gov

This page is intentionally left blank.

Contents

1	Introduction	1
1.1	About this manual	1
1.2	Licensing terms	3
1.3	Copyrights and trademarks	5
1.4	The development group	5
1.5	Acknowledgments	9
2	Governing equations	11
2.1	Introduction	11
2.2	Propagation	13
2.3	Source terms	14
2.3.1	General concepts	14
2.3.2	S_{nl} : Discrete Interaction Approximation (DIA)	16
2.3.3	S_{nl} : Full Boltzmann Integral (WRT)	18
2.3.4	S_{nl} : Generalized Multiple DIA (GMD)	22
2.3.5	S_{nl} : Two-Scale Approximation (TSA)	25
2.3.6	S_{nl} : Nonlinear Filter	29
2.3.7	$S_{in} + S_{ds}$: WAM cycle 3	31
2.3.8	$S_{in} + S_{ds}$: Tolman and Chalikov 1996	32
2.3.9	$S_{in} + S_{ds}$: WAM cycle 4 (ECWAM)	39
2.3.10	$S_{in} + S_{ds}$: Ardhuin et al. 2010	42
2.3.11	$S_{in} + S_{ds}$: Zieger et al. 2015	48
2.3.12	S_{ln} : Cavaleri and Malanotte-Rizzoli 1981	55
2.3.13	S_{bot} : JONSWAP bottom friction	56
2.3.14	S_{bot} : SHOWEX bottom friction	57
2.3.15	S_{mud} : Dissipation by viscous mud (D&L)	59
2.3.16	S_{mud} : Dissipation by viscous mud (Ng)	60
2.3.17	S_{db} : Battjes and Janssen 1978	61
2.3.18	S_{tr} : Triad nonlinear interactions (LTA)	62
2.3.19	S_{bs} : Bottom scattering	64
2.4	Source terms for wave-ice interactions	66
2.4.1	S_{ice} : Damping by sea ice (simple)	67
2.4.2	S_{ice} : Damping by sea ice (generalization of Liu et al.)	68
2.4.3	S_{ice} : Damping by sea ice (Shen et al.)	70
2.4.4	S_{ice} : Frequency-dependent damping by sea ice	73
2.4.5	S_{is} : Diffusive scattering by sea ice (simple)	75

2.4.6	S_{is} : Floe-size dependent scattering and dissipation . . .	75
2.4.7	S_{ref} : Energy reflection at shorelines and icebergs . . .	79
2.4.8	Second-order spectrum and free infragravity waves . . .	83
2.4.9	S_{xx} : User defined	85
2.5	Air-sea processes	86
2.5.1	General concepts	86
2.5.2	Sea-state dependent τ : Reichl et al. 2014	88
2.5.3	Sea-state dependent τ : Donelan et al. 2012	90
2.6	Output parameters	91
3	Numerical approaches	100
3.1	Spectral discretization	100
3.2	Splitting of the wave action equation	101
3.3	Depth variations in time	103
3.4	Spatial propagation	104
3.4.1	General concepts	104
3.4.2	Traditional regular grids	106
	First-order scheme	107
	Second-order scheme (UNO)	108
	Third-order scheme (UQ)	108
3.4.3	Curvilinear grids	111
3.4.4	Triangular unstructured grids	112
3.4.5	Spherical Multiple-Cell (SMC) grid	115
3.4.6	The Garden Sprinkler Effect	120
	No GSE alleviation	120
	Booij and Holthuijsen 1987	121
	Spatial averaging	124
3.4.7	Unresolved obstacles	126
3.4.8	Continuously moving grids	127
	General concepts	127
3.4.9	Rotated grids	129
3.5	Intra-spectral propagation	131
3.5.1	General concepts	131
3.5.2	First-order scheme	132
3.5.3	Second-order scheme (UNO)	133
3.5.4	Third-order scheme (UQ)	133
3.6	Non-ice source term integration	134
3.7	Ice source terms integration	138

3.8	Simple ice blocking (IC0)	139
3.9	Winds and currents	140
3.10	Use of tidal analysis	141
3.11	Wave crest and height space-time extremes	142
3.12	Spectral partitioning	145
3.13	Spatial and temporal tracking of wave systems	148
3.14	Nesting	150
3.14.1	Traditional one-way nesting	150
3.14.2	Two-way nesting	151
4	Wave Model Structure and Data Flow	155
4.1	Program design	155
4.2	The wave model routines	156
4.3	The data assimilation interface	159
4.4	Auxiliary programs	160
4.4.1	General concepts	160
4.4.2	The grid preprocessor	162
4.4.3	The initial conditions program	180
4.4.4	The boundary conditions program	182
4.4.5	The NetCDF boundary conditions program	184
4.4.6	The input field preprocessor	185
4.4.7	The NetCDF input field preprocessor	188
4.4.8	The tide prediction program	190
4.4.9	The generic shell	192
4.4.10	Automated grid splitting for ww3_multi (ww3_gspl)	201
4.4.11	The multi-grid shell	204
4.4.12	Grid Integration	216
4.4.13	Gridded output post-processor	218
4.4.14	Gridded NetCDF output post-processor	220
4.4.15	Gridded output post-processor for GrADS	222
4.4.16	Gridded GRIB output post-processor	224
4.4.17	Point output post-processor	226
4.4.18	Point output NetCDF post-processor	231
4.4.19	Point output post-processor for GrADS	234
4.4.20	Track output post-processor	236
4.4.21	Spatial and temporal tracking of wave systems	237

5	Installing, Compiling and Running the wave model	242
5.1	Introduction	242
5.2	Installing files	242
5.3	Compiling and linking	252
5.4	Selecting model options	256
5.4.1	Mandatory switches	256
5.4.2	Optional switches	260
5.4.3	Default model settings	264
5.5	Modifying the source code	264
5.6	Running test cases	266
6	System documentation	272
6.1	Introduction	272
6.2	The preprocessor	272
6.3	Program files	274
6.3.1	Wave model modules	274
6.3.2	Multi-grid modules	287
6.3.3	Data assimilation module	289
6.3.4	Auxiliary programs	289
6.4	Optimization	292
6.5	Internal data storage	293
6.5.1	Grids	293
6.5.2	Distributed memory concepts.	298
6.5.3	Multiple grids	301
6.6	Variables in modules	303
6.6.1	Parameter settings in modules	304
6.6.2	Data structures	308
	References	310
APPENDICES		
A	Managing multiple model versions	A.1

B	Setting model time steps	B.1
B.1	Individual grids	B.1
B.2	Mosaics of grids	B.3
C	Setting up nested runs	C.1
C.1	Using <code>ww3_shel</code>	C.1
C.2	Using <code>ww3_bound</code> and/or unstructured grids	C.3
C.3	Using <code>ww3_multi</code>	C.4
D	Setting up for distributed machines (MPI)	D.1
D.1	Model setup	D.1
D.2	Common errors	D.4
D.3	MPI point-to-point communication errors	D.5
E	Mosaic approach with non-regular grids	E.1
E.1	Introduction	E.1
E.2	SCRIP-WW3	E.1
E.3	SCRIP Operation	E.2
E.4	Optimization and common problems	E.3
E.5	Limitations	E.5
F	Ocean-Waves-Atmosphere coupling with OASIS	F.1
F.1	Introduction	F.1
F.2	Interfacing with OASIS3-MCT	F.2
F.3	Compiling with OASIS3-MCT	F.2
F.4	Launch a coupling simulation	F.3
F.5	Limitations	F.3

This page is intentionally left blank.

1 Introduction

1.1 About this manual

This document describes the governing equations (**Chapter 2**), numerical approaches (**Chapter 3**), model structure and data flow (**Chapter 4**), installing, compiling and running (**Chapter 5**) of WAVEWATCH III. Further details on the general code structure and implementation of different aspects are given in **Chapter 6**. A user wishing to install the model may thus jump directly to **Chapter 5**, and then successively modify input files in example runs (**Chapter 4**). However this will not replace a thorough knowledge of WAVEWATCH III that can be obtained by following Chapters 2 through 5.

This is the user manual and system documentation of version 5.16 of the third-generation wind-wave modeling framework WAVEWATCH III[®]. While code management of this system is undertaken by the National Center for Environmental Prediction (NCEP) the model development relies on a community of developers (see below). It is based on WAVEWATCH I and WAVEWATCH II as developed at Delft University of Technology, and NASA Goddard Space Flight Center, respectively. WAVEWATCH III differs from its predecessors in all major aspects; i.e., governing equations, program structure, numerical and physical approaches.

The format of a combined user manual and system documentation has been chosen to give users the necessary background to include new physical and numerical approaches in the framework according to their own specifications. This approach became more important as WAVEWATCH III developed into a wave modeling framework. By design, a user can apply his or her numerical and/or physical approaches, and thus develop a new wave model based on the WAVEWATCH III framework. In such an approach, optimization, parallelization, nesting, input and output service programs from the framework can be easily shared between actual models. Whereas this document is intended to be complete and self-contained, this is not the case for all elements in the system documentation. For additional system details, reference is made to the source code, which is fully documented. Note that a best practices guide for code development for WAVEWATCH III is now available (Tolman, 2010c, 2014b).

The present model version (5.16) is the new public version based on the last official model release (version 4.18). Since the latter release the following modifications have been made:

- Preparing for next model version, adding optional instrumentation to code for profiling of memory use (model version 5.00).
- Optimization of IC3 (ice source function). Added non-dispersive variant of "turbulence under ice" ice source function to IC2. This is simpler than the existing version and requires fewer free parameters. Method is selected by the user. Added fluxes for momentum and energy associated with ice source functions. Preliminary scheme for scattering of waves by ice (model version 5.01).
- Revisiting OpenMP parallelisms in the model. Revising previous OpenMP-only approach and introducing Hybrid MPI-OpenMP approach initiated by Farid Parpia of IBM (model version 5.02).
- Implementing tripole grid functionality for first order scheme, and for gradient calculations (e.g. for refraction by depth/current gradients). Adding test case for tripole grid to regtests (model version 5.03).
- Adding capability to handle cpp macros (model version 5.04).
- Upgrade to ST6 physics (model version 5.05).
- Adding the NCEP coupler capability (model version 5.06).
- Adding OASIS coupler capability (model version 5.07).
- Series of bug fix updates (model version 5.08).
- Updates to SMC grid type (model version 5.09).
- Adding sea ice scattering and creep dissipation source terms (model version 5.10).
- Introducing namelists formats for input files. Traditional way of providing inputs is still possible using the inp suffix (model version 5.11).
- Sea-state dependent stress-calculations are added. Updates to the restart files related to file size and optimization of initialization from restart files. Note, this means restart files are not backwards compatible (model version 5.12).
- Adding TSA as a nonlinear wave-wave interaction source term option (model version 5.13).
- Adding the capability for calculating space-time extremes (model version 5.14).

- Optimization of wvae system tracking (model version 5.15).
- Final preparations for distribution (model version 5.16).

Up to date information on this model can be found (including bugs and bug fixes) on the WAVEWATCH III web page,

<http://polar.ncep.noaa.gov/waves/wavewatch/>

and comments, questions and suggestions should be directed to the code manager, Jessica Meixner (jessica.meixner@noaa.gov), or the general WAVEWATCH III users mailing group list

ncep.list.wwatch3.users@lstsrv.ncep.noaa.gov

NCEP will redirect questions regarding contributions from outside NCEP to the respective authors of the codes. You may subscribe to the WAVEWATCH III users mailing list at the following web page:

<https://www.lstsrv.ncep.noaa.gov/mailman/listinfo/ncep.list.wwatch3.users>

1.2 Licensing terms

Starting with model version 3.14, WAVEWATCH III is distributed under the following licensing terms:

————— start of licensing terms —————

Software, as understood herein, shall be broadly interpreted as being inclusive of algorithms, source code, object code, data bases and related documentation, all of which shall be furnished free of charge to the Licensee.

Corrections, upgrades or enhancements may be furnished and, if furnished, shall also be furnished to the Licensee without charge. NOAA, however, is not required to develop or furnish such corrections, upgrades or enhancements.

NOAA's software, whether that initially furnished or corrections or upgrades, are furnished as is. NOAA furnishes its software without any warranty

whatsoever and is not responsible for any direct, indirect or consequential damages that may be incurred by the Licensee. Warranties of merchantability, fitness for any particular purpose, title, and non-infringement, are specifically negated.

The Licensee is not required to develop any software related to the licensed software. However, in the event that the Licensee does so, the Licensee is required to offer same to NOAA for inclusion under the instant licensing terms with NOAA's licensed software along with documentation regarding its principles, use and its advantages. This includes changes to the wave model proper including numerical and physical approaches to wave modeling, and boundary layer parameterizations embedded in the wave model. The Licensee is encouraged but not obligated to provide pre-and post processing tools for model input and output. The software required to be offered shall not include additional models to which the wave model may be coupled, such as oceanic or atmospheric circulation models. The software provided by the Licensee shall be consistent with the latest model version available to the Licensee, and interface routines to the software provided shall conform to programming standards as outlined in the model documentation. The software offered to NOAA shall be offered as is, without any warranties whatsoever and without any liability for damages whatsoever. NOAA shall not be required to include a Licensee's software as part of its software. Licensee's offered software shall not include software developed by others.

A Licensee may reproduce sufficient software to satisfy its needs. All copies shall bear the name of the software with any version number as well as replicas of any applied copyright notice, trademark notice, other notices and credit lines. Additionally, if the copies have been modified, e.g. with deletions or additions, this shall be so stated and identified.

All of Licensee's employees who have a need to use the software may have access to the software but only after reading the instant license and stating, in writing, that they have read and understood the license and have agreed to its terms. Licensee is responsible for employing reasonable efforts to assure that only those of its employees that should have access to the software, in fact, have access.

The Licensee may use the software for any purpose relating to sea state prediction.

No disclosure of any portion of the software, whether by means of a media or verbally, may be made to any third party by the Licensee or the Licensee's employees

The Licensee is responsible for compliance with any applicable export or import control laws of the United States.

end of licensing terms

The software will be distributed through our web site after the Licensee has agreed to the license terms.

1.3 Copyrights and trademarks

WAVEWATCH III[®] © 2009-2016 National Weather Service, National Oceanic and Atmospheric Administration. All rights reserved. WAVEWATCH III[®] is a trademark of the National Weather Service. No unauthorized use without permission.

1.4 The development group

The development of WAVEWATCH III[®] relies on the efforts of a team of developers that have worked tirelessly to make this an effective community tool. With the expansion of physical and numerical parameterizations available, the list of contributors to this model keeps growing. The development group consists of a core group of developers that are involved in overall code development, debugging and optimization as well as a larger group that has either made or continues to make contributions to physics packages and numerics. The following is a list of contributors (both past and present) of this development group (in alphabetic order) :

Mickael Accensi (Ifremer, France)

NetCDF for input and output (ww3_prnc , ww3_ounf, ww3_ounp),
namelist input files for ww3_multi, and general code development support.

Jose-Henrique Alves (SRG at NOAA/NCEP/EMC, USA)

Support of code development at NCEP, shallow water physics packages,
development of space-time wave-height extremes approach.

- Fabrice Ardhuin (CNRS, France, previously at SHOM then Ifremer)
Various physics packages (ST3, ST4, BS1, BT4, IG1, REF1, IS2...),
interface with unstructured grid schemes, tidal analysis, and some I/O
aspects (estimation of fluxes, adaptation of NetCDF).
- Francesco Barbariol (ISMAR-CNR, Italy)
Development of a space-time wave-height extremes approach.
- Alvise Benetazzo (ISMAR-CNR, Italy)
Development of a space-time wave-height extremes approach.
- Anne-Claire Bennis (University of Caen, France, previously at SHOM, France)
Coupling with 3D flow model using PALM.
- Jean Bidlot (ECMWF, UK)
Updates to physics package ST3.
- Nico Booij (Delft University of Technology, The Netherlands, retired)
Original design of source code pre-processor (`w3adc`), basic method
of documentation and other programming habits. Spatially varying
wavenumber grid.
- Guillaume Boutin (Ifremer, France)
Contribution to IS2 and IC2.
- Tim Campbell (Naval Research Laboratory, USA)
Search and regrid utilities, irregular grids, regression testing shell script,
and overall code development support.
- Dmitry V. Chalikov (Formerly UCAR at NOAA/NCEP/EMC)
Co-author of the [Tolman and Chalikov \(1996\)](#) input and dissipation
parameterizations and source code.
- Arun Chawla (NOAA/NCEP/EMC, USA)
Support of code development at NCEP, GRIB packing, automated grid
generation software ([Chawla and Tolman, 2007, 2008](#)).
- Sukun Cheng (while at Clarkson University, USA)
Original author of the code that was ported into WW3 (for model
version 5) as the improved “IC3” parameterization for effect of sea ice
on waves.

Clarence Collins (while an NRL/ASEE post-doc, USA)
Origination of IC4 (sea ice source function).

Jean-François Filipot (France Energy Marine, formerly at SHOM then Ifremer, France).
Unification of whitecapping and breaking in ST4.

Mike Foreman (IOS, Canada)
Versatile tidal analysis package.

Peter Janssen (ECMWF, United Kingdom)
Original version of WAM-Cycle 4 package (ST3), canonical transform for the second order wave spectrum.

Fabien Leckler (Ifremer, France)
Breaking parameters from source terms and contributions to ST4.

Jian-Guo Li (UK MetOffice, United Kingdom)
SMC grid, second order UNO schemes and rotated grids.

Kevin Lind (DoD PETTTT, USA)
Improvements to performance of some multi-grid functions.

Jessica Meixner (IMSG at NOAA/NCEP/EMC, USA)
Coupled modeling development, tripole grids, general code development support and code manager for WAVEWATCH III.

Mark Orzech (Naval Research Laboratory, USA)
Source terms for effects of mud (BT8, BT9).

Roberto Padilla-Hernández (IMSG at NOAA/NCEP/EMC, USA)
Support of code development at NCEP, editing.

William Perrie (Bedford Institute of Oceanography, Canada)
Two-Scale Approximations for non-linear interactions (NL4).

Arshad Rawat (MIO, Mauritius and Ifremer, France)
Contribution to second order spectrum and free infragravity wave sources (IG1).

W. Erick Rogers (Naval Research Laboratory, USA)

Irregular grids, source terms for effects of sea ice (e.g. in IC1, IC2, IC3, IC4, IC5) and mud (BT8, BT9), adaptation/interfaces of conservative remapping software, tripole grid, regression tests, and overall code development support.

Aron Roland (T. U. Darmstadt, Germany)

Advection on unstructured (triangle-based) grids and meshing tools.

Caroline Sevigny (UQAR, Canada)

Contribution to ice scattering including ice break-up.

Hayley Shen (Clarkson Univ.)

Supervised contributions by Zhao and Cheng on the “IC3” parameterization for effect of sea ice on waves.

Mathieu Dutour Sikiric (IRB, Croatia)

Multi-grid computations with unstructured (triangle-based) grids.

Mark Szyszka (RPS Group, Australia)

Identifying several bugs in the code development process and providing fixes for Openmp issues.

Hendrik L. Tolman (DOC/NOAA/NWS/OSTI, USA).

General code architecture, original WAVEWATCH-I, II and III models. Ongoing model development.

Bash Toulany (Bedford Institute of Oceanography, Canada)

Two-Scale Approximations for non-linear interactions (NL4).

Barbara Tracy (US Army Corps of Engineers, ERDC-CHL, USA, retired)

Spectral partitioning.

Gerbrant Ph. van Vledder (Delft University of Technology, NL)

Webb-Resio-Tracy exact nonlinear interaction routines, as well as some of the original service routines.

André van der Westhuysen (IMSG at NOAA/NCEP/EMC, USA)

Support of code development at NCEP, wave system tracking, addition of triad interactions.

Xin Zhao (while at Clarkson University, USA)

Original author of the code that was ported into WW3 (model version 4) as the “IC3” parameterization for effect of sea ice on waves.

Stefan Zieger (Bureau of Meteorology, Australia)

Deepwater source term package (ST6) and source terms for effects of sea ice.

1.5 Acknowledgments

The WAVEWATCH III wind wave model started by Hendrik Tolman with the development of the WAVEWATCH model at Delft University and WAVEWATCH II at NASA, Goddard Space Flight Center in the early 1990s. The development of WAVEWATCH III has transitioned from being a task undertaken by a single person or group to a community modeling framework. We are thankful to all our partners in the scientific community who have undertaken the development of this modeling system as part of their research activities. We are also extremely grateful to the larger user community who have tirelessly worked with us to identify bugs and other issues in the model.

WAVEWATCH III Development Team, October 2016

This page is intentionally left blank.

2 Governing equations

2.1 Introduction

Waves or spectral wave components in water with limited depth and non-zero mean currents are generally described using several phase and amplitude parameters. Phase parameters are the wavenumber vector \mathbf{k} , the wavenumber k , the direction θ and several frequencies. If effects of mean currents on waves are to be considered, a distinction is made between the relative or intrinsic (radian) frequency σ ($= 2\pi f_r$), which is observed in a frame of reference moving with the mean current, and the absolute (radian) frequency ω ($= 2\pi f_a$), which is observed in a fixed frame of reference. The direction θ is by definition perpendicular to the crest of the wave (or spectral component), and equals the direction of \mathbf{k} . Equations given here follow the geometrical optics approximation, which is exact in the limit when scales of variation of depths and currents are much larger than those of an individual wave¹. Diffraction, scattering and interference effects that are neglected by this approximation can be added a posteriori as source terms in the wave action equation. Under this approximation of slowly varying current and depth, the quasi-uniform (linear) wave theory then can be applied locally, giving the following dispersion relation and Doppler-type equation to interrelate the phase parameters

$$\sigma^2 = gk \tanh kd, \quad (2.1)$$

$$\omega = \sigma + \mathbf{k} \cdot \mathbf{U}, \quad (2.2)$$

where d is the mean water depth and \mathbf{U} is the (depth- and time- averaged over the scales of individual waves) current velocity. The assumption of slowly varying depths and currents implies a large-scale bathymetry, for which wave diffraction can generally be ignored. The usual definition of \mathbf{k} and ω from the phase function of a wave or wave component implies that the number of wave crests is conserved (see, e.g., Phillips, 1977; Mei, 1983)

¹Even with a factor 5 change in wave height over half a wavelength, the geometrical optics approximation can provide reasonable results as was shown over submarine canyons (Magne et al., 2007)

$$\frac{\partial \mathbf{k}}{\partial t} + \nabla \omega = 0. \quad (2.3)$$

From Eqs. (2.1) through (2.3) the rates of change of the phase parameters can be calculated (e.g., Christoffersen, 1982; Mei, 1983; Tolman, 1990, equations not reproduced here).

For monochromatic waves, the amplitude is described as the amplitude, the wave height, or the wave energy. For irregular wind waves, the (random) variance of the sea surface is described using the surface elevation variance density spectra (in the wave modeling community usually denoted as energy spectra). The variance spectrum F is a function of all independent phase parameters, i.e., $F(\mathbf{k}, \sigma, \omega)$, and furthermore varies in space and time at scales larger than those of individual waves, e.g., $F(\mathbf{k}, \sigma, \omega; \mathbf{x}, t)$. However, it is usually assumed that the individual spectral components satisfy the linear wave theory (locally), so that Eqs. (2.1) and (2.2) interrelate \mathbf{k} , σ and ω . Consequently only two independent phase parameters exist, and the local and instantaneous spectrum becomes two-dimensional. Within WAVEWATCH III the basic spectrum is the wavenumber-direction spectrum $F(k, \theta)$, which has been selected because of its invariance characteristics with respect to physics of wave growth and decay for variable water depths. The output of WAVEWATCH III, however, consists of the more traditional frequency-direction spectrum $F(f_r, \theta)$. The different spectra can be calculated from $F(k, \theta)$ using straightforward Jacobian transformations

$$F(f_r, \theta) = \frac{\partial k}{\partial f_r} F(k, \theta) = \frac{2\pi}{c_g} F(k, \theta), \quad (2.4)$$

$$F(f_a, \theta) = \frac{\partial k}{\partial f_a} F(k, \theta) = \frac{2\pi}{c_g} \left(1 + \frac{\mathbf{k} \cdot \mathbf{U}}{kc_g} \right)^{-1} F(k, \theta), \quad (2.5)$$

$$c_g = \frac{\partial \sigma}{\partial k} = n \frac{\sigma}{k}, \quad n = \frac{1}{2} + \frac{kd}{\sinh 2kd}, \quad (2.6)$$

where c_g is the so-called group velocity. From any of these spectra one-dimensional spectra can be generated by integration over directions, whereas integration over the entire spectrum by definition gives the total variance E (in the wave modeling community usually denoted as the wave energy).

In cases without currents, the variance (energy) of a wave package is a conserved quantity. In cases with currents the energy or variance of a spectral component is no longer conserved, due to the work done by current

on the mean momentum transfer of waves (Longuet-Higgins and Stewart, 1961, 1962). In a general sense, however, wave action $A \equiv E/\sigma$ is conserved (e.g., Whitham, 1965; Bretherton and Garrett, 1968). This makes the wave action density spectrum $N(k, \theta) \equiv F(k, \theta)/\sigma$ the spectrum of choice within the model. Wave propagation then is described by

$$\frac{DN}{Dt} = \frac{S}{\sigma}, \quad (2.7)$$

where D/Dt represents the total derivative (moving with a wave component) and S represents the net effect of sources and sinks for the spectrum F . Because the left side of Eq. (2.7) generally considers linear propagation without scattering, effects of nonlinear wave propagation (i.e., wave-wave interactions) and partial wave reflections arise in S . Propagation and source terms will be discussed separately in the following sections.

2.2 Propagation

In a numerical model, a Eulerian form of the balance equation (2.7) is needed. This balance equation can either be written in the form of a transport equation (with velocities outside the derivatives), or in a conservation form (with velocities inside the derivatives). The former form is valid for the vector wavenumber spectrum $N(\mathbf{k}; \mathbf{x}, t)$ only, whereas valid equations of the latter form can be derived for arbitrary spectral formulations, as long as the corresponding Jacobian transformation as described above is well behaved (e.g., Tolman and Booij, 1998). Furthermore, the conservation equation conserves total wave energy/action, unlike the transport equation. This is an important feature of an equation when applied in a numerical model. The balance equation for the spectrum $N(k, \theta; \mathbf{x}, t)$ as used in WAVEWATCH III is given as (for convenience of notation, the spectrum is henceforth denoted simply as N):

$$\frac{\partial N}{\partial t} + \nabla_x \cdot \dot{\mathbf{x}}N + \frac{\partial}{\partial k} \dot{k}N + \frac{\partial}{\partial \theta} \dot{\theta}N = \frac{S}{\sigma}, \quad (2.8)$$

$$\dot{\mathbf{x}} = \mathbf{c}_g + \mathbf{U}, \quad (2.9)$$

$$\dot{k} = -\frac{\partial \sigma}{\partial d} \frac{\partial d}{\partial s} - \mathbf{k} \cdot \frac{\partial \mathbf{U}}{\partial s}, \quad (2.10)$$

$$\dot{\theta} = -\frac{1}{k} \left[\frac{\partial \sigma}{\partial d} \frac{\partial d}{\partial m} + \mathbf{k} \cdot \frac{\partial \mathbf{U}}{\partial m} \right], \quad (2.11)$$

where $\mathbf{c}_g = (c_g \sin \theta, c_g \cos \theta)$, s is a coordinate in the direction θ and m is a coordinate perpendicular to s . Equation (2.8) is valid for Cartesian coordinates. For large-scale applications, this equation is usually transferred to spherical coordinates, defined by longitude λ and latitude ϕ , but maintaining the definition of the local variance (i.e., per unit surface, as in WAMDIG, 1988)

$$\frac{\partial N}{\partial t} + \frac{1}{\cos \phi} \frac{\partial}{\partial \phi} \dot{\phi} N \cos \theta + \frac{\partial}{\partial \lambda} \dot{\lambda} N + \frac{\partial}{\partial k} \dot{k} N + \frac{\partial}{\partial \theta} \dot{\theta}_g N = \frac{S}{\sigma}, \quad (2.12)$$

$$\dot{\phi} = \frac{c_g \cos \theta + U_\phi}{R}, \quad (2.13)$$

$$\dot{\lambda} = \frac{c_g \sin \theta + U_\lambda}{R \cos \phi}, \quad (2.14)$$

$$\dot{\theta}_g = \dot{\theta} - \frac{c_g \tan \phi \cos \theta}{R}, \quad (2.15)$$

where R is the radius of the earth and U_ϕ and U_λ are current components. Equation (2.15) includes a correction term for propagation along great circles, using a Cartesian definition of θ where $\theta = 0$ corresponds to waves traveling from west to east. WAVEWATCH III can be run using either Cartesian or Spherical coordinates. Note that unresolved obstacles such as islands can be included in the equations. In WAVEWATCH III this is done at the level of the numerical scheme, as is discussed in section 3.4.7. Also, depth variations at the scale of the wavelength can be introduced by a scattering source term described in section 2.3.19.

Finally, both Cartesian and spherical coordinates can be discretized in many ways, using quadrangles (rectangular, curvilinear or SMC grids) and triangles. That aspect is treated in chapter 3.

2.3 Source terms

2.3.1 General concepts

In deep water, the net source term S is generally considered to consist of three parts, an atmosphere-wave interaction term S_{in} , which is usually a

positive energy input but can also be negative in the case of swell, a nonlinear wave-wave interactions term S_{nl} and a wave-ocean interaction term that generally contains the dissipation S_{ds} . The input term S_{in} is dominated by the exponential wind-wave growth term, and this source term generally describes this dominant process only. For model initialization, and to provide more realistic initial wave growth, a linear input term S_{ln} can also be added in WAVEWATCH III.

In shallow water additional processes have to be considered, most notably wave-bottom interactions S_{bot} (e.g., [Shemdin et al., 1978](#)). In extremely shallow water, depth-induced breaking (S_{db}) and triad wave-wave interactions (S_{tr}) also become important. Also available in WAVEWATCH III are source terms for scattering of waves by bottom features (S_{sc}), wave-ice interactions (S_{ice}), reflection off shorelines or floating objects such as icebergs (S_{ref}), which can include sources of infragravity wave energy, and a general purpose slot for additional, user defined source terms (S_{xx}).

This defines the general source terms used in WAVEWATCH III as

$$S = S_{ln} + S_{in} + S_{nl} + S_{ds} + S_{bot} + S_{db} + S_{tr} + S_{sc} + S_{ice} + S_{ref} + S_{xx} . \quad (2.16)$$

Other source terms could be easily added. Those source terms are defined for the *energy* spectra. In the model, however, most source terms are directly calculated for the action spectrum. The latter source terms are denoted as $\mathcal{S} \equiv S/\sigma$.

The explicit treatment of the nonlinear interactions defines third-generation wave models. Therefore, the options for the calculation of S_{nl} will be discussed first, starting in section [2.3.2](#). S_{in} and S_{ds} represent separate processes, but are often interrelated, because the balance of these two source terms governs the integral growth characteristics of the wave energy. Several combinations of these basic source terms are available, and are described in section [2.3.7](#) and following. The description of linear input starts in section [2.3.12](#), and section [2.3.13](#) and following describe available additional processes, mostly related to shallow water and sea ice.

A third-generation wave model effectively integrates the spectrum only up to a cut-off frequency f_{hf} (or wavenumber k_{hf}), that is ideally equal to the highest discretization frequency. In practice the source terms parameterization or the time step used may not allow a proper balance to be obtained, and thus f_{hf} may be taken within the model frequency range. Above the cut-off frequency a parametric tail is applied (e.g., [WAMDIG, 1988](#))

$$F(f_r, \theta) = F(f_{r,hf}, \theta) \left(\frac{f_r}{f_{r,hf}} \right)^{-m}, \quad (2.17)$$

which is easily transformed to any other spectrum using the Jacobian transformations as discussed above. For instance, for the present action spectrum, the parametric tail can be expressed as (assuming deep water for the wave components in the tail)

$$N(k, \theta) = N(k_{hf}, \theta) \left(\frac{f_r}{f_{r,hf}} \right)^{-m-2}, \quad (2.18)$$

the actual values of m and the expressions for $f_{r,hf}$ depend on the source term parameterization used, and will be given below.

Before actual source term parameterizations are described, the definition of the wind requires some attention. In cases with currents, one can either consider the wind to be defined in a fixed frame of reference, or in a frame of reference moving with the current. Both definitions are available in WAVEWATCH III, and can be selected during compilation. The output of the program, however, will always be the wind speed which is not in any way corrected for the current.

The treatment of partial ice coverage (ice concentration) in the source terms follows the concept of a limited air-sea interface. This means that the momentum transferred from the atmosphere to the waves is limited. Therefore, input and dissipation terms are scaled by the fraction of ice concentration. The nonlinear wave-wave interaction term can be used in areas of open water and ice (Polnikov and Lavrenov, 2007). The scaling is implemented so that it is independent of the source term selected.

2.3.2 S_{nl} : Discrete Interaction Approximation (DIA)

Switch:	NL1
Origination:	WAM model
Provided by:	H. L. Tolman

Nonlinear wave-wave interactions can be modeled using the discrete interaction approximation (DIA, Hasselmann et al., 1985). This parameterization

	λ_{nl}	C
ST6	0.25	$3.00 \cdot 10^7$
WAM-3	0.25	$2.78 \cdot 10^7$
ST4 (Ardhuin et al.)	0.25	$2.50 \cdot 10^7$
Tolman and Chalikov	0.25	$1.00 \cdot 10^7$

Table 2.1: Default constants in DIA for input-dissipation packages.

was originally developed for the spectrum $F(f_r, \theta)$. To assure the conservative nature of S_{nl} for this spectrum (which can be considered as the "final product" of the model), this source term is calculated for $F(f_r, \theta)$ instead of $N(k, \theta)$, using the conversion (2.4).

Resonant nonlinear interactions occur between four wave components (quadruplets) with wavenumber vector \mathbf{k}_1 through \mathbf{k}_4 . In the DIA, it is assumed that $\mathbf{k}_1 = \mathbf{k}_2$. Resonance conditions then require that

$$\left. \begin{aligned} \mathbf{k}_1 + \mathbf{k}_2 &= \mathbf{k}_3 + \mathbf{k}_4 \\ \sigma_2 &= \sigma_1 \\ \sigma_3 &= (1 + \lambda_{nl})\sigma_1 \\ \sigma_4 &= (1 - \lambda_{nl})\sigma_1 \end{aligned} \right\}, \quad (2.19)$$

where λ_{nl} is a constant. For these quadruplets, the contribution δS_{nl} to the interaction for each discrete (f_r, θ) combination of the spectrum corresponding to \mathbf{k}_1 is calculated as

$$\begin{pmatrix} \delta S_{nl,1} \\ \delta S_{nl,3} \\ \delta S_{nl,4} \end{pmatrix} = D \begin{pmatrix} -2 \\ 1 \\ 1 \end{pmatrix} C g^{-4} f_{r,1}^{11} \times \left[F_1^2 \left(\frac{F_3}{(1 + \lambda_{nl})^4} + \frac{F_4}{(1 - \lambda_{nl})^4} \right) - \frac{2F_1 F_3 F_4}{(1 - \lambda_{nl}^2)^4} \right], \quad (2.20)$$

where $F_1 = F(f_{r,1}, \theta_1)$ etc. and $\delta S_{nl,1} = \delta S_{nl}(f_{r,1}, \theta_1)$ etc., C is a proportionality constant. The nonlinear interactions are calculated by considering a limited number of combinations (λ_{nl}, C) . In practice, only one combination is used. Default values for different source term packages are presented in Table 2.1.

This source term is developed for deep water, using the appropriate dispersion relation in the resonance conditions. For shallow water the expression is scaled by the factor D (still using the deep-water dispersion relation, however)

$$D = 1 + \frac{c_1}{\bar{k}d} [1 - c_2 \bar{k}d] e^{-c_3 \bar{k}d}. \quad (2.21)$$

Recommended (default) values for the constants are $c_1 = 5.5$, $c_2 = 5/6$ and $c_3 = 1.25$ (Hasselmann and Hasselmann, 1985). The overbar notation denotes straightforward averaging over the spectrum. For an arbitrary parameter z the spectral average is given as

$$\bar{z} = E^{-1} \int_0^{2\pi} \int_0^\infty z F(f_r, \theta) df_r d\theta, \quad (2.22)$$

$$E = \int_0^{2\pi} \int_0^\infty F(f_r, \theta) df_r d\theta. \quad (2.23)$$

For numerical reasons, however, the mean relative depth is estimated as

$$\bar{k}d = 0.75 \hat{k}d, \quad (2.24)$$

where \hat{k} is defined as

$$\hat{k} = \left(\overline{1/\sqrt{k}} \right)^{-2}. \quad (2.25)$$

The shallow water correction of Eq. (2.21) is valid for intermediate depths only. For this reason the mean relative depth $\bar{k}d$ is not allowed to become smaller than 0.5 (as in WAM). All above constants can be reset by the user in the input files of the model (see Section 4.4.2).

2.3.3 S_{nl} : Full Boltzmann Integral (WRT)

Switch:	NL2
Origination:	Exact-NL model
Provided by:	G. Ph. van Vledder

The second method for calculating the nonlinear interactions in WAVEWATCH III is the so-called Webb-Resio-Tracy method (WRT), which is

based on the original work on the six-dimensional Boltzmann integral formulation of Hasselmann (1962, 1963a,b), and additional considerations by Webb (1978), Tracy and Resio (1982) and Resio and Perrie (1991).

The Boltzmann integral describes the rate of change of action density of a particular wavenumber due to resonant interactions between pairs of four wavenumbers. To interact, these wavenumbers must satisfy the following resonance conditions

$$\left. \begin{aligned} \mathbf{k}_1 + \mathbf{k}_2 &= \mathbf{k}_3 + \mathbf{k}_4 \\ \sigma_1 + \sigma_2 &= \sigma_3 + \sigma_4 \end{aligned} \right\} , \quad (2.26)$$

which is a more general version of the resonance conditions (2.19). The rate of change of action density N_1 at wavenumber \mathbf{k}_1 due to all quadruplet interactions involving \mathbf{k}_1 is given by

$$\begin{aligned} \frac{\partial N_1}{\partial t} &= \iiint G(\mathbf{k}_1, \mathbf{k}_2, \mathbf{k}_3, \mathbf{k}_4) \delta(\mathbf{k}_1 + \mathbf{k}_2 - \mathbf{k}_3 - \mathbf{k}_4) \delta(\sigma_1 + \sigma_2 - \sigma_3 - \sigma_4) \\ &\quad \times [N_1 N_3 (N_4 - N_2) + N_2 N_4 (N_3 - N_1)] d\mathbf{k}_2 d\mathbf{k}_3 d\mathbf{k}_4 , \end{aligned} \quad (2.27)$$

where the action density N is defined in terms of the wavenumber vector \mathbf{k} , $N = N(\mathbf{k})$. The term G is a complicated coupling coefficients for which expressions have been given by Herterich and Hasselmann (1980). In the WRT method a number of transformations are made to remove the delta functions. A key element in the WRT method is to consider the integration space for each $(\mathbf{k}_1, \mathbf{k}_3)$ combination (see Resio and Perrie, 1991)

$$\frac{\partial N_1}{\partial t} = 2 \int T(\mathbf{k}_1, \mathbf{k}_3) d\mathbf{k}_3 , \quad (2.28)$$

in which the function T is given by

$$\begin{aligned} T(\mathbf{k}_1, \mathbf{k}_3) &= \iint G(\mathbf{k}_1, \mathbf{k}_2, \mathbf{k}_3, \mathbf{k}_4) \delta(\mathbf{k}_1 + \mathbf{k}_2 - \mathbf{k}_3 - \mathbf{k}_4) \\ &\quad \times \delta(\sigma_1 + \sigma_2 - \sigma_3 - \sigma_4) \theta(\mathbf{k}_1, \mathbf{k}_3, \mathbf{k}_4) \\ &\quad \times [N_1 N_3 (N_4 - N_2) + N_2 N_4 (N_3 - N_1)] d\mathbf{k}_2 d\mathbf{k}_4 , \end{aligned} \quad (2.29)$$

in which

$$\theta(\mathbf{k}_1, \mathbf{k}_3, \mathbf{k}_4) = \begin{cases} 1 & \text{when } |\mathbf{k}_1 - \mathbf{k}_3| \leq |\mathbf{k}_1 - \mathbf{k}_4| \\ 0 & \text{when } |\mathbf{k}_1 - \mathbf{k}_3| > |\mathbf{k}_1 - \mathbf{k}_4| \end{cases} \quad (2.30)$$

The delta functions in Eq. (2.29) determine a region in wavenumber space along which the integration should be carried out. The function θ determines a section of the integral which is not defined due to the assumption that \mathbf{k}_1 is closer to \mathbf{k}_3 than \mathbf{k}_2 . The crux of the Webb method consists of using a local coordinate system along a so-named locus, that is, the path in \mathbf{k} space given by the resonance conditions for a given combination of \mathbf{k}_1 and \mathbf{k}_3 . To that end the (k_x, k_y) coordinate system is replaced by a (s, n) coordinate system, where s (n) is the tangential (normal) direction along the locus. After some transformations, the transfer integral can then be written as a closed line integral along the closed locus

$$T(\mathbf{k}_1, \mathbf{k}_3) = \oint G \left| \frac{\partial W(s, n)}{\partial n} \right|^{-1} \theta(\mathbf{k}_1, \mathbf{k}_3, \mathbf{k}_4) \times [N_1 N_3 (N_4 - N_2) + N_2 N_4 (N_3 - N_1)] ds \quad , \quad (2.31)$$

in which G is the coupling coefficient and $|\partial W/\partial n|$ is the gradient term of a function representing the resonance conditions (see Van Vledder, 2000). Numerically, the Boltzmann integral is computed as the finite sum of many line integrals T for all discrete combinations of \mathbf{k}_1 and \mathbf{k}_3 . The line integral (2.31) is solved by dividing the locus in typically 30 pieces, such that the discretized version is given as:

$$T(\mathbf{k}_1, \mathbf{k}_3) \approx \sum_{i=1}^{n_s} G(s_i) W(s_i) P(s_i) \Delta s_i \quad , \quad (2.32)$$

in which $P(s_i)$ is the product term for a given point on the locus, n_s is the number of segments, and s_i is the discrete coordinate along the locus. Finally, the rate of change for a given wavenumber \mathbf{k}_1 is given by

$$\frac{\partial N(\mathbf{k}_1)}{\partial t} \approx \sum_{i_{k3}=1}^{n_k} \sum_{i_{\theta3}=1}^{n_\theta} k_3 T(\mathbf{k}_1, \mathbf{k}_3) \Delta k_{i_{k3}} \Delta \theta_{i_{\theta3}} \quad , \quad (2.33)$$

where n_k and n_θ are the discrete number of wavenumbers and directions in the computational grid, respectively. Note that although the spectrum is defined in terms of the vector wavenumber \mathbf{k} , the computational grid in a wave model is more conveniently defined in terms of the absolute wavenumber and wave direction (k, θ) to assure directional isotropy of the calculations. Taking all wavenumbers \mathbf{k}_1 into account produces the complete source term

due to nonlinear quadruplet wave-wave interactions. Details of the efficient computation of a locus for a given combination of the wavenumbers \mathbf{k}_1 and \mathbf{k}_3 can be found in Van Vledder (2000, 2002a,b).

It should be noted that these exact interaction calculations are extremely expensive, typically requiring 10^3 to 10^4 times more computational effort than the DIA. Presently, these calculations can therefore only be made for highly-idealized test cases involving a limited spatial grid.

The nonlinear interactions according to the WRT method have been implemented in WAVEWATCH III using the portable subroutines developed by Van Vledder (2002b). In this implementation, the computational grid of the WRT method is taken identical to the discrete spectral grid of WAVEWATCH III. In addition, the WRT routines inherit the power of the parametric spectral tail as in the DIA. Choosing a higher resolution than the computational grid of WAVEWATCH III for computing the nonlinear interactions is possible in theory, but this does not improve the results and is therefore not implemented.

Because nonlinear quadruplet wave-wave interactions at high frequencies are important, it is recommended to choose the maximum frequency of the wave model about five times the peak frequency of the spectra that are expected to occur in a wave model run. Note that this is important as the spectral grid determines the range of integration in Eq. (2.33). The recommended number of frequencies is about 40, with a frequency increment factor 1.07. The recommended directional resolution for computing the nonlinear interactions is about 10° . For specific purposes other resolutions may be used, and some testing with other resolutions may be needed.

An important feature of most algorithms for the evaluation of the Boltzmann integral is that the integration space can be pre-computed. This is also the case for the subroutine version of the WRT method used in WAVEWATCH III. In the initialization phase of the wave model the integration space, consisting of the discretized paths of all loci, together with the interaction coefficients and gradient terms, are computed and stored in a binary data file. For each water depth such a data file is generated and stored in the current directory. The names of these data files consist of a keyword, “quad”, followed by the keyword “*xxxx*”, with *xxxx* the water depth in meters, or 9999 for deep water. The extension of the binary data file is “bqf” (Binary Quadruplet File, BQF). If a BQF file exists, the program checks if this BQF file has been generated with the proper spectral grid. If this is not the case, the existing BQF file is overwritten with the correct BQF file.

During a wave model run with various depths, the optimal BQF is used, by looking at the nearest water depths for which a valid BQF file has been generated. In addition, the result is rescaled using the ratio of the depth scaling factors (2.21) for the target depth and the depth corresponding to the BQF file.

2.3.4 S_{nl} : Generalized Multiple DIA (GMD)

Switch:	NL3
Origination:	WAVEWATCH III
Provided by:	H. L. Tolman

The GMD has been developed as an extension to the DIA. Its development is documented in a set of Technical notes (Tolman, 2003a, 2005, 2008b, 2010b), reports (Tolman and Krasnopolsky, 2004; Tolman, 2009a, 2011b), and papers (Tolman, 2004, 2013a). As part of the development of the GMD, a holistic genetic optimization technique was developed (Tolman and Grumbine, 2013). A package to perform this optimization within WAVEWATCH III was first provided by Tolman (2010a). The most recent version of this package is version 1.5 (Tolman, 2014a).

The GMD expands on the DIA in three ways. First, the definition of the representative quadruplets is expanded. Second, the equations are developed for arbitrary depths, including the description of strong interactions in extremely shallow water (e.g., Webb, 1978). Third, multiple representative quadruplets are used.

The GMD allows for arbitrary configurations of the representative quadruplet, by expanding on the resonance conditions (2.19) as

$$\left. \begin{aligned} \sigma_1 &= a_1 \sigma_r \\ \sigma_2 &= a_2 \sigma_r \\ \sigma_3 &= a_3 \sigma_r \\ \sigma_4 &= a_4 \sigma_r \\ \theta_{12} &= \theta_1 \pm \theta_{12} \end{aligned} \right\} , \quad (2.34)$$

where $a_1 + a_2 = a_3 + a_4$ to satisfy the general resonance conditions (2.26), σ_r is a reference frequency, and θ_{12} is the angular gap between the wavenumbers \mathbf{k}_1 and \mathbf{k}_2 . The latter parameter can either be implicit to the

Table 2.2: One, two, or three parameter definitions of the representative quadruplet in the GMD. \mathbf{k}_d or (σ_d, θ_d) represents the discrete spectral grid point for which the discrete interaction contributions are evaluated. All quadruplets are aligned with the discrete directions by taking $\mathbf{k}_1 + \mathbf{k}_2 // \mathbf{k}_d$.

parameters	a_1	a_2	a_3	a_4	θ_{12}	σ_r
(λ)	1	1	$1 + \lambda$	$1 - \lambda$	0	σ_d
(λ, μ)	$1 + \mu$	$1 - \mu$	$1 + \lambda$	$1 - \lambda$	implied*	σ_d
$(\lambda, \mu, \theta_{12})$	$1 + \mu$	$1 - \mu$	$1 + \lambda$	$1 - \lambda$	free	$\frac{\sigma_d}{1+\mu}$

* assuming $\mathbf{k}_1 + \mathbf{k}_2 = \mathbf{k}_3 + \mathbf{k}_4 = 2\mathbf{k}_d$

quadruplet definition, or can be an explicitly tunable parameter. With this, a one- (λ) , two- (λ, μ) or three-parameter $(\lambda, \mu, \theta_{12})$ quadruplet definition have been constructed as outlined in Table 2.2. Note that, unlike in the DIA, all quadruplets are evaluated for the actual water depth and frequency.

In the GMD, the discrete interaction are computed for arbitrary depths. Somewhat surprisingly, interactions computed for the $F(f, \theta)$ spectrum and converted to the native WAVEWATCH III spectrum $N(k, \theta)$ using a Jacobian transformation proved more easily optimizable than computing the interaction contributions for the latter spectrum directly. Furthermore, a two-component scaling function was introduced with a ‘deep’ scaling function for the traditionally represented weak interactions in intermediate to deep water, and a ‘shallow’ scaling function representing strong interactions in extremely shallow water. With these modifications, the discrete interac-

tion contributions (2.20) of the DIA become

$$\begin{pmatrix} \delta S_{nl,1} \\ \delta S_{nl,2} \\ \delta S_{nl,3} \\ \delta S_{nl,4} \end{pmatrix} = \begin{pmatrix} -1 \\ -1 \\ 1 \\ 1 \end{pmatrix} \left(\frac{1}{n_{q,d}} C_{\text{deep}} B_{\text{deep}} + \frac{1}{n_{q,s}} C_{\text{shal}} B_{\text{shal}} \right) \times \left[\begin{aligned} & \frac{c_{g,1} F_1}{k_1 \sigma_1} \frac{c_{g,2} F_2}{k_2 \sigma_2} \left(\frac{c_{g,3} F_3}{k_3 \sigma_3} + \frac{c_{g,4} F_4}{k_4 \sigma_4} \right) \\ & - \frac{c_{g,3} F_3}{k_3 \sigma_3} \frac{c_{g,4} F_4}{k_4 \sigma_4} \left(\frac{c_{g,1} F_1}{k_1 \sigma_1} + \frac{c_{g,2} F_2}{k_2 \sigma_2} \right) \end{aligned} \right] \quad (2.35)$$

where B_{deep} and B_{shal} are the deep and shallow water scaling functions

$$B_{\text{deep}} = \frac{k^{4+m} \sigma^{13-2m}}{(2\pi)^{11} g^{4-m} c_g^2}, \quad (2.36)$$

$$B_{\text{shal}} = \frac{g^2 k^{11}}{(2\pi)^{11} c_g} (kd)^n, \quad (2.37)$$

with m and n as tunable parameters, C_{deep} and C_{shal} in Eq. (2.35) are the corresponding deep and shallow water tunable proportionality constants, and $n_{q,d}$ and $n_{q,s}$ are the number of representative quadruplets with deep and shallow water scaling, respectively, representing the feature of the GMD that multiple representative quadruplets can be used.

In the namelists `SNL3` and `ANL3` the user defines the number of quadruplets, and per quadruplet λ , μ , θ_{12} , C_{deep} and C_{shal} . Values of m and n are defined once, and used for all quadruplets. Finally relative depth below which deep water scaling is not used and above which shallow water scaling is not used are defined. Examples of some of the GMD configurations from Tolman (2010b) are included in the example input file `ww3_grid.inp` in Section 4.4.2. The default setting is to reproduce the traditional DIA.

Note that the GMD is significantly more complex than the DIA formulation, and requires evaluation of the quadruplet layout for every spectral frequency (compared to a single layout used for the DIA). For effective computation, quadruplet layouts are pre-computed and stored in memory for a set of nondimensional depths. Even with these and other optimizations, the GMD is roughly twice as expensive to compute for a single representative quadruplet than the DIA when using the one-parameter quadruplet layout. Using the two- or three-parameter quadruplet layout, the GMD has four

rather than two quadruplet realizations, making the GMD per quadruplet four times as expensive as the traditional DIA. Using multiple representative quadruplets is linearly additive in computational costs. For more in depth assessment of computational costs of a model including the GMD, see [Tolman \(2010b\)](#) and [Tolman \(2013a\)](#).

2.3.5 S_{nl} : The Two-Scale Approximation (TSA) and the Full Boltzmann Integral (FBI)

Switch:	NL4 with INDTSA=1 for TSA or 0 for FBI
Origination:	Full Boltzmann Integral
Provided by:	B. Toulany, W. Perrie, D. Resio & M. Casey

The Boltzmann integral describes the rate of change of action density of a particular wavenumber due to resonant interactions among four wavenumbers. The wavenumbers must satisfy a resonance:

$$\mathbf{k}_1 + \mathbf{k}_2 = \mathbf{k}_3 + \mathbf{k}_4. \quad (2.38)$$

The Two-Scale Approximation (TSA) for calculating the nonlinear interactions that is implemented in WAVEWATCH III is based on papers by [Resio and Perrie \(2008\)](#) (hereafter RP08), [Perrie and Resio \(2009\)](#), [Resio et al. \(2011\)](#) and [Perrie et al. \(2013\)](#). A description of TSA with respect to the Boltzmann integral is similar to the description for the WRT method. Here, we focus on the TSA derivation and the differences with the WRT method.

Starting from RP08 Eq. (2), the integral of the transfer rate from wavenumber \mathbf{k}_3 to wavenumber \mathbf{k}_1 , denoted $T(\mathbf{k}_1, \mathbf{k}_3)$, satisfies:

$$\frac{\partial n(\mathbf{k}_1)}{\partial t} = \int \int T(\mathbf{k}_1, \mathbf{k}_3) d\mathbf{k}_3 \quad (2.39)$$

which can be re-written (as in RP08) as:

$$\begin{aligned} T(\mathbf{k}_1, \mathbf{k}_3) &= 2 \oint [n_1 n_3 (n_4 - n_2) + n_2 n_4 (n_3 - n_1)] C(\mathbf{k}_1, \mathbf{k}_2, \mathbf{k}_3, \mathbf{k}_4) \\ &\quad \vartheta(|\mathbf{k}_1 - \mathbf{k}_4| - |\mathbf{k}_1 - \mathbf{k}_3|) \left| \frac{\partial W}{\partial \eta} \right|^{-1} ds \\ &\equiv 2 \oint N^3 C \vartheta \left| \frac{\partial W}{\partial \eta} \right|^{-1} ds \end{aligned} \quad (2.40)$$

as a line integral on contour s and where the function W is given by

$$W = \omega_1 + \omega_2 - \omega_3 - \omega_4 \quad (2.41)$$

where ϑ is the Heaviside function and $\mathbf{k}_2 = \mathbf{k}_2(s, \mathbf{k}_1, \mathbf{k}_3)$. Here, n_i is the action density at \mathbf{k}_i and function W is given by $W = \omega_1 + \omega_2 - \omega_3 - \omega_4$ requiring that the interactions conserve energy on s , which is the locus of points satisfying $W = 0$ and η is the local orthogonal to the locus s . Note that Eq.(2.40) is similar to Eq. (2.31) of WRT in section 2.3.3 with coupling coefficient C equal to the WRT coupling coefficient G divided by 2.

TSA and FBI For FBI, as well as for WRT, we numerically compute the discretized form of Eq.(2.40) as a finite sum of many line integrals (around locus s) of $T(\mathbf{k}_1, \mathbf{k}_3)$ for all discrete combinations of \mathbf{k}_1 and \mathbf{k}_3 . The line integral is determined by dividing the locus into a finite number of segments, each with the length ds . A complete ‘exact’ computation is expensive, requiring $10^3 - 10^4$ times DIAs run time.

The methodology for TSA is to decompose a directional spectrum into a *parametric (broad-scale)* spectrum and a (*local-scale*) nonparametric *residual* component. The residual component allows the decomposition to retain the same number of degrees of freedom as the original spectrum, a prerequisite for the nonlinear transfer source term in 3G models. As explained in the cited literature, this decomposition leads to a representation of the nonlinear wave-wave interactions in terms of the *broad-scale* interactions, *local-scale* interactions, and the *cross terms*: the interactions between the broadscale and local-scale components of the spectrum. This method allows the broad-scale interactions and certain portions of the local-scale interactions to be *pre-computed*. TSA’s accuracy is dependent on the accuracy of the parameterization used to represent the broadscale component.

We begin by decomposing a given action density spectrum n_i into the *parametric* broadscale term \hat{n}_i and a *residual* local-scale (or ‘*perturbation-scale*’) term n'_i . The broadscale term \hat{n}_i is assumed to have a JONSWAP-type form, depending on only a few parameters,

$$n'_i = n_i - \hat{n}_i \quad (2.42)$$

TSA’s accuracy depends on \hat{n}_i , in that if the number of degrees of freedom used for \hat{n}_i approaches the number of degrees of freedom in a given wave spectrum n_i , the local-scale n'_i becomes quite small, and thus, TSA is very

accurate. However, it is time-consuming to set up large multi-dimensional sets of pre-computed matrices for \hat{n}_i . Therefore an optimal TSA formulation must minimize the number of parameters needed for \hat{n}_i . However, even for complicated multi-peaked spectra n_i , a small set of parameters can be used to let \hat{n}_i capture *most* of the spectra so that the residual n'_i , can be small (RP08; Perrie and Resio (2009)).

RP08 describe the partitioning of n_i so that the transfer integral T in Eq. (2.40) consists of the sum of *broad-scale* terms \hat{n}_i , denoted B , *local-scale* terms n'_i , denoted L , and *cross-scale terms* of \hat{n}_i and n'_i , denoted X . Thus the nonlinear transfer term can be represented as,

$$S_{nl}(f, \theta) = B + L + X \quad (2.43)$$

where B depends on JONSWAP-type parameters x_i and can be pre-computed,

$$S_{nl}(f, \theta)_{broad-scale} = B(f, \theta, x_1, \dots, x_n). \quad (2.44)$$

TSA needs to find accurate efficient approximations for $L + X$. If all terms in Eq. (2.43) are computed as in FBI, this might result in an $8\times$ increase in the computations, compared to B in Eq. (2.43). While this approach can provide a means to examine the general problem of bimodal wave spectra, for example in mixed seas and swells, by subtracting the interactions for a single spectral region from the interactions for the sum of the two spectral regions, it does not provide the same insight as the use of the *split* density function, where the cross-interaction terms can be examined algebraically.

In any case, to simplify Eq. (2.43), terms involving n'_2 and n'_4 are neglected assuming that these local-scale terms are deviations about the broad-scale terms, \hat{n}_2 and \hat{n}_4 , which are supposed to capture most of the spectra, whereas n'_2 and n'_4 , with their positive/negative differences and products tend to cancel. TSA's ability to match the FBI (or WRT) results for test spectra is used to justify the approach. Moreover, the broadscale terms \hat{n}_2 and \hat{n}_4 , tend to have much longer lengths along locus s and therefore should contribute more to the net transfer integral. Thus, RP08 show that

$$S_{nl}(k_1) = B + L + X = B + \int \int \oint N_*^3 C \left| \frac{\partial W}{\partial n} \right|^{-1} ds k_3 d\theta_3 dk_3, \quad (2.45)$$

where N_*^3 is what's left from all the cross terms, after neglecting terms involving n'_2 and n'_4 ,

$$N_*^3 = \hat{n}_2 \hat{n}_4 (n'_3 - n'_1) + n'_1 n'_3 (\hat{n}_4 - \hat{n}_2) + \hat{n}_1 n'_3 (\hat{n}_4 - \hat{n}_2) + n'_1 \hat{n}_3 (\hat{n}_4 - \hat{n}_2), \dots \quad (2.46)$$

and they use known scaling relations, with specific parameterizations, for example for f^{-4} or f^{-5} based spectra. To implement this formulation, we generally fit each peak separately.

It should be noted that to speed up the computation, a pre-computed set of multi-dimensional arrays, for example the grid geometry arrays and the gradient array, which are functions of spectral parameters, number of segments on the locus and depth, are generated and saved in a file with filename 'grd_dfrq_nrng_nang_npts_ndep.dat', for example, 'grd.1.1025-.35.36_30_37.dat', etc.

The flow chart for TSA's main subroutine W3SNL4 in w3snl4md.ftn is as follows:

```

/
|
|*** It's called from:
|-----
|   (1) W3SRCE in w3srcemd.ftn; to calc. & integrate source term
|       at single pt
|   (2) GXEXP0 in gx_outp.ftn; to perform point output
|   (3) W3EXP0 in ww3_outp.ftn; to perform point output
|   (4) W3EXNC in ww3_oump.ftn; to perform point output
|*** It can also be called from:
|   (5) W3IOGR in w3iogrmd.ftn; to perform I/O of "mod_def.ww3"
|
W3SNL4 -->|
|
|*** It calls:
|-----
|
|           /
|           |
|           |*** It's called from:
|           |-----
|           |   W3SNL4 in w3snl4md.ftn; main TSA subr.
|           |*** It can also be called from: subr W3IOGR
|           |   W3IOGR in w3iogrmd.ftn; I/O of mod_def.ww3
|           |
|           |*** It calls:
|           |-----
|           |--> wkfnc (function)
|           |--> cgfnc (function)
| (1)       |
|--> INSNL4 -->|           /
|           |           |--> shloxr (uses function wkfnc)
|           |--> gridsetr -->|--> shlocr

```

```

|          |          |--> cplshr
|          |          \
|(2)       |          \
|--> optsa2
|
|          |          /
|(3)       |          |   if (ialt=2)
|--> snlr_tsa -->|--> interp2
|          |          \
|
|          |          /
|(4)       |          |   if (ialt=2)
|--> snlr_fbi -->|--> interp2
|          |          \
|
|
\

```

2.3.6 S_{nl} : Nonlinear Filter

Switch:	NLS
Origination:	WAVEWATCH III
Provided by:	H. L. Tolman

When the DIA of Eqs. (2.19) and (2.20) is applied with a quadruplet where λ_{nl} is small enough so that the resulting quadruplet is *not* resolved by the discrete spectral grid, then the resulting numerical form of the DIA corresponds to a simple diffusion tensor. If this tensor is filtered so that it is applied to the high-frequency tail of the spectrum only, then a conservative filter results, which retains all conservation properties of the nonlinear interactions (Tolman, 2008b, 2011a). This filter can be used as a part of a parameterization of nonlinear interactions. For instance, it was shown to be effective in removing high-frequency spectral noise in some GMD configurations in Figs. 5 and 6 of Tolman (2011a). Since it is essential that the quadruplet is not resolved by the spectral grid, the free parameter of the filter defining the quadruplet is the relative offset of quadruplets 3 and 4 in the discrete frequency grid (α_{34} , $0 < \alpha_{34} < 1$), from which λ_{nl} is computed as

$$\lambda_{nl} = \alpha_{34}(X_\sigma - 1), \quad (2.47)$$

where X_σ is the increment factor for the discrete frequency grid, typically $X_\sigma = 1.1$ [Eq. (3.1)]. Using the native spectral description of WAVEWATCH III, the change in spectral density δN_i at quadruplet component i , is written in the form of a discrete diffusion equation as (Tolman, 2011a, page 294)

$$\begin{pmatrix} \delta N_3 \\ \delta N_1 \\ \delta N_4 \end{pmatrix} = N_1 \begin{pmatrix} 0 \\ 1 \\ 0 \end{pmatrix} + N_1 \frac{S\Delta t}{N_1} \begin{pmatrix} 1 \\ -2 \\ 1 \end{pmatrix}, \quad (2.48)$$

with

$$S = \frac{C_{nlf} k^4 \sigma^{12}}{(2\pi)^9 g^4 c_g} \left[\frac{N_1^2}{k_1^2} \left(\frac{N_3}{k_3} + \frac{N_4}{k_4} \right) - 2 \frac{N_1 N_3 N_4}{k_1 k_3 k_4} \right], \quad (2.49)$$

where C_{nlf} is the proportionality constant of the DIA used in the filter. The DIA results in changes S for two mirror-image quadruplets (S_a and S_b). A JONSWAP style filter (Φ) is applied to localize the smoother at higher frequencies only, with

$$\Phi(f) = \exp \left[-c_1 \left(\frac{f}{c_2 f_p} \right)^{-c_3} \right], \quad (2.50)$$

where c_1 through c_3 are tunable parameters. The latter three parameters need to be chosen such that $\Phi(f_p) \approx 0$, $\Phi(f > 3f_p) \approx 1$ and that $\Phi \approx 0.5$ for frequencies moderately larger than f_p . This can be achieved by setting

$$c_1 = 1.25, \quad c_2 = 1.50, \quad c_3 = 6.00. \quad (2.51)$$

Accounting for the redistribution of the changes $S_{a,b}$ over the neighboring discrete spectral grids points, the effective nondimensional strengths ($\tilde{S}_{a,b}$) of the interactions for both quadruplets become

$$\tilde{S}_a = \Phi(f) M_1 S_a \Delta t / N_1, \quad \tilde{S}_b = \Phi(f) M_1 S_b \Delta t / N_1, \quad (2.52)$$

where N_1 is the action density at the center component of the quadruplet, and M_1 is a factor accounting for the redistribution of the contribution over the discrete spectral grid (for details, see Tolman, 2011a). To convert this DIA into a stable diffusive filter, $|\tilde{S}_{a,b}|$ should be limited to $\tilde{S}_{\max} \approx 0.5$

(e.g., Fletcher, 1988). The maximum change is distributed over the two quadruplets using

$$\tilde{S}_{m,a} = \frac{|\tilde{S}_a|\tilde{S}_{\max}}{|\tilde{S}_a| + |\tilde{S}_b|}, \quad \tilde{S}_{m,b} = \frac{|\tilde{S}_b|\tilde{S}_{\max}}{|\tilde{S}_a| + |\tilde{S}_b|}, \quad (2.53)$$

and the normalized changes \tilde{S}_a and \tilde{S}_b are limited as

$$-\tilde{S}_{m,a} \leq \tilde{S}_a \leq \tilde{S}_{m,a}, \quad -\tilde{S}_{m,b} \leq \tilde{S}_b \leq \tilde{S}_{m,b}. \quad (2.54)$$

With this, the free parameters of the conservative nonlinear filter are α_{34} in Eq. (2.47), C_{nlf} in Eq. (2.49), \tilde{S}_{\max} in Eq. (2.53), and c_1 through c_3 in Eq. (2.50). All these parameters can be adjusted by the user through the namelist SNLS in `ww3_grid.inp` (parameters A34, FHFC, DNM, FC1, FC2 and FC3, respectively). Note that this filter is applied in addition to a parameterization of S_{nl} , but does not replace it. Hence, it is used in concert with a full parameterization of S_{nl} , described in the preceding sections.

2.3.7 $S_{in} + S_{ds}$: WAM cycle 3

Switch:	ST1
Origination:	WAM model
Provided by:	H. L. Tolman

The input and dissipation source terms of WAM cycles 1 through 3 are based on Snyder et al. (1981) and Komen et al. (1984) (see also WAMDIG, 1988). The input source term is given as

$$\mathcal{S}_{in}(k, \theta) = C_{in} \frac{\rho_a}{\rho_w} \max \left[0, \left(\frac{28 u_*}{c} \cos(\theta - \theta_w) - 1 \right) \right] \sigma N(k, \theta), \quad (2.55)$$

$$u_* = u_{10} \sqrt{(0.8 + 0.065 u_{10}) 10^{-3}}, \quad (2.56)$$

where C_{in} is a constant ($C_{in} = 0.25$), ρ_a (ρ_w) is the density of air (water), u_* is the wind friction velocity (Charnock, 1955; Wu, 1982), c is the phase velocity σ/k , u_{10} is the wind speed at 10 m above the mean sea level and θ_w is the mean wind direction. The corresponding dissipation term is given as

$$\mathcal{S}_{ds}(k, \theta) = C_{ds} \hat{\sigma} \frac{k}{\hat{k}} \left(\frac{\hat{\alpha}}{\hat{\alpha}_{PM}} \right)^2 N(k, \theta), \quad (2.57)$$

$$\hat{\sigma} = \left(\overline{\sigma^{-1}} \right)^{-1}, \quad (2.58)$$

$$\hat{\alpha} = E \hat{k}^2 g^{-2}, \quad (2.59)$$

where C_{ds} is a constant ($C_{ds} = -2.36 \cdot 10^{-5}$), $\hat{\alpha}_{PM}$ is the value of $\hat{\alpha}$ for a PM spectrum ($\hat{\alpha}_{PM} = 3.02 \cdot 10^{-3}$) and where \hat{k} is given by Eq. (2.25).

The parametric tail [Eqs. (2.17) and (2.18)] corresponding to these source terms is given by² $m = 4.5$ and by

$$f_{hf} = \max \left[2.5 \hat{f}_r, 4 f_{PM} \right], \quad (2.60)$$

$$f_{PM} = \frac{g}{28 u_*}, \quad (2.61)$$

where f_{PM} is the [Pierson and Moskowitz \(1964\)](#) frequency, estimated from the wind friction velocity u_* . The shape and attachment point of this tail is hardcoded to the present model. The tunable parameters C_{in} , C_{ds} and α_{PM} are preset to their default values, but can be redefined by the user in the input files of the model.

2.3.8 $S_{in} + S_{ds}$: Tolman and Chalikov 1996

Switch:	ST2
Origination:	WAVEWATCH III
Provided by:	H. L. Tolman

The source term package of [Tolman and Chalikov \(1996\)](#) consists of the input source term of [Chalikov and Belevich \(1993\)](#) and [Chalikov \(1995\)](#), and two dissipation constituents. The input source term is given as

$$\mathcal{S}_{in}(k, \theta) = \sigma \beta N(k, \theta), \quad (2.62)$$

² originally, WAM used $m = 5$, present setting used for consistent limit behavior (e.g., [Tolman, 1992](#)).

where β is a nondimensional wind-wave interaction parameter, which is approximated as

$$10^4\beta = \begin{cases} -a_1\tilde{\sigma}_a^2 - a_2 & , & \tilde{\sigma}_a < -1 \\ a_3\tilde{\sigma}_a(a_4\tilde{\sigma}_a - a_5) - a_6 & , & -1 \leq \tilde{\sigma}_a < \Omega_1/2 \\ (a_4\tilde{\sigma}_a - a_5)\tilde{\sigma}_a & , & \Omega_1/2 \leq \tilde{\sigma}_a < \Omega_1 \\ a_7\tilde{\sigma}_a - a_8 & , & \Omega_1 \leq \tilde{\sigma}_a < \Omega_2 \\ a_9(\tilde{\sigma}_a - 1)^2 + a_{10} & , & \Omega_2 \leq \tilde{\sigma}_a \end{cases} \quad (2.63)$$

where

$$\tilde{\sigma}_a = \frac{\sigma u_\lambda}{g} \cos(\theta - \theta_w) \quad (2.64)$$

is the non-dimensional frequency of a spectral component, θ_w is the wind direction and u_λ is the wind velocity at a height equal to the ‘apparent’ wave length

$$\lambda_a = \frac{2\pi}{k|\cos(\theta - \theta_w)|}. \quad (2.65)$$

The parameters $a_1 - a_{10}$ and Ω_1, Ω_2 in Eq. (2.63) depend on the drag coefficient C_λ at the height $z = \lambda_a$:

$$\begin{aligned} \Omega_1 &= 1.075 + 75C_\lambda & \Omega_2 &= 1.2 + 300C_\lambda \\ a_1 &= 0.25 + 395C_\lambda, & a_3 &= (a_0 - a_2 - a_1)/(a_0 + a_4 + a_5) \\ a_2 &= 0.35 + 150C_\lambda, & a_5 &= a_4\Omega_1 \\ a_4 &= 0.30 + 300C_\lambda, & a_6 &= a_0(1 - a_3) \\ a_9 &= 0.35 + 240C_\lambda, & a_7 &= (a_9(\Omega_2 - 1)^2 + a_{10})/(\Omega_2 - \Omega_1) \\ a_{10} &= -0.05 + 470C_\lambda, & a_8 &= a_7\Omega_1 \\ & & a_0 &= 0.25a_5^2/a_4 \end{aligned} \quad (2.66)$$

The wave model takes the wind u_r at a given reference height z_r as its input, so that u_λ and C_λ need to be derived as part of the parameterization. Excluding a thin surface layer adjusting to the water surface, the mean wind profile is close to logarithmic

$$u_z = \frac{v_*}{\kappa} \ln\left(\frac{z}{z_0}\right), \quad (2.67)$$

where $\kappa = 0.4$ is the Von Kàrmàn constant, and z_0 is the roughness parameter. This equation can be rewritten in terms of the drag coefficient C_r at the reference height z_r as (Chalikov, 1995)

$$C_r = \kappa^2 [R - \ln(C)]^2, \quad (2.68)$$

where

$$R = \ln \left(\frac{z_r g}{\chi \sqrt{\alpha} u_r^2} \right), \quad (2.69)$$

where $\chi = 0.2$ is a constant, and where α is the conventional nondimensional energy level at high frequencies. An accurate explicit approximation to these implicit relations is given as

$$C_r = 10^{-3} \left(0.021 + \frac{10.4}{R^{1.23} + 1.85} \right). \quad (2.70)$$

The estimation of the drag coefficient thus requires an estimate of the high-frequency energy level α , which could be estimated directly from the wave model. However, the corresponding part of the spectrum is generally not well resolved, tends to be noisy, and is tainted by errors in several source terms. Therefore, α is estimated parametrically as (Janssen, 1989)

$$\alpha = 0.57 \left(\frac{u_*}{c_p} \right)^{3/2}. \quad (2.71)$$

As the latter equation depends on the drag coefficient, Eqs. (2.69) through (2.71) formally need to be solved iteratively. Such iterations are performed during the model initialization, but are not necessary during the actual model run, as u_* generally changes slowly. Note that Eq. (2.71) can be considered as an internal relation to the parameterization of C_r , and can therefore deviate from actual model behavior without loss of generality. In Tolman and Chalikov (1996), C_r is therefore expressed directly in terms of c_p .

Using the definition of the drag coefficient and Eq. (2.67) the roughness parameter z_0 becomes

$$z_0 = z_r \exp \left(-\kappa C_r^{-1/2} \right), \quad (2.72)$$

and the wind velocity and drag coefficient at height λ become

$$u_\lambda = u_r \frac{\ln(\lambda_a/z_0)}{\ln(z_r/z_0)}, \quad (2.73)$$

$$C_\lambda = C_r \left(\frac{u_a}{u_\lambda} \right)^2, \quad (2.74)$$

Finally, Eq. (2.71) requires an estimate for the peak frequency f_p . To obtain a consistent estimate of the peak frequency of actively generated waves, even in complex multimodal spectra, this frequency is estimated from the equivalent peak frequency of the positive part of the input source term (see Tolman and Chalikov, 1996)

$$f_{p,i} = \frac{\int \int f^{-2} c_g^{-1} \max[0, \mathcal{S}_{wind}(k, \theta)] df d\theta}{\int \int f^{-3} c_g^{-1} \max[0, \mathcal{S}_{wind}(k, \theta)] df d\theta}, \quad (2.75)$$

from which the actual peak frequency is estimated as (the tilde identifies nondimensional parameter based on u_* and g)

$$\tilde{f}_p = 3.6 \cdot 10^{-4} + 0.92 \tilde{f}_{p,i} - 6.3 \cdot 10^{-10} \tilde{f}_{p,i}^{-3}. \quad (2.76)$$

All constants in the above equations are defined within the model. The user only defines the reference wind height z_r .

During testing of a global implementation of WAVEWATCH III including this source term (Tolman, 2002f), it was found that its swell dissipation due to opposing or weak winds was severely overestimated. To correct this deficiency, a filtered input source term is defined as

$$\mathcal{S}_{i,m} = \begin{cases} \mathcal{S}_i & \text{for } \beta \geq 0 \quad \text{or} \quad f > 0.8f_p \\ X_s \mathcal{S}_i & \text{for } \beta < 0 \quad \text{and} \quad f < 0.6f_p \\ \mathcal{X}_s \mathcal{S}_i & \text{for } \beta < 0 \quad \text{and} \quad 0.6f_p < f < 0.8f_p \end{cases}, \quad (2.77)$$

where f is the frequency, f_p is the peak frequency of the wind sea as computed from the input source term, \mathcal{S}_i is the input source term (2.62), and $0 < X_s < 1$ is a reduction factor for \mathcal{S}_i , which is applied to swell with negative β only (defined by the user). \mathcal{X}_s represents a linear reduction of X_s with f_p providing a smooth transition between the original and reduced input.

The drag coefficient that follows from Eq. (2.71) becomes unrealistically high for hurricane strength wind speeds, leading to unrealistically high wave growth rates. To alleviate this, the drag coefficient at the reference height

C_r can be capped with a maximum allowed drag coefficient $C_{r,max}$, either as a simple hard limit

$$C_r = \min(C_r, C_{r,max}) \quad , \quad (2.78)$$

or with a smooth transition

$$C_r = C_{r,max} \tanh(C_r/C_{r,max}) \quad . \quad (2.79)$$

Selection of the capped drag coefficient occurs at the compile stage of the code. The cap level and cap type can be set by the user. Defaults settings are $C_{r,max} = 2.5 \cdot 10^{-3}$ and Eq. (2.78).

The corresponding dissipation source term consists of two constituents. The (dominant) low-frequency constituent is based on an analogy with energy dissipation due to turbulence,

$$\mathcal{S}_{ds,l}(k, \theta) = -2 u_* h k^2 \phi N(k, \theta) \quad , \quad (2.80)$$

$$h = 4 \left(\int_0^{2\pi} \int_{f_h}^{\infty} F(f, \theta) df d\theta \right)^{1/2} \quad . \quad (2.81)$$

$$\phi = b_0 + b_1 \tilde{f}_{p,i} + b_2 \tilde{f}_{p,i}^{-b_3} \quad . \quad (2.82)$$

where h is a mixing scale determined from the high-frequency energy content of the wave field and where ϕ is an empirical function accounting for the development stage of the wave field. The linear part of Eq. (2.82) describes dissipation for growing waves. The nonlinear term has been added to allow for some control over fully grown conditions by defining a minimum value for ϕ (ϕ_{\min}) for a minimum value of $f_{p,i}$ ($f_{p,i,\min}$). If ϕ_{\min} is below the linear curve, b_2 and b_3 are given as

$$b_2 = \tilde{f}_{p,i,\min}^{b_3} \left(\phi_{\min} - b_0 - b_1 \tilde{f}_{p,i,\min} \right) \quad , \quad (2.83)$$

$$b_3 = 8 \quad . \quad (2.84)$$

If ϕ_{\min} is above the linear curve, b_2 and b_3 are given as

$$\tilde{f}_a = \frac{\phi_{\min} - b_0}{b_1} \quad , \quad \tilde{f}_b = \max \left\{ \tilde{f}_a - 0.0025 \quad , \quad \tilde{f}_{p,i,\min} \right\} \quad , \quad (2.85)$$

$$b_2 = \tilde{f}_b^{b_3} \left[\phi_{\min} - b_0 - b_1 \tilde{f}_b \right] \quad , \quad (2.86)$$

$$b_3 = \frac{b_1 \tilde{f}_b}{\phi_{\min} - b_0 - b_1 \tilde{f}_b} . \quad (2.87)$$

The above estimate of b_3 results in $\partial\phi/\partial\tilde{f}_{p,i} = 0$ for $\tilde{f}_{p,i} = \tilde{f}_b$. For $\tilde{f}_{p,i} < \tilde{f}_b$, ϕ is kept constant ($\phi = \phi_{\min}$).

The empirical high-frequency dissipation is defined as

$$\mathcal{S}_{ds,h}(k, \theta) = -a_0 \left(\frac{u_*}{g} \right)^2 f^3 \alpha_n^B N(k, \theta) , \quad (2.88)$$

$$B = a_1 \left(\frac{f u_*}{g} \right)^{-a_2} ,$$

$$\alpha_n = \frac{\sigma^6}{c_g g^2 \alpha_r} \int_0^{2\pi} N(k, \theta) d\theta , \quad (2.89)$$

where α_n is Phillips' nondimensional high-frequency energy level normalized with α_r , and where a_0 through a_2 and α_r are empirical constants. This parameterization implies that $m = 5$ in the parametric tail, which has been preset in the model. Note that in the model Eq. (2.89) is solved assuming a deep water dispersion relation, in which case α_n is evaluated as

$$\alpha_n = \frac{2 k^3}{\alpha_r} F(k) . \quad (2.90)$$

The two constituents of the dissipation source term are combined using a simple linear combination, defined by the frequencies f_1 and f_2 .

$$\mathcal{S}_{ds}(k, \theta) = \mathcal{A} \mathcal{S}_{ds,l} + (1 - \mathcal{A}) \mathcal{S}_{ds,h} , \quad (2.91)$$

$$\mathcal{A} = \begin{cases} 1 & \text{for } f < f_l , \\ \frac{f-f_2}{f_1-f_2} & \text{for } f_1 \leq f < f_2 , \\ 0 & \text{for } f_2 \leq f . \end{cases} \quad (2.92)$$

To enhance the smoothness of the model behavior for frequencies near the parametric cut-off f_{hf} , a similar transition zone is used between the prognostic spectrum and the parametric high-frequency tail as in Eq. (2.18)

$$N(k_i, \theta) = (1 - \mathcal{B}) N(k_i, \theta) + \mathcal{B} N(k_{i-1}, \theta) \left(\frac{f_i}{f_{i-1}} \right)^{-m-2} , \quad (2.93)$$

Tuned to :	a_0	a_1	a_2	b_0	b_1	ϕ_{\min}
KC stable	4.8	$1.7 \cdot 10^{-4}$	2.0	$0.3 \cdot 10^{-3}$	0.47	0.003
KC unstable	4.5	$2.3 \cdot 10^{-3}$	1.5	$-5.8 \cdot 10^{-3}$	0.60	0.003

Table 2.3: Suggested constants in the source term package of Tolman and Chalikov. KC denotes [Kahma and Calkoen \(1992, 1994\)](#). First line represents default model settings.

where i is a discrete wavenumber counter, and \mathcal{B} is defined similarly to \mathcal{A} , ranging from 0 to 1 between f_2 and f_{hf} .

The frequencies defining the transitions and the length scale h are predefined in the model as

$$\left. \begin{aligned} f_{hf} &= 3.00 f_{p,i} \\ f_1 &= 1.75 f_{p,i} \\ f_2 &= 2.50 f_{p,i} \\ f_h &= 2.00 f_{p,i} \end{aligned} \right\} . \quad (2.94)$$

Furthermore, $f_{p,i,\min} = 0.009$ and $\alpha_r = 0.002$ are preset in the model. All other tunable parameters have to be provided by the user. Suggested and default values are given in [Table 2.3](#).

Test results of these source terms in a global model implementation ([Tolman, 2002f](#)) suggested that (i) the model tuned in the classical way to fetch-limited growth for stable conditions underestimates deep-ocean wave growth (a deficiency apparently shared by the WAM model) and that (ii) effects of stability on the growth rate of waves ([Kahma and Calkoen, 1992, 1994](#)) should be included explicitly in the parameterization of the source terms. Ideally, both problems would be dealt with by theoretical investigation of the source terms. Alternatively, the wind speed u can be replaced by an effective wind speed u_e . In [Tolman \(2002f\)](#) the following effective wind speed is used :

$$\frac{u_e}{u} = \left(\frac{c_o}{1 + C_1 + C_2} \right)^{-1/2}, \quad (2.95)$$

$$C_1 = c_1 \tanh [\max(0, f_1 \{ST - ST_o\})], \quad (2.96)$$

$$C_2 = c_2 \tanh [\max(0, f_2 \{ST - ST_o\})], \quad (2.97)$$

$$\mathcal{ST} = \frac{hg}{u_h^2} \frac{T_a - T_s}{T_0}, \quad (2.98)$$

where \mathcal{ST} is a bulk stability parameter, and T_a , T_s and T_0 are the air, sea and reference temperature, respectively. Furthermore, $f_1 \leq 0$, c_1 and c_2 have opposite signs and $f_2 = f_1 c_1 / c_2$. Following Tolman (2002f), default settings of $c_0 = 1.4$, $c_1 = -0.1$, $c_2 = 0.1$, $f_1 = -150$ and $\mathcal{ST}_o = -0.01$ in combination with the tuning to stable stratification wave growth data ('KC stable' parameter values in Table 2.3) are used. Note that this effective wind speed was derived for winds at 10 m height. The wind correction can be switched off by the user during compilation of the model, and default parameter settings can be redefined by the user in the program input files.

2.3.9 $S_{in} + S_{ds}$: WAM cycle 4 (ECWAM)

Switch:	ST3
Origination:	WAM model
Provided by:	F. Ardhuin

The wind-wave interaction source terms described here are based on the wave growth theory of Miles (1957), modified by Janssen (1982). The pressure-slope correlations that give rise to part of the wave generation are parameterized following Janssen (1991). A wave dissipation term due to shear stresses variations in phase with the orbital velocity is added for the swell part of the spectrum, based on the swell decay observations of Ardhuin et al. (2009a).

This parameterization was further extended by Abdalla and Bidlot (2002) to take into account a stronger gustiness in unstable atmospheric conditions. This effect is included in the present parameterization and is activated with the STAB3 switch. Efforts have been made to make the present implementation as close as possible to the one in the ECWAM model (Bidlot et al., 2005), in particular the stress lookup tables were verified to be identical. Later modifications include the addition of a negative part in the wind input to represent swell dissipation.

The source term reads (Janssen, 2004)

$$\mathcal{S}_{in}(k, \theta) = \frac{\rho_a}{\rho_w} \frac{\beta_{\max}}{\kappa^2} e^Z Z^4 \left(\frac{u_*}{C} + z_\alpha \right)^2 \cos^{p_{in}}(\theta - \theta_u) \sigma N(k, \theta) + S_{out}(k, \theta), \quad (2.99)$$

where ρ_a and ρ_w are the air and water densities, β_{\max} is a non-dimensional growth parameter (constant), κ is von Kármán' constant, and p_{in} is a constant that controls the directional distribution of \mathcal{S}_{in} . In the present implementation the air/water density ratio ρ_a/ρ_w is constant. We define $Z = \log(\mu)$ where μ is given by Janssen (1991) Eq. (16), and corrected for intermediate water depths, so that

$$Z = \log(kz_1) + \kappa / [\cos(\theta - \theta_u)(u_\star/C + z_\alpha)], \quad (2.100)$$

where z_1 is a roughness length modified by the wave-supported stress τ_w , and z_α is a wave age tuning parameter³. The roughness z_1 is defined as,

$$U_{10} = \frac{u_\star}{\kappa} \log\left(\frac{z_u}{z_1}\right) \quad (2.101)$$

$$z_1 = \alpha_0 \frac{\tau}{\sqrt{1 - \tau_w/\tau}}, \quad (2.102)$$

where $\tau = u_\star^2$, and z_u is the height at which the wind is specified. These two equations provide an implicit functional dependence of u_\star on U_{10} and τ_w/τ . This relationship is then tabulated (Janssen, 1991; Bidlot et al., 2007).

An important part of the parameterization is the calculation of the wave-supported stress τ_w ,

$$\tau_w = \left| \int_0^{k_{\max}} \int_0^{2\pi} \frac{\mathcal{S}_{in}(k', \theta)}{C} (\cos \theta, \sin \theta) dk' d\theta + \tau_{\text{hf}}(u_\star, \alpha) (\cos \theta_u, \sin \theta_u) \right|, \quad (2.103)$$

which includes the resolved part of the spectrum, up to k_{\max} , as well as the stress supported by shorter waves, τ_{hf} . Assuming a f^{-X} diagnostic tail beyond the highest frequency, τ_{hf} is given by

³Although this tuning parameter z_α is not well described in WAM-Cycle4 documentation, it has an important effect on wave growth. Essentially it shifts the wave age of the long waves, which typically increases the growth, and even generates waves that travel faster than the wind. This accounts for some gustiness in the wind and should possibly be resolution-dependent. For reference, this parameter was not properly set in early versions of the SWAN model, as discovered by R. Lalbeharry.

$$\begin{aligned} \tau_{\text{hf}}(u_*, \alpha) &= \frac{u_*^2}{g^2} \frac{\sigma_{\text{max}}^X 2\pi\sigma}{2\pi C_g(k_{\text{max}})} \int_0^{2\pi} N(k_{\text{max}}, \theta) \max\{0, \cos(\theta - \theta_u)\}^3 d\theta \\ &\quad \times \frac{\beta_{\text{max}}}{\kappa^2} \int_{\sigma_{\text{max}}}^{0.05g/u_*} \frac{e^{Z_{\text{hf}}} Z_{\text{hf}}^4}{\sigma^{X-4}} d\sigma \end{aligned} \quad (2.104)$$

where the second integral is a function of u_* and the Charnock coefficient α only, which is easily tabulated. In practice the calculation is coded with $X = 5$, and the variable Z_{hf} is defined by,

$$Z_{\text{hf}}(\sigma) = \log(kz_1) + \min\{\kappa/(u_*/C + z_\alpha), 20\}. \quad (2.105)$$

This parameterization is sensitive to the spectral level at k_{max} . A higher spectral level will lead to a larger value of u_* and thus positive feedback on the wind input via z_1 . This sensitivity is exacerbated by the sensitivity of the high-frequency spectral level to the presence of swell via the dissipation term.

A linear damping of swells was introduced in the operational ECWAM model in September 2009. It takes the form given by [Janssen \(2004\)](#)

$$S_{\text{out}}(k, \theta) = 2s_1\kappa \frac{\rho_a}{\rho_w} \left(\frac{u_*}{C}\right)^2 \left[\cos(\theta - \theta_u) - \frac{\kappa C}{u_* \log(kz_0)} \right] \quad (2.106)$$

where s_1 is set to 1 when this damping is used and 0 otherwise. For $s_1 = 0$ the parameterization is the WAM4 or BJA parameterization (see [Table 2.4](#)).

Due to the increase in high-frequency input compared to WAM3, the dissipation function was adapted by [Janssen \(1994\)](#) from the WAM3 dissipation, and later reshaped by [Bidlot et al. \(2005\)](#). That later modification is referred to as "BJA" for Bidlot, Janssen and Abdallah. A more recent modification, strongly improved the model results for Pacific swells, at the price of an underestimation of the highest sea states. This corresponds to the ECMWF WAM model contained in the IFS version CY38R1 ([Bidlot, 2012](#)). Note that these parameters were optimized for use of neutral winds from the operational ECMWF analysis. Using these with other wind products may require a re-tuning of these coefficients. For example, with NCEP or CF-SRR winds, the value of BETAMAX should probably be reduced or ZWND increased.

The generic form of the WAM4 dissipation term is,

$$S_{ds}(k, \theta)^{\text{WAM}} = C_{ds} \bar{\alpha}^2 \bar{\sigma} \left[\delta_1 \frac{k}{\bar{k}} + \delta_2 \left(\frac{k}{\bar{k}} \right)^2 \right] N(k, \theta) \quad (2.107)$$

where C_{ds} is a non-dimensional constant δ_1 and δ_2 are weight parameters,

$$\bar{k} = \left[\frac{\int k^p N(k, \theta) d\theta}{\int N(k, \theta) d\theta} \right]^{1/p} \quad (2.108)$$

with p a constant power. Similarly, the mean frequency is defined as

$$\bar{\sigma} = \left[\frac{\int \sigma^p N(k, \theta) d\theta}{\int N(k, \theta) d\theta} \right]^{1/p}, \quad (2.109)$$

so that the mean steepness is $\bar{\alpha} = E\bar{k}^2$.

The mean frequency also occurs in the definition of the maximum frequency of prognostic integration of the source terms. Since the definition of that frequency may be different from that of the source term it is defined with another exponent p_{tail} .

Unfortunately these parameterizations are sensitive to swell. An increase in swell height typically reduces dissipation at the windsea peak because the mean wavenumber \bar{k} and thus the mean steepness $\bar{\alpha}$ are reduced. For $p < 2$, as in the WAM-Cycle 4 and BJA parameterizations, this sensitivity is much larger and opposite to the expected effect of short wave modulation by long waves.

The source term code was generalized to allow the use of WAM4, BJA or others ECWAM parameterization, via a simple change of the parameters in the namelists SIN3 and SDS3, see Tables 2.4 and 2.5. At present, the default values of the namelist parameters correspond to BJA (Bidlot et al., 2005).

2.3.10 $S_{in} + S_{ds}$: Ardhuin et al. 2010

Switch:	ST4
Origination:	WAVEWATCH III
Provided by:	F. Ardhuin

Par.	WWATCH var.	namelist	WAM4	BJA	Bidlot 2012
z_u	ZWND	SIN3	10.0	10.0	10.0
α_0	ALPHA0	SIN3	0.01	0.0095	0.0095
β_{\max}	BETAMAX	SIN3	1.2	1.2	1.2
p_{in}	SINTHP	SIN3	2	2	2
z_α	ZALP	SIN3	0.0110	0.0110	0.0080
s_1	SWELLF	SIN3	0.0	0.0	1.0

Table 2.4: Parameter values for WAM4, BJA and the 2012 update in the ECWAM model. Source term parameterizations that can be reset via the SIN3 and SDS3 namelist. BJA is generally better than WAM4. The default parameters in ST3 corresponds to BJA. Please note that the name of the variables only apply to the namelists. In the source term module the names are slightly different, with a doubled first letter, in order to differentiate the variables from the pointers to these variables.

Par.	WWATCH var.	namelist	WAM4	BJA	Bidlot 2012
C_{ds}	SDSC1	SDS3	-4.5	-2.1	-1.33
p	WNMEANP	SDS3	-0.5	0.5	0.5
p_{tail}	WNMEANPTAIL	SDS3	-0.5	0.5	0.5
δ_1	SDSDELTA1	SDS3	0.5	0.4	0.5
δ_2	SDSDELTA2	SDS3	0.5	0.6	0.5

Table 2.5: Parameter values for WAM4, BJA and the update by Bidlot (2012). Source term parameterizations that can be reset via the SDS3 namelist. BJA is generally better than WAM4. Please note that the name of the variables only apply to the namelists. In the source term module the names are slightly different, with a doubled first letter, in order to differentiate the variables from the pointers to these variables.

This parameterization uses a positive part of the wind input taken from WAM cycle 4, with an ad hoc reduction of u_\star is implemented in order to allow a balance with a saturation-based dissipation. This correction also reduces the drag coefficient at high winds. This is done by reducing the wind input for high frequencies and high winds. For this, u_\star in eq. (2.99) is replaced by $u'_\star(k)$ defined for each frequency as

$$(u'_\star)^2 = \left| u_\star^2 (\cos \theta_u, \sin \theta_u) - |s_u| \int_0^k \int_0^{2\pi} \frac{S_{in}(k', \theta)}{C} (\cos \theta, \sin \theta) dk' d\theta, \right| \quad (2.110)$$

where the sheltering coefficient $|s_u| \sim 1$ can be used to tune the stresses at high winds, which would be largely overestimated for $s_u = 0$. For $s_u > 0$ this sheltering is also applied within the diagnostic tail in eq. (2.104), which requires the estimation of a 3-dimensional look-up table for the high frequency stress, the third parameter being the energy level of the tail.

The swell dissipation parameterization of [Ardhuin et al. \(2009a\)](#) is activated by setting s_1 to a non-zero integer value, and is given by a combination of the viscous boundary layer value,

$$\mathcal{S}_{out,vis}(k, \theta) = -s_5 \frac{\rho_a}{\rho_w} \left\{ 2k\sqrt{2\nu\sigma} \right\} N(k, \theta), \quad (2.111)$$

with the turbulent boundary layer expression

$$\mathcal{S}_{out,tur}(k, \theta) = -\frac{\rho_a}{\rho_w} \left\{ 16f_e\sigma^2 u_{orb,s}/g \right\} N(k, \theta), \quad (2.112)$$

giving the full term

$$\mathcal{S}_{out}(k, \theta) = r_{vis}\mathcal{S}_{out,vis}(k, \theta) + r_{tur}\mathcal{S}_{out,tur}(k, \theta), \quad (2.113)$$

where the two weights r_{vis} and r_{tur} are defined from a modified air-sea boundary layer significant Reynolds number $\text{Re} = 2u_{orb,s}H_s/\nu_a$

$$r_{vis} = 0.5(1 - \tanh((\text{Re} - \text{Re}_c)/s_7)), \quad (2.114)$$

$$r_{tur} = 0.5(1 + \tanh((\text{Re} - \text{Re}_c)/s_7)). \quad (2.115)$$

The significant surface orbital velocity is defined by

$$u_{orb,s} = 2 \left[\iint \sigma^3 N(k, \theta) dk d\theta \right]^{1/2}. \quad (2.116)$$

The first equation (2.111) is the linear viscous decay by Dore (1978), with ν_a the air viscosity and s_5 is an $O(1)$ tuning parameter. A few tests have indicated that a threshold $\text{Re}_c = 2 \times 10^5 \times (4 \text{ m}/H_s)^{(1-s_6)}$ provides reasonable result with $s_6 = 0$, although it may also be a function of the wind speed, and we have no explanation for the dependence on H_s . With $s_6 = 1$, a constant threshold close to 2×10^5 provides similar – but less accurate – results.

Eq. (2.112) is a parameterization for the nonlinear turbulent decay. When comparing model results to observations, it was found that the model tended to underestimate large swells and overestimate small swells, with regional biases. This defect is likely due, in part, to errors in the generation or non-linear evolution of these swells. However, it was chosen to adjust f_e as a function of the wind speed and direction,

$$f_e = s_1 f_{e,GM} + [|s_3| + s_2 \cos(\theta - \theta_u)] u_* / u_{\text{orb}}, \quad (2.117)$$

where $f_{e,GM}$ is the friction factor given by Grant and Madsen's (1979) theory for rough oscillatory boundary layers without a mean flow, using a roughness length adjusted to r_z times the roughness for the wind z_1 . The coefficient s_1 is an $O(1)$ tuning parameter, and the coefficients s_2 and s_3 are two other adjustable parameters for the effect of the wind on the oscillatory air-sea boundary layer. When $s_2 < 0$, wind opposing swells are more dissipated than following swells. Further, if $s_3 > 0$, \mathcal{S}_{out} is applied to the entire spectrum and not just the swell.

The dissipation term is parameterized from the wave spectrum saturation. Because the directional wave spectra were too narrow when using a saturation spectrum integrated over the full circle (Ardhuin and Boyer, 2006), the integration is restricted over a sector of half-width Δ_θ ,

$$B'(k, \theta) = \int_{\theta - \Delta_\theta}^{\theta + \Delta_\theta} \sigma k^3 \cos^{s_B}(\theta - \theta') N(k, \theta') d\theta'. \quad (2.118)$$

As a result, a sea state with two systems of same energy but opposite direction will typically produce less dissipation than a sea state with all the energy radiated in the same direction.

We finally define our dissipation term as the sum of the saturation-based

Par.	WWATCH var.	namelist	TEST471	TEST471f	TEST405	TEST500
z_u	ZWND	SIN4	10.0	10.0	10.0	10.0
α_0	ALPHA0	SIN4	0.0095	0.0095	0.0095	0.0095
β_{\max}	BETAMAX	SIN4	1.43	1.33	1.55	1.52
p_{in}	SINTHP	SIN4	2	2	2	2
z_α	ZALP	SIN4	0.006	0.006	0.006	0.006
s_u	TAUWSHELTER	SIN4	0.3	0.3	0.0	1.0
s_1	SWELLF	SIN4	0.66	0.66	0.8	0.8
s_2	SWELLF2	SIN4	-0.018	-0.018	-0.018	-0.018
s_3	SWELLF3	SIN4	0.022	0.022	0.015	0.015
Re_c	SWELLF4	SIN4	1.5×10^5	1.5×10^5	10^5	10^5
s_5	SWELLF5	SIN4	1.2	1.2	1.2	1.2
s_6	SWELLF6	SIN4	0.	0.	0.	0.
s_7	SWELLF7	SIN4	3.6×10^5	3.6×10^5	0.0	0.0
z_r	ZORAT	SIN4	0.04	0.04	0.04	0.04
$z_{0,\max}$	ZOMAX	SIN4	1.002	1.002	0.002	1.002

Table 2.6: Parameter values for TEST471, TEST471f, TEST405 and TEST500 source term parameterizations that can be reset via the SIN4 namelist. TEST471 generally provides the best results at global scale when using ECMWF winds, with the only serious problem being a low bias for $H_s > 8$ m. TEST451f corresponds to a retuning for CSFR wind reanalysis from NCEP/NCAR (Saha et al., 2010), and has almost no bias all the way to $H_s = 15$ m. Simulations and papers prepared before March 2012, used slightly different values, *e.g.* TEST441 and TEST441f can be recovered by setting SWELLF7 to 0, and TEST471 also used $s_u = 1$ and a few other adjustments (see manual of version 4.18). TEST405 is slightly superior for short fetches, and TEST500 is intermediate in terms of quality but it also includes depth-induced breaking in the same formulation, and thus may be more appropriate for depth-limited conditions. Please note that the name of the variables only apply to the namelists. In the source term module the names are slightly different, with a doubled first letter, in order to differentiate the variables from the pointers to these variables, and the SWELLFx are combined in one array SSWELLF. Bold values are different from the default values set by ww3_grid.

term and a cumulative breaking term $S_{\text{bk,cu}}$,

$$\begin{aligned} \mathcal{S}_{ds}(k, \theta) &= \sigma \frac{C_{\text{ds}}^{\text{sat}}}{B_r^2} \left[\delta_d \max \{B(k) - B_r, 0\}^2 \right. \\ &\quad \left. + (1 - \delta_d) \max \{B'(k, \theta) - B_r, 0\}^2 \right] N(k, \theta) \\ &\quad + \mathcal{S}_{\text{bk,cu}}(k, \theta) + \mathcal{S}_{\text{turb}}(k, \theta). \end{aligned} \quad (2.119)$$

where

$$B(k) = \max \{B'(k, \theta), \theta \in [0, 2\pi[\}. \quad (2.120)$$

The combination of an isotropic part (the term that multiplies δ_d) and a direction-dependent part (the term with $1 - \delta_d$) was intended to allow some control of the directional spread in resulting spectra.

The cumulative breaking term $\mathcal{S}_{\text{bk,cu}}$ represents the smoothing of the surface by big breakers with celerity C' that wipe out smaller waves of phase speed C . Due to uncertainties in the estimation of this effect in various observations, we use the theoretical model of [Ardhuin et al. \(2009b\)](#). Briefly, the relative velocity of the crests is the norm of the vector difference, $\Delta_C = |\mathbf{C} - \mathbf{C}'|$, and the dissipation rate of short wave is simply the rate of passage of the large breaker over short waves, i.e. the integral of $\Delta_C \Lambda(\mathbf{C}) d\mathbf{C}$, where $\Lambda(\mathbf{C}) d\mathbf{C}$ is the length of breaking crests per unit surface that have velocity components between C_x and $C_x + dC_x$, and between C_y and $C_y + dC_y$ ([Phillips, 1985](#)). Here Λ is inferred from breaking probabilities. Based on [Banner et al. \(2000, figure 6, \$b_T = 22\(\varepsilon - 0.055\)^2\$ \)](#), and taking their saturation parameter ε to be of the order of $1.6\sqrt{B'(k, \theta)}$, the breaking probability of dominant waves is approximately

$$P = 56.8 \left(\max \{ \sqrt{B'(k, \theta)} - \sqrt{B_r}, 0 \} \right)^2. \quad (2.121)$$

However, because they used a zero-crossing analysis, for a given wave scale, there are many times when waves are not counted because the record is dominated by another scale: in their analysis there is only one wave at any given time. This tends to overestimate the breaking probability by a factor of 2 ([Filipot et al., 2010](#)), compared to the present approach in which it is considered that several waves (of different scales) may be present at the same place and time. This effect is corrected simply dividing P by 2.

With this approach the spectral density of crest length (breaking or not) per unit surface $l(\mathbf{k})$ such that $\int l(\mathbf{k}) dk_x dk_y$, we take

$$l(\mathbf{k}) = 1/(2\pi^2 k), \quad (2.122)$$

and the spectral density of breaking crest length per unit surface is $\Lambda(\mathbf{k}) = l(\mathbf{k})P(\mathbf{k})$. Assuming that any breaking wave instantly dissipates all the energy of all waves with frequencies higher than a factor r_{cu} or more, the cumulative dissipation rate is simply given by the rate at which these shorter waves are taken over by larger breaking waves, times the spectral density, namely

$$\mathcal{S}_{\text{bk,cu}}(k, \theta) = -C_{\text{cu}}N(k, \theta) \int_{f' < r_{\text{cu}}f} \Delta_C \Lambda(\mathbf{k}') d\mathbf{k}', \quad (2.123)$$

where r_{cu} defines the maximum ratio of the frequencies of long waves that will wipe out short waves. This gives the source term,

$$\begin{aligned} \mathcal{S}_{\text{bk,cu}}(k, \theta) &= \frac{-14.2C_{\text{cu}}}{\pi^2} N(k, \theta) \\ &\int_0^{r_{\text{cu}}^2 k} \int_0^{2\pi} \max \left\{ \sqrt{B(f', \theta')} - \sqrt{B_r}, 0 \right\}^2 d\theta' dk' \end{aligned} \quad (2.124)$$

We shall take $r_{\text{cu}} = 0.5$, and C_{cu} is a tuning coefficient expected to be of order 1, which also corrects for errors in the estimation of l .

Finally, the wave-turbulence interaction term of [Teixeira and Belcher \(2002\)](#) and [Ardhuin and Jenkins \(2006\)](#), is given by

$$\mathcal{S}_{\text{ds}}^{\text{TURB}}(k, \theta) = -2C_{\text{turb}}\sigma \cos(\theta_u - \theta) k \frac{\rho_a u_*^2}{g\rho_w} N(k, \theta). \quad (2.125)$$

The coefficient C_{turb} is of order 1 and can be used to adjust for ocean stratification and wave groupiness.

All relevant source term parameters can be set via the namelists SIN4 and SDS4 to yield parameterizations TEST441b, TEST405, both described by [Ardhuin et al. \(2010\)](#) or TEST500 described by [Filipot and Ardhuin \(2012\)](#) (see Tables 2.6 and 2.7). Please note that the DIA constant C has been slightly adjusted in TEST441b, $C = 2.5 \times 10^7$. TEST441f corresponds to a re-tuned wind input formulation when using NCEP/NCAR winds.

2.3.11 $S_{\text{in}} + S_{\text{ds}}$: Zieger et al. 2015

Switch:	ST6
Origination:	AUSWEX, Lake George
Provided by:	A. Babanin, I. Young, M. Donelan, E. Rogers, S. Zieger

Par.	WWATCH var.	namelist	TEST471	TEST451	TEST405	TEST500
p	WNMEANP	SDS4	0.5	0.5	0.5	0.5
p_{tail}	WNMEANPTAIL	SDS4	0.5	0.5	0.5	0.5
f_{FM}	FXFM3	SDS4	2.5	9.9	2.5	9.9
	SDSC1	SDS4	0	0	0	1.0
$C_{\text{ds}}^{\text{sat}}$	SDSC2	SDS4	-2.2×10^{-5}	-2.2×10^{-5}	-2.2×10^{-5}	0.0
$C_{\text{ds}}^{\text{BCK}}$	SDSBCK	SDS4	0	0	0	0.185
$C_{\text{ds}}^{\text{HCK}}$	SDSHCK	SDS4	0	0	1.5	1.5
$\Delta_{\text{ds}}^{\theta}$	SDSDTH	SDS4	80	80	80	80
B_r	SDSBR	SDS4	0.0009	0.0009	0.00085	0.0009
C_{cu}	SDSCUM	SDS4	-0.40344	-0.40344	0.0	-0.40344
s_{B}	SDSCOS	SDS4	2.0	2.0	0.0	2.0
B_0	SDSC4	SDS4	1.0	1.0	1.0	1.0
p^{sat}	SDSP	SDS4	2.0	2.0	2.0	2.0
C_{turb}	SDSC5	SDS4	0.0	0.0	0.0	0.0
δ_d	SDSC6	SDS4	0.3	0.3	0.3	0.3
C	NLPROP	SNL1	2.5×10^7	2.5×10^7	2.7×10^7	2.5×10^7

Table 2.7: Same as Table 2.6, for the SDS4 and SNL1 namelists. Bold values are different from the default values set by ww3_grid.

This version implements observation-based physics for deep-water source/sink terms. These include wind input source term, and sink terms due to negative wind input, whitecapping dissipation and wave-turbulence interactions (swell dissipation). The wind input and whitecapping dissipation source terms are based on measurements taken at Lake George, Australia; wave-turbulence dissipation on laboratory experiments and field observations of swell decay; negative input on laboratory testing. Constraint is imposed on the total wind energy input through the wind stress, known independently.

Wind input. Apart from first direct field measurements of the wind input under strong wind forcing, the Lake George experiment revealed a number of new physical features for wind-wave exchange, previously not accounted for: (i) full air-flow separation that leads to a relative reduction of wind input for conditions of strong winds/steep waves; (ii) dependence of the wave growth rate on wave steepness, which signifies nonlinear behavior of the wind-input source function; (iii) enhancement of input in the presence of wave breaking (Donelan et al., 2006; Babanin et al., 2007) (the last feature was not implemented in here). Following Rogers et al. (2012), this input source

term is formulated as

$$S_{in}(k, \theta) = \frac{\rho_a}{\rho_w} \sigma \gamma(k, \theta) N(k, \theta), \quad (2.126)$$

$$\gamma(k, \theta) = G \sqrt{B_n} W, \quad (2.127)$$

$$G = 2.8 - \left(1 + \tanh(10\sqrt{B_n}W - 11)\right), \quad (2.128)$$

$$B_n = A(k) N(k) \sigma k^3, \quad (2.129)$$

$$W = \left(\frac{U}{c} - 1\right)^2. \quad (2.130)$$

In (2.126)–(2.130) ρ_a and ρ_w are densities of air and water, respectively, U is wind speed, c refers to wave phase speed, σ is radian frequency and k is wavenumber. The spectral saturation (2.129), introduced by Phillips (1984), is a spectral measure of steepness ak . The omni-directional action density is obtained by integration over all directions: $N(k) = \int N(k, \theta) d\theta$. The inverse of the directional spectral narrowness $A(k)$ is defined as $A^{-1}(k) = \int_0^{2\pi} [N(k, \theta)/N_{\max}(k)] d\theta$, where $N_{\max}(k) = \max\{N(k, \theta)\}$, for all directions $\theta \in [0, 2\pi]$ (Babanin and Soloviev, 1987).

Donelan et al. (2006) parameterized the growth rate (2.127) in terms of winds 10 m above the mean surface. Wave models typically employ friction velocity $u_* = \tau/\rho_a$. Wind speed scaling $U = 28u_*$ is adopted from Snyder et al. (1981) and Komen et al. (1984) following equation (2.55).

$$W_1 = \max^2 \left\{ 0, \frac{U}{c} \cos(\theta - \theta_w) - 1 \right\}, \quad (2.131)$$

$$W_2 = \min^2 \left\{ 0, \frac{U}{c} \cos(\theta - \theta_w) - 1 \right\}. \quad (2.132)$$

The directional distribution of W is implemented as the sum of favorable winds (2.131) and adverse winds (2.132), so that they complement one another (i.e. $W = \{W_1 \cup W_2\}$, see *Negative Input* later this section):

$$W = W_1 - a_0 W_2. \quad (2.133)$$

Wind input constraint. One important part of the input is the calculation of the momentum flux from the atmosphere to the ocean, which must agree with the flux received by the waves. At the surface, the stress $\vec{\tau}$ can be written as the sum of the viscous and wave-supported stress: $\vec{\tau} = \vec{\tau}_v + \vec{\tau}_w$.

The wave-supported stress $\vec{\tau}_w$ is used as the principal constraint for the wind input and cannot exceed the total stress $\vec{\tau} \leq \vec{\tau}_{tot}$. Here the total stress is determined by the flux parameterization: $\vec{\tau}_{tot} = \rho_a u_* |u_*|$. The wave-supported stress τ_w can be calculated by integration over the wind-momentum-input function:

$$\vec{\tau}_w = \rho_w g \int_0^{2\pi} \int_0^{k_{max}} \frac{S_{in}(k', \theta)}{c} (\cos \theta, \sin \theta) dk' d\theta. \quad (2.134)$$

Computation of the wave-supported stress (2.134) includes the resolved part of the spectrum up to the highest discrete wavenumber k_{max} , as well as the stress supported by short waves. To account for the latter, an f^{-5} diagnostic tail is assumed beyond the highest frequency in the energy density spectrum. In order to satisfy the constraint and in the case of $\vec{\tau} > \vec{\tau}_{tot}$, a wavenumber dependent factor L is applied to reduce energy from the high frequency part of the spectrum: $S_{in}(k') = L(k') S_{in}(k')$ with

$$L(k') = \min \left\{ 1, \exp(\mu [1 - U/c]) \right\}. \quad (2.135)$$

The reduction (2.135) is a function of wind speed and phase speed and follows an exponential form designed to reduce energy from the discrete part of the spectrum. The strength of reduction is controlled by coefficient μ , which has a greater impact at high frequencies and only little impact on the energy-dominant part of the spectrum. The value of μ is dynamically calculated by iteration at each integration time step (Tsagareli et al., 2010).

The drag coefficient is given by

$$C_d \times 10^4 = 8.058 + 0.967U_{10} - 0.016U_{10}^2, \quad (2.136)$$

which was selected and implemented as switch **FLX4**. The parameterization was proposed by Hwang (2001) and accounts for saturation, and further decline for extreme winds, of the sea drag at wind speeds in excess of 30 m s^{-1} . To prevent u_* from dropping to zero at very strong winds ($U_{10} \geq 50.33 \text{ m s}^{-1}$) expression (2.136) was modified to yield $u_* = 2.026 \text{ m s}^{-1}$. *Important!* In ST6, bulk adjustment to any uniform bias in the wind input field is done in terms of the wind stress parameter u_* rather than U_{10} . In order to achieve that, the factor in expression $C_d \times 10^4$ on the left hand side of (2.136) was substituted with $C_d \times \text{FAC}$ and added as the **FLX4** namelist parameter **CDFAC** (see *Bulk Adjustment* at the end of this section). The viscous drag

coefficient,

$$C_v \times 10^3 = 1.1 - 0.05U_{10}, \quad (2.137)$$

was parameterized by Tsagareli et al. (2010) as a function of wind speed using data from Banner and Peirson (1998).

Negative Input. Apart from the positive input, ST6 also has a negative input term in order to attenuate growth of waves in those parts of wave spectrum where adverse component of the wind stress is present (2.131–2.132). The growth rate for adverse winds is negative (Donelan, 1999) and is applied after the constraint of the wave-supported stress τ_w is met. The value of a_0 (in 2.133) is a tuning parameter in the parameterization of the input and is adjustable through the SIN6 namelist parameter SINA0.

Whitecapping Dissipation. For dissipation due to wave breaking, the Lake George field study revealed a number of new features: (i) the threshold behavior of wave breaking (Babanin et al., 2001). The waves do not break unless they exceed a generic steepness in which case the wave breaking probability depends on the level of exceedence above this threshold steepness. For waves below the critical threshold, whitecapping dissipation is zero. (ii) the cumulative dissipative effect due to breaking and dissipation of short waves affected by longer waves (Donelan, 2001; Babanin and Young, 2005; Moon et al., 2006; Young and Babanin, 2006; Babanin et al., 2010), (iii) non-linear dissipation function at strong winds (Moon et al., 2006; Babanin et al., 2007), (iv) bimodal distribution of the directional spreading of the dissipation (Young and Babanin, 2006; Babanin et al., 2010) (the last feature was not implemented in ST6). Following Rogers et al. (2012), the whitecapping dissipation term is implemented as:

$$S_{ds}(k, \theta) = \left[T_1(k, \theta) + T_2(k, \theta) \right] N(k, \theta), \quad (2.138)$$

where T_1 is the inherent breaking term, expressed as the traditional function of wave spectrum, and T_2 , expressed as an integral of the wave spectrum below wavenumber k , accounts for the cumulative effect of short-wave breaking or dissipated due to longer waves at each frequency/wavenumber. The inherent breaking term T_1 is the only breaking-dissipation term if this frequency is at or below the spectral peak. Once the peak moves below this particular frequency, T_2 becomes active and progressively more important as the peak downshifts further.

The threshold spectral density F_T is calculated as

$$F_T(k) = \frac{\varepsilon_T}{A(k) k^3}, \quad (2.139)$$

where k is the wavenumber and with $\varepsilon_T = 0.035^2$ being an empirical constant (Babanin et al., 2007; Babanin, 2011).

$$F_T(k) = \frac{\varepsilon_T}{A(k) k^3}. \quad (2.140)$$

Let the level of exceedence above the critical threshold spectral density (at which stage wave breaking is predominant) be defined as $\Delta(k) = F(k) - F_T(k)$. Furthermore, let $\mathcal{F}(k)$ be a generic spectral density used for normalization, then the inherent breaking component can be calculated as

$$T_1(k) = a_1 A(k) \frac{\sigma}{2\pi} \left[\frac{\Delta(k)}{\mathcal{F}(k)} \right]^{p_1}. \quad (2.141)$$

The cumulative dissipation term is not local in frequency space and is based on an integral that grows towards higher frequencies, dominating at smaller scales:

$$T_2(k) = a_2 \int_0^k A(k) \frac{c_g}{2\pi} \left[\frac{\Delta(k)}{\mathcal{F}(k)} \right]^{p_2} dk. \quad (2.142)$$

The dissipation terms (2.141)–(2.142) depend on five parameters: a generic spectral density $\mathcal{F}(k)$ used for normalization, and four coefficients a_1 , a_2 , p_1 , and p_2 . The coefficients p_1 and p_2 control the strength of the normalized threshold spectral density $\Delta(k)/\mathcal{F}(k)$ of the dissipation terms. Namelist parameter **SDSET** changes between the spectral density $F(k)$ and threshold spectral density $F_T(k)$ for normalization in (2.141)–(2.142). According to Babanin et al. (2007) and Babanin (2009), the directional narrowness parameter is set to unity $A(k) \approx 1$ in Eqs. (2.140)–(2.142).

Rogers et al. (2012) calibrated the dissipation terms based on duration-limited academic tests. Calibration coefficients used in ST6 and listed in Table 2.8 differ somewhat from those of Rogers et al. (2012) mainly due to the fact that the wave-supported stress $\vec{\tau}_w$ is implemented in the form of vector components and the scaling model for wind speed is customizable in the wind input parameterization.

Parameter	WWATCH var.	namelist	vers. 4.18	vers. 5.16
F_T	SDSET	SDS6	T	T
a_1	SDSA1	SDS6	6.24E-7	3.74E-7
p_1	SDSP1	SDS6	4	4
a_2	SDSA2	SDS6	8.74E-6	5.24E-6
p_2	SDSP2	SDS6	4	4
a_0	SINA0	SIN6	0.04	0.09
b_1 is constant	CSTB1	SWL6	n/a	F
b_1, B_1	SWLB1	SWL6	0.25E-3	0.0032
FAC	CDFAC	FLX4	1.00E-4	1.00E-4
C	NLPROP	SNL1	3.00E7	3.00E7

Table 2.8: Summary of calibration parameters for ST6 source terms. Values tabulated represent default model settings. Abbreviation “n/a” indicates that the variable is not applicable in that release of the code.

Swell Dissipation. In the absence of wave breaking, other mechanisms of wave attenuation are present. Here, they are referred to as swell dissipation and parameterized in terms of the interaction of waves with oceanic turbulence (Babanin, 2011). This mechanism, however, remains active for the wind-generated waves too. Its contribution across the spectrum is small, if the spectrum is above the wave-breaking threshold, but it is dominant at the front face of the spectrum, or even at the peak in case of the full Pierson-Moscowitz development.

$$S_{swl}(k, \theta) = -\frac{2}{3} b_1 \sigma \sqrt{B_n} N(k, \theta). \quad (2.143)$$

By making coefficient b_1 in Eq. (2.143) dependent on steepness the large gradient in the spatial bias in wave height can be reduced:

$$b_1 = B_1 2\sqrt{E} k_p. \quad (2.144)$$

In Eq. (2.144), B_1 is a scaling coefficient, E is the total sea surface variance Eq. (2.23) and k_p is the peak wavenumber. Eq. (2.144) can be flagged through the SWL6 namelist parameter CSTB1. The value for the coefficient B_1 in Eq. (2.144) and/or b_1 in Eq. (2.143) is customizable through the SWL6 namelist parameter SWLB1 (see Table 2.8).

Bulk Adjustments. The source term ST6 has been calibrated with flux parameterization FLX4. Bulk adjustment to the wind field can be achieved by re-scaling the drag parameterization FLX4 through the FLX4 namelist parameter CDFAC=1.0E-4. This has a similar effect to tuning variable β_{max} in ST4 source term package, equations (2.99) and (2.104), which is customizable through namelist parameter BETAMAX (see section 2.3.9–2.3.10). Ardhuin et al. (2011a) and Rasche and Ardhuin (2013) listed different sets of values that allow us to adjust to different wind fields. When optimizing the wave model, it is recommended to only re-tune parameters a_0 , b_1 and FAC. Again, FAC can potentially eliminate a bias in the wind field, which typically changes with the selection of the reanalysis product. This reduction was tested for extreme wind conditions such as hurricanes (Zieger et al., 2015). In global hindcast, the coefficient for the negative input can be used to tune the bulk of wave height in scatter comparisons, whereas the scaling coefficient for swell dissipation primarily effect large sea states. When the discrete interaction approximation (DIA) is used to compute the four-wave interaction the default value for the proportionality constant changes to $C = 3.00 \cdot 10^7$.

Limitations of the code: In cases where the minimum time step for dynamical source term integration is much smaller than the overall time step (i.e. less than 1/15th) the model becomes unstable. The issue is known and will be removed in a future revision.

2.3.12 S_{ln} : Cavaleri and Malanotte-Rizzoli 1981

Switch:	LN1
Origination:	Pre-WAM
Provided by:	H. L. Tolman

A linear input source term is useful to allow for the consistent spin-up of a model from quiescent conditions, and to improve initial wave growth behavior. The parameterization of Cavaleri and Malanotte-Rizzoli (1981) is available in WAVEWATCH III, with a filter for low-frequency energy as introduced by Tolman (1992). The input term can be expressed as

$$\mathcal{S}_{lin}(k, \theta) = 80 \left(\frac{\rho_a}{\rho_w} \right)^2 g^{-2} k^{-1} \max[0, u_* \cos(\theta - \theta_w)]^4 G \quad , \quad (2.145)$$

where ρ_a and ρ_w are the densities of air and water, respectively, and where G is the filter function

$$G = \exp \left[- \left(\frac{f}{f_{filt}} \right)^{-4} \right] . \quad (2.146)$$

In Tolman (1992) the filter frequency f_{filt} was given as the Pierson-Moskowitz frequency f_{PM} , which in turn was estimated as in Eq. (2.61). In the present implementation, the filter can be related to both f_{PM} and the cut-off frequency of the prognostic part of the spectrum f_{hf} as defined in Eq. (2.17)

$$f_{filt} = \max [\alpha_{PM} f_{PM}, \alpha_{hf} f_{hf}] , \quad (2.147)$$

where the constants α_{PM} and α_{hf} are user-defined. Default values of these constants are set to $\alpha_{PM} = 1$ and $\alpha_{hf} = 0.5$. Addition of the dependency on f_{hf} assures consistent growth behavior at all fetches, without the possibility of low-frequency linear growth to dominate at extremely short fetches.

2.3.13 S_{bot} : JONSWAP bottom friction

Switch:	BT1
Origination:	JONSWAP experiment
Provided by:	H. L. Tolman

A simple parameterization of bottom friction is the empirical, linear JONSWAP parameterization (Hasselmann et al., 1973), as used in the WAM model (WAMDIG, 1988). Using the notation of Tolman (1991), this source term can be written as

$$\mathcal{S}_{bot}(k, \theta) = 2\Gamma \frac{n - 0.5}{gd} N(k, \theta) , \quad (2.148)$$

where Γ is an empirical constant, which is estimated as $\Gamma = -0.038 \text{ m}^2\text{s}^{-3}$ for swell (Hasselmann et al., 1973), and as $\Gamma = -0.067 \text{ m}^2\text{s}^{-3}$ for wind seas (Bouws and Komen, 1983). n is the ratio of phase velocity to group velocity given by (2.6). The default value for $\Gamma = -0.067$ can be redefined by the user by changing the SBT1 namelist parameter **GAMMA**.

2.3.14 S_{bot} : SHOWEX bottom friction

Switch:	BT4
Origination:	Crest model
Provided by:	F. Ardhuin

A more realistic parameterization for sandy bottoms is based on the eddy viscosity model by [Grant and Madsen \(1979\)](#) and a roughness parameterization that includes the formation of ripples and transition to sheet flow. The parameterization of [Tolman \(1994\)](#), was adjusted by [Ardhuin et al. \(2003\)](#) to field measurements from the DUCK'94 and SHOWEX experiments on the North Carolina continental shelf. The parameterization has been adapted to WAVEWATCH III by also including a sub-grid parameterization for the variability of the water depth, as given by [Tolman \(1995b\)](#). This parameterization is activated by the switch BT4.

The source term can be written as

$$S_{bot}(k, \theta) = -f_e u_b \frac{\sigma^2}{2g \sinh^2(kd)} N(k, \theta), \quad (2.149)$$

where f_e is a dissipation factor that is a function of the r.m.s. bottom orbital displacement amplitude a_b and the Nikuradse roughness length k_N , and u_b is the r.m.s. of the bottom orbital velocity.

The present bed roughness parameterization (2.150)–(2.156) contains seven empirical coefficients listed in Table 2.9.

The roughness k_N is decomposed in a ripple roughness k_r and a sheet flow roughness k_s ,

$$k_r = a_b \times A_1 \left(\frac{\psi}{\psi_c} \right)^{A_2}, \quad (2.150)$$

$$k_s = 0.57 \frac{u_b^{2.8}}{[g(s-1)]^{1.4}} \frac{a_b^{-0.4}}{(2\pi)^2}. \quad (2.151)$$

In Eqs. (2.150) and (2.151) A_1 and A_2 are empirical constants, s is the sediment specific density, ψ is the Shields number determined from u_b and the median sand grain diameter D_{50} ,

$$\psi = f'_w u_b^2 / [g(s-1) D_{50}], \quad (2.152)$$

Par.	WWATCH var.	namelist	SHOWEX	Tolman (1994)
A_1	RIPFAC1	BT4	0.4	1.5
A_2	RIPFAC2	BT4	-2.5	-2.5
A_3	RIPFAC3	BT4	1.2	1.2
A_4	RIPFAC4	BT4	0.05	0.0
σ_d	SIGDEPTH	BT4	0.05	user-defined
A_5	BOTROUGHMIN	BT4	0.01	0.0
A_6	BOTROUGHFAC	BT4	1.00	0.0

Table 2.9: Parameter values for the SHOWEX bottom friction (default values) and the original parameter values used by Tolman (1994). Source term parameters can be modified via the BT4 namelist. Please note that the name of the variables only apply to the namelists. In the source term module the seven variables are contained in the array SBTCX.

with f'_w the friction factor of sand grains (determined in the same way as f_e with D_{50} instead of k_r as the bottom roughness), and ψ_c is the critical Shields number for the initiation of sediment motion under sinusoidal waves on a flat bed. We use an analytical fit (Soulsby, 1997)

$$\psi_c = \frac{0.3}{1 + 1.2D_*} + 0.055 [1 - \exp(-0.02D_*)], \quad (2.153)$$

$$D_* = D_{50} \left[\frac{g(s-1)}{\nu^2} \right]^{1/3}, \quad (2.154)$$

where ν is the kinematic viscosity of water.

When the wave motion is not strong enough to generate vortex ripples, i.e. for values of the Shields number less than a threshold ψ_{tr} , k_N is given by a relic ripple roughness k_{tr} . The threshold is

$$\psi_{\text{tr}} = A_3 \psi_c. \quad (2.155)$$

Below this threshold, k_N is given by

$$k_{\text{tr}} = \max \{A_5 m, A_6 D_{50}, A_4 a_b\} \text{ for } \psi < \psi_{\text{tr}}. \quad (2.156)$$

2.3.15 S_{mud} : Dissipation by viscous mud (D&L)

Switch:	BT8
Origination:	NRL/SWAN
Provided by:	M. Orzech and E. Rogers

Two formulations for wave damping by viscous fluid mud have been implemented in WAVEWATCH III based on earlier implementations in a SWAN code at NRL. As with wave damping by ice (Sect. 2.4.1), both rely on the concept of complex wave number (Eq. (2.176)). Both treat the mud layer as a viscous fluid, and both assume that the mud depth is comparable to its Stokes' boundary layer thickness. The first formulation (Dalrymple and Liu (1978); hereafter D&L) is a numerical solution. The second formulation (Ng (2000); hereafter Ng) is an analytical, asymptotic solution, so calculations tend to be much faster than with D&L. For the range of mud characteristics used by Rogers and Holland (2009), which are based on field measurements (and estimates), the methods produce very similar results.

In each case, the mud-induced dissipation is added to contributions from other source/sink terms in Eq. (2.8).

$$S_{mud} = 2k_i C_{g,mud}, \quad (2.157)$$

where $k_i = \text{imag}(k_{mud})$ and $C_{g,mud}$ is the mud-modified wave group velocity.

The above follows from exponential decay of a single wave train with initial amplitude a_0 :

$$a = a_0 e^{-k_i x}. \quad (2.158)$$

Both methods operate by solving for a modified dispersion relation, where the wavenumber being solved for, k_{mud} , is a complex number. The D&L method uses an iterative procedure for this dispersion relation. For details, see Section 2 and Appendix B of Dalrymple and Liu (1978). Descriptions specific to BT9 (Ng) are given in the following section.

To activate viscous mud effects with the (D&L) routines, the user specifies BT8 in the switch parameter file.

In the case where any of the new ice and mud source functions are activated with the switches IC1, IC2, IC3, BT8, or BT9, `ww3_shel` will anticipate instructions for 8 new fields (5 for ice, then 3 for mud). These are given prior to the “water levels” information. The new fields can also be specified as

homogeneous field using `ww3_shel.inp`. The mud parameters are mud density (kg/m^3), mud thickness (m), and mud viscosity (m^2/s), in that order.

The user is referred to the regression tests `ww3_tbt1.1` `ww3_tbt2.1` for examples of how to use the new mud source functions.

Limitations of the code: In the case of `ww3_multi`, the interface for the necessary mud and ice forcing fields has only been implemented when using the namelist type of input file. In the case of mud, though the k_r is calculated, its effect is not passed back to the main program. The only effect is via k_i (dissipation). Full implementation of k_r , already possible with IC3, and will be available in a future version of the model.

Limitations of the physics: 1) Both models (BT8, BT9) neglect elasticity in the mud layer. 2) Non-Newtonian response of the mud (e.g. as a thixotropic fluid) is not available. 3) Mud thickness should be interpreted not as the total mud thickness, but rather as the thickness of the fluidized mud layer. This value is notoriously difficult to determine in practice (Rogers and Holland (2009)). Fortunately, since WAVEWATCH III supports nonstationary and non-uniform input for the mud parameters, it is possible to address items (2) and (3) via coupling with a numerical model of the mud layer: no additional changes to the WAVEWATCH III code are required for this.

2.3.16 S_{mud} : Dissipation by viscous mud (Ng)

Switch:	BT9
Origination:	NRL/SWAN
Provided by:	M. Orzech and E. Rogers

To activate viscous mud effects with the Ng routines, the user specifies BT9 in the switch parameter file. The Ng method computes k_i as:

$$k_i \approx D_{mud} \equiv \frac{\delta_m (B'_r + B'_i) k_1^2}{\sinh 2k_1 d + 2k_1 d}, \quad (2.159)$$

Here, δ_m is the Stokes boundary layer thickness for mud, d is water depth, and k_1 is leading order term of the real part of the mud-modified wave number k_{mud} , respectively, in a Taylor expansion about the mud-water interface, and D_{mud} is the leading order term in the full expansion of k_i . B' is a complex coefficient affecting the depth profile of the velocities. For additional details, see Section 2.3.15 and Ng (2000).

2.3.17 S_{ab} : Battjes and Janssen 1978

Switch:	DB1 / MLIM
Origination:	Pre-WAM
Provided by:	J. H. G. M. Alves

The implementation in WAVEWATCH III of depth-induced breaking algorithms is intended to extend the applicability of the model to within shallow water environments, where wave breaking, among other depth-induced transformation processes, becomes important.

For this reason the approach of [Battjes and Janssen \(1978\)](#), henceforth denoted as BJ78), which is based on the assumption that all waves in a random field exceeding a threshold height, defined as a function of bottom topography parameters, will break. For a random wave field, the fraction of waves satisfying this criterion is determined by a statistical description of surf-zone wave heights (i.e., a Rayleigh-type distribution, truncated at a depth-dependent wave-height maximum).

The bulk rate δ of spectral energy density dissipation of the fraction of breaking waves, as proposed by BJ78, is estimated using an analogy with dissipation in turbulent bores as

$$\delta = 0.25 Q_b f_m H_{\max}^2, \quad (2.160)$$

where Q_b is the fraction of breaking waves in the random field, f_m is the mean frequency and H_{\max} is the maximum individual height a component in the random wave field can reach without breaking (conversely, above which all waves would break). In BJ78 the maximum wave height H_{\max} is defined using a Miche-type criterion ([Miche, 1944](#)),

$$\bar{k}H_{\max} = \gamma_M \tanh(\bar{k}d), \quad (2.161)$$

where γ_M is a constant factor. This approach also removes energy in deep-water waves exceeding a limiting steepness. This can potentially result in double counting of dissipation in deep-water waves. Alternatively, H_{\max} can be defined using a McCowan-type criterion, which consists of simple constant ratio

$$H_{\max} = \gamma d, \quad (2.162)$$

where d is the local water depth and γ is a constant derived from field and laboratory observation of breaking waves. This approach will exclusively represent depth-induced breaking. Although more general breaking criteria for H_{\max} as a simple function of local depth exist (e.g., Thornton and Guza, 1983), it should be noted that the coefficient γ refers to the maximum height of an individual breaking wave within the random field. McCowan (1894) calculated the limiting wave-height-to-depth ratio for a solitary wave propagating on a flat bottom to be 0.78, which is still used presently as a conservative criteria in engineering applications. The average value found by Battjes and Janssen (1978) was $\gamma = 0.73$. More recent analyses of waves propagating over reefs by Nelson (1994, 1997) suggest a ratio of 0.55.

The fraction of breaking waves Q_b is determined in terms of a Rayleigh-type distribution truncated at H_{\max} (i.e., all broken waves have a height equal to H_{\max}), which results in the following expression:

$$\frac{1 - Q_b}{-\ln Q_b} = \left(\frac{H_{rms}}{H_{\max}} \right)^2, \quad (2.163)$$

where H_{rms} is the root-mean-square wave height. In the current implementation, the implicit equation (2.163) is solved for Q_b iteratively. With the assumption that the total spectral energy dissipation δ is distributed over the entire spectrum so that it does not change the spectral shape (Eldeberky and Battjes, 1996) the following depth-induced breaking dissipation source function is obtained

$$\mathcal{S}_{db}(k, \theta) = -\alpha \frac{\delta}{E} F(k, \theta) = -0.25 \alpha Q_b f_m \frac{H_{\max}^2}{E} F(k, \theta), \quad (2.164)$$

where E is the total spectral energy, and $\alpha = 1.0$ is a tunable parameter. The user can select between Eqs. (2.161) and (2.162), and adjust γ and α . Defaults are Eq. (2.162), $\gamma = 0.73$ and $\alpha = 1.0$.

2.3.18 S_{tr} : Triad nonlinear interactions (LTA)

Switch:	TR1
Origination:	SWAN
Provided by:	A. Van der Westhuysen

Nonlinear triad interactions are modelled using the LTA model of (Eldeberky, 1996). This stochastic model is based on the Boussinesq-type deterministic equations of (Madsen and Sorensen, 1993). These deterministic equations are ensemble averaged, and the hierarchy of spatial evolution equations truncated by a zero-fourth-order-cumulant assumption, yielding a set of equations for the spectral and bispectral evolution in one-dimension. The bispectrum appearing in the spectral evolution equation is split up into a biamplitude and a biphas. The biphas corresponding to the self interaction of the peak frequency σ_p is parameterised as a function of the local Ursell number by

$$\beta(\sigma_p, \sigma_p) = -\frac{\pi}{2} + \frac{\pi}{2} \tanh\left(\frac{0.2}{Ur}\right), \quad (2.165)$$

in which the spectrally based Ursell number Ur is given by

$$Ur = \frac{g}{8\sqrt{2}\pi^2} \frac{H_s T_{m01}^2}{d^2}. \quad (2.166)$$

The biamplitude is obtained by spatially integrating the evolution equation for the bispectrum, by which the biamplitude is rendered a spatially local function. This results in an expression for the biamplitude which has a spatially slowly-varying component and a fast-oscillating component, of which the latter is neglected. Using the derived expressions for the biphas and biamplitude, the spectral evolution equation (a one-equation model) can be solved. To reduce the computational cost even further, the complete set of all interacting triads are represented by only the set of *self sum interactions*, that is, triads in which a component of frequency σ interacts with a component of the same frequency to exchange energy flux with a component of frequency $\sigma + \sigma = 2\sigma$. The final expression for the effect of triad interactions on a component with frequency σ is made up of two contributions—one adding energy flux to σ (transferred flux arriving from $1/2\sigma$) and one subtracting energy flux from σ (transfer going to 2σ). The expression implemented, adapted for radian frequencies, reads:

$$S_{nl3}(\sigma, \theta) = S_{nl3}^-(\sigma, \theta) + S_{nl3}^+(\sigma, \theta), \quad (2.167)$$

with

$$S_{nl3}^+(\sigma, \theta) = \max[0, \alpha_{EB} 2\pi c c_g J^2 |\sin \beta| \{E^2(\sigma/2, \theta) - 2E(\sigma/2, \theta)E(\sigma, \theta)\}], \quad (2.168)$$

and

$$S_{\text{nl}3}^-(\sigma, \theta) = -2S_{\text{nl}3}^+(2\sigma, \theta) . \quad (2.169)$$

Because of a Jacobian in the transfer of the energy flux from σ to 2σ , the flux density arriving at 2σ is half that leaving σ (hence the factor 2 appearing in Eq. (2.169)). The interaction coefficient J , describing self interaction in the nonlinearity range $0 \leq Ur \leq 1$, is given by (Madsen and Sorensen, 1993):

$$J = \frac{k_{\sigma/2}^2(gd + 2c_{\sigma/2}^2)}{k_{\sigma}d(gd + \frac{2}{15}gd^3k_{\sigma}^2 - \frac{2}{5}\sigma^2d^2)} . \quad (2.170)$$

The LTA formulation is implemented along each propagation direction of the directional spectrum, yielding an isotropic, directionally decoupled representation of triad interaction. The value of the proportionality coefficient is set at $\alpha_{\text{EB}} = 0.05$. The results produced by the LTA are furthermore quite sensitive to the choice of the frequency up to which the interactions are calculated, denoted here as $f_{\text{max},\text{EB}}$. (Eldeberky, 1995) recommends that the interactions be computed up to a frequency of 2.5 times the mean frequency ($f_{\text{max},\text{EB}} = 2.5f_{m01}$).

2.3.19 S_{bs} : Bottom scattering

Switch:	BS1
Origination:	CREST model
Provided by:	F. Ardhuin

Waves propagating over a sloping bottom are partially reflected. In the limit of small variation in water depth Δd with respect to the mean water depth d , the reflection coefficient is proportional to the bottom spectrum Kreisel (1949) and leads to a redistribution of wave energy in direction. This process may be formulated as a source term, which leads to accurate reflection coefficients when considering the evolution of the spectrum over scales larger than the bottom auto-correlation length, with reasonable accuracy up to $\Delta d/d \simeq 0.6$ (Ardhuin and Magne, 2007). The source term reads,

$$\mathcal{S}_{\text{bs}}(\mathbf{k}) = \frac{\pi}{2} \int_0^{2\pi} \frac{k'^2 M^2(\mathbf{k}, \mathbf{k}')}{\sigma \sigma' (k' C'_g + \mathbf{k} \cdot \mathbf{U})} F^B(\mathbf{k} - \mathbf{k}') [N(\mathbf{k}') - N(\mathbf{k})] d\theta', \quad (2.171)$$

with the coupling coefficient

$$M(\mathbf{k}, \mathbf{k}') \simeq M_b(\mathbf{k}, \mathbf{k}') = \frac{g\mathbf{k} \cdot \mathbf{k}'}{\cosh(kd) \cosh(k'd)} \quad (2.172)$$

where the effect of bottom-induced current and elevation changes are neglected, as appropriate for low to moderate current velocity relative to the intrinsic phase speed, i.e. $U/C < 0.3$. For larger Froude numbers, in particular in near-blocking conditions, the present implementation is not expected to be accurate. In Eq. (2.171), k and k' are related by the resonance condition, $\omega = \omega'$, i.e. $\sigma + \mathbf{k} \cdot \mathbf{U} = \sigma' + \mathbf{k}' \cdot \mathbf{U}$, where \mathbf{U} is the phase advection velocity (see, e.g., [WISE Group, 2007](#)).

The bottom spectrum $F^B(\mathbf{k})$ is specified in the file `bottom_spectrum.inp`. This spectrum may be determined from multi-beam bathymetric data. In the absence of detailed bathymetric data, the sand dune spectrum may be parameterized based on the work of [Hino \(1968\)](#). Recent observations generally confirm the earlier data on sand dune spectra ([Ardhuin and Magne, 2007](#)), with a non-dimensional constant spectrum for large k , i.e. $F^B(\mathbf{k}) \sim k^{-4}$.

The bottom spectrum is double-sided for simplicity of calculation and normalized such that the bottom variance (in square meters) is

$$\langle d^2 \rangle = \int_{-\infty}^{\infty} \int_{-\infty}^{\infty} F^B(k_x, k_y) dk_x dk_y. \quad (2.173)$$

In the present implementation this bottom spectrum is assumed to be the same at all grid points.

The source term is computed according to different methods depending on the value of the current. For zero current, the interactions only involves waves of the same frequency and the interaction is always the same and linear in terms of the directional spectrum. In this case the interaction is expressed as a matrix problem. Namely, the directional spectrum F is a vector of NTH components, and the source term is a vector of same size that is obtained by the matrix multiplication $S = MF$ with M a square (NTH,NTH) array. This array is a function of the bottom spectrum and the non-dimensional depth kd . This scattering matrix is precomputed and diagonalized as a preprocessing step for a finite number of wavenumber magnitudes ([Ardhuin and Herbers, 2002](#)). The cost of this preprocessing increases linearly with the number of discrete wavenumbers.

For non-zero current, the interaction pattern depends on the current magnitude and direction (magnitude only for an isotropic bottom spectrum), and

a precomputation of the scattering matrix would increase the overhead cost by at least one order of magnitude. In the present implementation, the interaction integration with non-zero current is recomputed at every source term call.

2.4 Source terms for wave-ice interactions

Wave-ice interaction processes have been the topic of many investigations. In general, wave-ice interactions require a description of the ice properties that usually include at least the ice concentration (fraction of ocean surface covered by ice), mean ice thickness, and maximum floe diameter. Indeed, the ice is often broken into pieces (the floes) that can have a wide variety of sizes, and these sizes strongly modify the dispersion and wave-ice interaction processes.

In the present version of WAVEWATCH III[®], the different options for treating the ice are the result of ongoing research effort and are not completely self-consistent. In particular, the forcing fields may take different meanings for different source terms. There are now 4 different version of dissipation processes activated with the switches IC1, IC2, IC3, and IC4 that can be combined with 2 different versions of scattering effects IS1 and IS2. The second scattering routine, because it was the only routine to use a maximum floe diameter, also contains an estimation of ice break-up and resulting maximum floe diameter and some dissipation due to creep.

At present it is not possible to combine dissipation parametrizations designed for frazil or pancake ice (IC3 or IC4) with a parametrization designed for the ice pack, such as IC2. Further, all parameterizations are not yet completely consistent: for example the floe size is not yet taken into account in some modified dispersion relations that take into account the ice, and the spatial variability of the ice properties, in particular the thickness, is generally not taken into account. As a result, the various ice effects have only been tested in very few real conditions (e.g. [Ardhuin et al., 2016](#)). We expect to have a more streamlined way of combining various processes in future versions of WAVEWATCH III[®], possibly using a maximum floe diameter to call one or the other routines.

In several source terms, a modified dispersion relation can be used. In particular IC2 and IS2 share the optional use of the [Liu and Mollo-Christensen](#)

(1988) dispersion relation for unbroken ice,

$$\sigma^2 = (gk_{ice} + Bk_{ice}^5) / \left(1 / \tanh(k_{ice}H) + \frac{\rho_{ice}hk_{ice}}{\rho_w} \right), \quad (2.174)$$

$$c_g = (g + (5 + 4k_{ice}M)Bk_{ice}^5) / (2\sigma(1 + k_{ice}M)^2). \quad (2.175)$$

B and M quantify the effects of, respectively, ice bending due to waves and ice inertia. The group velocity under the ice, derived from the same relation, is used in the module W3SIS2MD and computed in W3DISPMD. See Liu and Mollo-Christensen (1988) for details.

This equation is only solved when ICEDISP=TRUE in the MISC namelist. Otherwise, $k_{ice} = k$, just like in open water. Note that the effect of k_{ice} is limited to wave breaking and dissipation, and is not passed back to the main program.

2.4.1 S_{ice} : Damping by sea ice (simple)

Switch:	IC1
Origination:	WAVEWATCH III/NRL
Provided by:	E. Rogers and S. Zieger

Experimental routines for representation of the effect of ice on waves have been implemented using the switches IC1, IC2, and IC3. These effects can be presented in terms of a complex wavenumber

$$k = k_r + ik_i, \quad (2.176)$$

with the real part k_r representing impact of the sea ice on the physical wavelength and propagation speeds, producing effects analogous to shoaling and refraction by bathymetry, whereas the imaginary part of the complex wavenumber, k_i , is an exponential decay coefficient $k_i(x, y, t, \sigma)$ (depending on location, time and frequency, respectively), producing wave attenuation. The k_i is introduced as $S_{ice}/E = -2c_g k_i$, where S_{ice} is a source term (see also Komen et al. (1994), pg. 170).

The effect of sea ice on k_i is used for all three of the source functions (IC1, IC2, IC3). The effect of sea ice on k_r has been implemented for IC3, does not apply to IC1, and has not been implemented for IC2.

With the ice source functions, IC1, IC2, and IC3, ice concentration is not a required input, but if ice concentration has been read in, the source function will be scaled by ice concentration.

In the case of ice, up to five parameters are allowed. These can be referred to generically as $C_{ice,1}, C_{ice,2}, \dots, C_{ice,5}$. The meaning of the ice parameters will vary depending on which S_{ice} routine is selected.

In the case where any of the ice and mud source functions are activated with the switches IC1, IC2, IC3, BT8, or BT9, `ww3_shel` will anticipate intructions for 8 fields (5 for ice, then 3 for mud). These are given prior to the “water levels” information. The new fields can also be specified as homogeneous field using `ww3_shel.inp`.

The reader is referred to the regression tests `ww3_tic1.1-3` and `ww3_tic2.1` for examples of how to use the new ice source functions.

The first implemented method (IC1) is for the user to specify $k_i(x, t)$, which is uniform in frequency space, $C_{ice,1} = k_i$. The parameters $C_{ice,2}, \dots, C_{ice,5}$ are not used. An example setting is $C_{ice,1} = 2 \times 10^{-5}$. Descriptions specific to IC2 and IC3 are given in following sections.

Limitations of the code: The interface for the new mud and ice coefficients have only been implemented for `ww3_shel`. Interface for `ww3_multi` will be available in a future revision.

Limitations of the physics: The scattering of waves from sea ice is not considered via IC1, IC2, IC3. This is an important physical process (Wadhams, 1975), but since it is conservative, it should be treated separately from the source functions IC1, IC2, IC3, which are intended to represent non-conservative effects of sea ice. This work is in progress.

2.4.2 S_{ice} : Damping by sea ice (generalization of Liu et al.)

Switch:	IC2
Origination:	WAVEWATCH III/NRL
Provided by:	E. Rogers, S. Zieger, F. Ardhuin

This method for representing the dissipation of wave energy by wave-ice inter-

action is based on the papers by [Liu and Mollo-Christensen \(1988\)](#), [Liu et al. \(1991\)](#) and [Ardhuin et al. \(2015\)](#). The main input ice parameters is the ice thickness (in meters) that can vary spatially and temporally and is the forcing field $C_{ice,1}$.

This is a model for attenuation by a sea ice cover, derived on the assumption that dissipation is caused by friction in the boundary layer below the ice, with the ice modeled as a continuous thin elastic plate. The original form by [Liu and Mollo-Christensen \(1988\)](#) is activated by setting the IC2 namelist SIC2 parameter `IC2DISPER = .TRUE.`. That form assumes that the boundary layer is always laminar but it uses an eddy viscosity ν that can vary spatially and is the forcing field $C_{ice,2}$.

With IC2 and IC3, the sea ice effects requires solution of a new dispersion relation. For IC2, the key equations are:

$$\sigma^2 = (gk_r + Bk_r^5)/(\coth(k_r h_w) + k_r M), \quad (2.177)$$

$$c_g = (g + (5 + 4k_r M)Bk_r^5)/(2\sigma(1 + k_r M)^2), \quad (2.178)$$

$$\alpha = (\sqrt{\nu\sigma}k_r)/(c_g\sqrt{2}(1 + k_r M)). \quad (2.179)$$

In our notation, h_w is water depth and h_i is ice thickness. The variables B and M quantify the effects of the bending of the ice and inertia of the ice, respectively. Both of these variables depend on h_i (see [Liu and Mollo-Christensen, 1988](#); [Liu et al., 1991](#)).

In the case of IC2, though the k_r is calculated, its effect is not passed back to the main program. The only effect is via k_i (dissipation).

[Ardhuin et al. \(2015\)](#) distinguish between laminar and turbulent regimes, allowing this is activated by setting `IC2DISPER = .FALSE.`. In that case the dissipation goes from a laminar form using the molecular viscosity multiplied by an empirical adjustment factor `IC2VISC` to a turbulent form, amplified by a factor `IC2TURB`, for Reynolds numbers above a user-defined threshold `IC2REYNOLDS`. This transition is smoothed over a range `IC2SMOOTH` to take into account the random nature of the wave field. In the turbulent regime, the friction factor is estimated from a user-specified under-ice roughness length `IC2ROUGH`, expected to be of the order of 10^{-4} m. The parameter `IC2TURBS` is an ad hoc enhancement of turbulent dissipation in the Southern hemisphere that was introduced for test purposes to investigate sources of bias. This will be deprecated in future versions. It now appears that combining IC2 with

creep dissipation in IS2 can provide good results for dominant waves in both hemispheres.

2.4.3 S_{ice} : Damping by sea ice (Shen et al.)

Switch:	IC3
Origination:	Clarkson U. Fortran-77 code
Provided by:	E. Rogers, X. Zhao, S. Cheng, S. Zieger

The third method for representing wave-ice interaction is taken from Wang and Shen (2010). This model treats the ice as a visco-elastic layer. $C_{ice,1}$ is used for ice thickness (m); $C_{ice,2}$ is used for the viscosity ($\text{m}^2 \text{s}^{-1}$); $C_{ice,3}$ is used for density (kg m^{-3}); $C_{ice,4}$ is used for effective shear modulus (Pa); $C_{ice,5}$ is not used. An example setting is $C_{ice,1..4} = [0.1, 1.0, 917.0, 0.0]$.

In WAVEWATCH III version 4, this method of S_{ice} (IC3) was much more expensive than IC1 or IC2. This issue is largely addressed in model version 5.

The namelist SIC3 is introduced in model version 5. The namelist parameters are summarized in a list here, and some are discussed in further detail below.

IC3CHENG	Solution technique new in version 5. Default = TRUE.
IC3HILIM	Optional limiter on ice thickness. Default=100 (i.e. by default, the option is not used).
IC3KILIM	Optional limiter on dissipation rate k_i . Default=100 (i.e. by default, the option is not used).
USECGICE	When set to TRUE, the model will include the effect of ice on the group velocity. Default = FALSE.
IC3VISC	If user wishes to use an effective viscosity that is constant and uniform, this can now be done via namelist. Default=N/A.
IC3ELAS	As with IC3VISC, but for effective elasticity. Default=N/A.
IC3DENS	As with IC3VISC, but for ice density. Default=N/A.
IC3HICE	As with IC3VISC, but for ice thickness. Default=N/A.

IC3MAXCNC	Parameter which can be used to optionally switch to another dissipation for some ice conditions (see below). Default=100 (i.e. option is not used). Normal range is 0 to 1.
IC3MAXTHK	Idem. Default=100 (i.e. option is not used). Normal range is 0 to 10 meters.
IC2REYNOLDS	Parameter associated with IC2 non-dispersive turbulent boundary layer scheme. Default=1.5e+5.
IC2ROUGH	Idem. Default=0.02.
IC2SMOOTH	Idem. Default=7.0e+4.
IC2VISC	Idem. Default=2.0.
IC2TURB	Idem. Default=2.0.
IC2TURBS	Idem. Default=0.0.

The IC3CHENG option is new in model version 5. When set to `TRUE`, the model will use an alternative solution technique provided by S. Cheng. This has two important features. First, stability is improved, such that there is no need to use the ice limiter, i.e. the IC3HILIM parameter. Second, this method requires that three of four ice rheology parameters be stationary and uniform, input via namelist parameters (see below).

If IC3CHENG is set to `FALSE`, the user is advised to use the ice thickness limiter IC3HILIM to ensure stability (value of 25 to 100 cm is suggested). The parameter IC3KILIM was required for stable and fast computations in some prior development versions of WAVEWATCH III, but is now unnecessary and may be ignored by the user.

In model version 4.18, four ice rheology parameters (ice thickness, effective viscosity, effective elasticity, and ice density) were allowed to be non-stationary and non-uniform. This could be provided using `ww3_prep`. Or in cases where `ww3_shel` is used and non-uniform input is unnecessary, the “homogeneous” option of `ww3_shel` was available for rheology input. In model version 5, an option is added to specify the four ice rheology parameters via the namelist SIC3. Two restrictions apply: 1) If IC3CHENG is set to `FALSE` and USECGICE is set to `TRUE`, the namelist method cannot be used, and 2) If IC3CHENG is set to `TRUE`, the namelist method must be used for three of the rheology parameters (effective viscosity, effective elasticity, and ice density). If IC3CHENG is set to `TRUE` or USECGICE is set to `FALSE`, the fourth ice rheology parameter (ice thickness) can be input by either method (namelist or non-namelist). The model performs error checking to ensure that the user

has specified input for each parameter by a single method (neither method of input is assumed to supercede the other).

The k_r , modified by ice is incorporated into the governing equation (2.8) via the c_g (group velocity) and c (phase velocity) calculations on the left-hand side; e.g. Rogers and Holland (2009, and subsequent unpublished work). The modified wavenumber k_r produces effects analogous to shoaling and refraction by bathymetry. To activate the shoaling effect, the model should be operated with namelist variable `USECGICE = TRUE`. To activate the refraction effect, the model should be compiled with switch `REFRX`. With this switch, the model computes refraction based on spatial gradients in phase velocity that include ice effects, rather than the simpler wave dispersion relation without ice. These effects are demonstrated in the regression test `ww3_tic1.3` which is provided with the code.

The group velocity using `IC3CHENG` solver with zero ice thickness does not collapse exactly to that from the open water dispersion relation. [This is caused by numerical error in the calculation $c_g = \frac{\partial \sigma}{\partial k} = \frac{\Delta \sigma}{\Delta k}$. This calculation will be improved in a subsequent patch.] These small differences in group speed will result in slight shoaling and refraction errors if these effects are turned on. Error for ice thickness=zero was found to be less than 10% and was frequency dependent. This has been avoided by skipping the solver if ice thickness is exactly zero. If ice thickness is close to but not exactly zero, then the issue may persist. The solutions from `CHENG` for other parameters (effective viscosity, effective shear modulus) as they approach zero were not tested. Small but material difference have also noted between the solutions from `IC3CHENG` set to `FALSE` vs. `TRUE` for the same ice inputs.

As noted above, `USECGICE = TRUE` is required for the shoaling effect. However, since some ice rheology will lead to an increase in group velocity, the user is advised to be careful with this option. The group velocity affects the CFL criterion, which may require that the user reduce the time step size. `USECGICE = FALSE` is recommended for users that do not wish to worry about this issue.

In model version 5, a non-default option is added which causes the dissipation parameterization to change for some ice conditions. If ice concentration exceeds `IC3MAXCNC` and ice thickness exceeds `IC3MAXTHK`, the `IC2` dissipation (more specifically, the non-default, non-dispersive boundary layer scheme sub-option of `IC2`) is used in place of the dispersion-based dissipation estimate of Wang and Shen (2010). See description of `IC2` for more information. Since it is non-dispersive, this feature should not be used with `USECGICE =`

TRUE.

2.4.4 S_{ice} : Frequency-dependent damping by sea ice

Switch:	IC4
Origination:	WAVEWATCH III/NRL
Provided by:	C. Collins and E. Rogers

The fourth option (IC4) for damping of waves by sea ice gives methods to implement one of several simple, empirical/parametric forms for the dissipation of wave energy by sea ice. The motivation for IC4 is to provide a simple, flexible, and efficient source term which reproduces, albeit in a highly parameterized way, some basic physics of wave-ice interaction. The method is set by the integer value (presently 1 to 6) for IC4METHOD namelist parameter: 1) an exponential fit to the field data of [Wadhams et al. \(1988\)](#), 2) the polynomial fit in [Meylan et al. \(2014\)](#), 3) a quadratic fit to the calculations of [Kohout and Meylan \(2008\)](#) given in [Horvat and Tziperman \(2015\)](#), 4) Eq. 1 of [Kohout et al. \(2014\)](#), 5) a simple step function with up to 4 steps (may be nonstationary and non-uniform), and 6) a simple step function with up to 10 steps (must be stationary and uniform). All but the fourth method of IC4 feature frequency-dependent attenuation. With the fourth method, attenuation varies with waveheight but is uniform across the frequencies.

In the following discussion we use IC4M1 to denote IC4 method 1, and so forth. IC4 appears in the `switch` and namelist `IC4METHOD=1` (for example) appears in the file `ww3_grid.inp`. Whereas in IC1, $C_{ice,1}$ is the user-determined attenuation, for IC4M1, IC4M2, and IC4M4 $C_{ice,n}$ are constants of the equations. For IC4M3, $C_{ice,1}$ is ice thickness. For IC4M5, $C_{ice,n}$ controls the step function. Note that $C_{ice,n}$ may be provided by the user as non-stationary and non-uniform using methods analogous to methods used to input water levels.

IC4M1: an exponential equation was chosen to fit the data contained in table 2 of [Wadhams et al. \(1988\)](#) which results in preferential attenuation of high frequency waves. This parameterizes the well-known low-pass filtering effect of ice. The equation has the following form:

$$\alpha = \exp \left[\frac{-2\pi C_{ice,1}}{\sigma} - C_{ice,2} \right] \quad (2.180)$$

The values determined from the data are $C_{ice,1...2} = [0.18, 7.3]$ but these may be tweaked for attenuation of a qualitatively similar character.

IC4M2: [Meylan et al. \(2014\)](#) used a polynomial to fit their data. The additional physics parameterized here is the so-called roll-over effect where the attenuation levels off at the higher frequencies. The equation is the following:

$$\alpha = C_{ice,1} + C_{ice,2} \left[\frac{\sigma}{2\pi} \right] + C_{ice,3} \left[\frac{\sigma}{2\pi} \right]^2 + C_{ice,4} \left[\frac{\sigma}{2\pi} \right]^3 + C_{ice,5} \left[\frac{\sigma}{2\pi} \right]^4 \quad (2.181)$$

From [Meylan et al. \(2014\)](#), the suggested values for the coefficients are $C_{ice,1...5} = [0, 0, 2.12 \times 10^{-3}, 0, 4.59 \times 10^{-2}]$.

IC4M3: [Horvat and Tziperman \(2015\)](#) fit a quadratic equation to the attenuation coefficient calculated by [Kohout and Meylan \(2008\)](#) as a function of frequency, T , and ice thickness, h . Attenuation increases for thicker ice and higher frequencies (lower periods). The number of coefficients of the quadratic equation were prohibitively large to be user-determined, so the equation is hardwired in and the tunable parameter, $C_{ice,1}$, is ice thickness h . For reference, the equation is the following:

$$\ln \alpha(T, h) = -0.3203 + 2.058h - 0.9375T - 0.4269h^2 + 0.1566hT + 0.0006T^2 \quad (2.182)$$

Be advised, the equation itself was an extrapolation of the original range of h used to calculate the attenuation coefficients in [Kohout and Meylan \(2008\)](#) which was between 0.5 and 3 m, see [Horvat and Tziperman \(2015\)](#).

IC4M4: [Kohout et al. \(2014\)](#) found that attenuation was a function of significant wave height. Attenuation increased linearly with H_s until $H_s = 3m$ at which point attenuation is capped, thus:

$$\begin{cases} \alpha = C_{ice,1} \times H_s & \text{for } H_s \leq 3m \\ \alpha = C_{ice,2} & \text{for } H_s > 3m \end{cases} \quad (2.183)$$

The values given in [Kohout et al. \(2014\)](#) are $C_{ice,1...2} = [5.35 \times 10^{-6}, 16.05 \times 10^{-6}]$. See regression test `ww3_tic1.1/input_IC4/M4` for examples.

IC4M5: This is a simple step function with up to 4 steps. It is controlled by the optionally nonstationary and non-uniform parameters $C_{ice,1...7}$. Parameters $C_{ice,1...4}$ control the step levels, which are in terms of dissipation rate, k_i , in radians per meter. Parameters $C_{ice,5...7}$ control the step boundaries (given in Hz). See regression test `ww3_tic1.1/input_IC4/M5` for examples.

IC4M6: This is a simple step function with up to 10 steps. It is controlled by the stationary and uniform namelist parameters **IC4KI** and **IC4FC**. Array **IC4KI** controls the step levels, which are in terms of dissipation rate, k_i , in radians per meter. Array **IC4FC** controls the step boundaries (given in Hz). See regression test `ww3_tic1.1/input.IC4/M6` for examples.

2.4.5 S_{is} : Diffusive scattering by sea ice (simple)

Switch:	IS1
Origination:	WAVEWATCH III/NRL
Provided by:	S. Zieger

The non-conservative effect of ice on waves has been implemented in switches **IC1** through **IC3** (see Section 2.4.1–2.4.3). The conservative effect of sea ice has been implemented in switch **IS1** and represents a simple form of scattering. It is assumed that the floe size is smaller than the grid size and that a fraction α_{ice} of the incoming wave energy is scattered isotropically. The fraction is determined from sea ice concentration **ICE** using a simple linear transfer function

$$\alpha_{ice} = \max \{0, C_1 \text{ ICE} + C_2\} \quad . \quad (2.184)$$

The coefficients C_1 and C_2 are customizable through namelist **SIS1** with namelist parameters **ISC1** and **ISC2**. At each discrete frequency and direction the wave energy is reduced by the amount of α_{ice} and redistributed to all direction in the same discrete frequency to conserve energy.

2.4.6 S_{is} : Floe-size dependent scattering and dissipation

Switch:	IS2
Origination:	WAVEWATCH III
Provided by:	F. Ardhuin, C. Sevigny, G. Boutin, D. Dumont, T. Williams

The implementation of this scattering term generally follows the approach of [Meylan and Masson \(2006\)](#), to which has been added an estimation of the

breakup of the ice by waves to be able to update a maximum floe size diameter. Finally a creep-based dissipation was also combined with the scattering.

The scattering source term currently uses a back-scatter that is uniform in all directions, giving the action-conserving formulation,

$$\frac{S_{\text{is}}(k, \theta)}{\sigma} = \int_0^{2\pi} \beta_{\text{is,MIZ}} [s_{\text{scat}} N(k, \theta') - N(k, \theta)] d\theta'. \quad (2.185)$$

where s_{scat} is set to 1.0 by default but can be modified by `IS2BACKSCAT` in namelist `SIS2`.

The determination of scattering coefficients $\beta_{\text{is,MIZ}}$ is based on the theoretical reflection coefficient $\alpha_n(\sigma, h)$ for waves with a normal incidence going from a half-plane of open water to a half-plane of ice-covered water with a constant ice thickness h . Values of $\alpha_n(\sigma, h)$ as computed by [Kohout and Meylan \(2008\)](#) are tabulated in the `W3SIS2MD` module. Following [Dumont et al. \(2011\)](#), the broken ice is treated as a series of such ice-water interfaces. Neglecting multiple reflections, the scattering parameterization defines the attenuation per unit time as if the ice-covered part of a grid cell was a succession of floes of mean diameter D_m with a partial reflection $\alpha_n(\sigma, h)$ for each floe, giving,

$$\beta_{\text{is,MIZ}} = \text{ICE } c_g \alpha_n(\sigma, h) / D_m, \quad (2.186)$$

where `ICE` is the ice concentration.

The estimation of the mean floe diameter D_m is based on an assumed power law for the number of floes of diameter D , taken proportional to $D^{-\gamma}$. This power law is further assumed to apply for D ranging from the minimum D_{min} and a maximum D_{max} . The average is thus given by

$$D_m = \frac{\gamma}{\gamma - 1} \times \frac{D_{\text{max}}^{-\gamma+1} - D_{\text{min}}^{-\gamma+1}}{D_{\text{max}}^{-\gamma} - D_{\text{min}}^{-\gamma}}. \quad (2.187)$$

At present D_{min} is a user-supplied value. D_{max} can either be provided as a forcing field, e.g. from an ice model or some observations, or, if the namelist parameter `IS2BREAK` is set to `TRUE`, estimated from the breaking of the ice by the local wave field. If the namelist parameter `IS2DUPATE` is set to `TRUE`, small values of D_{max} will persist even if the waves become too small to be able to break the ice to that size. This is probably the proper model use

when external forcing/coupling is available (e.g. advection of ice properties in an ice model). On the contrary, if `IS2DUPDATE` is set to `FALSE`, the value of D_{\max} will be always adjusted to the local sea state, even if that means increasing D_{\max} .

Ice breaking by waves of wavelength λ is assumed to produce floes of diameter $\lambda/2$. In the parametrization, ice breaking occurs if the three following criteria are fulfilled (Williams et al., 2013):

1. $\lambda/2 \geq D_{\min}$ and $\lambda/2 \leq D_{\max}$
2. $D_{\max} > D_c$, as it exists a critical diameter, which depends on ice properties, below which no flexural failure is possible
3. $\varepsilon > \varepsilon_c$, the strain due to the incoming wave has to be greater than a defined critical strain

The first criterion is simply checking that the new value of D_{\max} will be larger than D_{\min} and smaller than the previous value of D_{\max} .

The second criterion relies on Mellor (1986), who defines D_c as

$$D_c = \left(\frac{\pi^4 Y^* h^3}{48 \rho g (1 - \nu^2)} \right)^{1/4}. \quad (2.188)$$

The third criterion corresponds to the flexural strain threshold. The horizontal strain caused by waves is related to the curvature of the ice layer, which, in one dimension is $\varepsilon = 0.5h\partial^2\eta_{ice}/\partial x^2$. The strain variance is given

$$\langle \varepsilon^2 \rangle = \left(\frac{h}{2} \right)^2 \int_{k_1}^{k_2} k_{ice}^4 F(k) dk, \quad (2.189)$$

where h is the ice thickness and k_{ice} is the wavenumber $2\pi/\lambda_{ice}$. Borrowing from wave breaking ideas (Banner et al., 2000), the integration of the curvature variance is limited around the local wavenumber k_{ice} . We also note that we have defined an effective minimum ice thickness h_{\min} so that, if $h < h_{\min}$, the strain variance is computed with $h = h_{\min}$ to avoid unbreakable elastic thin ice in the model that does not correspond to usual observations. We thus take D_{\max} to be half the wavelength of the shortest waves for which the following criterion is met

$$F_{break} \sqrt{\varepsilon^2} > \frac{\sigma_c}{Y^*}, \quad (2.190)$$

where σ_c is the ice flexural strength. F_{break} is a factor representing random waves and adjustable with the SIS2 namelist parameter `IS2BREAKF`. It should in theory depend on the duration for which the ice is forced by the waves, and, based on the typical maximum value over 500 Rayleigh-distributes waves, was taken to be $F_{break} = 3.6$. $F_{break} E_s$ is thus the maximum strain for random waves.

Creep dissipation was added in this routine, following [Wadhams \(1973\)](#), because it critically depends on the floe size. It assumes that the floes deformation is not fully elastic, and that the secondary creep under the wave-induced cyclic causes the dissipation of wave energy into heat. We use the ice flow law

$$\left(\frac{d\varepsilon}{dt}\right)_{ij} = \frac{\tau^2}{B^3} \sigma'_{i,j}, \quad (2.191)$$

B is the flow law constant and is a function of ice temperature. Using the normalized parameter estimated by [Cole et al. \(1998\)](#) from laboratory experiments, $A = 10^{11}$, and a uniform ice temperature of 270 K gives a value of $B = 10^7 \text{ s}^{1/3}$. The volumic dissipation rate is

$$\frac{de}{dt} = |\sigma_{xx}^4 / (2B)^3|. \quad (2.192)$$

Also, the cyclic deformation of the ice can require a much larger elastic energy than the gravity potential energy, but this is only true if the ice is not broken. As a result, working with a wave elevation spectrum $E(k)$ could introduce large changes in $E(k)$ when the ice is broken or reformed. Instead we prefer to work with an energy spectrum $RC_g E(k)/C_{g,ice}$, using the coefficient R introduced by [Wadhams \(1973\)](#), which is the ratio of elastic to gravity potential energies. For unbroken ice R is

$$R = 1 + C_R \frac{4Y^* h^3 \pi^4}{3\rho g \lambda^4 (1 - \nu^2)}, \quad (2.193)$$

where we have been careful that [Wadhams \(1973\)](#) used $2h$ for the ice thickness, and C_R is by default set to 1.0 using the namelist parameter `IS2BREAKE`, but it can be set to zero to work with the true elevation spectrum instead. This factor R is also applied in the calculation of ice breakup by the waves.

The creep dissipation is linearized as $S_{\text{creep}} = -\alpha_{\text{creep}} E_{\text{ice}}$. The coefficient α_{creep} was adapted from the [Wadhams \(1973\)](#) monochromatic formula and is equal to

$$\alpha_{\text{creep}} = 0.05 B h^5 \left(\frac{Y^*}{2B(1-\nu^2)} \right)^4 I_3 k^4 \frac{C_g^2}{\rho g C_{g_{\text{ice}}} R^2} F \int_{k_1}^{k_2} k_{\text{ice}}^4 E(k) dk, \quad (2.194)$$

where $I_3 = \frac{1}{\pi} \int_0^\pi \sin^4 \beta d\beta$. F_{broken} is a heuristic smooth transition from unbroken to broken ice, so that the dissipation gradually goes to zero for waves much longer than the floe sizes, because in that case the ice does not deform and produces no dissipation of wave energy,

$$F_{\text{broken}} = \tanh \left(\frac{D_{\text{max}} - C_\lambda \lambda_{\text{ice}}}{D_{\text{max}} C_{\text{smooth}}} \right). \quad (2.195)$$

Creep is computed after updating D_{max} . The two parameters in this smooth transition C_λ and C_{smooth} are set to 0.4 and 0.2 by the adjustable namelist parameters `IS2CREEPD` and `IS2CREEPC`.

Finally we recall the various model parameters used in IS2 in the following table. Some are defined as constants in the `W3IS2MD` module, others can be adjusted with the `SIS2` namelist.

Parameters	Symbol	namelist parameter	default values
Minimum floe size	D_{min}	N. A.	20 m
Initial floe size	D_{init}	N. A.	1000 m
Ice fragility	ξ	N. A.	0.9
Ice density	ρ_{ice}	N. A.	922.5 kg m ⁻³
Effective Young Modulus	Y^*	N. A.	5.49 GPa
Poisson Coefficient	ν	N. A.	0.3
Flexural strength	σ_c	N. A.	0.27 MPa
Flow law parameter	n	<code>IS2CREEPN</code>	3
Flow law parameter	B	<code>IS2CREEPB</code>	10 ⁷ s ^{1/3}
Correction for elastic energy	C_R	<code>IS2BREAKE</code>	1.0

2.4.7 S_{ref} : Energy reflection at shorelines and icebergs

Switch:	REF1
Origination:	WAVEWATCH III
Provided by:	F. Ardhuin

Reflections by shorelines and icebergs is activated by using the REF1 switch and setting namelist parameters REF1, REF1COAST, REF1SUBGRID or REF1BERG (in namelist REF1) to non-zero values that are the target reflection coefficients R_0^2 for the wave energy. If the IG1 switch is also used, then the energy source at the shoreline also includes free infragravity waves in both ingoing and outgoing directions. That particular source is described in section 2.4.8.

From these values R_0^2 may be varied with wave height and period following a Miche-type parameter: this is activated by setting REFFREQ to a non-zero value, and is based on the field measurements of Elgar et al. (1994). These coefficients can also be made to vary spatially, by setting REFMAP to a non-zero value. In that case ww3_grid will expect to find a extra line after the reading of the water depths and obstructions in ww3_grid.inp.

Wave reflection at the shoreline varies from a fraction of a percent to about 50% of the incoming wave energy, and may have important consequences for the directional wave spectrum, and the wave climate in otherwise sheltered locations (O'Reilly et al., 1999). Wave reflection is also extremely important for the generation of seismic noise by ocean waves.

Because reflection involve wave trains with different directions, in a model like WAVEWATCH III, their interaction can only be represented through a source term in the right hand side. Nevertheless, this is physically linked to propagation.

In practice, for the regular and curvilinear grids, the reflection source term puts into the reflected wave directions the proper amount of energy that will be taken away by propagation at the next time step. When neglecting the cross-shore current, this is

$$\mathcal{S}_{ref}(k, \theta) = \int R^2(k, \theta, \theta') \frac{C_g(k)}{\Delta A} [\cos(\theta - \theta_q) \Delta q + \sin(\theta - \theta_p) \Delta p] N(k, \theta') d\theta' , \quad (2.196)$$

where R^2 is an energy reflection coefficient, and Δp and Δq are the grid spacing along the two axes of the grid, and ΔA is the cell area. The definition of the shoreline direction from the land/sea mask is explained in Ardhuin et al. (2011b). This has not been tested for the SMC grids, and it is not expected to work for that type of grid.

In the case of unstructured grids, the spectral density of outgoing directions on the boundary is directly set to the expected reflected value and the boundary condition is handled specifically by the the numerical schemes.

The reflection coefficient R^2 is taken to be non-zero only for the directions for which $\cos(\theta - \theta') < 0$, and its magnitude is the product of a reflection coefficient $R_0^2(k)$, integrated over the scattered directions θ , and a directional distribution $R_2(\theta, \theta')$ around the specular direction θ_s ,

$$R^2(k, \theta, \theta') = R_0^2(k)R_2(\theta, \theta') \quad . \quad (2.197)$$

This directional distribution takes three forms:

- isotropic in all directions opposite to the incoming direction: this is for sub-grid islands and icebergs or sharp shoreline angles,
- proportional to $\cos(\theta - \theta_s)^2$ for moderate shoreline angles,
- proportional to $\cos(\theta - \theta_s)^n$ for small shoreline angles (nearly straight shoreline). Where $n = 4$ by default and can be changed to any value using the `REFCOSP_STRAIGHT` namelist parameter in the `REF1` namelist.

That parameterization is described in detail by [Ardhuin and Roland \(2012\)](#).

In the case of icebergs and sub-grid islands, the reflected energy is redistributed evenly in all directions within 90° of the direction opposite to the incoming waves. For resolved lands, a mean direction perpendicular to shore θ_n was defined from the land or sea status of the 8 grid points surrounding the local point (Fig. 2.1).

For each model grid point adjacent to land, the analysis of the land-sea geometry gives one value of θ_n among 16 possible directions. Together with any incoming wave direction θ_i this defines a specular reflection direction $\theta_r = 2\theta_n - \theta_i + \pi$. For each spectral component of direction θ_i going towards the coast (i.e. such that $\cos(\theta_i - \theta_n) > 0$), the total reflection is R^2 times the incoming energy. This reflected energy $R^2 E(f)M(f, \theta_i)$ is redistributed over directions around the specular reflection direction θ_r , with a broad distribution taken proportional to $\cos^n(\theta - \theta_r)$, where the power n is a function of the local shoreline geometry.

For this purpose we distinguish three different shoreline geometries relative to the local point as illustrated by Fig. 2.1: we set $n = 2$ for a straight coast (three connected land points among the neighbors), $n = 1$ for a mild corner (two land points among the neighbors), and $n = 0$ at a sharp corner (only one land point, among the 4 closest neighbors) which corresponds to the same treatment done for sub-grid islands and icebergs. Changing these values of n in the range 0 to 2 has little effect on our results. $n = 1$ corresponds to

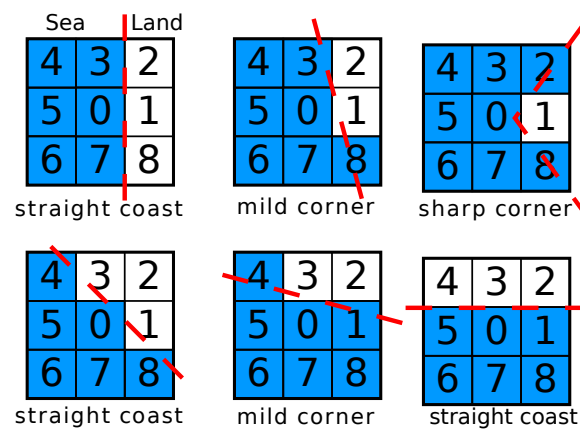


Figure 2.1: Examples of determination of the shoreline orientation and geometry using the land/sea mask. For any sea point (number 0) which is the ocean (in blue) and has at least one neighbor in land (in white) the eight neighbors, numbered from 1 to 8 are used to define the shoreline geometry. For ‘mild’ corners and straight coasts, the estimated shoreline orientation (dashed line) is used to compute the directional distribution of the reflected wave energy.

a Lambertian surface approximation, which is used for electromagnetic wave scattering from rough surfaces. A pure specular reflection would be obtained with n infinite. A more rigorous treatment should use the distribution of the shoreline orientation at the scale of the ocean wavelength, namely of the order of 100 m.

2.4.8 Second-order spectrum and free infragravity waves

Switch:	IG1
Origination:	WAVEWATCH III
Provided by:	F. Ardhuin

WARNING: A bug has been identified with IG wave sources in unstructured grids. A model patch using an older version of the code will be provided shortly.

The linear dispersion relation used in section 2.1 is a good approximation for most of the wave energy but a significant part of the spectrum at high frequencies, with typical frequencies above three times the windsea wave peak (e.g. Leckler, 2013). In shallow water, another strongly nonlinear part of the spectrum is found at very low frequencies, which are called infragravity waves.

In the case of horizontally homogeneous conditions over a flat bottom, both low and high frequency non-linear components can be estimated from the linear wave spectrum, using perturbation theory (e.g. Hasselmann, 1962). Also, the non-linear evolution of a homogeneous wave field is better described in terms of this ‘linearized spectrum’. It is thus practical to work with this ‘linearized spectrum’ and convert to the observable spectrum that contains non-linear components when post-processing the model results. One method to perform this transformation is a canonical transformation proposed by Krasitskii (1994). The properties of this transformation were further explored by Janssen (2009) and implemented for post-processing in the ECMWF version of the WAM model.

The code for the canonical transform written by P. Janssen was interfaced with WAVEWATCH III. Using the IG1 switch and setting the parameter IGADDOUTP = 2 in the SIG1 namelist, this canonical transformed, which conserves energy, will be used for the output point spectra. If IGADDOUTP =

1, then the second-order spectrum is added on top of the model spectrum using the theory (e.g. Hasselmann, 1962). That option does not conserve energy and is not consistent at high frequency because the quasi-linear term in the second-order spectrum are ignored (Janssen, 2009).

However, when comparing to measurements, one should be aware that different measuring devices have different responses to the nonlinear part of the spectrum. In particular surface-following buoys also linearize the spectrum, and the second-order pressure field is not related to the second-order elevation via the relations used for linear waves. The canonical transform is thus only applicable for wave gauges that measure elevation at a fixed location.

When the wave field is not homogeneous, the nonlinear properties of the waves lead to an exchange of energy between different modes. In shallow water this usually results in the transfer of energy to infragravity waves, that are released along shorelines and travel as free waves. The IG1 switch allows the parameterization of that effect with several methods. These are very crude parameterizations compared to the full hydrodynamic solution that would require solving the bispectral evolution across the surf zone at a very high spatial resolution (e.g. Herbers and Burton, 1997). The default namelist settings correspond to the parameterization presented by Ardhuin et al. (2014). In practice the free infragravity wave energy is added via the S_{ref} source term, by setting the SIG1 namelist IGSOURCE to 1 or 2.

In the first method, activated with IGSOURCE =1, the second-order spectrum is computed using either the Hasselmann perturbation (IGMETHOD = 1) or the canonical transform (any other value of IGMETHOD) as described in Janssen (2009). This approach may lead to better directional distribution of IG wave energy but it is still being tested. The second method, activated with IGSOURCE = 2, and the free IG spectrum is given by the following expressions,

$$A_{IG} = H_s T_{m0,-2}^2, \quad (2.198)$$

$$\widehat{E}_{IG}(f) = 1.2\alpha_1^2 \frac{kg^2}{c_g 2\pi f} \frac{(A_{IG}/4)^2}{\Delta_f} [\min(1., 0.015\text{Hz}/f)]^{1.5}, \quad (2.199)$$

$$\widehat{E}_{IG}(f, \theta) = \widehat{E}_{IG}(f)/(2\pi), \quad (2.200)$$

where the mean period is defined as $T_{m0,-2} = \sqrt{m_{-2}/m_0}$ with the moments

$$m_n = \int_{f_{min} \text{ Hz}}^{0.5 \text{ Hz}} E(f) f^n df, \quad (2.201)$$

and the empirical coefficient α_1 is of the order of 10^{-3} s^{-1} , and is set by the **SIG1** namelist parameter **IGEMPIRICAL**. The minimum frequency f_{min} used to define $T_{m0,-2}$ is set by the namelist parameter **IGMAXFREQ** and it is also the maximum frequency of the IG band over which this source of energy is applied. Also, in this band the IG energy at the coast can be added on top of pre-existing energy, or the pre-existing energy can be reset to zero. That latter behavior is the default and controlled by **IGBCOVERWRITE = 1**. For other choices, (**IGBCOVERWRITE = 0**), the results are very sensitive to the maximum shoreline reflection coefficient allowed (**REFRMAX** parameter in namelist **REF1**).

Finally, IG energy can also be added for frequencies beyond f_{min} , this is the default behavior and it is activated by setting **IGSWELLMAX = TRUE**. For that part of the IG wave field, the IG wave source is now reduced by a factor 4 which is now hard-coded in **w3ref1md.ftn**. This should be adjusted together with the maximum reflection which is defined by the **REF1** namelist parameter **REFRMAX**. In the present version, the option **IGSWELLMAX = TRUE** does not work well with unstructured grids. We thus advise to use **IGSWELLMAX = FALSE** for these grids, this will unfortunately lead to a spectral gap between the IG band and the swell-windsea band.

2.4.9 S_{xx} : User defined

Switch:	XXn
Origination:	—
Provided by:	user

This slot is intended for a source term that is not yet classified in Eq. (2.16). Almost by definition, it cannot be provided here.

2.5 Air-sea processes

2.5.1 General concepts

Additional subroutines are provided within WAVEWATCH III for use as part of coupled ocean-wave or ocean-atmosphere systems. These subroutines are designed to compute additional quantities related to the surface wave field which are intended to be passed to external models (e.g. ocean models). The motivation for these subroutines is to allow the external model to include the impact of waves on quantities such as the wind stress and the upper ocean turbulence.

Sea-state dependent air-sea fluxes The air-sea momentum flux, or the total wind stress, is the sum of the momentum flux into both surface waves and subsurface currents. Coupled atmosphere-ocean models that do not consider the impact of the surface gravity wave field typically compute the total wind stress based on an empirical relationship between the wind speed and the wind stress (via a drag coefficient, C_d). The provided *FLD* subroutines allows the computation of the total wind stress based on the WAVEWATCH III wavenumber-direction spectrum for use in coupled numerical models.

To the leading order, the total wind stress is equal to the sum of the momentum flux into surface waves (form drag of surface waves) and the momentum flux directly into the subsurface currents (through viscous stress). The momentum flux into the waves may be expressed as an integral of the wave variance spectrum multiplied by the wave growth rate (momentum-uptake rate). A few assumptions are needed to calculate the wave form drag. First, the wave form drag is sensitive at the leading order to the level of the high frequency waves (or the spectral tail). This part of the wave spectrum contains a great deal of uncertainty within the wave model, and therefore may need to be separately parameterized for computing the wind stress. An assumption must therefore be made to parameterize the high frequency, which is not constrained by observational data and wind speeds above 15 m/s. Second, assumptions of the wave growth-rate function are needed since it has historically been parameterized from either the wind speed or the wind stress. In either case, empirical coefficients are needed within the growth-rate function based on wavelength and wave direction relative to the wind and/or stress. Third, there is feedback due to the wave form drag on the turbulence

profile and the wind profile within the wave boundary layer (roughly the upper 10 meters above the air-sea interface). How important this feedback is on determining the wind stress and the mean wind profile is not entirely understood. Finally, the growth rate is known to be different over breaking and non-breaking waves. However, there are no simple methods for explicitly including the breaking wave impact within wind-stress calculation models. Therefore, no separation is made in either of the present *FLD* subroutines between breaking and non-breaking wave growth-rates.

The total air-sea momentum flux can be expressed (to the leading order) as:

$$\vec{\tau} = \vec{\tau}_\nu + \vec{\tau}_f, \quad (2.202)$$

where $\vec{\tau}_\nu$ is the viscous stress vector and $\vec{\tau}_f$ is the wave form drag. At the air-sea interface, the wave form drag can be computed as the contribution of the momentum flux into all waves:

$$\vec{\tau}_f = \rho_w \int_{k_{min}}^{k_{max}} \int_{-\pi}^{\pi} \beta_g(k, \theta) \sigma F(k, \theta) d\theta \vec{k} dk, \quad (2.203)$$

where ρ_w is the water density, k is the wavenumber, θ is the wave direction, σ is the angular frequency, $\beta_g(k, \theta)$ is the growth rate, $F(k, \theta)$ is the wave variance spectrum, and k_{min} and k_{max} are the minimum and maximum wavenumbers of contributing waves. The expression for the growth rate varies based on the theory applied in the model, and will be described separately for each theory in their following descriptions.

The spectral tail at wind speeds above 15 m/s is not well constrained observationally or theoretically. Therefore, the spectral tail level in the *FLD* subroutines has been empirically parameterized such that the mean drag coefficient corresponds to the standard bulk drag coefficient used within the modeling system. In this way, the mean value of the wind stress will not be modified by using any explicit sea state dependent wind stress formulation, but the stress will deviate from the mean based on the sea-state. It is assumed that the tail level is a function of a wind speed only and is independent of sea states.

2.5.2 Sea-state dependent τ : Reichl et al. 2014

Switch:	FLD1
Origination:	WAVEWATCH III
Provided by:	B. Reichl

Wind stress according to Reichl et al., 2014 In Reichl et al. (2014) the total stress is constant in height, but is decomposed into two components as a function of height as:

$$\vec{\tau} = \vec{\tau}_t(z) + \vec{\tau}_f(z), \quad (2.204)$$

where τ_t is the turbulent stress and is equal to the viscous stress very near the surface. The wave form stress can be expressed as:

$$\vec{\tau}_f(z) = \rho_w \int_{k_{min}}^{k=\delta/z} \int_{-\pi}^{\pi} \beta_g(k, \theta) \sigma F(k, \theta) d\theta \vec{k} dk, \quad (2.205)$$

that is, the wave form stress at height z is equal to the integration of the wave form stress at the surface for wavenumbers below $k = \delta/z$, where δ/k is the inner layer height (Hara and Belcher, 2004) for waves at a wavenumber k . This expression is derived by assuming that the wave-induced stress is significant from the surface up to the inner layer height, but is negligible further above. Since at the surface

$$\vec{\tau} = \vec{\tau}_\nu + \vec{\tau}_f(z=0) = \vec{\tau}_\nu + \rho_w \int_{k_{min}}^{k_{max}} \int_{-\pi}^{\pi} \beta_g(k, \theta) \sigma F(k, \theta) d\theta \vec{k} dk, \quad (2.206)$$

the turbulent stress at a height z can be expressed as:

$$\vec{\tau}_t(z) = \vec{\tau}_\nu + \rho_w \int_{k=\delta/z}^{k_{max}} \int_{-\pi}^{\pi} \beta_g(k, \theta) \sigma F(k, \theta) d\theta \vec{k} dk. \quad (2.207)$$

In this model it is assumed that the turbulent stress at the inner layer height $z = \delta/k$ determines the growth rate of waves at wavenumber k :

$$\beta_g(k, \theta) = c_\beta \sigma \frac{|\tau_t(z = \delta/k)|}{\rho_w c^2} \cos^2(\theta - \theta_\tau), \quad (2.208)$$

where θ_τ is the direction of the turbulent stress at the inner layer height. The turbulent stress at the inner layer height is used in place of the total wind stress because longer waves reduce the effective wind forcing on shorter waves (wave sheltering).

The growth rate coefficient c_β varies depending on the ratio of the wave phase speed to the local turbulent friction velocity (friction velocity at the inner layer height), $u_\star^l = \sqrt{\tau_t(z = \delta/k)/\rho_a}$.

$$c_\beta = \begin{cases} 25 & : \cos(\theta - \theta_w) > 0 & : c/u_\star^l < 10 \\ 10 + 15 \cos[\pi(c/u_\star - 10)/15] & : & : 10 \leq c/u_\star^l < 25 \\ -5 & : & : 25 \leq c/u_\star^l \\ -25 & : \cos(\theta - \theta_w) < 0 & \end{cases} \quad (2.209)$$

The wind profile is explicitly calculated using the energy conservation constraint in the wave boundary layer. From the top of the viscous sublayer to the inner layer height of the shortest waves the wind shear is expressed as:

$$\frac{d\vec{u}}{\partial z} = \frac{\rho_a}{\kappa z} \left| \frac{\vec{\tau}_\nu}{\rho_a} \right|^{3/2} \frac{\vec{\tau}_\nu}{\vec{\tau}_\nu \cdot \vec{\tau}_{tot}} \quad \text{for } z_\nu < z < \delta/k_l. \quad (2.210)$$

Between the inner layer height of the shortest waves and that of the longest waves the wind shear is expressed as:

$$\frac{d\vec{u}}{\partial z} = \left[\frac{\delta}{z^2} \tilde{F}_w \left(k = \frac{\delta}{z} \right) + \frac{\rho_a}{\kappa z} \left| \frac{\vec{\tau}_t(z)}{\rho_a} \right|^{3/2} \right] \times \frac{\vec{\tau}_t(z)}{\vec{\tau}_t(z) \cdot \vec{\tau}_{tot}} \quad \text{for } \delta/k_l \leq z, \quad (2.211)$$

where $\tilde{F}_w(k = \delta/z)$ is the energy uptake by surface waves:

$$\tilde{F}_w(k = \delta/z) = \rho_w \int_{-\pi}^{\pi} \beta_g(k, \theta) g F(k, \theta) k d\theta. \quad (2.212)$$

Finally, above the inner layer height of the longest waves the wave effect is negligible and the wind shear is aligned in the direction of the wind stress:

$$\frac{d\vec{u}}{dz} = \frac{u_\star}{\kappa z} \frac{\vec{\tau}_{tot}}{|\vec{\tau}_{tot}|}. \quad (2.213)$$

Note that when using the FLD1 switch, internal variables and output values of the viscous stress, friction velocity, surface roughness length and Charnock parameter are recalculated and overwritten.

2.5.3 Sea-state dependent τ : Donelan et al. 2012

Switch:	FLD2
Origination:	UMWM
Provided by:	B. Reichl

Wind stress according to Donelan et al., 2012 In Donelan et al. (2012) the growth rate parameter in Eq. (2.203) is expressed as:

$$\beta_g(k, \theta) = A_1 \sigma \frac{[u_{\lambda/2} \cos(\theta - \theta_w) - c] |u_{\lambda/2} \cos(\theta - \theta_w) - c| \rho_a}{c^2 \rho_w}, \quad (2.214)$$

$$A_1 = \begin{cases} 0.11, & : u_{\lambda/2} \cos \theta > c, & \text{for wind forced sea} \\ 0.01 & : 0 < u_{\lambda/2} \cos \theta < c, & \text{for swell faster than the wind} \\ 0.1 & : \cos \theta < 0, & \text{for swell opposing the wind} \end{cases} \quad (2.215)$$

where A_1 is the proportionality coefficient determined empirically (so that modeled wave spectra agree with field observations), $u_{\lambda/2}$ is the wind speed at the height of half the wavelength (up to 20 m), θ_w is the wind direction, and c is the wave phase speed. The wind speed is calculated using the law of the wall for rough surfaces:

$$u(z) = \frac{u_*}{\kappa} \ln \left(\frac{z}{z_0} \right), \quad (2.216)$$

where κ is the von Kármán coefficient (default 0.4). The viscous stress is calculated from the law of the wall for smooth surfaces. The viscous drag coefficient, Cd_ν is adjusted to account for sheltering:

$$Cd'_\nu = \frac{Cd_\nu}{3} \left(1 + \frac{2Cd_\nu}{Cd_\nu + Cd_f} \right), \quad (2.217)$$

where Cd_f is the wave form drag coefficient. The viscous stress can then be solved for as:

$$\vec{\tau}_\nu = \rho_a Cd'_\nu |\mathbf{u}_z| \mathbf{u}_z. \quad (2.218)$$

Note that when using the FLD2 switch, internal variables and output values of the viscous stress, friction velocity, surface roughness length and Charnock parameter are recalculated and overwritten.

	Group Name	Elements
I	Forcing Fields	10
II	Mean Wave Parameters	16
III	Spectrum Parameters	6
IV	Partitions Parameters	8
V	Atmosphere-Waves Layer	10
VI	Wave-Ocean Layer	11
VII	Wave-Bottom Layer	5
VIII	Spectrum parameters	6
IX	Numerical Diagnostics	5
X	User Defined	2

Table 2.10: Groups in new double-indexing output field structure.

2.6 Output parameters

The wave model provides output of gridded fields of mean wave parameters. Some of these parameters can also be found in the output for selected points. For activation of the output see Section 4.4.9

Since version 4.XX (...), WAVEWATCH III output fields are defined by a double-indexing structure, where the first index refers to a functional group that parameters belong to, and the second number is the index for a given parameter within its group. Groups are defined according to Table 2.10.

Below, a brief definition of output field parameters is provided. A table with definitions may be found in the sample `ww3_shel.inp` file, in Section 4.4.9. That input file also provides a list of flags indicating if output parameters are available in different field output file types (ASCII, grib, igrads, NetCDF).

Selection of field outputs in input files for a given output type, may be made in two ways. For F and T flags, this option is activated if the user adds F or T to the first line of the output field selection part for a given inp file. There are 10 groups of parameters the user can choose from (reflecting the internal double-index structure of the code itself). If the first flag of a group line is set to F then that group will not produce output, and a second line for parameter flags is not expected. If the group flag is set to T, then a second

group line is expected containing parameter flags. Examples of F/T flag use are given in Section 4.4.9. All parameters that are a function of frequency (e.g. **EF** or **USF**) require the setting of specific namelist parameters, in the OUTS namelist. This is to reduce the memory use if these parameters are not needed.

For namelists, the first line is set to N, and the next line contains parameter symbols. Examples are given in Section 4.4.11 and Section 4.4.14. The names for these namelists are the bold names below, for example **HS**.

All parameters listed below are available in ASCII and NetCDF output files. If selected output file types are grads or grib, some parameters may not be available. Availability (or not) is identified in the first two columns in the field output parameter table within the example input file in Section 4.4.9. That table also identifies, for all parameters, the internal WAVEWATCH III code tags, the output tags (names used is ASCII file extensions, NetCDF variable names and namelist-based selection (see also Section 4.4.14), and the long parameter name/definition.

I) Forcing fields

- 1) **DPT** The mean water depth (m). This includes varying water levels.
- 2) **CUR** The mean current velocity (vector, m/s).
- 3) **WND** The mean wind speed (vector, m/s). This wind speed is always the speed as input to the model, i.e., is not corrected for the current speed.
- 4) **AST** The air-sea temperature difference (°C).
- 5) **WLV** Water level.
- 6) **ICE** Ice concentration.
- 7) **IBG** Wave attenuation due to icebergs: this parameter is the inverse of the e-folding scale associated to the loss of wave energy in a field of small icebergs (Ardhuin et al., 2011b).
- 8) **D50** Sediment median grain size (D_{50}).
- 9) **IC1** Ice thickness.
- 10) **IC5** Ice flow diameter.

II) Standard mean wave parameters

- 1) **HS** Significant wave height (m) [see Eq. (2.23)]

$$H_s = 4\sqrt{E}. \quad (2.219)$$

- 2) **LM** Mean wave length (m) [see Eq. (2.22)]

$$L_m = 2\pi\overline{k^{-1}}. \quad (2.220)$$

- 3) **T02** Mean wave period (s) [see Eq. (2.22)]

$$T_{m02} = 2\pi/\sqrt{\overline{\sigma^2}}. \quad (2.221)$$

- 4) **T0M1** Mean wave period (s) [see Eq. (2.22)]

$$T_{m0,-1} = 2\pi\overline{\sigma^{-1}}. \quad (2.222)$$

- 5) **T01** Mean wave period (s) [see Eq. (2.22)]

$$T_{m0,1} = 2\pi\overline{\sigma}. \quad (2.223)$$

- 6) **FP** Peak frequency (Hz), calculated from the one-dimensional frequency spectrum using a parabolic fit around the discrete peak.

- 7) **DIR** Mean wave direction (degr., meteorological convention)

$$\theta_m = \text{atan}\left(\frac{b}{a}\right), \quad (2.224)$$

$$a = \int_0^{2\pi} \int_0^\infty \cos(\theta)F(\sigma, \theta) d\sigma d\theta, \quad (2.225)$$

$$b = \int_0^{2\pi} \int_0^\infty \sin(\theta)F(\sigma, \theta) d\sigma d\theta. \quad (2.226)$$

- 8) **SPR** Mean directional spread (degr.; Kuik et al., 1988)

$$\sigma_\theta = \left[2\left\{1 - \left(\frac{a^2 + b^2}{E^2}\right)^{1/2}\right\}\right]^{1/2}, \quad (2.227)$$

- 9) **DP** Peak direction (degr.), defined like the mean direction, using the frequency/wavenumber bin containing of the spectrum $F(k)$ that contains the peak frequency only.

- 10) **HIG** Infragravity height.

- 11) **MXE** Max surface elev (Space-time extreme, STE)

- 12) **MXES** St Dev of max surface elev (STE)

- 13) **MXH** Max wave height (STE)

- 14) **MXHC** Max wave height from crest (STE)
- 15) **SDMH** St Dev of MXC (STE)
- 16) **SDMHC** St Dev of MXHC (STE)

III) Spectral parameters (first 5 moments and wavenumbers).

All these parameters are a function of frequency and thus these are three-dimensional arrays. Because of the large memory use, the computation of these parameters requires the activation of switches in the OUTS namelist.

- 1) **EF** Wave frequency spectrum (m^2/Hz)

$$E(f) = 2\pi \int F(\sigma, \theta) d\theta . \quad (2.228)$$

- 2) **TH1M** Mean direction for each frequency (degr.; [Kuik et al., 1988](#))

$$\theta_1(f) = \text{atan} \left(\frac{b_1(f)}{a_1(f)} \right) , \quad (2.229)$$

$$a_1(f) = 2\pi \int_0^{2\pi} \int_0^\infty \cos(\theta) F(\sigma, \theta) d\theta , \quad (2.230)$$

$$b_1(f) = 2\pi \int_0^{2\pi} \int_0^\infty \sin(\theta) F(\sigma, \theta) d\theta . \quad (2.231)$$

- 3) **STH1M** First directional spread for each frequency (degr.;)

$$\sigma_1(f) = \left[2 \left\{ 1 - \left(\frac{a_1(f)^2 + b_1(f)^2}{E(f)^2} \right)^{1/2} \right\} \right]^{1/2} , \quad (2.232)$$

- 4) **TH2M** Mean direction from a_2 and b_2 (degr.)

$$\theta_2(f) = \text{atan} \left(\frac{b_2(f)}{a_2(f)} \right) , \quad (2.233)$$

$$a_2(f) = 2\pi \int_0^{2\pi} \int_0^\infty \cos(2\theta) F(\sigma, \theta) d\theta , \quad (2.234)$$

$$b_2(f) = 2\pi \int_0^{2\pi} \int_0^\infty \sin(2\theta) F(\sigma, \theta) d\theta . \quad (2.235)$$

- 5) **STH2M** Directional spreading from a_2 and b_2 (degr.)

$$\sigma_2(f) = \left[0.5 \left\{ 1 - \left(\frac{a_2(f)^2 + b_2(f)^2}{E(f)^2} \right)^{1/2} \right\} \right]^{1/2}, \quad (2.236)$$

- 6) **WN** Wavenumbers $k(\sigma)$ (rad/m)

$$\sigma^2 = gk \tanh(kD), \quad (2.237)$$

IV) Spectral partition parameters

These output parameters are based on partitioning of the spectrum into individual wave fields.

- 1) **PHS** Wave heights H_s of partitions of the spectrum (see below).
- 2) **PTP** Peak (relative) periods of partitions of the spectrum (parabolic fit).
- 3) **PLP** Peak wave lengths of partitions of the spectrum (from peak period).
- 4) **PSP** Mean direction of partitions of the spectrum.
- 5) Directional spread of partition of the spectrum Cf. Eq. (2.227).
- 6) **PWS** Wind sea fraction of partition of the spectrum. The method of Hanson and Phillips (2001) is used, implemented as described in Tracy et al. (2007). With this, a ‘wind sea fraction’ W is introduced

$$W = E^{-1} E|_{U_p > c}, \quad (2.238)$$

where E is the total spectral energy, and $E|_{U_p > c}$ is the energy in the spectrum for which the projected wind speed U_p is larger than the local wave phase velocity $c = \sigma/k$. The latter defines an area in the spectrum under the direct influence of the wind. To allow for nonlinear interactions to shift this boundary to lower frequencies, and subsequently to have fully grown wind seas inside this area, U_p includes a multiplier C_{mult}

$$U_p = C_{mult} U_{10} \cos(\theta - \theta_w) . \quad (2.239)$$

The multiplier can be set by the user. The default value is $C_{mult} = 1.7$.

- 7) **TWS** Wind sea fraction of the entire spectrum.
- 8) **PNR** Number of partitions found in the spectrum.

V) Atmosphere-waves layer

- 1) **UST** The friction velocity u_* (scalar). Definition depends on selected source term parameterization (m/s). An alternative vector version of the stresses is available for research (requires user intervention in the code).
- 2) **CHA** Charnock parameter for air-sea friction (without dimensions)
- 3) **CGE** Energy flux (W/m)

$$C_g E = \rho_w g \overline{C_g} E. \quad (2.240)$$

- 4) **FAW** Wind to wave energy flux
- 5) **TAW** Net wave-supported stress (wind to wave momentum flux)
- 6) **TWA** Negative part of the wave-supported stress
- 7) **WCC** Wave to wind momentum flux
- 8) **WCF** Whitecap coverage (without dimensions)
- 9) **WCH** Whitecap mean thickness (m)
- 10) **WCM** Mean breaking wave height (m) (NOT AVAILABLE YET)

VI) Wave-ocean layer

- 1) **SXY** Radiation stresses

$$S_{xx} = \rho_w g \iint (n - 0.5 + n \cos^2 \theta) F(k, \theta) dk d\theta, \quad (2.241)$$

$$S_{xy} = \rho_w g \iint n \sin \theta \cos \theta F(k, \theta) dk d\theta, \quad (2.242)$$

$$S_{yy} = \rho_w g \iint (n - 0.5 + n \sin^2 \theta) F(k, \theta) dk d\theta, \quad (2.243)$$

where

$$n = \frac{1}{2} + \frac{kd}{\sinh 2kd}. \quad (2.244)$$

- 2) **TWO** Wave to ocean momentum flux
- 3) **BHD** Bernoulli head (m^2/s^2)

$$J = g \iint \frac{k}{\sinh 2kd} F(k, \theta) dk d\theta, \quad (2.245)$$

- 4) **FOC** Wave to ocean energy flux (W/m²)
 5) **TUS** Stokes volume transport (m²/s)

$$(M_x^w, M_y^w) = g \iint \frac{(k \cos(\theta), k \sin(\theta))}{\sigma} F(k, \theta) dk d\theta, \quad (2.246)$$

- 6) **USS** Stokes drift at the sea surface (m/s)

$$(U_{ssx}, U_{ssy}) = g \iint \sigma \cosh 2kd \frac{(k \cos(\theta), k \sin(\theta))}{\sinh^2 kd} F(k, \theta) dk d\theta, \quad (2.247)$$

- 7) **P2S** Second order pressure variance (m²) and peak period of this pressure (s) which contributes to acoustic and seismic noise,

$$F_{p2D}(k=0) = \int_0^\infty \frac{4\sigma}{C_g} \int_0^\pi F(k, \theta) F(k, \theta + \pi) d\theta dk, \quad (2.248)$$

- 8) **USF** Frequency spectrum of Stokes drift at the sea surface (m/s/Hz)

$$(U_{ssx}(f), U_{ssy}(f)) = g \iint \sigma \cosh 2kd \frac{(k \cos(\theta), k \sin(\theta))}{\sinh^2 kd} F(k, \theta) \frac{2\pi}{C_g} d\theta, \quad (2.249)$$

- 9) **P2L** Frequency spectrum of the second order pressure (m²s) which contributes to acoustic and seismic noise,

$$F_{p2D}(k=0, f) = \frac{2\sigma}{\pi} \int_0^\pi \frac{4\pi^2}{C_g^2} F(k, \theta) F(k, \theta + \pi) d\theta. \quad (2.250)$$

- 10) **TWI** Wave to sea ice stress
 11) **FIC** Wave to sea ice energy flux

VII) Wave-bottom layer

- 1) **ABR** Near-bottom rms excursion amplitude

$$a_{b,rms} = \left[2 \iint \frac{1}{\sinh^2 kd} F(k, \theta) dk d\theta \right]^{1/2}. \quad (2.251)$$

- 2) **UBR** Near-bottom rms orbital velocity

$$u_{b,rms} = \left[2 \iint \frac{\sigma^2}{\sinh^2 kd} F(k, \theta) dk d\theta \right]^{1/2}. \quad (2.252)$$

- 3) **BED** Bedform parameters: ripple height and directions (NOT TESTED YET)
- 4) **FBB** Energy dissipation in WBBL
- 5) **TBB** Momentum loss in WBBL

VIII) Spectrum parameters

- 1) **MSS** Mean square slopes in x and y directions (zonal and meridional components of slopes variances).
- 2) **MSC** Spectral tail level (without dimensions)
- 3) **WL02** East/X North/Y mean wavelength component
- 4) **AXT** Correl sea surface gradients (x,t)
- 5) **AYT** Correl sea surface gradients (y,t)
- 6) **AXY** Correl sea surface gradients (x,y)

IX) Numerical diagnostics

- 1) **DTD** Average time step in the source term integration (s).
- 2) **FC** Cut-off frequency f_c (Hz, depends on parameterization of input and dissipation).
- 3) **CFX** Maximum CFL number for spatial advection
- 4) **CFD** Maximum CFL number for angular advection
- 5) **CFK** Maximum CFL number for wavenumber advection

X) User defined

- 1) **U1** Slot for user defined parameter (requires modification of code).
- 2) **U2** Idem.

This page is intentionally left blank.

3 Numerical approaches

The Wave Action Equation in Cartesian (2.8) or spherical (2.12) coordinates is the basic equations of the wave model. However, modified versions of these equations are used in the model, where (a) they are solved on a variable wavenumber grid (see below), where (b) modified versions of these equations are used to properly describe dispersion for discretized equations in selected numerical schemes (see Section 3.4), and where (c) sub-grid obstacles such as islands are considered (see Section 3.4).

3.1 Spectral discretization

If Eq. (2.8) or Eq. (2.12) is solved directly, an effective reduction of spectral resolution occurs in shallow water (see Tolman and Booij, 1998). This loss of resolution can be avoided if the equation is solved on a variable wavenumber grid, which implicitly incorporates the kinematic wavenumber changes due to shoaling. Such a wavenumber grid corresponds to a spatially and temporally invariant grid in relative frequency (Tolman and Booij, 1998). The corresponding local wavenumber grid can be calculated directly from the invariant frequency grid and the dispersion relation (2.1), and hence becomes a function of the local depth d . To accommodate economical calculations of S_{nl} and allow a good separation of swell frequencies, a frequency discretization with exponentially increasing increments is adopted, so that the varying frequency resolution is proportional to the local frequency,

$$\sigma_{m+1} = X_\sigma \sigma_m, \quad (3.1)$$

where m is a discrete grid counter in k -space. X_σ is defined by the user in the input files of the program. Traditionally, in most applications of third-generation models $X_\sigma \simeq 1.1$ is used.

The effects of a spatially varying grid will be discussed for the Cartesian Eq. (2.8) only. Adaptation to the spherical grid is trivial. Denoting the variable wavenumber grid with κ , the balance equation becomes

$$\frac{\partial N}{\partial t c_g} + \frac{\partial \dot{x}N}{\partial x c_g} + \frac{\partial \dot{y}N}{\partial y c_g} + \frac{\partial \dot{\kappa}N}{\partial \kappa c_g} + \frac{\partial \dot{\theta}N}{\partial \theta c_g} = \frac{S}{\sigma c_g}, \quad (3.2)$$

$$\dot{\kappa} \frac{\partial k}{\partial \kappa} = c_g^{-1} \frac{\partial \sigma}{\partial d} \left(\frac{\partial d}{\partial t} + \mathbf{U} \cdot \nabla_x d \right) - \mathbf{k} \cdot \frac{\partial \mathbf{U}}{\partial s}. \quad (3.3)$$

3.2 Splitting of the wave action equation

In WAVEWATCH III Eq. (3.2) is solved using a fractional step method. The first step treats the temporal variations of the depth, and corresponding changes in the wavenumber grid. As is discussed by Tolman and Booij (1998), this step can be invoked sparsely. By splitting off effects of (temporal) water level variations, the grid becomes invariant, and the depth becomes quasi-steady for the remaining fractional steps. Other fractional steps consider spatial propagation, intra-spectral propagation and source terms. Starting with version 5.10, the source term S is further split into non-ice $S_{no\ ice}$ and ice S_{ice} source term. For a single model grid, the following sequence of integration is performed by the W3WAVE routine:

1. Update of water level
2. Intra-spectral part 1: integration over $\Delta t_g/2$ of $\frac{\partial}{\partial t} \frac{N}{c_g} + \frac{\partial}{\partial \kappa} \frac{\dot{\kappa} N}{c_g} + \frac{\partial}{\partial \theta} \frac{\dot{\theta} N}{c_g} = 0$
3. Spatial propagation: integration over Δt_g of $\frac{\partial}{\partial t} \frac{N}{c_g} + \frac{\partial}{\partial x} \frac{\dot{x} N}{c_g} + \frac{\partial}{\partial y} \frac{\dot{y} N}{c_g} = 0$
4. Intra-spectral part 2: integration over $\Delta t_g/2$ of $\frac{\partial}{\partial t} \frac{N}{c_g} + \frac{\partial}{\partial \kappa} \frac{\dot{\kappa} N}{c_g} + \frac{\partial}{\partial \theta} \frac{\dot{\theta} N}{c_g} = 0$
5. Source term integration: integration over Δt_g of $\frac{\partial}{\partial t} \frac{N}{c_g} = \frac{S_{no\ ice}}{\sigma c_g}$
6. Ice source term integration: integration over Δt_g of $\frac{\partial}{\partial t} \frac{N}{c_g} = \frac{S_{ice}}{\sigma c_g}$

The succession of these 6 steps is, in the limit $\Delta t_g \rightarrow 0$, equivalent to the integration of Eq. (3.2) over a global time step Δt_g .

This splitting in multiple steps allows an efficient vectorization and parallelization at the same time. The time splitting furthermore allows for the use of separate partial or dynamically adjusted time steps in the different fractional steps of the model. WAVEWATCH III makes a distinction between 4 different time steps.

- 1) The ‘global’ time step Δt_g , is the common step of all the splitted sub-integrations. In that sense, it is the smallest time step for which a physically meaningful solution can be obtained, because all terms in the equation have been integrated. As a result, this is a possible time step for evaluating model output or coupling with other models, and, in the case of a multi-grid system, it is the time step at which communication between grids is performed. In the case of a forced – not coupled – model, input winds and currents are interpolated at this global step. This time step is provided by the user in the input file of `ww3_grid`, but can be reduced within the model to reach a requested input or output time.
- 2) The second time step is the time step for spatial propagation. This is not used for triangular-based grids, for which the advection step is – in the case of explicit schemes – adjusted internally for each spectral component. For other grid types, the user supplies a reference maximum propagation time step for the lowest model frequency $\Delta t_{p,r}$, assuming no currents, and no grid motion. For the frequency with counter m , the maximum time step $\Delta t_{p,m}$ is calculated within the model as

$$\Delta t_{p,m} = \frac{\dot{x}_{p,r}}{\dot{x}_{p,m}} \Delta t_{p,r} , \quad (3.4)$$

where $\dot{x}_{p,r}$ is the maximum advection speed for the longest waves without currents or grid motion, and $\dot{x}_{p,m}$ is the actual maximum advection speed (including current) for frequency m . If the propagation time step is smaller than the global time step, the propagation effects are calculated with a number of successive smaller time steps. This generally implies that several partial time steps are used for the lowest frequency, but that the highest frequencies are propagated over the interval Δt_g with a single calculation. The latter results in a significantly more efficient model, particularly if higher-order accurate propagation schemes are used. Note that $\Delta t_{p,m}$ may be defined bigger than Δt_g , and that this has potential impact in model economy for cases with (strong) currents.

- 3) The third time step is the time step for intra-spectral propagation. For large-scale and deep-water grids this time step can generally be taken equal to the global time step Δt_g . For shallow water grids, smaller intra-spectral propagation time steps allow for larger effects

of refraction within the stability constraints of the scheme. Note that the order of invoking spatial and intra-spectral propagation is alternated to enhance numerical accuracy. If strong refraction of long period swells occur, this may result in a notable undulation of mean wave parameters. This can be avoided by setting this time step to an even integer fraction of Δt_g .

- 4) The final time step is the time step for the integration of the source terms, which is dynamically adjusted for each separate grid point and global time step Δt_g (see Section 3.6). This results in more accurate calculations for rapidly changing wind and wave conditions, and a more economical integration for slowly varying conditions. In order to limit the calculation time, a minimum time step is defined by the user.

The following sections deal with the separate steps in the fractional step method, and various subjects associated with this. The main issue are covered in Section 3.3, which addresses treatment of temporal variations of the water depth, Section 3.4 which addresses spatial propagation, Section 3.5 which addresses intra-spectral propagation, and Sections 3.6 and 3.7 which address the numerical integration of non-icea and ice source terms. The other sections deal with additional numerical approaches and techniques, covering the treatment of winds and currents (Section 3.9), including tides (Section 3.10), calculating space-time extremes (Section 3.11), treatment of ice (Section 3.8), spectral partitioning and the corresponding tracking of wave systems in space and time (Sections 3.12, 3.13), and nesting (Section 3.14).

3.3 Depth variations in time

Temporal depth variations result in a change of the local wavenumber grid. Because the wavenumber spectrum is invariant with respect to temporal changes of the depth, this corresponds to a simple interpolation of the spectrum from the old grid to the new grid, without changes in the spectral shape. As discussed above, the new grid simply follows from the globally invariant frequency grid, the new water depth d and the dispersion relation Eq. (2.1).

The time step of updating the water level is generally dictated by physical time scales of water level variations, but not by numerical considerations (Tolman and Booij, 1998).

The interpolation to the new wavenumber grid is performed with a simple conservative interpolation method. In this interpolation the old spectrum is first converted to discrete action densities by multiplication with the spectral bin widths. This discrete action then is redistributed over the new grid cf. a regular linear interpolation. The new discrete actions then are converted into a spectrum by division by the (new) spectral bin widths. The conversion requires a parametric extension of the original spectrum at high and low frequencies because the old grid generally will not completely cover the new grid. Energy/action in the old spectrum at low wavenumbers that are not resolved by the new grid is simply removed. At low wavenumbers in the new grid that are not resolved by the old grid zero energy/action is assumed. At high wavenumbers in the new grid the usual parametric tail is applied if necessary. The latter correction is rare, as the highest wavenumbers usually correspond to deep water.

In practical applications the grid modification is usually relevant for a small fraction of the grid points only. To avoid unnecessary calculations, the grid is transformed only if the smallest relative depth kd in the discrete spectrum is smaller than 4. Furthermore, the spectrum is interpolated only if the spatial grid point is not covered by ice, and if the largest change of wavenumber is at least $0.05\Delta k$.

3.4 Spatial propagation

3.4.1 General concepts

Spatial propagation in WAVEWATCH III is described by the first terms of Eq. (3.2). For spherical coordinates [Eq. (2.12)], the corresponding spatial propagation step becomes

$$\frac{\partial \mathcal{N}}{\partial t} + \frac{\partial}{\partial \phi} \dot{\phi} \mathcal{N} + \frac{\partial}{\partial \lambda} \dot{\lambda} \mathcal{N} = 0, \quad (3.5)$$

where the propagated quantity \mathcal{N} is defined as $\mathcal{N} \equiv N c_g^{-1} \cos \phi$. For the Cartesian grid, a similar equation is found for $\mathcal{N} \equiv N c_g^{-1}$. In this section

equations for the more complicated spherical grid are presented only. Conversion to a Cartesian grid is generally a simplification and is trivial.

Equation (3.5) in form is identical to the conventional deep-water propagation equation, but includes effects of both limited depths and currents. At the land-sea boundaries, wave action propagating toward the land is assumed to be absorbed without reflection, and waves propagating away from the coast are assumed to have no energy at the coastline. For so-called ‘active boundary points’ where boundary conditions are prescribed, a similar approach is used. Action traveling toward such points is absorbed, whereas action at the boundary points is used to estimate action fluxes for components traveling into the model.

The spatial grids can use two different coordinate systems, either a ‘flat’ Cartesian coordinate system typically used for small scale and idealized test applications, and a spherical (latitude-longitude) system used for most real-world applications. In model version 3.14, the coordinate system was selected at compile time with the `XYG` or `LLG` switches. In more recent model versions, the grid type is now a variable defined in `ww3_grid` and stored in the `mod_def.ww3` file.

There is an option for spherical grids to have simple closure, to be periodic in the longitude direction, e.g. so that energy can propagate east from the maximum longitude in the grid to the minimum longitude in the grid. This closure is “simple” insofar as the index for latitude does not change across this “seam”. A “not simple” type of closure is also permitted: this is associated with tripole grids. The tripole grid is a type of irregular grid and so this closure is discussed further in (3.4.3).

Up to model version 3.14, WAVEWATCH III considered only regular discrete grids, where the two main grid axes (x, y) are discretized using constant increments Δx and Δy . In model version 5.16 additional options have been included, including curvilinear grids and unstructured grids. In the following sections these grid approaches will be discussed, before additional propagation issues are addressed, covering the Garden Sprinkler Effect (3.4.6), continuously moving grids (3.4.8) unresolved islands (3.4.7), and rotated grids (3.4.9).

3.4.2 Traditional regular grids

Propagation schemes for traditional regular grids are selected at compile time using switches. Several schemes are available in WAVEWATCH III. These schemes are described in order of complexity below.

First-order scheme

Switch:	PR1
Origination:	WAVEWATCH III
Provided by:	H. L. Tolman

A simple and cheap first order upwind scheme has been included, mainly for testing during development of WAVEWATCH III. To assure numerical conservation of action, a flux or control volume formulation is used. The flux between grid points with counters i and $i - 1$ in ϕ -space ($\mathcal{F}_{i,-}$) is calculated as

$$\mathcal{F}_{i,-} = \left[\dot{\phi}_b \mathcal{N}_u \right]_{j,l,m}^n, \quad (3.6)$$

$$\dot{\phi}_b = 0.5 \left(\dot{\phi}_{i-1} + \dot{\phi}_i \right)_{j,l,m}, \quad (3.7)$$

$$\mathcal{N}_u = \begin{cases} \mathcal{N}_{i-1} & \text{for } \dot{\phi}_b \geq 0 \\ \mathcal{N}_i & \text{for } \dot{\phi}_b < 0 \end{cases}, \quad (3.8)$$

where j , l and m are discrete grid counters in λ -, θ - and k -spaces, respectively, and n is a discrete time step counter. $\dot{\phi}_b$ represents the propagation velocity at the ‘cell boundary’ between points i and $i - 1$, and the subscript u denotes the ‘upstream’ grid point. At land-sea boundaries, $\dot{\phi}_b$ is replaced by $\dot{\phi}$ at the sea point. Fluxes between points i and $i + 1$ ($\mathcal{F}_{i,+}$) are obtained by replacing $i - 1$ with i and i with $i + 1$. Fluxes in λ -space are calculated similarly, changing the appropriate grid counters and increments. The ‘action density’ (\mathcal{N}^{n+1}) at time $n + 1$ is estimated as

$$\mathcal{N}_{i,j,l,m}^{n+1} = \mathcal{N}_{i,j,l,m}^n + \frac{\Delta t}{\Delta \phi} [\mathcal{F}_{i,-} - \mathcal{F}_{i,+}] + \frac{\Delta t}{\Delta \lambda} [\mathcal{F}_{j,-} - \mathcal{F}_{j,+}], \quad (3.9)$$

where Δt is the propagation time step, and $\Delta \phi$ and $\Delta \lambda$ are the latitude and longitude increments, respectively. Equations (3.6) through (3.8) with $\mathcal{N} = 0$ on land and applying Eq. (3.9) on sea points only automatically invokes the required boundary conditions.

Note that Eq. (3.9) represents a two-dimensional implementation of the scheme, for which the norm of the actual advection vectors needs to be used in Eq. (3.4). Note furthermore, that this implies a CFL criterion for the full equation, which is generally more stringent than that for a scheme where λ and ϕ propagation are treated separately as in the third order schemes

discussed below. For a grid with equal increments in both directions, this results in a maximum time step that is a factor $1/\sqrt{2}$ smaller for the first order scheme than for the third order schemes.

Second-order scheme (UNO)

Switch:	UNO
Origination:	MetOffice
Provided by:	J.-G. Li

The upstream non-oscillatory 2nd order (UNO) advection scheme (Li, 2008) is an extension of the MINMOD scheme (Roe, 1986). In the UNO scheme, the interpolated wave action value at the mid-flux point for the cell face between cell $i-1$ and cell i is given by

$$N_{i-}^* = N_c + \text{sign}(N_d - N_c) \frac{(1 - C)}{2} \min(|N_u - N_c|, |N_c - N_d|) \quad , \quad (3.10)$$

where $i-$ is the cell face index; $C = \left| \dot{\phi}_b \right| \Delta t / \Delta \phi$ is the absolute CFL number; and the subscripts u , c and d indicate the *upstream*, *central* and *downstream* cells, respectively, relative to the given $i-$ cell face velocity $\dot{\phi}_b$. If $\dot{\phi}_b > 0$, $u = i-2$, $c=i-1$, $d=i$ for the cell face between cell $i-1$ and cell i . If $\dot{\phi}_b \leq 0$ then $u=i+1$, $c=i$, $d=i-1$. Details of the UNO scheme are given in Li (2008) alongside standard numerical tests which demonstrate that the UNO scheme on Cartesian multiple-cell grids is non-oscillatory, conservative, shape-preserving, and faster than its classical counterpart as long as the CFL number is less than 1.0.

The flux and cell value update follow the same formulations as the first order upstream scheme, that is,

$$\mathcal{F}_{i-} = \phi_b \dot{N}_{i-}^*; \quad N_i^{n+1} = N_i^n + \frac{\Delta t}{\Delta \phi} (\mathcal{F}_{i-} - \mathcal{F}_{i+}) \quad , \quad (3.11)$$

where \mathcal{F}_{i+} is the flux for the cell face between cell i and cell $i+1$. It can be estimated with a mid-flux value similar to (3.10) but with i replaced with $i+1$. An advective-conservative hybrid operator (Leonard et al., 1996) that reduces the time-splitting error is used to extend the UNO schemes to multi-dimensions.

Third-order scheme (UQ)

Switch:	UQ
Origination:	WAVEWATCH III
Provided by:	H. L. Tolman

The third-order accurate scheme available in WAVEWATCH III is the QUICKEST scheme (Leonard, 1979; Davis and More, 1982) combined with the ULTIMATE TVD (total variance diminishing) limiter (Leonard, 1991). This is the default propagation scheme for WAVEWATCH III. This scheme is third-order accurate in both space and time, and has been selected based on the extensive intercomparison of higher-order finite difference schemes for water quality models (see Cahyono, 1994; Falconer and Cayhono, 1993; Tolman, 1995a). This scheme is applied to propagation in longitudinal and latitudinal directions separately, alternating the direction to be treated first.

In the QUICKEST scheme the flux between grid points with counters i and $i - 1$ in ϕ -space ($\mathcal{F}_{i,-}$) is calculated as⁴

$$\mathcal{F}_{i,-} = \left[\dot{\phi}_b \mathcal{N}_b \right]_{j,l,m}^n, \quad (3.12)$$

$$\dot{\phi}_b = 0.5 \left(\dot{\phi}_{i-1} + \dot{\phi}_i \right), \quad (3.13)$$

$$\mathcal{N}_b = \frac{1}{2} \left[(1 + C)\mathcal{N}_{i-1} + (1 - C)\mathcal{N}_i \right] - \left(\frac{1 - C^2}{6} \right) \mathcal{CU} \Delta\phi^2, \quad (3.14)$$

$$\mathcal{CU} = \begin{cases} (\mathcal{N}_{i-2} - 2\mathcal{N}_{i-1} + \mathcal{N}_i) \Delta\phi^{-2} & \text{for } \dot{\phi}_b \geq 0 \\ (\mathcal{N}_{i-1} - 2\mathcal{N}_i + \mathcal{N}_{i+1}) \Delta\phi^{-2} & \text{for } \dot{\phi}_b < 0 \end{cases}, \quad (3.15)$$

$$C = \frac{\dot{\phi}_b \Delta t}{\Delta\phi}, \quad (3.16)$$

where \mathcal{CU} is the (upstream) curvature of the action density distribution, and where C is a CFL number including a sign to identify the propagation direction. Like the first order scheme, this scheme gives stable solutions for $|C| \leq 1$. To assure that this scheme does not generate aphysical extrema, it is used in combination with the ULTIMATE limiter. This limiter uses the central, upstream and downstream action density (suffices c , u and d , respectively), which are defined as

⁴ Fluxes ($\mathcal{F}_{i,+}$) between grid points with counters $i + 1$ and i again are obtained by substituting the appropriate indices.

$$\begin{aligned} \mathcal{N}_c = \mathcal{N}_{i-1}, \quad \mathcal{N}_u = \mathcal{N}_{i-2}, \quad \mathcal{N}_d = \mathcal{N}_i & \text{ for } \dot{\phi}_b \geq 0 \\ \mathcal{N}_c = \mathcal{N}_i, \quad \mathcal{N}_u = \mathcal{N}_{i+1}, \quad \mathcal{N}_d = \mathcal{N}_{i-1} & \text{ for } \dot{\phi}_b < 0 \end{aligned} \quad (3.17)$$

To assess if the initial state and the solution show similar monotonic or non-monotonic behavior, the normalized action $\tilde{\mathcal{N}}$ is defined

$$\tilde{\mathcal{N}} = \frac{\mathcal{N} - \mathcal{N}_u}{\mathcal{N}_d - \mathcal{N}_u}. \quad (3.18)$$

If the initial state is monotonic (i.e., $0 \leq \tilde{\mathcal{N}}_c \leq 1$), the (normalized) action at the cell boundary \mathcal{N}_b is limited to

$$\tilde{\mathcal{N}}_c \leq \tilde{\mathcal{N}}_b \leq 1, \quad \tilde{\mathcal{N}}_b \leq \tilde{\mathcal{N}}_c C^{-1}. \quad (3.19)$$

otherwise

$$\tilde{\mathcal{N}}_b = \tilde{\mathcal{N}}_c. \quad (3.20)$$

An alternative scheme is necessary if one of the two grid points adjacent to the cell boundary is on land or represents an active boundary point. In such cases, Eqs. (3.7) and (3.14) are replaced by

$$\dot{\phi}_b = \dot{\phi}_s, \quad (3.21)$$

$$\mathcal{N}_b = \mathcal{N}_u, \quad (3.22)$$

where the suffix s indicates the (average of) the sea point(s). This boundary condition represents a simple first order upwind scheme, which does not require the limiter (3.17) through (3.20).

The final propagation scheme, similar to Eq. (3.9), becomes

$$\mathcal{N}_{i,j,l,m}^{n+1} = \mathcal{N}_{i,j,l,m}^n + \frac{\Delta t}{\Delta \phi} [\mathcal{F}_{i,-} - \mathcal{F}_{i,+}]. \quad (3.23)$$

The scheme for propagation in λ -space is simply obtained by rotating indices and increments in the above equations.⁵

Note that the ULTIMATE QUICKEST scheme is implemented as alternate one-dimensional schemes, for which the maxima of component advection

⁵ The ‘soft’ boundary treatment as described on page 31 of Tolman (2002e) is no longer available, because it is incompatible with the advanced nesting techniques introduced in model version 3.14.

speeds need to be used in Eq. (3.4). For consistency, the same time steps are always used for λ and ϕ propagation for a given component.

3.4.3 Curvilinear grids

Origination:	WAVEWATCH III(NRL Stennis)
Provided by:	W. E. Rogers, T. J. Campbell

As an extension to traditional “regular” grids, computations may be made on “irregular” grids within WAVEWATCH III . This makes it possible to run the model on alternate grid projections (e.g. Lambert conformal conic), rotated grids, or shoreline-following grids with higher resolution near shore, though the restrictions on time step from the conditionally stable schemes still apply. The same propagation schemes are utilized for irregular grids as for regular grids (Section 3.4.2).

The implementation is described in detail in [Rogers and Campbell \(2009\)](#), and summarized here: a Jacobian is used to convert the entire domain between the normal, curving space, and a straightened space. This conversion is performed only within the propagation routine, rather than integrating the entire model in straightened space. A simple, three step process is used every time the propagation subroutine is called (i.e. every time step and every spectral component): first, the dependent variable (wave action density) is converted to straightened space using a Jacobian; second, the wave action density is propagated via subroutine calls for each (of two) grid axes; third, the wave action density is converted back to normal, curved space. The actual flux computation is not significantly modified from its original, regular grid form. The same process occurs, regardless of grid type (regular or irregular); for regular grids, the Jacobian is unity.

Regarding the user interface: in `ww3_grid.inp`, a string is used to indicate the grid type. In cases where this grid string is ‘RECT’, the model processes input for a regular grid. In case where this grid string is ‘CURV’, the model processes input for an irregular grid. [Note that with WAVEWATCH III version 4.00, the coordinate system (i.e. degrees vs. meters) and the closure type (e.g. global/wrapping grid) are also specified in `ww3_grid.inp`; the switches `LLG` and `XYG` are deprecated.]

With WAVEWATCH III version 5, capability is added to run on a special

type of curvilinear grid, the “tripole grid” using the first-order propagation scheme. In the northern hemisphere, this grid type uses two poles instead of one, and both are over land to prevent singularities in grid spacing. This type of grid is sometimes used in ocean models, e.g. (Murray, 1996) and (Metzger et al., 2014). No special switch is required, and the grid is read in as any other irregular grid would be, but the user must specify a closure type (CSTRG) of TRPL in `ww3_grid.inp`. Specific details can be found in the documentation for `ww3_grid.inp` in Section 4.4.2. Propagation and gradient calculations are modified to deal with the new closure method. The TRPL closure type is compatible only with the first-order PR1 propagation scheme. An attractive feature of the tripole grid is that it allows the user to run a single grid which extends all the way to the North Pole. However, though the three poles are over land, there is still a convergence of meridians at the sea points nearest to them, meaning that the grid spacing in terms of real distances (which determines the maximum propagation time step) is still highly variable. More efficient grid spacing (meaning: with less variation of grid spacing in terms of real distances) can be achieved through the use of the multi-grid capability. Though this scheme addresses singularities in grid spacing at the pole, it does not address the singularity associated with definition of wave direction.

3.4.4 Triangular unstructured grids

Origination:	WWM-II
Provided by:	A. Roland, F. Ardhuin, M. Dutour-Sikirić

Triangle-based grids can be used in WAVEWATCH III by using numerical schemes based on contour residual distribution (RD) (see Roland, 2009, for a review). These efficient schemes have initially been implemented in the Wind Wave Model-II (WWM-II) and have subsequently been evaluated in WWIII (e.g. Ardhuin et al., 2009b; Magne et al., 2010). This option is activated by setting the grid string to ‘UNST’ in `ww3_grid.inp`. Four schemes have been implemented, and the choice of one or the other is done with the UNST namelist. These are the CRD-N-scheme (1st order), the CRD-PSI-scheme (better than 1st order, 2nd order on triangular structured grids), the CRD-FCT-scheme (2nd order space-time), and the implicit N-scheme. The default

is the most efficient but diffusive explicit N-scheme. An implicit variant of the RD-Schemes using the method of lines and the N-Scheme for the space discretization was implemented in the SWAN model by [Zijlema \(2010\)](#). We note that these advection schemes do not include corrections for the garden sprinkler effect (GSE). These can be particularly visible for waves going around islands surrounded by deep water. In that case, the diffusion of the N scheme can compensate the GSE.

In practice the grid can be easily generated, using the PolyMesh interface (software developed by Aron Roland), from a shoreline polygons database (e.g. [Wessel and Smith, 1996](#)) and a list of depth soundings, regular or irregular.

In this method the evolution of the spectrum at the nodes, where it is evaluated, is based on the redistribution over the nodes of the flux convergence into the median dual cells associated with the nodes (see [Figure 3.1](#)). For any spectral component, the advection equation, [Eq. \(3.5\)](#), is solved on the median dual cells: the incoming flux into a cell gives the rate of change of the wave action at the corresponding node. The various schemes implemented have different discretizations for the estimation of this flux. The schemes have been presented in (see [Roland, 2009](#), for a review) and [Roland \(2012\)](#).

The equivalent of the CFL condition for explicit finite difference schemes on regular grids is the ratio of the dual cell area divided by the product of the time step and all positive flux into the dual cell. Because the spectral levels are imposed on the boundary for the positive fluxes, the boundary nodes are excluded from this CFL calculation and the incoming energy is set to zero, whereas the outgoing energy is fully absorbed.

The boundary condition at the shoreline depends on the wave direction relative to the shoreline orientation. This particular treatment is enforced using the ‘IOBPD’ array which is updated whenever the grid points status map ‘MAPSTA’ changes. The grid geometry is also used to define local gradients of the water depth and currents. All other operations, such as interpolation of the forcing on the grid and interpolation from the grid onto output locations, is performed using linear interpolation in triangles.

All the triangle geometry operations assume a locally flat Earth. Depth and current gradients on the grid are estimated at the nodes by weighting with their angle the gradients over each triangle connected to the node.

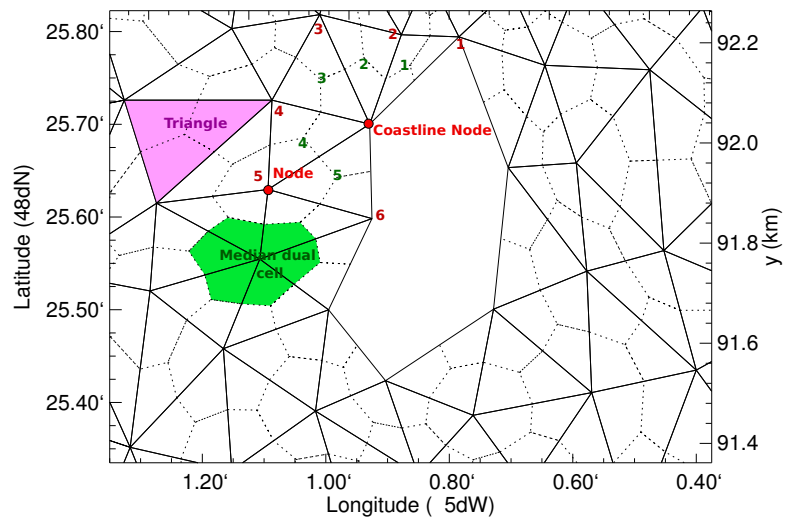


Figure 3.1: Example of a region of a triangle-based mesh, with in this case the small Island of Bannec, France. If the depth is greater than the minimum depth, the nodes of the shoreline are active. These are characterized by a larger number of neighbor nodes (6 in the example chosen) than neighbor triangles (5 in the same example).

3.4.5 Spherical Multiple-Cell (SMC) grid

Switch:	SMC
Origination:	WAVEWATCH III(MetOffice)
Provided by:	J.-G. Li

The Spherical Multiple-Cell (SMC) grid⁶ (Li, 2011) is an extension of the Cartesian multiple-cell grid (Li, 2003) onto the spherical coordinate system. It is an unstructured grid but retains the conventional lat-lon grid cells so that all propagation formulations on the spherical coordinates are still applicable and hence all the finite difference schemes. The SMC grid relaxes the CFL restriction at high latitudes in a similar fashion as the reduced grid (Rasch, 1994). Polar cells are introduced to remove the polar singularity of the differential transport equation by switching to an integral equation. The upstream non-oscillatory 2nd order (UNO) advection schemes (Li, 2008) is implemented on the SMC grid for both spatial and inter-spectral propagation. This 2nd order scheme can be replaced with a 3rd order scheme using the PSMC namelist logical variable UNO3. The UNO3 scheme is similar to the UQ scheme but replacing the flux limiters with the UNO 2nd order scheme. A simple rotation scheme is used for wave refraction-induced rotation and the great circle turning (Li, 2012). The refraction scheme is unconditionally stable for any time step but the maximum refraction induced rotation angle is limited by the maximum possible refraction angle towards the local gradient direction. Diffusion term similar to the Booij and Holthuijsen (1987) for alleviation of the garden sprinkler effect is used but the diffusion coefficient is simplified to a single homogeneous parameter (D_{nn} as in Eq. (3.32)). An additional 1-2-1 weighted averaging scheme is also available by the PSMC namelist logic variable AVERG. Reduction of computing time with this SMC grid is significant in comparison with the conventional grid, thanks to the relaxed time step restriction at high latitudes and removal of land points from the model. A remedy for the invalidated scalar assumption at high latitude is provided to extend the global wave model into the entire Arctic Ocean (Li, 2016). This Arctic part can be activated by adding the ARC switch along side the SMC switch.

The SMC grid can be used for replacing the regular lat-lon grid so that

⁶ Presently this grid is activated by a compile switch and can only be used as a stand-alone grid. This will become a run time option in upcoming model versions.

the model domain can be extended to high latitudes or even the North Pole without reducing the time step. This application requires few changes to the regular grid model except for preparing a few extra input files, including the cell array and face array files. The cell array can be generated with the existing regular grid bathymetry by using the sea points only and merging cells in the longitudinal directions at a few latitude steps (Li, 2011).

Another important use of the SMC grid is for multi-resolution grids. The base level SMC grid cell can be refined into 4 quarterly cells by halving both the longitude and latitude grid lengths. Any cell on this refined level can be further divided into another 4 quarterly cells. This refinement can go on as required, resulting in multi-resolution grids in a few refined levels. For consistency, the single resolution SMC grid is considered to have only one level. Wind forcing will remain to be at the base level resolution for all SMC grids (one level or multi-level) and it will be interpolated on to the refined levels (if any) inside the WW3 model. The normal regular grid input files, such as the water depth, land-sea masks, and sub-grid obstruction, are no longer required, replaced with sea-point only cell and face arrays and a sub-grid obstruction file. The water depth is stored in the cell array in the last (5-th) column as an integer in meter. The masks will be defined inside `ww3_grid` with the sea-point cell array.

One important feature of the SMC grid is that it is an unstructured grid, that is, the cells are not required to be listed side by side as in their physical position. For the convenience of multi-resolution SMC grid, the cells are sorted by their sizes so that cells on one given level are grouped together in one sub-loop for a shared sub-time-step. The base level time step is halved as the grid length for the refined level sub-step. This effectively avoids the model to be slowed down by the refined cells due to their CFL restrictions. Neighboring cells information for propagation schemes are provided with cell face arrays, which are pre-calculated for the given cell array list. So there is no need to expand the sea point only SMC grid cells onto a full grid for propagation. Fig. 3.2 illustrates how SMC cell arrays are defined and Fig. 3.3 shows the Arctic region in a 6-12-25 km three level SMC grid. The golden and red circles mark the global and Arctic parts in the SMC6-25 grid. The Arctic part within the golden circle requires a fixed reference direction to define its wave directional bins. The global part (up to the golden circle) can be run independently without the Arctic part. The 4 rows from the red to the golden circles are duplicated in the Arctic part as boundary cells if the Arctic part is activated with the ARC option. Separate cell and face arrays

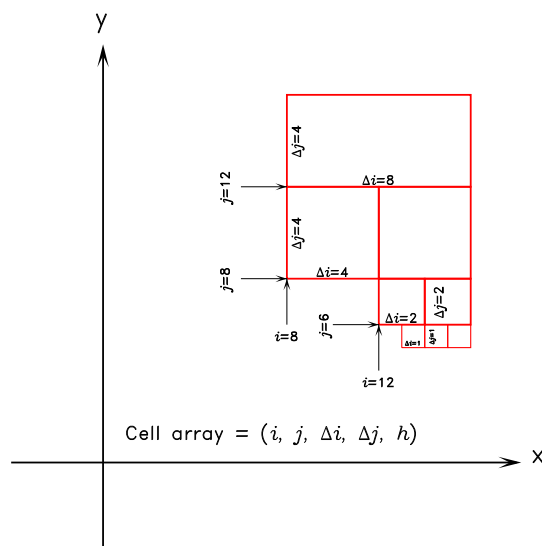


Figure 3.2: Illustration of cell arrays used in the SMC grid.

are used for the Arctic part and they are merged into the global ones within the wave model for propagation.

Some IDL and F90 programs have been developed for generation of SMC grid cell and face arrays and visualization of the grid mesh and wave fields but they have not been formally included in the WW3 package yet. An IDL program (Glob50SMCells.pro) is provided in `smc_docs/SMCG_TKs/` to generate a global 50km SMC grid using a 50km regular grid bathymetry ASCII input file (G50kmBathy.dat). Face array generation is done with two F90 programs, one for the global part (G50SG1Side.f90) and one for the Arctic part (G50SAcSide.f90). Due to the special treatment of the polar cell (Li, 2012), face arrays for the Arctic polar cell requires a different approach than other cells. The cell array file has to be sorted with a simple Linux script (countcells) before it is fed into the face array generation program. The face arrays also need to be sorted with a Linux script (countijsd) to determine the multi-level sub-loop counts. An independent spectral propagation test (G50SMCSRGD.f90) can be run to test the cell and face arrays and its output can be visualized with an IDL script, `g50smstrspb.pro`, which uses the saved projection files from the SMC grid visualization program, `g50smcgrids.pro`.

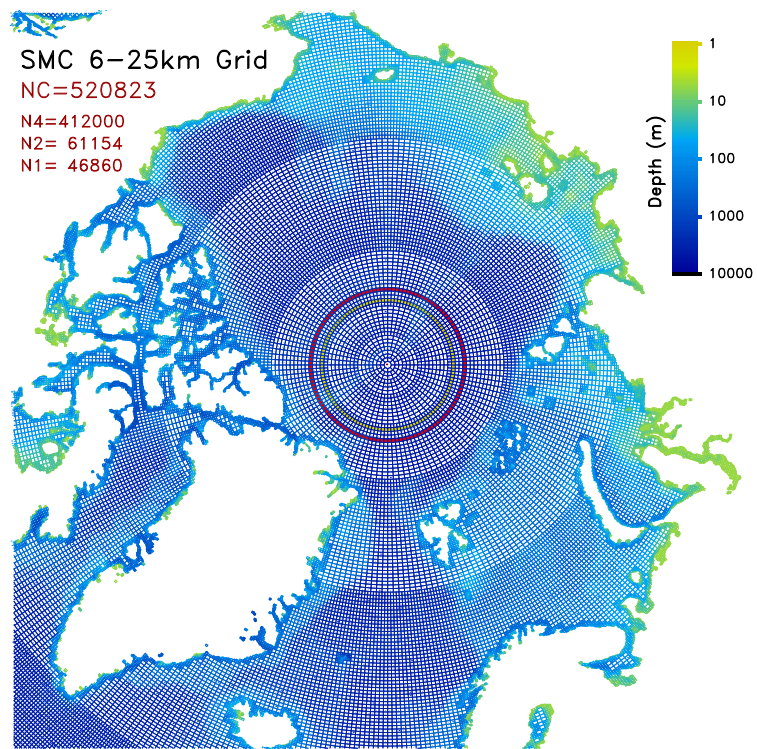


Figure 3.3: The Arctic region in a 6-12-25km multi-resolution SMC grid.

By modifying the projection parameters in `g50smcgrids.pro`, users can choose a projection view point (in lat-lon degree) and save the projection for model output visualization. The sub-grid obstruction file can be generated with the idl script `Glob50SMCObstr.pro`.

Compilation of the SMC grid option is similar to that for the regular lat-lon grid except for that the SMC switch is substituted for the PR2 UNO combination switches. Note that the SMC grid is built inside the regular lat-lon grid type so regular lat-lon grid parameters, such as `NX`, `NY`, `SX`, `SY`, `X1`, and `Y1`, are still required for SMC grid in `ww3_grid.inp` file at the base resolution level. The regular lat-lon grid water depth, land-sea masks, and sub-grid obstruction input files are no longer required and they are replaced with SMC grid sea point only files (depth is stored in the cell array and subgrid obstruction in `G50GObstr.dat`). The depth and land-sea mask input lines in `ww3_grid.in` are, however, kept for passing parameters, such as the minimumu depth. Due to the merges at high latitudes and refined resolutions if any, regular grid mapping arrays are modified slightly for consistency with the SMC grid cells. Refer to the regression test `regtests/ww3_tp2.10` for an example of a 3-level SMC grid model for the Lake Erie.

Output for the SMC grid can be processed by the `ww3_outf` program as either the fully expanded regular lat-lon grid output at the base resolution level or as ASCII output at all SMC grid cell points (type-4). The regular grid format output can be viewed as other regular grid output but the refined resolution cells have been converted into corresponding base resolution cells for a multi-resolution grid. The all cell ASCII output gives field values at the cell center so its resolution conforms with the SMC grid. Visualization of the all cell ASCII output can be done with the aid of the input cell array file because the output cell sequency is the same as the input cell array. The IDL script `g50smcswhglb.pro` is an example program to plot the global 50km SMC grid SWH output. It uses the projection files produced by `g50smcgrids.pro`. Users are encouraged to develop their own grid-generating and post-processing programs in other languages.

It is recommended to read the `smc_docs/SMC_Grid_Guide.pdf` for more information or to contact Jian-Guo.Li@metoffice.gov.uk for any help about the SMC grid.

3.4.6 The Garden Sprinkler Effect

The higher-order accurate propagation schemes are sufficiently free of numerical diffusion for the so-called ‘Garden Sprinkler Effect’ (GSE) to occur, i.e., a continuous swell field disintegrates into a set of discrete swell fields due to the discrete description of the spectrum (Booij and Holthuijsen, 1987, Fig. 3c). Several GSE alleviation methods are available in WAVEWATCH III, as described in the following sections.

No GSE alleviation

Switch:	PR0 / PR1
Origination:	WAVEWATCH III
Provided by:	H. L. Tolman

In case of no propagation (switch PR0) or for the first-order propagation scheme in a traditional or curvilinear grid no GSE alleviation is available or needed.

Booij and Holthuijsen 1987

Switch:	PR2
Origination:	WAVEWATCH III
Provided by:	H. L. Tolman

The classical GSE alleviation method is from [Booij and Holthuijsen \(1987\)](#), who derived an alternative propagation equation for the discrete spectrum, including a diffusive correction to account for continuous dispersion in spite of the discrete spectral description. This correction influences spatial propagation only, which for general spatial coordinates (x, y) becomes

$$\frac{\partial \mathcal{N}}{\partial t} + \frac{\partial}{\partial x} \left[\dot{x} \mathcal{N} - D_{xx} \frac{\partial \mathcal{N}}{\partial x} \right] + \frac{\partial}{\partial y} \left[\dot{y} \mathcal{N} - D_{yy} \frac{\partial \mathcal{N}}{\partial y} \right] - 2D_{xy} \frac{\partial^2 \mathcal{N}}{\partial x \partial y} = 0, \quad (3.24)$$

$$D_{xx} = D_{ss} \cos^2 \theta + D_{nn} \sin^2 \theta, \quad (3.25)$$

$$D_{yy} = D_{ss} \sin^2 \theta + D_{nn} \cos^2 \theta, \quad (3.26)$$

$$D_{xy} = (D_{ss} - D_{nn}) \cos \theta \sin \theta, \quad (3.27)$$

$$D_{ss} = (\Delta c_g)^2 T_s / 12, \quad (3.28)$$

$$D_{nn} = (c_g \Delta \theta)^2 T_s / 12, \quad (3.29)$$

where D_{ss} is the diffusion coefficient in the propagation direction of the discrete wave component, D_{nn} is the diffusion coefficient along the crest of the discrete wave component and T_s is the time elapsed since the generation of the swell. In the present fractional step method the diffusion can be added as a separate step

$$\frac{\partial \mathcal{N}}{\partial t} = \frac{\partial}{\partial x} \left[D_{xx} \frac{\partial \mathcal{N}}{\partial x} \right] + \frac{\partial}{\partial y} \left[D_{yy} \frac{\partial \mathcal{N}}{\partial y} \right] + 2D_{xy} \frac{\partial^2 \mathcal{N}}{\partial x \partial y}. \quad (3.30)$$

This equation is incorporated with two simplifications, the justification of which is discussed in [Tolman \(1995a\)](#). First, the swell ‘age’ T_s is kept constant throughout the model (defined by the user, no default value available). Secondly, the diffusion coefficients D_{ss} and D_{nn} are calculated assuming deep water

$$D_{ss} = \left((X_\sigma - 1) \frac{\sigma_m}{2k_m} \right)^2 \frac{T_s}{12}, \quad (3.31)$$

$$D_{nn} = \left(\frac{\sigma_m}{2k_m} \Delta\theta \right)^2 \frac{T_s}{12}, \quad (3.32)$$

where X_σ is defined as in Eq. (3.1). With these two assumptions, the diffusion tensor becomes constant throughout the spatial domain for each separate spectral component.

Equation (3.30) is solved using a forward-time central-space scheme. At the cell interface between points i and $i - 1$ in $\phi(x)$ space, the term in brackets in the first term on the right side of Eq. (3.30) (denoted as $\mathcal{D}_{i,-}$) is estimated as

$$D_{xx} \frac{\partial \mathcal{N}}{\partial x} \approx \mathcal{D}_{i,-} = D_{xx} \left(\frac{\mathcal{N}_i - \mathcal{N}_{i-1}}{\Delta x} \right) \Big|_{j,l,m}. \quad (3.33)$$

Corresponding values for counters i and $i + 1$, and for gradients in $\lambda(y)$ space again are obtained by rotating indices and increments. If one of the two grid points is located on land, Eq. (3.33) is set to zero. The mixed derivative at the right side of Eq. (3.30) (denoted as $\mathcal{D}_{ij,-}$) is estimated for the grid point i and $i - 1$ in x -space and j and $j - 1$ in y -space as

$$\mathcal{D}_{ij,-} = D_{xy} \left(\frac{-\mathcal{N}_{i,j} + \mathcal{N}_{i-1,j} + \mathcal{N}_{i,j-1} - \mathcal{N}_{i-1,j-1}}{0.5(\Delta x_j + \Delta x_{j-1}) \Delta y} \right) \Big|_{l,m}. \quad (3.34)$$

Note that the increment Δx is a function of y due to the use of the spherical grid. This term is evaluated only if all four grid points considered are sea points, otherwise it is set to zero. Using a forward in time discretization of the first term in Eq. (3.30), and central in space discretizations for the remainder of the first and second term on the right side, the final algorithm becomes

$$\begin{aligned} \mathcal{N}_{i,j,l,m}^{n+1} = & \mathcal{N}_{i,j,l,m}^n + \frac{\Delta t}{\Delta x} (\mathcal{D}_{i,+} - \mathcal{D}_{i,-}) + \frac{\Delta t}{\Delta y} (\mathcal{D}_{j,+} - \mathcal{D}_{j,-}) \\ & + \frac{\Delta t}{4} (\mathcal{D}_{ij,-} + \mathcal{D}_{ij,-} + \mathcal{D}_{ij,+} + \mathcal{D}_{ij,+}). \end{aligned} \quad (3.35)$$

Stable solutions are obtained for (e.g., Fletcher, 1988, Part I section 7.1.1)

$$\frac{D_{\max} \Delta t}{\min(\Delta x, \Delta y)^2} \leq 0.5, \quad (3.36)$$

where D_{\max} is the maximum value of the diffusion coefficient (typically $D_{\max} = D_{nn}$). Because this stability criterion is a quadratic function of the grid increment, stability can become a serious problem at high latitudes for large scale applications. To avoid this putting undue constraints on the time step of a model, a corrected swell age $T_{s,c}$ is used

$$T_{s,c} = T_s \min \left\{ 1, \left(\frac{\cos(\phi)}{\cos(\phi_c)} \right)^2 \right\}, \quad (3.37)$$

where ϕ_c is a cut-off latitude defined by the user.

The above diffusion is needed for swell propagation, but is not realistic for growing wind seas. For wind seas, the ULTIMATE QUICKEST scheme without the dispersion correction is sufficiently smooth to render stable fetch-limited growth curves (Tolman, 1995a). To remove minor oscillations, a small isotropic diffusion is used for growing wave components. To assure that this diffusion is small and equivalent for all spectral components, it is calculated from a preset cell Reynolds (or cell Peclet) number $\mathcal{R} = c_g \Delta x D_g^{-1} = 10$, where D_g is the isotropic diffusion for growing components

$$D_g = \frac{c_g \min(\Delta x, \Delta y)}{\mathcal{R}}. \quad (3.38)$$

The diffusion for swell and for wind seas are combined using a linear combination depending on the nondimensional wind speed or inverse wave age $u_{10}c^{-1} = u_{10}k\sigma^{-1}$ as

$$X_g = \min \left\{ 1, \max \left[0, 3.3 \left(\frac{k u_{10}}{\sigma} \right) - 2.3 \right] \right\}, \quad (3.39)$$

$$D_{ss} = X_g D_g + (1 - X_g) D_{ss,p}, \quad (3.40)$$

$$D_{nn} = X_g D_g + (1 - X_g) D_{nn,p}, \quad (3.41)$$

where the suffix p denotes propagation diffusion as defined in Eqs. (3.31) and (3.32). The constants in Eqs (3.38) and (3.39) are preset in the model.

Spatial averaging

Switch:	PR3
Origination:	WAVEWATCH III
Provided by:	H. L. Tolman

The major drawback of the above GSE alleviation method is its potential impact on model economy as discussed in relation to Eq. (3.36) and in Tolman (2001, 2002a). For this reason, an alternative additional GSE alleviation method has been developed for WAVEWATCH III.

This method which represents the default for WAVEWATCH III, replaces the additional diffusion step (3.30) with a separate fractional step in which direct averaging of the field of energy densities for a given spectral component is considered. The area around each grid point over which the averaging is performed extends in the propagation (\mathbf{s}) and normal (\mathbf{n}) directions as

$$\pm \gamma_{a,s} \Delta c_g \Delta t \mathbf{s} \quad , \quad \pm \gamma_{a,n} c_g \Delta \theta \Delta t \mathbf{n} \quad , \quad (3.42)$$

where $\gamma_{a,s}$ and $\gamma_{a,n}$ are tunable constants, the default value of which is set to 1.5. This averaging is illustrated in Fig. 3.4. Note that these values may require some retuning for practical applications, as discussed in Tolman (2002a). Appendix A of the latter paper presents details of the averaging scheme, including conservation considerations. Consistency with the Booij and Holthuijsen (1987) approach furthermore implies that $\gamma_{a,s}$ and $\gamma_{a,n}$ should vary with the spatial grid resolution (see Chawla and Tolman, 2008, Appendix).

Note that this kind of averaging with dominant directions \mathbf{s} and \mathbf{n} is similar to the Booij and Holthuijsen (1987) diffusion method, that uses the same main directions. The averaging method, however, never influences the time step, because it is completely separated from the actual propagation. Moreover, if explicit schemes are used with typically $c_g \Delta t / \Delta x < 1$, it is obvious that the averaging over the area as defined in (3.42) will generally require information at directly neighboring spatial grid points only, as in Fig. 3.4. Furthermore, this method does not require high-latitude filtering.

As is illustrated in Tolman (2002a,d), this method gives virtually identical results as the previous method, but does so at slightly lower costs. For high-resolution applications, the averaging method may become dramatically more economical.

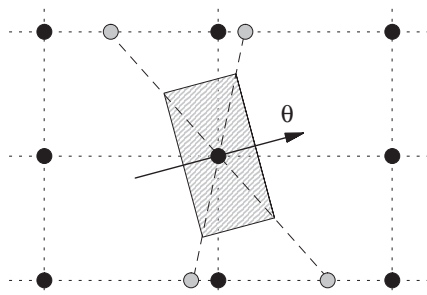


Figure 3.4: Schematic of spatial averaging GSE alleviation technique. Solid circles and dotted lines represent the spatial grid. Hatched area represent averaging area to be considered. Corner point values are obtained from the central grid point and the gray points. The latter values are obtained by interpolation from adjacent grid points (from Tolman, 2002a).

Finally, the GSE can be alleviated somewhat by assuring that the discrete spectral directions do not coincide with spatial grid lines. This can be achieved by defining the first discrete direction θ_1 as

$$\theta_1 = \alpha_\theta \Delta\theta \quad , \quad (3.43)$$

where $-0.5 \leq \alpha_\theta \leq 0.5$ can be defined by the user. Note that setting $\alpha \neq 0$ is beneficial to the first-order scheme, but has negligible impact on the third-order scheme.

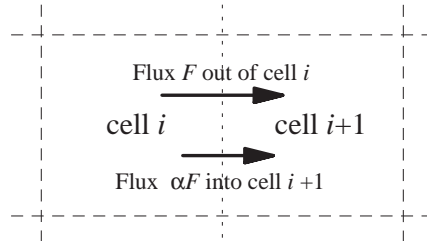


Figure 3.5: Treatment of unresolved obstacles. Common cell boundary (dotted line) has transparency α . Dashed lines represent other cell boundaries. Numerical flux from left to right.

3.4.7 Unresolved obstacles

Origination:	WAVEWATCH III
Provided by:	H. L. Tolman

Even at the time of the original tuning of WAVEWATCH III version 1.15 (Tolman, 2002f), it was clear that unresolved islands groups are a major source of local wave model errors. This was illustrated in some more detail in Tolman (2001, Fig. 3), and Tolman et al. (2002, Fig. 8). In WAVEWATCH III, a methodology from SWAN (Booij et al., 1999; Holthuijsen et al., 2001) was adopted to apply the effects of unresolved obstacles at the cell boundaries of the spatial grid within the numerical scheme. In this approach, the numerical fluxes between cells through their common boundary are suppressed according to the degree of obstruction provided by the unresolved obstacle. In this approach, the numerical propagation scheme of the ULTIMATE QUICKEST scheme of Eq. (3.23) is modified as

$$\mathcal{N}_{i,j,l,m}^{n+1} = \mathcal{N}_{i,j,l,m}^n + \frac{\Delta t}{\Delta \phi} [\alpha_{i,-} \mathcal{F}_{i,-} - \alpha_{i,+} \mathcal{F}_{i,+}] , \quad (3.44)$$

where $\alpha_{i,-}$ and $\alpha_{i,+}$ are ‘transmissions’ of the corresponding cell boundaries, ranging from 0 (closed boundary) to 1 (no obstructions). For outflow boundaries, transparencies by definition are 1, otherwise energy will artificially accumulate in cells. For inflow boundaries, transparencies less than 1 result in elimination of obstructed energy at the cell boundary. This approach is illustrated in Fig. 3.5. Note that a similar approach is easily adopted in the

first- and second-order schemes. Note, furthermore, that an alternate obstruction approach with obstructions as a function of the spectral direction θ has been used by [Hardy and Young \(1996\)](#) and [Hardy et al. \(2000\)](#).

Two methods for defining the obstructions are available in the model. The first defines the obstructions directly at the grid boundary. This requires the generation of staggered depth-transparency grids. The second allows the user to define depths and transparencies at the same grid. In this case, the transparency at the inflow boundary becomes $0.5(1 + \alpha_i)$, and the outflow transparency by definition is 1. To complete the total transparency α_i , the next cell in the flow direction will have an inflow transparency $2\alpha_i/(1 + \alpha_i)$. If consecutive cells are partially obstructed, the product of individual transparencies is applied.

This approach can also be used to continuously model the effects of ice coverage on wave propagation. This is discussed in [Section 3.8](#). Details of the sub-grid treatment of islands and ice can be found in [Tolman \(2003b\)](#). A study of impacts of this approach in large-scale wave models is presented in [Tolman \(2002d, 2003b\)](#).

The default setting of WAVEWATCH III is to not include sub-grid modeling of obstacles. Generating obstruction grids can be labor intensive. For this reason, an automated approach for generating bottom and obstruction grids was developed by [Chawla and Tolman \(2007, 2008\)](#). Note that this option does not involve compile-level choices, but is entirely controlled from the grid preprocessor (see [Chapter 4](#)).

3.4.8 Continuously moving grids

Switch:	MGx
Origination:	WAVEWATCH III
Provided by:	H. L. Tolman

In order to address wave growth issues in rapidly changing, small scale conditions such as hurricanes, an option to add a given continuous advection speed to the grid has been added to the model in model version 3.02. This model version is described in detail in [Tolman and Alves \(2005\)](#). Here, only a cursory description is given.

WARNING

The continuously moving grid version of WAVEWATCH III is only intended for testing wave model properties in highly-idealized conditions. This model version should only be used for deep water without mean currents and land masses. Furthermore, to avoid complications with great circle propagation, only a Cartesian grid should be used. The option is furthermore implemented only for propagation options PR1 and PR3. Note that this is not checked in the scripts or programs at either the compile or run time level. This option is not considered to be for general application.

WARNING

For the above described application Eq. (2.8) can be written as

$$\frac{\partial N}{\partial t} + (\dot{\mathbf{x}} - \mathbf{v}_g) \cdot \nabla_x N = \frac{S}{\sigma}, \quad (3.45)$$

where \mathbf{v}_g represents the advection velocity of the grid. This option is selected when compiling the model. A second compile level option allows for adding the grid advection velocity \mathbf{v}_g to the wind field. This allows for a simple method to assure mass conservation of a wind field independent of the actual and instantaneous grid advection velocity. The advection velocity \mathbf{v}_g can vary in time and is provided by the user at the run time of the model (see below).

For the simplified conditions for which Eq. (3.45) is valid, the implementation of the moving grids is trivial if it is considered that this equation is equivalent to

$$\frac{\partial N}{\partial t} + \nabla_x \cdot (\dot{\mathbf{x}} - \mathbf{v}_g) N = \frac{S}{\sigma}, \quad (3.46)$$

which in turn implies that the advection velocity \mathbf{v}_g can be added directly to $\dot{\mathbf{x}}$ for arbitrary numerical schemes solving Eq. (2.8). Because this influences the net advection velocity, it also influences stability characteristics. This impact has been accounted for automatically by including the moving grid velocity in the calculation of the actual propagation time step in Eq (3.4). Hence, the user need to provide a proper maximum propagation time step representative for $\mathbf{v}_g = \mathbf{0}$ only.

The motion of the grid has an apparent influence on the Garden Sprinkler Effect (GSE), due to the different retention time in the grid of spectral components with identical frequency but different propagation direction. Current GSE alleviation methods tend to be more efficient for younger swells than

for older swells. Hence, swells with longer retention time in the moving grid tend to show a more pronounced GSE (see Tolman and Alves, 2005). To mitigate this apparent imbalance in GSE alleviation, Eq. (3.42) is replaced with

$$\pm \gamma_a \gamma_{a,s} \Delta c_g \Delta t \mathbf{s} \quad , \quad \pm \gamma_a \gamma_{a,n} c_g \Delta \theta \Delta t \mathbf{n} \quad , \quad (3.47)$$

$$\gamma_a = \left(\frac{|\dot{\mathbf{x}}|}{|\dot{\mathbf{x}} - \mathbf{v}_g|} \right)^p \quad (3.48)$$

where γ_a is a correction factor accounting for the grid movement, and where the power p is a parameter allows for some tuning. With this modification, the effects of the GSE can be distributed more evenly over the grid by rescaling the amount of smoothing applied with the expected residence time of corresponding spectral component in the moving grid (see Tolman and Alves, 2005).

To switch on the moving grid option or the corrections of the wind field or GSE, three optional switches are added to the WAVEWATCH III source code (also see, Section 5.4:

- MGP Apply advection correction for continuous moving grid.
- MGW Apply wind correction for continuous moving grid.
- MGG Apply GSE alleviation for continuous moving grid.

The advection velocity and direction is input to the shell similar to the input of homogeneous currents (see bottom of file `ww3_shel.inp` in Section 4.4.9), exchanging the keyword ‘CUR’ with ‘MOV’. The advection velocity can be changed in time like all homogeneous input fields. An example of running with a moving grid model is given in test case `ww3_ts3`. A similar capability exist in `ww3_multi.inp` in Section 4.4.11, and is tested in test case `mww3_test_05`.

3.4.9 Rotated grids

Switch:	RTD
Origination:	WAVEWATCH III (MetOffice)
Provided by:	J.-G. Li

The rotated grid is a latitude-longitude (lat-lon) grid and is obtained by rotating the North Pole to a new position at latitude ϕ_p and longitude λ_p in the standard latitude-longitude system. The new pole position is chosen so that the model domain of interest may be placed around the rotated equatorial area for a evenly-spaced lat-lon mesh. For this reason the rotated grid is also known as *Equatorial grid*. For instance, the North Atlantic and European wave (NAEW) model used in the UK Met Office uses a rotated pole at 37.5N, 177.5E so that London, UK (~51.5N 0.0E) is almost on the rotated equator. This rotated grid allows a much more evenly spaced lat-lon mesh in the NAEW domain than the standard lat-lon grid in the same area. In WAVEWATCH III the rotated grid is implemented with minimum changes to the original lat-lon grid. In fact, the rotated grid is treated just like the standard lat-lon grid inside the model. Only input and output files are modified for the rotated grid. Users should choose the regular lat-lon grid along with the `RTD` switch to use the rotated grid. Model input files, like wind, current and ice files should be mapped on to the rotated grid. For convenience of nesting in standard lat-lon grid, boundary conditions for the rotated grid use standard lat-lon grid points, which are converted into rotated grid lat-lon inside WAVEWATCH III. The list of 2D spectral output locations in `ww3_shel.inp` are also specified in standard lat-lon. All directional output such as wind direction, peak direction, 2D spectra, etc. are converted into standard lat-lon orientation. The full grid output are still on rotated grid but 2D spectra locations have been converted into standard lat-lon.

Four subroutines are provided in module `w3servmd.ftn` for rotated grid conversion:

<code>W3SPECTN</code>	Turns wave spectrum anti-clockwise by AnglD
<code>W3ACTURN</code>	Turns wave action(k,nth) anti-clockwise by AnglD
<code>W3LLTOEQ</code>	Convert standard into rotated lat/lon plus AnglD
<code>W3EQTOLL</code>	Reverse of <code>w3lltoeq</code> , but AnglD unchanged

These subroutines are self-contained and can be extracted outside the model for pre- or post-processing of rotated grid files. Some conversion tools have been developed based on these subroutines but have not been included in WAVEWATCH III yet. Refer to the regression test `regtests/ww3_tp2.11` for an example of a rotated grid model (NAEW). Users may find more information in `smc_docs/Rotated_Grid.pdf` or contact Jian-Guo Li for help (Jian-Guo.Li@metoffice.gov.uk).

3.5 Intra-spectral propagation

3.5.1 General concepts

The third step of the numerical fractional step algorithm considers refraction and residual (current-induced) wavenumber shifts. Irrespective of the spatial grid discretization and coordinate system, the equation to be solved in this step becomes

$$\frac{\partial N}{\partial t} + \frac{\partial}{\partial k} \dot{k}_g N + \frac{\partial}{\partial \theta} \dot{\theta}_g N = 0, \quad (3.49)$$

$$\dot{k}_g = \frac{\partial \sigma}{\partial d} \frac{\mathbf{U} \cdot \nabla_x d}{c_g} - \mathbf{k} \cdot \frac{\partial \mathbf{U}}{\partial s}, \quad (3.50)$$

where \dot{k}_g is the wavenumber velocity relative to the grid, and $\dot{\theta}_g$ is given by (2.15) and (2.11). This equation does not require boundary conditions in θ -space, as the model by definition uses the full (closed) directional space. In k -space, however, boundary conditions are required. At low wavenumbers, it is assumed that no wave action exists outside the discrete domain. It is therefore assumed that no action enters the model at the discrete low-wavenumber boundary. At the high-wavenumber boundary, transport across the discrete boundary is calculated assuming a parametric spectral shape as given by Eq. (2.18). The derivatives of the depth as needed in the evaluation of $\dot{\theta}$ are mostly determined using central differences. For points next to land, however, one-sided differences using sea points only are used.

Propagation in θ -space can cause practical problems in an explicit numerical scheme, as the refraction velocity can become extreme for long waves in extremely shallow water or due to strong current shears. Similarly, the propagation in k -space suffers from similar problems in very shallow water. To avoid the need of extremely small time steps due to refraction, the propagation velocities in θ -space and k -space (2.11) are filtered,

$$\dot{\theta} = X_{rd}(\lambda, \phi, k) \left(\dot{\theta}_d + \dot{\theta}_c + \dot{\theta}_g \right), \quad (3.51)$$

where the indices d , c and g refer to the depth, current and great-circle related fraction of the refraction velocity in (2.11). The filter factor X_{rd} is calculated for every wavenumber and location separately, and is determined so that the CFL number for propagation in θ -space due to the *depth* refraction term

cannot exceed a pre-set (user defined) value (default 0.7). This corresponds to a reduction of the bottom slope for some low frequency wave components. For mid-latitudes, the affected components are expected to carry little energy because they are in extremely shallow water. Long wave components carrying significant energy are usually traveling toward the coast, where their energy is dissipated anyway. This filtering is also important for short waves, and close to the pole. The effect of this filter can be tested by reducing the time steps for intraspectral refraction and by looking at the maximum CFL numbers in the output of the model. These are computed just before the filter is applied.

The spectral space is always discretized with constants directional increments and a logarithmic frequency grid (3.1) to accommodate computations of the nonlinear interaction S_{nl} . First, second and third orders schemes are available, and are presented in the following sections.

3.5.2 First-order scheme

Switch:	PR1
Origination:	WAVEWATCH III
Provided by:	H. L. Tolman

In the first order scheme the fluxes in θ - and k -space are calculated using Eqs. (3.6) through (3.8) (replacing \mathcal{N} with N and rotating the appropriate counters). The complete first order scheme becomes

$$N_{i,j,l,m}^{n+1} = N_{i,j,l,m}^n + \frac{\Delta t}{\Delta \theta} [\mathcal{F}_{l,-} - \mathcal{F}_{l,+}] + \frac{\Delta t}{\Delta k_m} [\mathcal{F}_{m,-} - \mathcal{F}_{m,+}] , \quad (3.52)$$

where $\Delta \phi$ is the directional increment, and Δk_m is the (local) wavenumber increment. The low-wavenumber boundary conditions is applied by taking $\mathcal{F}_{m,-} = 0$ for $m = 1$, and the high wavenumber boundary condition is calculated using the parametric approximation (2.18) for N , extending the discrete grid by one grid point to high wavenumbers.

3.5.3 Second-order scheme (UNO)

Switch:	UNO
Origination:	Met Office
Provided by:	J.-G. Li

The UNO scheme for the directional θ -space is identical to the regular grid one assuming that the directional bins are regularly spaced. For the k -space, however, the UNO scheme uses its irregular version, which uses local gradients instead of differences to estimate wave action value at the mid-flux point for the cell face between spectral bin $i-1$ and i , that is:

$$N_{i-}^* = N_c + \text{sign}(N_d - N_c) \frac{(\Delta k_c - |\dot{k}_{i-}| \Delta t)}{2} \min \left(\left| \frac{N_u - N_c}{k_u - k_c} \right|, \left| \frac{N_c - N_d}{k_c - k_d} \right| \right), \quad (3.53)$$

where i - is the wave number k bin index; the subscripts u , c and d indicate the *upstream*, *central* and *downstream* cells, respectively, relative to the given i - face velocity \dot{k}_{i-} ; k_c is the central bin wave number and Δk_c is the central bin width. Details of the irregular grid UNO scheme are given in Li (2008).

Boundary conditions for the θ -space is the natural periodic condition. For the k -space, two more zero spectral bins are added to each end of the wave spectral domain as the UNO scheme is 2nd order in accuracy.

3.5.4 Third-order scheme (UQ)

Switch:	UQ
Origination:	WAVEWATCH III
Provided by:	H. L. Tolman

The ULTIMATE QUICKEST scheme for the θ -space is implemented similar to the scheme for physical space, with the exception that the closed direction space does not require boundary conditions. The variable grid spacing in k -space requires some modifications to the scheme as outlined by (Leonard, 1979, Appendix). Equations (3.12) through (3.16) then become

$$\mathcal{F}_{m,-} = \left[\dot{k}_{g,b} N_b \right]_{i,j,l}^n, \quad (3.54)$$

$$\dot{k}_{g,b} = 0.5 \left(\dot{k}_{g,m-1} + \dot{k}_{g,m} \right), \quad (3.55)$$

$$N_b = \frac{1}{2} \left[(1 + C)N_{i-1} + (1 - C)N_i \right] - \frac{1 - C^2}{6} \mathcal{CU} \Delta k_{m-1/2}^2, \quad (3.56)$$

$$\mathcal{CU} = \begin{cases} \frac{1}{\Delta k_{m-1}} \left[\frac{N_m - N_{m-1}}{\Delta k_{m-1/2}} - \frac{N_{m-1} - N_{m-2}}{\Delta k_{m,-3/2}} \right] & \text{for } \dot{k}_b \geq 0 \\ \frac{1}{\Delta k_m} \left[\frac{N_{m+1} - N_m}{\Delta k_{m+1/2}} - \frac{N_m - N_{m-1}}{\Delta k_{m-1/2}} \right] & \text{for } \dot{k}_b < 0 \end{cases}, \quad (3.57)$$

$$C = \frac{\dot{k}_{g,b} \Delta t}{\Delta k_{m-1/2}}, \quad (3.58)$$

where Δk_m is the discrete band or cell width at grid point m , and where $\Delta k_{m-1/2}$ is the distance between grid points with counters m and $m-1$. The ULTIMATE limiter can be applied as in Eqs. (3.17) through (3.20), if the CFL number of Eq. (3.58) is used. At the low- and high-wavenumber boundaries the fluxes again are estimated using a first-order upwind approach, with boundary conditions as above defined for the first-order scheme. The final scheme in k -space becomes

$$N_{i,j,l,m}^{n+1} = N_{i,j,l,m}^n + \frac{\Delta t}{\Delta k_m} [\mathcal{F}_{m,-} - \mathcal{F}_{m,+}], \quad (3.59)$$

3.6 Non-ice source term integration

The source terms not involving ice are accounted for by solving

$$\frac{\partial N}{\partial t} = \mathcal{S}_{no\ ice}. \quad (3.60)$$

As in WAM, a semi-implicit integration scheme is used. In this scheme the discrete change of action density ΔN becomes (WAMDIG, 1988)

$$\Delta N(k, \theta) = \frac{\mathcal{S}(k, \theta)}{1 - \epsilon D(k, \theta) \Delta t}, \quad (3.61)$$

where D represents the diagonal terms of the derivative of \mathcal{S} with respect to N (WAMDIG, 1988, Eqs. 4.1 through 4.10), and where ϵ defines the offset

of the scheme. Originally, $\epsilon = 0.5$ was implemented to obtain a second-order accurate scheme. Presently, $\epsilon = 1$ is used because it is more appropriate for the large time steps in the equilibrium range of the spectrum (Hargreaves and Annan, 1998, 2001) and it results in much smoother integration of the spectrum. The change of ϵ has little impact on mean wave parameters, but makes the dynamical time stepping as described below more economical.

The semi-implicit scheme is applied in the framework of a dynamic time-stepping scheme (Tolman, 1992). In this scheme, integration over the global time step Δt_g can be performed in several dynamic time steps Δt_d , depending on the net source term \mathcal{S} , a maximum change of action density ΔN_m and the remaining time in the interval Δt_g . For the n^{th} dynamic time step in the integration over the interval Δt_g , Δt_d^n is calculated in three steps as

$$\Delta t_d^n = \min_{f < f_{hf}} \left[\frac{\Delta N_m}{|\mathcal{S}|} \left(1 + \epsilon D \frac{\Delta N_m}{|\mathcal{S}|} \right)^{-1} \right], \quad (3.62)$$

$$\Delta t_d^n = \max [\Delta t_d^n, \Delta t_{d,\min}], \quad (3.63)$$

$$\Delta t_d^n = \min \left[\Delta t_d^n, \Delta t_g - \sum_{i=1}^{n-1} \Delta t_d^i \right], \quad (3.64)$$

where Δt_{\min} is a user-defined minimum time step, which is added to avoid excessively small time steps. The corresponding new spectrum N^n becomes

$$N^n = \max \left[0, N^{n-1} + \left(\frac{\mathcal{S} \Delta t_d}{1 - \epsilon D \Delta t_d} \right) \right]. \quad (3.65)$$

The maximum change of action density ΔN_m is determined from a parametric change of action density ΔN_p and a filtered relative change ΔN_r

$$\Delta N_m(k, \theta) = \min [\Delta N_p(k, \theta), \Delta N_r(k, \theta)], \quad (3.66)$$

$$\Delta N_p(k, \theta) = X_p \frac{\alpha}{\pi} \frac{(2\pi)^4}{g^2} \frac{1}{\sigma k^3}, \quad (3.67)$$

$$\Delta N_r(k, \theta) = X_r \max [N(k, \theta), N_f], \quad (3.68)$$

$$N_f = \max \left[\Delta N_p(k_{\max}, \theta), X_f \max_{\forall k, \theta} \{ N(k, \theta) \} \right], \quad (3.69)$$

	X_p	X_r	X_f	$\Delta t_{d,\min}$
WAM equivalent	$\frac{\pi}{24}10^{-3}\Delta t$	$\infty(\geq 1)$	–	Δt_g
suggested	0.1-0.2	0.1-0.2	0.05	$\approx 0.1\Delta t_g$
default setting	0.15	0.10	0.05	–

Table 3.1: User-defined parameters in the source term integration scheme

where X_p , X_r and X_f are user-defined constants (see Table 3.1), α is a PM spectrum energy level (set to $\alpha = 0.62 \times 10^{-4}$) and k_{\max} is the maximum discrete wavenumber. The parametric spectral shape in (3.67) corresponds in deep water to the well-known high-frequency shape of the one-dimensional frequency spectrum $F(f) \propto f^{-5}$. The link between the filter level and the maximum parametric change in (3.69) is used to assure that the dynamic time step remains reasonably large in cases with extremely small wave energies. A final safeguard for stability of integration is provided by limiting the discrete change of action density to the maximum parametric change (3.67) in conditions where Eq. (3.63) dictates Δt_d^n . In this case Eq. (3.63) becomes a limiter as in the WAM model. Impacts of limiters are discussed in detail in for instance Hersbach and Janssen (1999, 2001), Hargreaves and Annan (2001) and Tolman (2002c).

The dynamic time step is calculated for each grid point separately, adding additional computational effort only for grid points in which the spectrum is subject to rapid change. The source terms are re-calculated for every dynamic time step.

It is possible to compile WAVEWATCH III without using a linear growth term. In such a case, waves can only grow if some energy is present in the spectrum. In small-scale applications with persistent low wind speeds, wave energy might disappear completely from part of the model. To assure that wave growth can occur when the wind increases, a so-called seeding option is available in WAVEWATCH III (selected during compilation). If the seeding option is selected, the energy level at the seeding frequency $\sigma_{\text{seed}} = \min(\sigma_{\max}, 2\pi f_{hf})$ is required to at least contain a minimum action density

$$N_{\min}(k_{seed}, \theta) = 6.25 \times 10^{-4} \frac{1}{k_{seed}^3 \sigma_{seed}} \max [0., \cos^2(\theta - \theta_w)] \min \left[1, \max \left(0, \frac{|u_{10}|}{X_{seed} g \sigma_{seed}^{-1}} - 1 \right) \right], \quad (3.70)$$

where $g\sigma_{seed}^{-1}$ approximates the equilibrium wind speed for the highest discrete spectral frequency. This minimum action distribution is aligned with the wind direction, goes to zero for low wind speeds, and is proportional to the integration limiter (3.67) for large wind speeds. $X_{seed} \geq 1$ is a user-defined parameter to shift seeding to higher frequencies. Seeding starts if the wind speed reaches X_{seed} times the equilibrium wind speed for the highest discrete frequency, and reaches its full strength for twice as high wind speeds. The default model settings include the seeding algorithm, with $X_{seed} = 1$.

In model version 3.11, surf-zone physics parameterizations have been introduced. Such physics, particularly depth-induced breaking, operate on much smaller time scales than deep water and limited-depth physics outside the surf zone. To assure reasonable behavior for larger time steps, an additional optional limiter has been adopted from the SWAN model, which can be used instead of modeling surf-breaking explicitly. This limiter is similar to the Miche style maximum wave height in the depth-limited wave breaking source term of Eq. (2.161). In this limiter, the maximum wave energy E_m is computed as

$$E_m = \frac{1}{16} [\gamma_{lim} \tanh(\bar{k}d) / \bar{k}]^2, \quad (3.71)$$

where γ_{lim} is a factor comparable to γ_M in Eq. (2.161), with the caveat that γ_M is representative for an individual wave, whereas γ_{lim} is representative for the significant wave height. For monochromatic waves, the original expression by Miche (1944) would correspond to $\gamma_{lim} = 0.94$ and replacing H_s by the height H of the waves. Here this idea is applied to random waves. In shallow water, this limits H_s to be less than $\gamma_{lim}d$. If the total spectral energy E is larger than the maximum energy E_m , the limiter is applied by simply rescaling the spectrum by the factor E/E_m , loosely following the argumentation from Eldeberky and Battjes (1996) and used in Section 2.3.17.

This limiter can be switched on or off in the compilation of the model, and γ_{lim} can be adjusted by the user. The default is set to $\gamma_{lim} = 1.6$ because

H_{rms} values close to d have indeed been recorded and thus taking a ratio H_s/H_{rms} of 1.4, using 1.6 allows this large steepness to be exceeded by some margin. Note that this limiter should be used as a ‘safety valve’ only, and hence that it should be less strict than the breaking criterion in the surf-breaking or whitecapping source terms, if these source terms are modeled explicitly.

Also, this limiter does not guarantee that all parts of the spectrum are realistic. Indeed, the use of a mean wavenumber, as in the Komen et al. dissipation, makes it possible to have unrealistically steep short waves in the presence of swell. A future extension of this limiter could be to limit the steepness with a partial spectral integration in frequencies, to make sure that waves of all scales are indeed not too steep.

3.7 Ice source terms integration

Because the attenuation and scattering in the ice can be very strong (although they are linear), it is convenient to perform a separate integration of the ice terms $S_{ice} = S_{id} + S_{is}$. This combines a dissipation term

$$S_{id}/\sigma = \beta_{id}N, \quad (3.72)$$

and a scattering term which is of the form

$$\frac{S_{is}(k, \theta)}{\sigma} = \int_0^{2\pi} \beta_{is}[N(k, \theta') - N(k, \theta)]d\theta', \quad (3.73)$$

in which the scattering coefficient β_{is} is a priori a function of the difference in direction between incident θ' and scattered θ directions, as well as the shape of ice floes. In general the directional spectrum $N(k, \cdot)$ is a vector with NTH (number of directions) components, and the source term is a vector of the same size given by the matrix product $S/\sigma = MN(k, \cdot)$ where M is a positive symmetric square NTH by NTH matrix with components given from the β_{id} values. The matrix M is easily diagonalized as

$$M = VDVT, \quad (3.74)$$

where D is a diagonal matrix containing all eigenvalues and V is the array of eigenvectors, and V^T is its transpose. As a result the split wave action

equation for ice source terms

$$\frac{\partial N}{\partial t c_g} = \frac{S_{\text{id}}}{\sigma c_g}, \quad (3.75)$$

can be rewritten for the action N_i of each eigenvector V_i with eigenvalue λ_i as

$$\frac{\partial N_i}{\partial t c_g} = \frac{\beta_{\text{id}} + \lambda_i}{\sigma c_g} N_i, \quad (3.76)$$

which has the following exact solution

$$N_i(t + \Delta t_g) = N_i(t) \exp [(\beta_{\text{id}} + \lambda_i) \Delta t_g]. \quad (3.77)$$

In all cases the eigenvector corresponding to an isotropic spectrum has an eigenvalue $\lambda = \beta_{\text{id}}$. In the case of an isotropic back-scatter, the other eigenvalues are all equal to $(\beta_{\text{id}} + \beta_{\text{is}})$. This decomposition over the two eigenspaces simplifies the solution to

$$N(t + \Delta t_g) = \exp(\beta_{\text{id}} \Delta t_g) \bar{N}(t) + \exp [(\beta_{\text{id}} + \beta_{\text{is}}) \Delta t_g] [N(t) - \bar{N}(t)], \quad (3.78)$$

where \bar{N} is the average over all directions. As a result, for a spatially homogeneous field, the spectrum exponentially tends to isotropy over a time scale $1/(\beta_{\text{id}})$.

3.8 Simple ice blocking (IC0)

Switch:	IC0
Origination:	WAVEWATCH III
Provided by:	H. L. Tolman

Ice covered sea is considered as ‘land’ in WAVEWATCH III, assuming zero wave energy and boundary conditions at ice edges are identical to boundary conditions at shore lines. Grid points are taken out of the calculation if the ice concentration becomes larger than a user-defined concentration. If the ice concentration drops below its critical value, the corresponding grid point is ‘re-activated’. The spectrum is then initialized with a PM spectrum based on the local wind direction with a peak frequency corresponding to

the second-highest discrete frequency in the grid. A low energy spectrum is used to assure that spectra are realistic, even for shallow coastal points.

The above discontinuous ice treatment represents the default model setting in WAVEWATCH III. In the framework of the modeling of unresolved obstacles as discussed in Section 3.4.7, a continuous method is also available, as given by Tolman (2003b). In this method, a user-defined critical ice concentration at which obstruction begins ($\epsilon_{c,0}$) and is complete ($\epsilon_{c,n}$) are given (defaults are $\epsilon_{c,0} = \epsilon_{c,n} = 0.5$, i.e., discontinuous treatment of ice). From these critical concentrations, corresponding decay length scales are calculated as

$$l_0 = \epsilon_{c,0} \min(\Delta x, \Delta y), \quad (3.79)$$

$$l_n = \epsilon_{c,n} \min(\Delta x, \Delta y), \quad (3.80)$$

from which cell transmissions in x and y (α_x and α_y , respectively) are calculated as

$$\alpha_x = \begin{cases} 1 & \text{for } \epsilon\Delta x < l_0 \\ 0 & \text{for } \epsilon\Delta x > l_n \\ \frac{l_n - \epsilon\Delta x}{l_n - l_0} & \text{otherwise} \end{cases}, \quad \alpha_y = \begin{cases} 1 & \text{for } \epsilon\Delta y < l_0 \\ 0 & \text{for } \epsilon\Delta y > l_n \\ \frac{l_n - \epsilon\Delta y}{l_n - l_0} & \text{otherwise} \end{cases}. \quad (3.81)$$

Details of this model can be found in Tolman (2003b).

Updating of the ice map within the model takes place at the discrete model time approximately half way in between the valid times of the old and new ice maps. The map will not be updated, if the time stamps of both ice fields are identical.

The above description pertains to the switch IC0. Note that either ice transmissions for propagation (IC0), or ice as a source term can be used (IC1, IC2, IC3), but not both approaches at the same time.

3.9 Winds and currents

Model input mainly consists of wind and current fields. Within the model, winds and currents are updated at every time step Δt_g and represent values at the end of the time step considered. Several interpolation methods are available (selected during compilation). By default, the interpolation in time

consists of a linear interpolation of the velocity and the direction (turning the wind or current over the smallest angle). The wind speed or current velocity can optionally be corrected to (approximately) conserve the energy instead of the wind velocity. The corresponding correction factor X_u is calculated as

$$X_u = \max \left[1.25, \frac{u_{10,rms}}{u_{10,l}} \right], \quad (3.82)$$

where $u_{10,l}$ is the linearly interpolated velocity and $u_{10,rms}$ is the rms interpolated velocity. Finally, winds can optionally be kept constant and changed discontinuously (option not available for current).

Note that the auxiliary programs of WAVEWATCH III include a program to pre-process input fields (see Section 4.4.6). This program transfers gridded fields to the grid of the wave model. For winds and currents this program utilizes a bilinear interpolation of vector components. This interpolation can be corrected to (approximately) conserve the velocity or the energy of the wind or the current by utilizing a correction factor similar to Eq. (3.82).

3.10 Use of tidal analysis

Origination:	WAVEWATCH III
Provided by:	F. Ardhuin

In order to reduce the volume of input files, the water levels and currents can be defined by their tidal amplitudes and phases. This is made possible by using the TIDE switch which activates the detection of the needed information in current.ww3 and level.ww3 files. The tidal analysis can be performed from NetCDF current or water level files, using the `ww3_pnc` preprocessing program. In that case the analysis method uses the flexible tide analysis package by Foreman et al. (2009). The precomputed tidal constituents can be used at run time by `ww3_shel`.

However, that method may not be very efficient due to the large memory required to store a large number of tidal constituents because, like other forcing parameters, they are not decomposed across processors: each processor stores the full spatial grid of forcing parameters. To avoid this, the tidal constituents can be used to generate time series with the tidal prediction program `ww3_ptide`, which produces the usual `current.ww3` or `level.ww3` files.

The choice of tidal constituents for the analysis and prediction are specified in the input files for `ww3_prnc` and `ww3_ptide`. Two short-cuts are defined. `VFAST` is the following selection of 20 components, Z0 (mean), SSA, MSM, MSF, MF, 2N2, MU2, N2, NU2, M2, S2, K2, MSN2, MN4, M4, MS4, S4, M6, 2MS6, and M8. When using `ww3_shel` to do the tidal prediction, the time step for currents or water is set to 1800 s.

In `ww3_ptide`, there is also a quality check on the values of the tidal constituents that is performed: unrealistically large values of the amplitudes for some constituents can be defined in `ww3_ptide.inp`. For model grid points where these are exceeded, all components are set to zero, except for UNST grids, in which the neighbors are searched to provide a reasonable value and avoid strong gradients.

3.11 Wave crest and height space-time extremes

Origination:	WAVEWATCH III(ISMAR, NCEP)
Provided by:	Barbariol, F., Benetazzo, A., Alves, J.H.G.M.

Space-Time (ST) extreme waves are modeled in WAVEWATCH III based on the Euler Characteristics (EC) approach, which states that for a given multi-dimensional (2-D space + time), statistically homogeneous and stationary Gaussian random wave field, the probability of exceedance of the maximal sea surface elevation is approximated by means of the mean value of the EC (Fedele et al., 2012). The ST extreme elevation model used here was formulated by Fedele (2012) for Gaussian sea waves, and extended to second-order nonlinear spatial wave fields by Fedele et al. (2013) and spatio-temporal fields by Benetazzo et al. (2015). The proposed ST extreme linear model was assessed with numerical simulations (Barbariol et al., 2015), while the extension to second-order nonlinear waves was verified using stereo imaging (Fedele et al., 2013; Benetazzo et al., 2015). According to those models, the probability of exceedance of the second-order nonlinear ST maximal crest height η_{2ST_m} is approximated (for large threshold z_2 with respect to the standard deviation of the surface elevation σ) as:

$$P(\eta_{2ST_m} > z_2) \approx \left[N_{3D} \left(\frac{z_1}{\sigma} \right)^2 + N_{2D} \left(\frac{z_1}{\sigma} \right) + N_{1D} \right] \exp \left(-\frac{z_1^2}{2\sigma^2} \right), \quad (3.83)$$

where the nonlinear threshold z_2 is related to its linear approximation z_1 via the Tayfun quadratic equation using the steepness parameter μ , strictly valid in deep waters, which accounts for bandwidth effects. Parameters N_{3D} , N_{2D} , and N_{1D} express the average number of 3D, 2D, and 1D waves within the ST region, respectively, and are determined from the moments m_{ijl} of the directional wave spectrum $S(k, \theta)$ defined as follows:

$$m_{ijl} = \int k_x^i k_y^j \omega^l S(k, \theta) dk d\theta. \quad (3.84)$$

The average number of waves in Eq. (3.83) also depends on the size of the spatio-temporal domain, namely the spatial dimension X along the mean direction of wave propagation, the spatial dimension Y orthogonal to the mean direction of wave propagation, and the duration D . The expected value $\bar{\eta}_{2ST_m}$ (output parameter **STMACE**, in meters) of the random variable η_{2ST_m} is given by

$$\begin{aligned} \bar{\eta}_{2ST_m} &= \mathbb{E} \{ \eta_{2ST_m} \} = \\ &\sigma \left[\left(h_1 + \frac{\mu}{2} h_1^2 \right) + \gamma \left(h_1 - \frac{2N_{3D}h_1 + N_{2D}}{N_{3D}h_1^2 + N_{2D}h_1 + N_{1D}} \right)^{-1} (1 + \mu h_1) \right], \end{aligned} \quad (3.85)$$

where $\gamma \approx 0.5772$ is the Euler-Mascheroni constant, and h_1 is the dimensionless (with respect to the standard deviation σ) most probable (mode) extreme value, which is the largest solution of the implicit equation in h

$$[N_{3D}h^2 + N_{2D}h + N_{1D}] \exp \left(-\frac{h^2}{2} \right) = 1. \quad (3.86)$$

The standard deviation σ_{2_m} (output parameter **STMAXD**, in meters) of the crest height η_{2ST_m} is given by:

$$\sigma_{2_m} = std(\eta_{2ST_m}) = \sigma \frac{\pi}{\sqrt{6}} \left(h_1 - \frac{2N_{3D}h_1 + N_{2D}}{N_{3D}h_1^2 + N_{2D}h_1 + N_{1D}} \right)^{-1} (1 + \mu h_1). \quad (3.87)$$

The expected value of the ST extreme crest-to-trough wave height is obtained using the Quasi-Determinism (QD) model, which predicts the mean shape of ST wave groups close to the apex of their development. According to the QD model the expected value of the crest-to-trough height $\bar{H}_{1_{cm}}$ (output

parameter **HCMAXE**, in meters) of the wave with linear extreme crest height $\bar{\eta}_{1ST_m}$ is expressed as

$$\bar{H}_{1_{cm}} = \mathbb{E} \{H_{1_{cm}}\} = \bar{\eta}_{1ST_m} (1 - \psi_1^*/\sigma^2), \quad (3.88)$$

where $\psi_1^* < 0$ is the value of the first minimum of the temporal autocovariance function computed from the spectrum as

$$\psi_1(\tau) = \int S(\omega) \cos(\omega\tau) d\omega, \quad (3.89)$$

and $\bar{\eta}_{1ST_m} \psi_1^*/\sigma^2 < 0$ is the expected displacement of the wave trough preceding or following the expected linear extreme crest height $\bar{\eta}_{1ST_m}$, which is computed using Eq. (3.85) after letting the wave steepness $\mu = 0$. For a given linear group, the height $\bar{H}_{1_{cm}}$ is generally smaller than the maximum expected wave height \bar{H}_{1_m} (output parameter **HMAXE**, in meters), which is computed as

$$\bar{H}_{1_m} = \mathbb{E} \{H_{1_m}\} = \bar{\eta}_{1ST_m} \sqrt{2(1 - \psi_1^*/\sigma^2)}. \quad (3.90)$$

The effect on wave heights of second-order nonlinearities is generally small, particularly in narrow band seas, and it will be neglected in the present implementation to reduce the computational cost. Uncertainty of estimates of $\bar{H}_{1_{cm}}$ (output parameter **HCMAXD**, in meters) and \bar{H}_{1_m} (output parameter **HMAXD**, in meters) are determined using the standard deviation of η_{1ST_m} (σ_{1_m} , which is computed using Eq. (3.87) after letting the wave steepness $\mu = 0$) as follows:

$$\begin{aligned} std(H_{1_m}) &= \sigma_{1_m} \sqrt{2(1 - \psi_1^*/\sigma^2)}, \\ std(H_{1_{cm}}) &= \sigma_{1_m} (1 - \psi_1^*/\sigma^2). \end{aligned} \quad (3.91)$$

In WAVEWATCH III, for each time step at all grid points, ST extremes are computed over the spatio-temporal region XYD ; the default values for $X = 1000$ m, $Y = 1000$ m, and $D = 1200$ s can be redefined by the user in the model input file `ww3_grid.inp` as namelists **STDX** (variable X), **STDY** (variable Y), **STDT** (variable D). In the present implementation, only the prognostic part of the spectrum is used for extreme computation. For additional implementation details, underlying approximations, assumptions and a full set of references for the fundamental theoretical and empirical framework underlying the ST extremes parameters used here, see Fedele (2012) and Barbariol et al. (2016).

To activate the computation of wave crest and height space-time extremes in WAVEWATCH III, the user has to specify values of the MISC namelist parameters `STDX`, `STDY` and `STDT` in `ww3_grid.inp` different to -1 (the latter is a default value that avoids computer overheads when these parameters are not wanted). `STDX` and `STDY` are spatial dimensions over which extremes are calculated. `STDT` is the time length over which extremes are calculated. If `STDX` and `STDY` are left at default values (-1), but `STDT` has a namelist value different to default (e.g., greater than 0), then extreme values are provided over time, for a point. Conversely, if `STDT` is kept at default (-1) and `STDX` and `STDY` are greater than zero, instantaneous extreme values are computed over space. When all three parameters are greater than zero, space-time probabilities and values are computed.

Wave crest and height space-time extremes outputs follow the standard WAVEWATCH III parameter framework, and have to be specified as namelists or flags in `ww3_shel.inp` or `ww3_multi.inp`, in which case they are included in the standard gridded binary output files during a model run. Consequently, they also have to be specified in gridded output post-processors for obtaining a final human-readable form. Space-time extremes output parameters available in WAVEWATCH III are provided in Table 3.2.

Internal Label	User-Interface Label	Description
STMAXE	MXE	Max surface elev (STE)
STMAXD	MXES	STD of max crest (STE)
HMAXE	MXH	Max wave height (STE)
HCMAXE	MXHC	Max wvhgt from crest (STE)
HMAXD	SDMH	STD of MXH (STE)
HCMAXD	SDMHC	STD of MXHC (STE)

Table 3.2: User-defined parameters in the computation of wave crest and height space-time extremes.

3.12 Spectral partitioning

Origination:	APL Wave / XWaves / IMEDS
Provided by:	B. Tracy

Fig. 3.6 shows an example surface plot of an energy density spectrum at one grid point at a specific time. The amount of energy density at each frequency-direction intersection is shown by this surface. The surface is divided into shaded areas or partitions representing energy from sub-peaks within the spectrum. Fig. 3.6 shows four spectral partitions, an area of windsea and three swell trains. The total energy represented by this spectrum can be defined by bulk parameters, such as the significant wave height H_s . The shaded areas, called partitions of the spectrum, show spectral sub-features that give more information about this grid point's energy situation. WAVEWATCH III has point and field output options available to provide quantitative descriptions of these individual spectral partition such as partition wave height, peak period of partition (parabolic fit), peak wavelength of partition, mean direction of partition, wind-sea fraction of partition (W) using Eq. (2.238), and the number of partitions. In the field output, these parameters correspond to spectral partitioned output fields 1 through 8 and can be found in Section 2.6.

Since the two-dimensional spectrum in Fig. 3.6 looks like a topological surface, it is logical to apply an image processing partitioning algorithm that treats the spectral surface like a topographical surface. The partitioning shown in Fig. 3.6 is based on a digital image processing watershed algorithm (Vincent and Soille, 1991) first prototyped by Hanson and Jensen (2004) for the analysis of ocean wave data. The US continental divide where everything to the east goes into the Atlantic Ocean and everything to the west goes into the Pacific Ocean is a typical example of a watershed line. The oceans represent minima that determine the watershed line. If the spectral surface is inverted, the spectral peaks become catchments and watershed lines or partition boundaries can be determined using the Vincent and Soille (1991) algorithm. Calculation of parameters for each spectral partition can then be accomplished and wave system analysis as described in Hanson and Phillips (2001) can be applied. Hanson and Jensen (2004) and Hanson et al. (2006) used a MATLAB code to apply the Vincent and Soille (1991) algorithm⁷. This code has been transformed to an efficient FORTRAN routine for use in WAVEWATCH III since version 3.11. Coding follows the Vincent and Soille (1991) paper but incorporates an efficient sort routine ($O(n)$) discussed in Tracy et al. (2006).

⁷ Now available as XWaves from <http://www.WaveForceTechnologies.com>, replacing the previous APL WAVES package

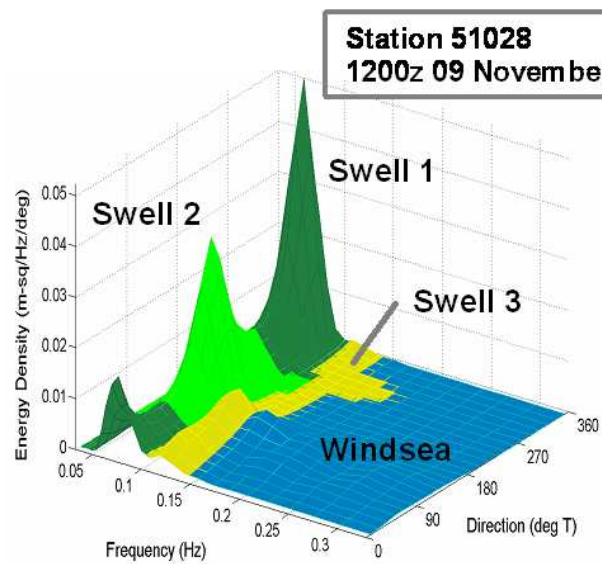


Figure 3.6: Surface plot of an energy density spectrum showing spectral partitions for windsea and three swell trains. This is a snapshot of hind-casted conditions at Christmas Island (NOAA buoy 51028) at 12:00 UTC on November 9, 2000.

3.13 Spatial and temporal tracking of wave systems

Origination:	IFP Swan
Provided by:	Van der Westhuysen, Hanson, Devaliere

The spectral partitioning procedure described above is carried out within the spectral space, independently at each geographical grid point. As a result, there is no coherence between the identified partitions over geographical space and in time. Following Voorrips et al. (1997), Hanson and Phillips (2001) and Devaliere et al. (2009), a spatial correlation step is therefore applied. This is done by means of an outwardly running spiral, originating at an arbitrary point (typically the center) inside the computational domain. Figure 3.7 presents an example of such a tracking spiral on a regular computational grid over a coastal domain featuring landmass. At the spiral origin (location 1), each spectral partition is assigned an initial system index. The spatial correlation is then determined for each subsequent geographical location (2, 3, 4, ...) moving outward along the spiral. At each new geographical location, the peak period T_p , peak direction θ_p and significant wave height H_{m0} of each of its spectral partitions are correlated with the spatial means $\tilde{T}_{p,i}^n$, $\tilde{\theta}_{p,i}^n$ and $\tilde{H}_{m0,i}^n$ of the corresponding parameters at its neighboring geographical grid points (indicated by the superscript n) previously assigned a system i . the partition at the present grid point is assigned to the neighboring system i that minimizes the following Goodness-of-Fit (GoF) function:

$$GoF_i = \left(\frac{T_p - \tilde{T}_{p,i}^n}{\Delta T_n} \right)^2 + \left(\frac{\theta_p - \tilde{\theta}_{p,i}^n}{\Delta \theta_n} \right)^2 + \left(\frac{H_{m0} - \tilde{H}_{m0,i}^n}{\Delta H_n} \right)^2, \quad (3.92)$$

where ΔT_n , $\Delta \theta_n$ and ΔH_n are combining criteria (Van der Westhuysen et al., 2016). If either of the first two terms on the right hand side of (3.92) exceed unity for the closest match, the difference is considered too great and a new wave system is assigned to that partition. Here, the search range for neighboring points is set at 1, so that a maximum of four previously-associated neighbors can be found (e.g. location 15 will have the previously processed neighbors 3, 4, 5 and 14). In some cases, iterative combining is required.

The next step is to correlate these wave systems over time. Each system i at the current time level t is associated with its closest match amongst the systems j at the previous time level ($t - 1$). Three characteristics of

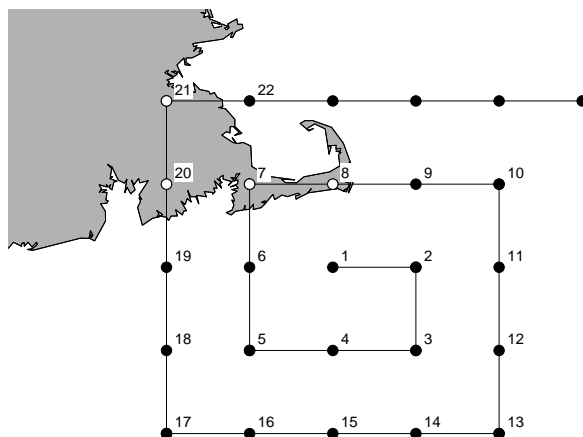


Figure 3.7: Example of a tracking spiral on a regular computational grid over a coastal domain featuring landmass (shaded). Black dots indicate active grid points and white dots indicate inactive (dry) grid points.

the wave systems are considered in this process, namely: (i) the spatial mean peak wave period over the system, $\tilde{T}_{p,t,i}^s$, with s denoting the system mean, (ii) the spatial mean peak wave direction, $\tilde{\theta}_{p,t,i}^s$ and (iii) the number of overlapping grid points between the two systems in geographical space $\cap_{i,j}$. These characteristics are combined to form the following GoF function:

$$GoF_{i,j} = \left(\frac{\tilde{T}_{p,t,i}^s - \tilde{T}_{p,t-1,j}^s}{\Delta T_s} \right)^2 + \left(\frac{\tilde{\theta}_{p,t,i}^s - \tilde{\theta}_{p,t-1,j}^s}{\Delta \theta_s} \right)^2 + \left(\frac{N_{t-1,j} - \cap_{i,j}}{0.5N_{t-1,j}} \right)^2, \quad (3.93)$$

where ΔT_s and $\Delta \theta_s$ are combining criteria, and N is the total number of grid points in a system, see [Van der Westhuysen et al. \(2016\)](#). In order to focus the tracking process on high-energy regions in the wave field, the spatial mean period and peak direction values of each system are weighted with the square of the significant wave height. System i at the current time level t is assigned the system j from the previous time level ($t-1$) that minimizes (3.93). If any of the three terms on the right hand side of (3.93) exceed unity for the system that minimizes (3.93), a new system number is assigned. For

the last term, this implies a minimum spatial overlap requirement, arbitrarily set at 50%. This term mostly has an impact over basin scale domains, where systems are typically smaller than the computational area. In order to improve robustness, the details of identified systems are stored for five time levels, after which the system association is released.

3.14 Nesting

Origination:	WAVEWATCH III
Provided by:	H. L. Tolman

Traditionally, wave models only consider one-way nesting, with boundary data from low-resolution grids being provided to high-resolution grids. This approach has always been available in WAVEWATCH III, and is discussed in Section 3.14.1. In model version 3.14, a multi-grid wave model driver was introduced, considering full two-way nesting between grids. This approach is discussed in Section 3.14.2. The illustrations below consider regular grids, but the principles discussed are applicable to curvilinear and triangular grids too.

3.14.1 Traditional one-way nesting

The conventional wave model program `ww3.shel` considers a single wave model grid. This program includes options to transfer boundary conditions from large-scale runs to small-scale runs. Each run can simultaneously accept one data set with boundary conditions, and generate up to 9 data sets with boundary conditions. To assure conservation of wave energy with incompatible depths and currents, the boundary data consists of energy spectra $F(\sigma, \theta)$. The data file consists of spectra at grid points of the generating run, and information needed to interpolate spectra at the requested boundary points. The size of the transfer files is thus minimized if the input points for a small-scale run are located on grid lines in the large-scale run. When used as input, the spectra are interpolated in space and time for every global time step Δt_g , using a linear interpolation of spectral components.

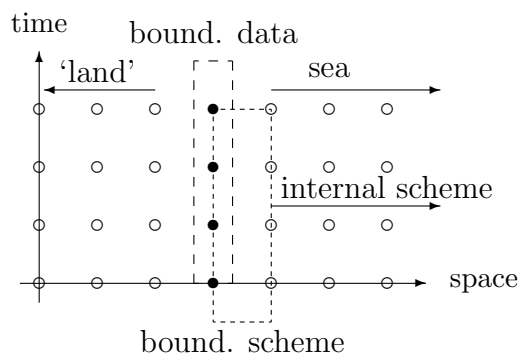


Figure 3.8: Traditional one-way nesting approach as used in `ww3_shel`. One-dimensional representation in space and time, symbols represent grid points.

The numerical approach for including boundary data in a wave model is illustrated in Fig. 3.8. Active boundary points are assigned in the grid to separate sea points from land points or from otherwise deactivated grid points. Between the active boundary points and sea points, a local boundary scheme is applied (typically first order). In the internal sea points of the model, the selected propagation scheme is used.

Practical aspects of the conventional one-way nesting approach are discussed in more detail in Appendix C.

3.14.2 Two-way nesting

Model version 3.14 includes an option to use the multi-grid or mosaic approach to wave modeling with the program `ww3_multi` (Tolman, 2006, 2007, 2008a). In this program, an arbitrary number of grids with arbitrary resolutions is considered, with data exchange between grids at each relevant model time step. The grids are given a rank number, where lower rank corresponds to lower resolution, and equal rank corresponds to similar resolution (but not necessarily equal resolution). Three types of data transfer between grids are considered:

- Transfer of data from lower to higher rank grids.

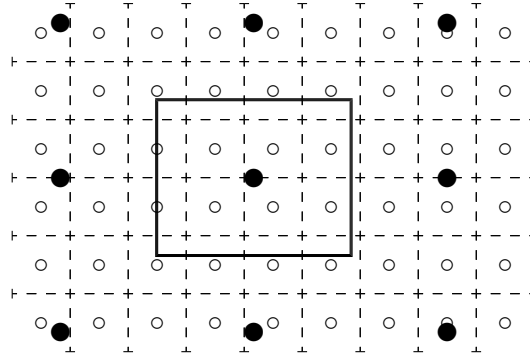


Figure 3.9: Concept for reconciling lower ranked grid with higher ranked grid in two-way nesting approach. \circ and hashed lines represent the higher ranked grid points and grid boxes, respectively, \bullet and solid lines represent lower ranked grid and central grid box.

- Transfer of data from higher to lower rank grids.
- Transfer of data between grids with equal rank.

Data transfer from lower to higher ranked grids is accomplished by providing boundary data to the higher ranked grid, as in the traditional one-way nesting approach described in the previous section and in Fig. 3.8.

When this approach is combined with data transfer from higher to lower rank, a full two-way nesting approach is established. In `ww3_multi` the data at the lower ranked grids is reconciled with the data at the higher ranked grids after the higher ranked grids have ‘caught up’ in time with the lower ranked grids. Considering that the resolution of the lower ranked grid by definition is lower than the resolution of the higher ranked grid, a natural way to estimate the wave energy in the lower ranked grid $E_{l,i}$ from energy in the higher ranked grid $E_{h,j}$ is

$$E_{l,i} = \sum w_{i,j} E_{h,j} \quad , \quad (3.94)$$

where i and j are grid counters in the two grids, and where $w_{i,j}$ are averaging weights. The weights can be defined consistent with conservation of wave energy as the surface of the grid box j in the higher ranked grid that covers the grid box i in the lower ranked grid, normalized with the surface of the

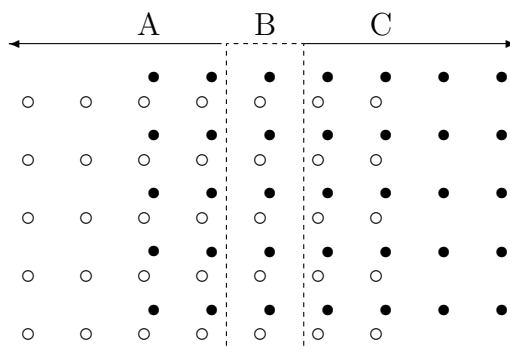


Figure 3.10: Concept for reconciling grids with identical rank and therefore similar resolution. \circ represents points of grid 1, \bullet represents grid 2.

lower ranked grid box i . This is illustrated in Fig. 3.9. To avoid circular reconciliation, grid points in the lower ranked grid that contribute to the boundary data in the higher ranked grid are not updated in this manner.

Overlapping grids with similar rank cannot use the above two-way nesting technique to consistently exchange data. Instead, all such grids are propagated one time step, after which the grids are reconciled as is illustrated in Fig. 3.10. For grid 1 (\circ in Fig. 3.10) two areas can be distinguished. In area C, the influence of the boundary has propagated into the grid since the last reconciliation. The actual depth of penetration depends on the stencil width of the numerical scheme, and the number of propagation time steps. In areas A and B, information from the boundary has not yet penetrated, and this area can be considered as the ‘interior’ of grid 1. Similarly, area A represents the boundary penetration depth for grid 2 (\bullet in Fig. 3.10) whereas B and C represent the interior of grid 2. A simple and consistent reconciliation between grid 1 and 2 uses data from grid 1 exclusively in area A (interpolating data from grid 1 to grid points in grid 2 as necessary), and uses data from grid 2 exclusively in area C. In area B, where interior parts of both grids overlap, a consistent solution can be found by using weighted averages from both grids. Note that this approach is easily extended to multiple overlapping grids.

Note that for explicit numerical propagation schemes and overlapping grids with identical resolution and coinciding grid points, solutions for over-

lapping grids and the compatible single grid can be identical, as long as the overlap areas are sufficiently wide.

The two-way nesting techniques in `ww3_multi` are largely automated. Each grid is prepared individually, with its own preferred time stepping information. Locations where each grid expects to get boundary data from lower ranked grids are marked as in the one-way nesting approach. All other book-keeping needed to implement the two-way nesting techniques are automated, although some iterations may be needed to assure that all input boundary points defined in each grid can be provided with boundary data from other grids in the multi-grid application. Alternatively, each grid can obtain data from an external data file as in the traditional nesting approach. In the present implementation, each grid has to obtain all boundary data from a single file, or from other grids in the multi-grid application, but cannot receive data from file and grids simultaneously. Details on the management algorithm developed to run all grid simultaneously can be found in [Tolman \(2007, section 3.4\)](#) and [Tolman \(2008a\)](#), and will not be reproduced here.

Note that the grids used in `ww3_multi` do not need to have the same spectral discretization. Spectra are converted on the fly in `ww3_multi`. Details on the numerical techniques used for this approach can be found in [Tolman \(2007, section 3.5.5\)](#). Grid generation for multiple grids in such an approach can be cumbersome, and consistency between grids is required for consistent model results. For this reason automated grid generation utilities have been developed by [Chawla and Tolman \(2007, 2008\)](#).

4 Wave Model Structure and Data Flow

4.1 Program design

The core of WAVEWATCH III is the wave model subroutine. The wave model routine can be called by either a stand-alone program shell or any other program that requires dynamically updated wave data. Two such programs are provided with the WAVEWATCH III release. Auxiliary programs include a grid preprocessor, a program to generate artificial initial conditions, a generic program shell (and a corresponding input pre-processor) and output post-processors. In the discussion of the model below, file names will be identified by the file type font, the contents of a file by the code type font and FORTRAN program elements by the FORTRAN type font.

The main wave model routine is `w3WAVE`. Data files are identified with the file extension `.ww3`, except in the multi-grid wave model `ww3_multi`, where the file extension identifies an individual grid. For simplicity, the file extension `.ww3` will be used throughout this chapter. A relational diagram including the basic data flow is presented in Fig. 4.1.

The grid preprocessor writes a model definition file `mod_def.ww3` with bottom and obstruction information and parameter values defining the physical and numerical approaches. The wave model requires initial conditions, consisting of a restart file `restart.ww3`, written by either the wave model itself, or by the initial conditions program. If this file is not available, the wave model will be initialized automatically, depending on the ability of the model to start from calm conditions. If linear growth or spectral seeding is switch on, the model will start from calm conditions ($H_s = 0$), otherwise the initial conditions will consist of a parametric fetch-limited spectrum based on the initial wind field (see the corresponding option in the initial conditions program).

The wave model routine (`w3WAVE`) optionally generates up to 9 restart files `restartn.ww3`, where n represents a single digit integer number. The wave model also optionally reads boundary conditions from the file `nest.ww3` and generates boundary conditions for consecutive runs in `nestn.ww3`. The model furthermore dumps raw data to the output files `out_grd.ww3`, `out_pnt.ww3`, `track_o.ww3` and `partition.ww3` (gridded mean wave parameters, spectra at locations, spectra along tracks, and partitioned wave data, respectively).

The tracks along which spectra are to be presented is defined in the file `track.i.ww3`. Note that the wave model does not write to standard output, because this would be inconvenient if WAVEWATCH III is part of an integrated model. Instead, it maintains its own log file `log.ww3` and optionally a test output files `test.ww3` for a shared memory version of the model, or `testnnn.ww3` for distributed memory versions, where *nnn* is the processor number starting with 1. Finally, various output post-processors are available (binary post-processing of raw gridded fields, point output and track output files; NetCDF and GRIB(2) packing of wave data; post-processing for later GrADS graphical processing of gridded and spectral data). A more detailed description of all program elements and their input files is given below. Note that the source codes of each routine are fully documented. This documentation is an additional source of information about WAVEWATCH III.

Files specific to WAVEWATCH III are opened by name within the program. The unit numbers, however, have to be defined by the user⁸, guaranteeing the largest possible flexibility for implementation in integrated models.

Next to the wave model subroutine, an initialization routine and an interface routine for data assimilation are provided. The latter routine is intended to be run side by side with the wave model routine. The routine includes a generic interface that provides all necessary model components to perform full spectral data assimilation. This routine is integrated into the generic wave model shell, which is set up to perform time step managements for a wave model with or without data assimilation. The shell also provides a simple yet flexible way to provide the data assimilation scheme with various types of data. Data assimilation has not yet been included in the multi-grid wave model shell.

4.2 The wave model routines

As discussed above, the actual wave model is a subroutine. To run the model, a program shell is needed. WAVEWATCH III is provided with a simple stand-alone shell as will be discussed in Section 4.4.9, and with a more complex multi-grid model shell as will be discussed in Section 4.4.11. The present section concentrates on the wave model subroutines.

⁸ Except for `ww3_multi`.

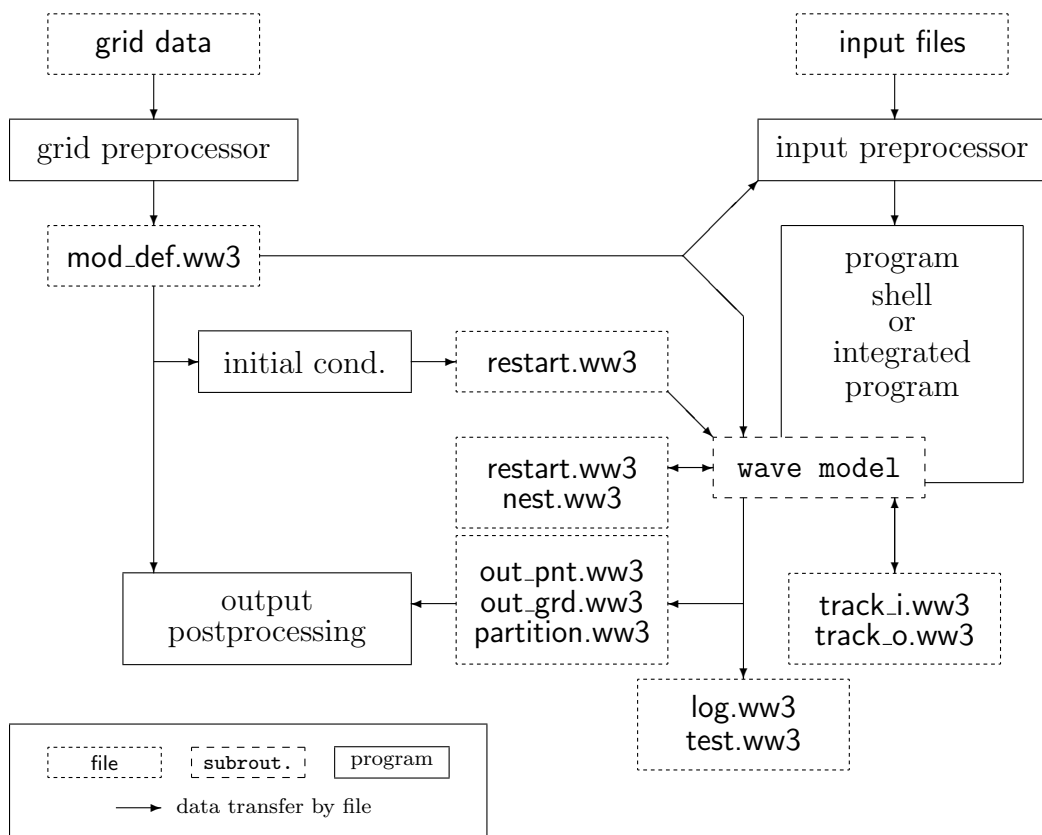


Figure 4.1: Basic program elements and data flow

step	pass	date	time	input				output						
				b	w	l	c	i	d	g	p	t	r	b
0	1	1968/06/06	00:00:00	F				X	X					
8	1		02:00:00					X						
12	1		03:00:00					X						
16	1		04:00:00					X						
24	1		06:00:00	X				X	X					
32	2		08:00:00					X						
36	2		09:00:00					L						
40	2		10:00:00					X						
48	2		12:00:00	X		X		L	L					

Figure 4.2: Example action table from file `log.ww3`.

The wave model initialization routine `w3INIT` performs model initialization for a single wave model grid. This includes setting up part of the I/O system by defining unit numbers, initializing internal time management, processing the model definition file (`mod_def.ww3`), processing initial conditions (`restart.ww3`), preparing model output, and calculating grid-dependent parameters. If the model is compiled for an MPI environment, all necessary communication for both calculations and output are determined and initialized (the model uses persistent MPI communication throughout).

The wave model routine `w3WAVE` can be called any number of times to propagate the wave field for a single grid in time after the initialization has taken place. After some initial checks, the subroutine interpolates winds and currents, updates ice concentrations and water levels, propagates the wave field, and applies the selected source terms for a number of time steps. The internal time step is defined by the interval for which the calculations are to be performed, and by the requested output times. At the end of the calculations, the routine provides the calling program with the requested fields of wave data. A documentation of the interface of `w3WAVE` can be found in the source code (`w3wavemd.ftn`).

Apart from the raw data files as described above, the program maintains a log file `log.ww3`. This file is opened by `w3INIT` (contained in `w3WAVE` in

`w3wavemd.ftn`), which writes some self-explanatory header information to this file. Each consecutive call to `w3WAVE` adds several lines to an ‘action table’ in this log file as is shown in Fig. 4.2. The column identified as ‘step’ shows the discrete time step considered. The column identified as ‘pass’ identifies the sequence number of the call to `w3WAVE`; i.e., 3 identifies that this action took place in the third call to `w3WAVE`. The third column shows the ending time of the time step. In the input and output columns the corresponding actions of the model are shown. An **X** identifies that the input has been updated, or that the output has been performed. An **F** indicates a first field read, and an **L** identifies the last output. The seven input columns identify boundary conditions (**b**), wind fields (**w**), water levels (**l**), current fields (**c**), ice concentrations (**i**), and data for assimilation (**d**), respectively. Note that data assimilation takes place at the end of the time step after the wave routine call. The seven output columns identify gridded output (**g**), point output (**p**), output along tracks (**t**), restart files (**r**), boundary data (**b**), and partitioned spectral data (**f**), and output for coupling (**c**), respectively.

For the multi-grid wave model (Tolman, 2008a, `ww3_multi`) a set of routines is build around the basic wave model routines. The three main routines are the initialization routine `WMINIT`, a time stepping routine `WMWAVE` and a finalization routine `WMFINL`, with similar functions as the routines for a single grid as described above. Note that the raw input and output files are generated for separate grid in the mosaic, and are identified by replacing the standard file extension `.ww3` with a unique identifier for each individual grid. Log files are maintained for each individual grid, as well as an overall log file `log.mww3`.

4.3 The data assimilation interface

As discussed above, the wave model subroutine is supplemented with a data assimilation interface routine (`w3WDAS` in `w3wdasmd.ftn`). This routine is integrated in the stand-alone shell (see Section 4.4.9) to provide time step management of a combined wave model / data assimilation scheme. It has not yet been integrated in the multi-grid model driver, although it is accounted for in the multi-grid model management algorithm. In this a fairly simple approach is assumed where data assimilation is performed at selected times, while the wave model marches forward in time. In the setup of the

shell, the data assimilation is performed after the model has reached the target time, but has not yet produced output. After the data assimilation is performed, the wave model routine is called again only to generate output as requested. Thus, the wave model output for a given time will include the effects of data assimilation for that specific target time.

The generic program shell also processes several types of data to be assimilated, and passes it on to the data assimilation interface routine. All data needs to be preprocessed using the wave model input preprocessor (see Section 4.4.6), and will be recognized by the generic shell by file name. Presently, up to three different data files can be used. Tentatively, these could be mean wave parameters, one dimensional spectral data, and two dimensional spectral data, respectively. This is, however, not hardwired to the model and in fact needs to be defined by the user.

Presently, no data assimilation packages are available. User supplied data assimilation schemes can be included in the wave model using the interface routine (`W3WDAS` in `w3wdasmd.ftn`), the documentation of which should be sufficient for the necessary programming. Details on how to add user supplied software to the WAVEWATCH III compilation system can be found in the following chapter. NCEP is presently working on wave data assimilation techniques, but presently has no plans to distribute wave data assimilation software.

4.4 Auxiliary programs

4.4.1 General concepts

All auxiliary programs presented here, with the exception of the track output post-processor, read input from a pre-defined input file. The first character on the first line of the input file will be considered to be the comment character, identifying comment lines in the input file. This comment character has to appear on the first position of input lines to be effective. In all examples in the following sections lines starting with '\$' therefore only contain comment. The programs furthermore all write formatted output to the standard output unit.

In the following sections, all available auxiliary programs are described using an example input file with all options included (partially as comment).

These files are identical to the distributed example input files. The sections furthermore show the name of the executable program, the program name (as appears in the program statement), the source code file and input and output files and their unit numbers (in brackets behind the file name). Input and output files marked with * are optional. The intermediate files mentioned below are all UNFORMATTED, and are not described in detail here. Each file is written and read by a single routine, to which reference is made for additional documentation.

mod_def.ww3	Subroutine W3IOGR (w3iogrmd.ftn).
out_grd.ww3	Subroutine W3IOGO (w3iogomd.ftn).
out_pnt.ww3	Subroutine W3IOPO (w3iopomd.ftn).
track_o.ww3	Subroutine W3IOTR (w3iotrmd.ftn).
restart.ww3	Subroutine W3IORS (w3iorsmd.ftn).
nest.ww3	Subroutine W3IOBC (w3iobcmd.ftn).
partition.ww3	Subroutine W3IOSF (w3iosfmd.ftn).

Preprocessing and compilation of the programs is discussed in the following two chapters. Examples of test runs of the model are provided with the source code.

4.4.2 The grid preprocessor

Program	:	ww3_grid		(W3GRID)
Code	:	ww3_grid.ftn		
Input	:	ww3_grid.inp	(10)	Formatted input file for program.
		'grid file' *	(user)	File with bottom depths.
		'obstr. file' *	(user)	File with sub-grid obstructions.
		'mask file' *	(user)	File with grid mask.
Output	:	standard out	(6)	Formatted output of program.
		mod_def.ww3	(20)	Model definition file in WAVE-WATCH III format.
		mask.ww3 *	(20)	Land-sea mask file (switch o2a).
Scratch	:	ww3_grid.scratch	(90)	Formatted scratch file.

Note that bottom and obstruction data may be in same file.

start of example input file (traditional form)

```

$ ----- $
$ WAVEWATCH III Grid preprocessor input file $
$ ----- $
$ Grid name (C*30, in quotes)
$
$ 'TEST GRID (GULF OF NOWHERE) '
$
$ Frequency increment factor and first frequency (Hz) ----- $
$ number of frequencies (wavenumbers) and directions, relative offset
$ of first direction in terms of the directional increment [-0.5,0.5].
$ In versions 1.18 and 2.22 of the model this value was by definition 0,
$ it is added to mitigate the GSE for a first order scheme. Note that
$ this factor is IGNORED in the print plots in ww3_outp.
$
$ 1.1 0.04118 25 24 0.
$
$ Set model flags ----- $
$ - FLDRY Dry run (input/output only, no calculation).
$ - FLCX, FLCY Activate X and Y component of propagation.
$ - FLCTH, FLCK Activate direction and wavenumber shifts.
$ - FLSOU Activate source terms.
$
$ F T T T F T
$
$ Set time steps ----- $

```



```

$                                     through (2.65) for definition of
$                                     effective wind speed (!/STAB2).
$ WAM4 and variants : Namelist SIN3
$           ZWND      : Height of wind (m).
$           ALPHA0    : minimum value of Charnock coefficient
$           ZOMAX     : maximum value of air-side roughness z0
$           BETAMAX   : maximum value of wind-wave coupling
$           SINTHP    : power of cosine in wind input
$           ZALP      : wave age shift to account for gustiness
$           TAUWSHELTER : sheltering of short waves to reduce u_star
$           SWELLPAR  : choice of swell attenuation formulation
$                       (1: TC 1996, 3: ACC 2008)
$           SWELLF    : swell attenuation factor
$ Extra parameters for SWELLPAR=3 only
$           SWELLF2, SWELLF3 : swell attenuation factors
$           SWELLF4 : Threshold Reynolds number for ACC2008
$           SWELLF5 : Relative viscous decay below threshold
$           ZORAT    : roughness for oscil. flow / mean flow
$ BYDRZ input      : Namelist SIN6
$           SINAO    : factor for negative input
$           SINU10   : wind speed scaling option
$
$ Nonlinear interactions - - - - -
$ Discrete I.A.      : Namelist SNL1
$           LAMBDA   : Lambda in source term.
$           NLPROP   : C in sourc term. NOTE : default
$                       value depends on other source
$                       terms selected.
$           KDCONV   : Factor before kd in Eq. (n.nn).
$           KDMIN, SNLCS1, SNLCS2, SNLCS3 :
$                       Minimum kd, and constants c1-3
$                       in depth scaling function.
$ Exact interactions : Namelist SNL2
$           IQTYPE   : Type of depth treatment
$                       1 : Deep water
$                       2 : Deep water / WAM scaling
$                       3 : Shallow water
$           TAILNL   : Parametric tail power.
$           NDEPTH   : Number of depths in for which
$                       integration space is established.
$                       Used for IQTYPE = 3 only
$           Namelist ANL2
$           DEPTHS   : Array with depths for NDEPTH = 3
$ Gen. Multiple DIA : Namelist SNL3
$           NQDEF    : Number of quadruplets.

```

```

$           MSC   : Scaling constant 'm'.
$           NSC   : Scaling constant 'N'.
$           KDFD  : Deep water relative filter depth,
$           KDFS  : Shallow water relative filter depth,
$           Namelist ANL3
$           QPARMS : 5 x NQDEF paramaters describing the
$                   quadruplets, repeating LAMBDA, MU, DT12.
$                   Cdeep and Cshal. See examples below.
$ Two Scale Approx. : Namelist SNL4
$                   IND TSA : Index for TSA/FBI computations
$                           (0 = FBI ; 1 = TSA)
$                   ALTLP  : Index for alternate looping
$                           (1 = no ; 2 = yes)
$
$ Traditional DIA setup (default):
$
$ &SNL3 NQDEF = 1, MSC = 0.00, NSC = -3.50 /
$ &ANL3 QPARMS = 0.250, 0.000, -1.0, 0.1000E+08, 0.0000E+00 /
$
$ GMD3 from 2010 report (G13d in later paper) :
$
$ &SNL3 NQDEF = 3, MSC = 0.00, NSC = -3.50 /
$ &ANL3 QPARMS = 0.126, 0.000, -1.0, 0.4790E+08, 0.0000E+00 ,
$               0.237, 0.000, -1.0, 0.2200E+08, 0.0000E+00 ,
$               0.319, 0.000, -1.0, 0.1110E+08, 0.0000E+00 /
$
$ G35d from 2010 report:
$
$ &SNL3 NQDEF = 5, MSC = 0.00, NSC = -3.50 /
$ &ANL3 QPARMS = 0.066, 0.018, 21.4, 0.170E+09, 0.000E+00 ,
$               0.127, 0.069, 19.6, 0.127E+09, 0.000E+00 ,
$               0.228, 0.065, 2.0, 0.443E+08, 0.000E+00 ,
$               0.295, 0.196, 40.5, 0.210E+08, 0.000E+00 ,
$               0.369, 0.226, 11.5, 0.118E+08, 0.000E+00 /
$
$ Nonlinear filter based on DIA - - - - -
$           Namelist SNLS
$           A34   : Relative offset in quadruplet
$           FHFC  : Proportionality constants.
$           DMN   : Maximum relative change.
$           FC1-3 : Constants in frequency filter.
$
$ Whitecapping dissipation - - - - -
$ WAM-3       : Namelist SDS1
$             CDIS, APM : As in source term.

```

```

$
$ Tolman and Chalikov : Namelist SDS2
$           SDSA0, SDSA1, SDSA2, SDSB0, SDSB1, PHIMIN :
$           Constants a0, a1, a2, b0, b1 and
$           PHImin.
$
$ WAM4 and variants   : Namelist SDS3
$           SDSC1      : WAM4 Cds coefficient
$           MNMEANP, WNMEANPTAIL : power of wavenumber
$           for mean definitions in Sds and tail
$           SDSDELTA1, SDSDELTA2 : relative weights
$           of k and k^2 parts of WAM4 dissipation
$           SDSLF, SDSHF : coefficient for activation of
$           WAM4 dissipation for unsaturated (SDSLF) and
$           saturated (SDSHF) parts of the spectrum
$           SDSC2      : Saturation dissipation coefficient
$           SDSC4      : Value of B0=B/Br for wich Sds is zero
$           SDSBR      : Threshold Br for saturation
$           SDSP       : power of (B/Br-B0) in Sds
$           SDSBR2     : Threshold Br2 for the separation of
$           WAM4 dissipation in saturated and non-saturated
$           SDSC5 : coefficient for turbulence dissipation
$           SDSC6 : Weight for the istropic part of Sds_SAT
$           SDSDTH: Angular half-width for integration of B
$
$ BYDRZ              : Namelist SDS6
$           SDSET      : Select threshold normalization spectra
$           SDSA1, SDSA2, SDSP1, SDSP2 :
$           Coefficients for dissipation terms T1 and T2
$           : Namelist SWL6
$           SWLB1      : Coefficient for swell dissipation
$
$ Bottom friction  - - - - -
$   JONSWAP        : Namelist SBT1
$           GAMMA      : Bottom friction emprical constant
$
$ Surf breaking   - - - - -
$   Battjes and Janssen : Namelist SDB1
$           BJALFA     : Dissipation constant (default = 1)
$           BJGAM      : Breaking threshold (default = 0.73)
$           BJFLAG     : TRUE  - Use Hmax/d ratio only (default)
$                       FALSE - Use Hmax/d in Mische formulation
$
$ Dissipation in the ice  - - - - -

```

```

$ Generalization of Liu et al. : Namelist SIC2
$           IC2DISPER  : If true uses Liu formulation with eddy viscosity
$                   If false, uses the generalization with turbulent
$                   to laminar transition
$           IC2TURB   : empirical factor for the turbulent part
$           IC2ROUGH  : under-ice roughness length
$           IC2REYNOLDS: Re number for laminar to turbulent transition
$           IC2SMOOTH : smoothing of transition representing random waves
$           IC2VISC   : empirical factor for viscous part
$
$
$ Scattering in the ice & creep dissipations- - - - -
$ Generalization of Williams et al. : Namelist SIS2
$           ISC1       : scattering coefficient (default = 1)
$           IS2BACKSCAT : fraction of energy back-scattered (default = 1 )
$           IS2BREAK   : TRUE  - changes floe max diameter
$                   : FALSE - does not change floe max diameter
$           IS2C1      : scattering in pack ice
$           IS2C2      : frequency dependance of scattering in pack ice
$           IS2C3      : frequency dependance of scattering in pack ice
$           ISBACKSCAT : fraction of scattered energy actually redistributed
$           IS2DISP    : use of ice-specific dispersion relation (T/F)
$           FRAGILITY  : parameter between 0 and 1 that gives the shape of
$           IS2DMIN    : minimum floe diameter in meters
$           IS2DAMP    : multiplicative coefficient for dissipation term f
$           IS2UPDATE  : TRUE  - updates the max floe diameter with forcin
$                   : FALSE - updates the max floe diameter at each tim
$
$ Triad nonlinear interactions - - - - -
$ Lumped Triad Interaction (LTA) : Namelist STR1 (To be implemented)
$           PTRIAD1 : Proportionality coefficient (default 0.05)
$           PTRIAD2 : Multiple of Tm01 up to which interaction
$                   is computed (2.5)
$           PTRIAD3 : Ursell upper limit for computing
$                   interactions (not used, default 10.)
$           PTRIAD4 : Shape parameter for biphas
$                   computation (0.2)
$           PTRIAD5 : Ursell number treshold for computing
$                   interactions (0.01)
$
$ Shoreline reflections - - - - -
$ ref. parameters      : Namelist REF1
$           REF Coast  : Reflection coefficient at shoreline
$           REF FREQ   : Activation of freq-dependent ref.
$           REF MAP    : Scale factor for bottom slope map

```

```

$          REFRMAX   : maximum ref. coefficient (default 0.8)
$          REFFREQPOW: power of frequency
$          REFICEBERG: Reflection coefficient for icebergs
$          REFSUBGRID: Reflection coefficient for islands
$          REFCOSP_STRAIGHT: power of cosine used for
$                               straight shoreline
$
$ Bound 2nd order spectrum and free IG - - - - -
$   IG1 parameters      : Namelist SIG1
$           IGMETHOD  : 1: Hasselmann, 2: Krasitskii-Janssen
$           IGADDOUTP  : activation of bound wave correction
$                               in ww3_outp / ww3_oump
$           IGSOURCE   : 1: uses bound waves, 2: empirical
$           IGSTERMS   : > 0 : no source term in IG band
$           IGMAXFREQ  : maximum frequency of IG band
$           IEMPIRICAL: constant in empirical free IG source
$           IGBCOVERWRITE: T: Replaces IG spectrum, does not add
$           IGWELLMAX  : T: activates free IG sources for all freq.
$
$
$ Propagation schemes ----- $
$   First order        : Namelist PRO1
$           CFLTM      : Maximum CFL number for refraction.
$
$   UQ/UNO with diffusion : Namelist PRO2
$           CFLTM      : Maximum CFL number for refraction.
$           DTIME     : Swell age (s) in garden sprinkler
$                               correction. If 0., all diffusion
$                               switched off. If small non-zero
$                               (DEFAULT !!!) only wave growth
$                               diffusion.
$           LATMIN    : Maximum latitude used in calc. of
$                               strength of diffusion for prop.
$
$   UQ/UNO with averaging : Namelist PRO3
$           CFLTM      : Maximum CFL number for refraction.
$           WPTHCG     : Tuning factor propag. direction.
$           WPTHTH     : Tuning factor normal direction.
$
$   Note that UQ and UNO schemes have no tunable parameters.
$   All tuneable parameters are associated with the refraction
$   limitation and the GSE alleviation.
$
$ Unstructured grids ----- $
$   UNST parameters    : Namelist UNST

```



```

$          UGOBCAUTO : TRUE: OBC points are taken from type 15 elements
$                      FALSE: OBC points must be listed in ww3_grid.inp
$          UGOBCDEPTH: Threshold ( < 0) depth for OBC points if UGOBCAUTO is
$          EXPFSN     : Activation of N scheme
$          EXPFSPSI   : Activation of PSI scheme
$          EXPFSFCT   : Activation of FCT scheme
$          IMPFSN     : Activation of N implicit scheme
$
$ SMC grid propagation : Namelist PSMC and default values
$          CFLTM     : Maximum CFL no. for propagation, 0.7
$          DTIME     : Swell age for diffusion term (s), 0.0
$          LATMIN    : Maximum latitude (deg) for GCT, 86.0
$          RFMAXD    : Maximum refraction turning (deg), 80.0
$          LvSMC     : No. of refinement level, default 1
$          ISHFT     : Shift number of i-index, default 0
$          JEQT      : Shift number of j-index, default 0
$          NBISMC    : No. of input boundary points, 0
$          UNO3      : Use 3rd order advection scheme, .FALSE.
$          UNO3      : Add extra spatial averaging, .FALSE.
$ &PSMC DTIME = 39600.0, LATMIN=85.0, RFMAXD = 36.0, LvSMC=3, JEQT=1344 /
$
$ Output of 3D arrays----- $
$ In order to limit the use of memory, arrays for 3D output fields (i.e.
$ variables that are a function of both space and frequency, are not
$ declared, and thus cannot be used, unless specified by namelists.
$ NB: Output of 'first 5' moments E, th1m, sth1m, th2, sth2m allows to estimate the full
$ directional spectrum using, e.g. MEM (Lygre&Krogstad 1986).
$
$ Parameters (integers) : Namelist OUTS
$ For the frequency spectrum E(f)
$          E3D       : <=0: not declared, > 0: declared
$          I1E3D     : First frequency index of output (default is 1)
$          I2E3D     : Last frequency index of output (default is NK)
$ For the mean direction th1m(f), and spread sth1m(f)
$          TH1MF, STH1MF : <=0: not declared, > 0: declared
$          I1TH1MF, I1STH1MF: First frequency index of output (default is 1)
$          I2TH1MF, I2STH1MF: First frequency index of output (default is 1)
$ For the mean direction th2m(f), and spread sth2m(f)
$          TH2MF, STH2MF : <=0: not declared, > 0: declared
$          I1TH2MF, I1STH2MF: First frequency index of output (default is 1)
$          I2TH2MF, I2STH2MF: First frequency index of output (default is 1)
$ For 2nd order pressure at K=0 (source of microseisms & microbaroms)
$          P2SF      : <=0: not declared, > 0: declared
$          I1P2SF    : First frequency index of output (default is 1)
$          I2P2SF    : Last frequency index of output (default is NK)

```

```

$
$ Miscellaneous ----- $
$ Misc. parameters : Namelist MISC
$ CICEO : Ice concentration cut-off.
$ CICEN : Ice concentration cut-off.
$ PMOVE : Power p in GSE alleviation for
$ moving grids in Eq. (D.4).
$ XSEED : Xseed in seeding alg. (!/SEED).
$ FLAGTR : Indicating presence and type of
$ subgrid information :
$ 0 : No subgrid information.
$ 1 : Transparencies at cell boun-
$ daries between grid points.
$ 2 : Transp. at cell centers.
$ 3 : Like 1 with cont. ice.
$ 4 : Like 2 with cont. ice.
$ XP, XR, XFILT
$ Xp, Xr and Xf for the dynamic
$ integration scheme.
$ IHMAX : Number of discrete levels in part.
$ HSPMIN : Minimum Hs in partitioning.
$ WSM : Wind speed multiplier in part.
$ WSC : Cut of wind sea fraction for
$ identifying wind sea in part.
$ FLC : Flag for combining wind seas in
$ partitioning.
$ NOSW : Number of partitioned swell fields
$ in field output.
$ FMICHE : Constant in Miche limiter.
$ STDX : Space-Time Extremes X-Length
$ STDY : Space-Time Extremes Y-Length
$ STDT : Space-Time Extremes Duration
$ P2SF : .....
$
$ Diagnostic Sea-state Dependent Stress- - - - -
$ Reichl et al. 2014 : Namelist FLD1
$ TAILTYPE : High Frequency Tail Method
$ 0: Constant value (prescribed)
$ 1: Wind speed dependent
$ (Based on GFDL Hurricane
$ Model Z0 relationship)
$ TAILLEV : Level of high frequency tail
$ (if TAILTYPE==0)
$ Valid choices:
$ Capped min: 0.001, max: 0.02

```

```

$           TAILT1      : Tail transition ratio 1
$                   TAILT1*peak input frequency
$                   is the first transition point of
$                   the saturation spectrum
$                   Default is 1.25
$           TAILT1      : Tail transition ratio 2
$                   TAILT2*peak input frequency
$                   is the second transition point of
$                   the saturation spectrum
$                   Default is 3.00
$ Donelan et al. 2012 : Namelist FLD2
$           TAILTYPE    : See above (FLD1)
$           TAILLEV     : See above (FLD1)
$           TAILT1      : See above (FLD1)
$           TAILT2      : See above (FLD1)
$
$ In the 'Out of the box' test setup we run with sub-grid obstacles
$ and with continuous ice treatment.
$
$ &MISC CICEO = 0.25, CICEN = 0.75, FLAGTR = 4 /
$ &FLX3 CDMAX = 3.5E-3 , CTYPE = 0 /
$ &SDB1 BJGAM = 1.26, BJFLAG = .FALSE. /
$
$ Mandatory string to identify end of namelist input section.
$
END OF NAMELISTS
$
$ Define grid ----- $
$
$ Five records containing :
$
$ 1 Type of grid, coordinate system and type of closure: GSTRG, FLAGLL,
$ CSTRG. Grid closure can only be applied in spherical coordinates.
$   GSTRG : String indicating type of grid :
$           'RECT' : rectilinear
$           'CURV' : curvilinear
$           'UNST' : unstructured (triangle-based)
$   FLAGLL : Flag to indicate coordinate system :
$           T : Spherical (lon/lat in degrees)
$           F : Cartesian (meters)
$   CSTRG : String indicating the type of grid index space closure :
$           'NONE' : No closure is applied
$           'SMPL' : Simple grid closure : Grid is periodic in the
$                   : i-index and wraps at i=NX+1. In other words,
$                   : (NX+1,J) => (1,J). A grid with simple closure

```

```

$           : may be rectilinear or curvilinear.
$           'TRPL' : Tripole grid closure : Grid is periodic in the
$           : i-index and wraps at i=NX+1 and has closure at
$           : j=NY+1. In other words, (NX+1,J<=NY) => (1,J)
$           : and (I,NY+1) => (NX-I+1,NY). Tripole
$           : grid closure requires that NX be even. A grid
$           : with tripole closure must be curvilinear.
$ 2 NX, NY. As the outer grid lines are always defined as land
$   points, the minimum size is 3x3.
$
$ Branch here based on grid type
$
$ IF ( RECTILINEAR GRID ) THEN
$
$ 3 Grid increments SX, SY (degr.or m) and scaling (division) factor.
$   If CSTRG='SMPL', then SX is set to 360/NX.
$ 4 Coordinates of (1,1) (degr.) and scaling (division) factor.
$
$ ELSE IF ( CURVILINEAR GRID ) THEN
$
$ 3 Unit number of file with x-coordinate.
$   Scale factor and add offset: x <= scale_fac * x_read + add_offset.
$   IDLA, IDFM, format for formatted read, FROM and filename.
$     IDLA : Layout indicator :
$           1 : Read line-by-line bottom to top.
$           2 : Like 1, single read statement.
$           3 : Read line-by-line top to bottom.
$           4 : Like 3, single read statement.
$     IDFM : format indicator :
$           1 : Free format.
$           2 : Fixed format with above format descriptor.
$           3 : Unformatted.
$     FROM : file type parameter
$           'UNIT' : open file by unit number only.
$           'NAME' : open file by name and assign to unit.
$
$   If the above unit number equals 10, then the x-coord is read from this
$   file. The x-coord must follow the above record. No comment lines are
$   allowed within the x-coord input.
$
$ 4 Unit number of file with y-coordinate.
$   Scale factor and add offset: y <= scale_fac * y_read + add_offset.
$   IDLA, IDFM, format for formatted read, FROM and filename.
$     IDLA : Layout indicator :
$           1 : Read line-by-line bottom to top.

```

```

$           2 : Like 1, single read statement.
$           3 : Read line-by-line top to bottom.
$           4 : Like 3, single read statement.
$   IDFM : format indicator :
$           1 : Free format.
$           2 : Fixed format with above format descriptor.
$           3 : Unformatted.
$   FROM : file type parameter
$           'UNIT' : open file by unit number only.
$           'NAME' : open file by name and assign to unit.
$
$   If the above unit number equals 10, then the y-coord is read from this
$   file. The y-coord must follow the above record. No comment lines are
$   allowed within the y-coord input.
$
$ ELSE IF ( UNSTRUCTURED GRID ) THEN
$   Nothing to declare: all the data will be read from the GMESH file
$ END IF ( CURVILINEAR GRID )
$
$ 5 Limiting bottom depth (m) to discriminate between land and sea
$   points, minimum water depth (m) as allowed in model, unit number
$   of file with bottom depths, scale factor for bottom depths (mult.),
$   IDLA, IDFM, format for formatted read, FROM and filename.
$   IDLA : Layout indicator :
$           1 : Read line-by-line bottom to top.
$           2 : Like 1, single read statement.
$           3 : Read line-by-line top to bottom.
$           4 : Like 3, single read statement.
$   IDFM : format indicator :
$           1 : Free format.
$           2 : Fixed format with above format descriptor.
$           3 : Unformatted.
$   FROM : file type parameter
$           'UNIT' : open file by unit number only.
$           'NAME' : open file by name and assign to unit.
$
$   If the above unit number equals 10, then the bottom depths are read from
$   this file. The depths must follow the above record. No comment lines are
$   allowed within the depth input. In the case of unstructured grids, the file
$   is expected to be a GMESH grid file containing node and element lists.
$
$ -----
$ Example for rectilinear grid with spherical (lon/lat) coordinate system.
$ Note that for Cartesian coordinates the unit is meters (NOT km).
$

```

```

      'RECT' T 'NONE'
      12      12
      1.      1.      4.
     -1.     -1.      4.
    -0.1 2.50 10 -10. 3 1 '(....)' 'NAME' 'bottom.inp'
$
6 6 6 6 6 6 6 6 6 6 6 6
6 6 6 5 4 2 0 2 4 5 6 6
6 6 6 5 4 2 0 2 4 5 6 6
6 6 6 5 4 2 0 2 4 5 6 6
6 6 6 5 4 2 0 0 4 5 6 6
6 6 6 5 4 4 2 2 4 5 6 6
6 6 6 6 5 5 4 4 5 6 6 6
6 6 6 6 6 5 5 6 6 6 6
6 6 6 6 6 6 6 6 6 6 6
6 6 6 6 6 6 6 6 6 6 6
6 6 6 6 6 6 6 6 6 6 6
6 6 6 6 6 6 6 6 6 6 6
$
$ -----
$ Example for curvilinear grid with spherical (lon/lat) coordinate system.
$ Same spatial grid as preceding rectilinear example.
$ Note that for Cartesian coordinates the unit is meters (NOT km).
$
$      'CURV' T 'NONE'
$      12      12
$
$      10 0.25 -0.5 3 1 '(....)' 'NAME' 'x.inp'
$
$ 1 2 3 4 5 6 7 8 9 10 11 12
$ 1 2 3 4 5 6 7 8 9 10 11 12
$ 1 2 3 4 5 6 7 8 9 10 11 12
$ 1 2 3 4 5 6 7 8 9 10 11 12
$ 1 2 3 4 5 6 7 8 9 10 11 12
$ 1 2 3 4 5 6 7 8 9 10 11 12
$ 1 2 3 4 5 6 7 8 9 10 11 12
$ 1 2 3 4 5 6 7 8 9 10 11 12
$ 1 2 3 4 5 6 7 8 9 10 11 12
$ 1 2 3 4 5 6 7 8 9 10 11 12
$ 1 2 3 4 5 6 7 8 9 10 11 12
$ 1 2 3 4 5 6 7 8 9 10 11 12
$
$      10 0.25 0.5 3 1 '(....)' 'NAME' 'y.inp'
$
$ 1 1 1 1 1 1 1 1 1 1 1 1

```

```

$ 2 2 2 2 2 2 2 2 2 2 2 2
$ 3 3 3 3 3 3 3 3 3 3 3 3
$ 4 4 4 4 4 4 4 4 4 4 4 4
$ 5 5 5 5 5 5 5 5 5 5 5 5
$ 6 6 6 6 6 6 6 6 6 6 6 6
$ 7 7 7 7 7 7 7 7 7 7 7 7
$ 8 8 8 8 8 8 8 8 8 8 8 8
$ 9 9 9 9 9 9 9 9 9 9 9 9
$ 10 10 10 10 10 10 10 10 10 10 10 10
$ 11 11 11 11 11 11 11 11 11 11 11 11
$ 12 12 12 12 12 12 12 12 12 12 12 12
$
$      -0.1 2.50  10  -10. 3 1 '(...)' 'NAME' 'bottom.inp'
$
$ 6 6 6 6 6 6 6 6 6 6 6 6
$ 6 6 6 5 4 2 0 2 4 5 6 6
$ 6 6 6 5 4 2 0 2 4 5 6 6
$ 6 6 6 5 4 2 0 2 4 5 6 6
$ 6 6 6 5 4 2 0 0 4 5 6 6
$ 6 6 6 5 4 4 2 2 4 5 6 6
$ 6 6 6 6 5 5 4 4 5 6 6 6
$ 6 6 6 6 6 6 5 5 6 6 6 6
$ 6 6 6 6 6 6 6 6 6 6 6 6
$ 6 6 6 6 6 6 6 6 6 6 6 6
$ 6 6 6 6 6 6 6 6 6 6 6 6
$ 6 6 6 6 6 6 6 6 6 6 6 6
$
$ -----
$ SMC grid use the same spherical lat-lon grid parameters
$   'RECT' T 'SMPL'
$   1024    704
$ SMC grid base level resolution dlon dlat and start lon lat
$ 0.35156250 0.23437500 1.
$ 0.17578125 -78.6328125 1.
$
$ Normal depth input line is used to passing the minimum depth
$ though the depth file is not read for SMC grid.
$ -0.1 10.0 30  -1. 1 1 '(...)' 'NAME' 'SMC25Depth.dat'
$ SMC cell and face arrays and obstruction ratio:
$ 32 1 1 '(...)' 'S6125MCels.dat'
$ 33 1 1 '(...)' 'S6125ISide.dat'
$ 34 1 1 '(...)' 'S6125JSide.dat'
$ 31 1.0 1 1 '(...)' 'NAME' 'SMC25Subtr.dat'
$ The input boundary cell file is only needed when NBISMC > 0.
$ 35 1 1 '(...)' 'S6125Bundy.dat'

```

```

$ Extra cell and face arrays for Arctic part if ARC is selected.
$ 36 1 1 '(...)' 'S6125MBArc.dat'
$ 37 1 1 '(...)' 'S6125AISid.dat'
$ 38 1 1 '(...)' 'S6125AJSid.dat'
$ Normal land-sea mask file input line is kept but file is not used.
$ 39 1 1 '(...)' 'NAME' 'S6125Masks.dat'
$   Boundary cell id list file (unit 35) is only required if boundary
$   cell number entered above is non-zero. The cell id number should be
$   the sequential number in the cell array (unit 32) S625MCels.dat.
$
$ If sub-grid information is available as indicated by FLAGTR above,
$ additional input to define this is needed below. In such cases a
$ field of fractional obstructions at or between grid points needs to
$ be supplied. First the location and format of the data is defined
$ by (as above) :
$ - Unit number of file (can be 10, and/or identical to bottom depth
$   unit), scale factor for fractional obstruction, IDLA, IDFM,
$   format for formatted read, FROM and filename
$
$   10 0.2 3 1 '(...)' 'NAME' 'obstr.inp'
$
$ *** NOTE if this unit number is the same as the previous bottom
$   depth unit number, it is assumed that this is the same file
$   without further checks. ***
$
$ If the above unit number equals 10, the bottom data is read from
$ this file and follows below (no intermediate comment lines allowed,
$ except between the two fields).
$
$   0 0 0 0 0 0 0 0 0 0 0 0
$   0 0 0 0 0 0 0 0 0 0 0 0
$   0 0 0 0 0 0 0 0 0 0 0 0
$   0 0 0 0 0 0 0 0 0 0 0 0
$   0 0 0 0 0 0 0 0 0 0 0 0
$   0 0 0 0 0 0 0 5 0 0 0 0
$   0 0 0 0 0 0 0 5 0 0 0 0
$   0 0 0 0 0 0 0 4 0 0 0 0
$   0 0 0 0 0 0 0 4 0 0 0 0
$   0 0 0 0 0 0 0 5 0 0 0 0
$   0 0 0 0 0 0 0 5 0 0 0 0
$   0 0 0 0 0 0 0 0 0 0 0 0
$
$   0 0 0 0 0 0 0 0 0 0 0 0
$   0 0 0 0 0 0 0 0 0 0 0 0
$   0 0 0 0 0 0 0 0 0 0 0 0

```



```

0 0 0 0 0 0 0 0 0 0 0 0
0 0 0 0 0 0 0 0 5 5 5 0
0 0 0 0 0 0 0 0 0 0 0 0
0 0 0 0 0 0 0 0 0 0 0 0
0 0 0 0 0 0 0 0 0 0 0 0
0 0 0 0 0 0 0 0 0 0 0 0
0 0 0 0 0 0 0 0 0 0 0 0
0 0 0 0 0 0 0 0 0 0 0 0
0 0 0 0 0 0 0 0 0 0 0 0
0 0 0 0 0 0 0 0 0 0 0 0
$
$ *** NOTE size of fields is always NX * NY ***
$
$ Input boundary points and excluded points ----- $
$   The first line identifies where to get the map data, by unit number
$   IDLA and IDFM, format for formatted read, FROM and filename
$   if FROM = 'PART', then segmented data is read from below, else
$   the data is read from file as with the other inputs (as INTEGER)
$
   10 3 1 '(....)' 'PART' 'mapsta.inp'
$
$ Read the status map from file ( FROM != PART ) ----- $
$
$ 3 3 3 3 3 3 3 3 3 3 3 3
$ 3 2 1 1 1 1 0 1 1 1 1 3
$ 3 2 1 1 1 1 0 1 1 1 1 3
$ 3 2 1 1 1 1 0 1 1 1 1 3
$ 3 2 1 1 1 1 0 0 1 1 1 3
$ 3 2 1 1 1 1 1 1 1 1 1 3
$ 3 2 1 1 1 1 1 1 1 1 1 3
$ 3 2 1 1 1 1 1 1 1 1 1 3
$ 3 2 1 1 1 1 1 1 1 1 1 3
$ 3 2 1 1 1 1 1 1 1 1 1 3
$ 3 2 1 1 1 1 1 1 1 1 1 3
$ 3 3 3 3 3 3 3 3 3 3 3 3
$
$ The legend for the input map is :
$
$   0 : Land point.
$   1 : Regular sea point.
$   2 : Active boundary point.
$   3 : Point excluded from grid.
$
$ Input boundary points from segment data ( FROM = PART ) ----- $
$   An unlimited number of lines identifying points at which input
$   boundary conditions are to be defined. If the actual input data is

```

```

$ not defined in the actual wave model run, the initial conditions
$ will be applied as constant boundary conditions. Each line contains:
$ Discrete grid counters (IX,IY) of the active point and a
$ connect flag. If this flag is true, and the present and previous
$ point are on a grid line or diagonal, all intermediate points
$ are also defined as boundary points.
$
    2  2  F
    2 11  T
$
$ Close list by defining point (0,0) (mandatory)
$
    0  0  F
$
$ Excluded grid points from segment data ( FROM != PART )
$ First defined as lines, identical to the definition of the input
$ boundary points, and closed the same way.
$
    0  0  F
$
$ Second, define a point in a closed body of sea points to remove
$ the entire body of sea points. Also close by point (0,0)
$
    0  0
$
$ Sedimentary bottom map if namelist &SBT4 SEDMAPD50 = T
$
    22  1.  1  1  '(f10.6)'  'NAME'  'SED.txt'
$
$ Output boundary points ----- $
$ Output boundary points are defined as a number of straight lines,
$ defined by its starting point (X0,Y0), increments (DX,DY) and number
$ of points. A negative number of points starts a new output file.
$ Note that this data is only generated if requested by the actual
$ program. Example again for spherical grid in degrees. Note, these do
$ not need to be defined for data transfer between grids in the multi
$ grid driver.
$
    1.75  1.50  0.25 -0.10    3
    2.25  1.50 -0.10  0.00   -6
    0.10  0.10  0.10  0.00  -10
$
$ Close list by defining line with 0 points (mandatory)
$
    0.    0.    0.    0.    0

```

```
$  
$ ----- $  
$ End of input file $  
$ ----- $
```

end of example input file (traditional form)

4.4.3 The initial conditions program

Program : ww3_strt (W3STRT)
 Code : ww3_strt.ftn
 Input : ww3_strt.inp (10) Formatted input file for program.
 mod_def.ww3 (20) Model definition file.
 Output : standard out (6) Formatted output of program.
 restart.ww3 (20) Restart file in WAVEWATCH III
 format.

start of example input file (traditional form)

```

$ ----- $
$ WAVEWATCH III Initial conditions input file $
$ ----- $
$ type of initial field ITYPE .
$
$ 1
$
$ ITYPE = 1 ----- $
$ Gaussian in frequency and space, cos type in direction.
$ - fp and spread (Hz), mean direction (degr., oceanographic
$ convention) and cosine power, Xm and spread (degr. or m) Ym and
$ spread (degr. or m), Hmax (m) (Example for lon-lat grid in degr.).
$
$ 0.10 0.01 270. 2 1. 0.5 1. 0.5 2.5
$ 0.10 0.01 270. 2 0. 1000. 1. 1000. 2.5
$ 0.10 0.01 270. 2 0. 1000. 1. 1000. 0.01
$ 0.10 0.01 270. 2 0. 1000. 1. 1000. 0.
$
$ ITYPE = 2 ----- $
$ JONSWAP spectrum with Hasselmann et al. (1980) direct. distribution.
$ - alfa, peak freq. (Hz), mean direction (degr., oceanographical
$ convention), gamma, sigA, sigB, Xm and spread (degr. or m) Ym and
$ spread (degr. or m) (Example for lon-lat grid in degr.).
$ alfa, sigA, sigB give default values if less than or equal to 0.
$
$ 0.0081 0.1 270. 1.0 0. 0. 1. 100. 1. 100.
$
$ ITYPE = 3 ----- $
$ Fetch-limited JONSWAP
$ - No additional data, the local spectrum is calculated using the
$ local wind speed and direction, using the spatial grid size as
$ fetch, and assuring that the spectrum is within the discrete
  
```

```

$ frequency range.
$
$ ITYPE = 4 ----- $
$ User-defined spectrum
$ - Scale factor., defaults to 1 if less than or equal 0.
$ - Spectrum F(f,theta) (single read statement)
$
$ -0.1
$ 0 0 0 0 0 0 0 0 0 0 0 0 0 0 0 0 0 0 0 0 0 0 0 0 0 0 0 0 0 0 0 0
$ 0 1 1 1 0 0 0 0 0 0 0 0 0 0 0 0 0 0 0 0 0 0 0 0 0 0 0 0 0 0 0 0
$ 0 1 4 2 1 0 0 0 0 0 0 0 0 0 0 0 0 0 0 0 0 0 0 0 0 0 0 0 0 0 0 0
$ 0 0 1 1 0 0 0 0 0 0 0 0 0 0 0 0 0 0 0 0 0 0 0 0 0 0 0 0 0 0 0 0
$ 0 0 0 0 0 0 0 0 0 0 0 0 0 0 0 0 0 0 0 0 0 0 0 0 0 0 0 0 0 0 0 0
$ 0 0 0 0 0 0 0 0 0 0 0 0 0 0 0 0 0 0 0 0 0 0 0 0 0 0 0 0 0 0 0 0
$ 0 0 0 0 0 0 0 0 0 0 0 0 0 0 0 0 0 0 0 0 0 0 0 0 0 0 0 0 0 0 0 0
$ 0 0 0 0 0 0 0 0 0 0 0 0 0 0 0 0 0 0 0 0 0 0 0 0 0 0 0 0 0 0 0 0
$ 0 0 0 0 0 0 0 0 0 0 0 0 0 0 0 0 0 0 0 0 0 0 0 0 0 0 0 0 0 0 0 0
$ 0 0 0 0 0 0 0 0 0 0 0 0 0 0 0 0 0 0 0 0 0 0 0 0 0 0 0 0 0 0 0 0
$ 0 0 0 0 0 0 0 0 0 0 0 0 0 0 0 0 0 0 0 0 0 0 0 0 0 0 0 0 0 0 0 0
$ 0 0 0 0 0 0 0 0 0 0 0 0 0 0 0 0 0 0 0 0 0 0 0 0 0 0 0 0 0 0 0 0
$ 0 0 0 0 0 0 0 0 0 0 0 0 0 0 0 0 0 0 0 0 0 0 0 0 0 0 0 0 0 0 0 0
$ 0 0 0 0 0 0 0 0 0 0 0 0 0 0 0 0 0 0 0 0 0 0 0 0 0 0 0 0 0 0 0 0
$ 0 0 0 0 0 0 0 0 0 0 0 0 0 0 0 0 0 0 0 0 0 0 0 0 0 0 0 0 0 0 0 0
$ 0 0 0 0 0 0 0 0 0 0 0 0 0 0 0 0 0 0 0 0 0 0 0 0 0 0 0 0 0 0 0 0
$ 0 0 0 0 0 0 0 0 0 0 0 0 0 0 0 0 0 0 0 0 0 0 0 0 0 0 0 0 0 0 0 0
$ 0 0 0 0 0 0 0 0 0 0 0 0 0 0 0 0 0 0 0 0 0 0 0 0 0 0 0 0 0 0 0 0
$ 0 0 0 0 0 0 0 0 0 0 0 0 0 0 0 0 0 0 0 0 0 0 0 0 0 0 0 0 0 0 0 0
$ 0 0 0 0 0 0 0 0 0 0 0 0 0 0 0 0 0 0 0 0 0 0 0 0 0 0 0 0 0 0 0 0
$
$ ITYPE = 5 ----- $
$ Starting from calm conditions.
$ - No additional data.
$
$ ----- $
$ End of input file $
$ ----- $

```

end of example input file (traditional form)

4.4.4 The boundary conditions program

Program	:	ww3_bound		(W3BOUND)
Code	:	ww3_bound.ftn		
Input	:	ww3_bound.inp	(10)	Formatted input file for program.
		mod_def.ww3	(20)	Model definition file.
		'spectra file' *	(user)	File(s) with wave spectra.
Output	:	standard out	(6)	Formatted output of program.
		nest.ww3	(33)	Boundary conditions file.

start of example input file (traditional form)

```

$ ----- $
$ WAVEWATCH III Ascii boundary input processing $
$ ----- $
$
$ Boundary option: READ or WRITE
$
WRITE
$
$ Interpolation method: 1: nearest
$                       2: linear interpolation
2
$
$ Verbose mode [0-1]
$
0
$
$ List of spectra files. These ASCII files use the WAVEWATCH III
$ format as described in the ww3_outp.inp file. The files are
$ defined relative to the directory in which the program is run.
$
$ Examples of such files can be found at (for example):
$ ftp://polar.ncep.noaa.gov/pub/waves/develop/glw.latest_run/
$                                     (the *.spec.gz files)
$ http://tinyurl.com/iowagaftp/HINDCAST/GLOBAL/2009_ECMWF/SPEC
$
$ If data is used other than from previous WAVEWATCH III runs, then
$ this data will need to be converted to the WAVEWATCH III format.
$
$ In the case of NetCDF files see ww3_bounc.inp
$
SPECTRI/mww3.W004N476.spec
SPECTRI/mww3.W0042N476.spec

```

```
SPECTRI/mww3.W0044N476.spec  
SPECTRI/mww3.W0046N476.spec  
SPECTRI/mww3.W0048N476.spec  
SPECTRI/mww3.W005N476.spec  
SPECTRI/mww3.W0052N476.spec  
SPECTRI/mww3.W0054N476.spec  
SPECTRI/mww3.W0056N476.spec  
SPECTRI/mww3.W0058N489.spec  
SPECTRI/mww3.W006N478.spec  
SPECTRI/mww3.W006N482.spec  
SPECTRI/mww3.W006N486.spec  
SPECTRI/mww3.W006N489.spec  
'STOPSTRING'
```

```
$  
$ ----- $  
$ End of input file $  
$ ----- $
```

end of example input file (traditional form)

4.4.5 The NetCDF boundary conditions program

Program : ww3_bounc (w3BOUNC)
 Code : ww3_bounc.ftn
 Input : ww3_bound.inp (10) Formatted input file for program.
 mod_def.ww3 (20) Model definition file.
 'spectra file' * (user) File(s) with wave spectra, in
 NetCDF.
 Output : standard out (6) Formatted output of program.
 nest.ww3 (33) Boundary conditions file.

start of example input file (traditional form)

```

$ ----- $
$ WAVEWATCH III NetCDF boundary input processing $
$ ----- $
$
$ Boundary option: READ or WRITE
$
WRITE
$
$ Interpolation method: 1: nearest
$                       2: linear interpolation
2
$ Verbose (0, 1, 2)
1
$
$ List of spectra files. These NetCDF files use the WAVEWATCH III
$ format as described in the ww3_ounp.inp file. The files are
$ defined relative to the directory in which the program is run.
$
SPECTRA_NC/ww3.62163_spec.nc
SPECTRA_NC/ww3.62069_spec.nc
'STOPSTRING'
$
$ ----- $
$ End of input file $
$ ----- $

```

end of example input file (traditional form)

4.4.6 The input field preprocessor

Program	:	ww3_prep		(W3PREP)
Code	:	ww3_prep.ftn		
Input	:	ww3_prep.inp	(10)	Formatted input file for program.
		mod_def.ww3	(11)	Model definition file.
		'user input'*	(user)	See example below.
Output	:	standard out	(6)	Formatted output of program.
		level.ww3*	(12)	Water levels file.
		current.ww3*	(12)	Current fields file.
		wind.ww3*	(12)	Wind fields file.
		ice.ww3*	(12)	Ice fields file.
		data0.ww3*	(12)	Assimilation data ('mean').
		data1.ww3*	(12)	Assimilation data ('1-D spectra').
		data2.ww3*	(12)	Assimilation data ('2-D spectra').

start of example input file (traditional form)

```

$ ----- $
$ WAVEWATCH III Field preprocessor input file $
$ ----- $
$ Major types of field and time flag
$ Field types : IC1 Ice thickness.
$               IC5 Ice floe mean diameter.
$               ICE Ice concentrations.
$               ISI Icebergs and sea ice.
$               LEV Water levels.
$               WND Winds.
$               WNS Winds (including air-sea temp. dif.)
$               CUR Currents.
$               DAT Data for assimilation.
$
$ Format types : AI Transfer field 'as is'.
$               LL Field defined on rectilinear grid (in same
$               coordinate system as model grid)
$               F1 Field defined on curvilinear grid (in same
$               coordinate system as model grid), coordinates
$               of each grid point given in separate file.
$               F2 Like F1, composite of 2 fields.
$
$ - Format type not used for field type 'DAT'.
$

```

```

$ Time flag      : If true, time is included in file.
$ Header flag   : If true, header is added to file.
$               (necessary for reading, FALSE is used only for
$               incremental generation of a data file.)
$
$ 'ICE' 'LL' F T
$
$ Additional time input ----- $
$ If time flag is .FALSE., give time of field in yyyyymmdd hhmmss format.
$
$ 19680606 053000
$
$ Additional input format type 'LL' ----- $
$ Grid range (degr. or m) and number of points for axes, respectively.
$ Example for longitude-latitude grid.
$
$ -0.25 2.5 15 -0.25 2.5 4
$
$ Additional input format type 'F1' or 'F2' ----- $
$ Three or four additional input lines, to define the file(s) with
$ the grid information :
$ 1) Discrete size of input grid (NXI,NYI) and T/F flag identifying
$ closure in longitudes ("CLO"). Tripole input is not supported.
$ 2) Define type of file using the parameters FROM, IDLA, IDFM (see
$ input for grid preprocessor), and a format
$ 3) Unit number and (dummy) name of first file.
$ 4) Unit number and (dummy) name of second file (F2 only).
$
$ 15 3
$ 'UNIT' 3 1 '(.L.L.)'
$ 10 'll_file.1'
$ 10 'll_file.2'
$
$ Additional input for data ----- $
$ Dimension of data (0,1,2 for mean pars, 1D or 2D spectra), "record
$ length" for data, data value for missing data
$
$ 0 4 -999.
$
$ Define data files ----- $
$ The first input line identifies the file format with FROM, IDLA and
$ IDFM, the second (third) lines give the file unit number and name.
$
$ 'UNIT' 3 1 '(..T..)' '(..F..)'
$ 10 'data_file.1'

```

```

$ 10 'data_file.2'
$
$ If the above unit numbers are 10, data is read from this file
$ (no intermediate comment lines allowed),
$ This example is an ice concentration field.
$
  1. 1. 1. 1. 1. 1. 0. 0. 0. 0. 0. 0. 0. 0. 0.
  1. 1. .5 .5 .5 0. 0. 0. 0. 0. 0. 0. 0. 0.
  0. 0. 0. 0. 0. 0. 0. 0. 0. 0. 0. 0. 0. 0.
  0. 0. 0. 0. 0. 0. 0. 0. 0. 0. 0. 0. 0. 0.
$
$ This example is mean parameter assimilation data
$ First record gives number of data records, data are read as as
$ individual records of reals with record length as given above
$
$ 3
$ 1.5 1.6 0.70 10.3
$ 1.7 1.5 0.75 9.8
$ 1.9 1.4 0.77 11.1
$
$ ----- $
$ End of input file $
$ ----- $

```

end of example input file (traditional form)

Note that the optional output files are specific to `ww3_shel` and `ww3_multi`, but are not processed by the actual wave model routines. These files are consequently not needed if the wave model routines are used in a different shell or in an integrated program. However, the routines reading and writing these files are system-independent and could therefore be used in customized applications of the basic wave model. The reading and writing of these files is performed by the subroutine `W3FLDG` (`w3fldsmd.ftn`). For additional documentation and file formats reference if made to this routine.

4.4.7 The NetCDF input field preprocessor

Program	:	ww3_pnc		(W3PRNC)
Code	:	ww3_pnc.ftn		
Input	:	ww3_pnc.inp	(10)	Formatted input file for program.
		mod_def.ww3	(11)	Model definition file.
		'user input'*	(user)	See example below.
Output	:	standard out	(6)	Formatted output of program.
		level.ww3*	(12)	Water levels file.
		current.ww3*	(12)	Current fields file.
		wind.ww3*	(12)	Wind fields file.
		ice.ww3*	(12)	Ice fields file.
		data0.ww3*	(12)	Assimilation data ('mean').
		data1.ww3*	(12)	Assimilation data ('1-D spectra').
		data2.ww3*	(12)	Assimilation data ('2-D spectra').

start of example input file (traditional form)

```

$ ----- $
$ WAVEWATCH III Field preprocessor input file $
$ ----- $
$ Major types of field and time flag
$ Field types : IC1 Ice thickness.
$               IC5 Ice floe mean diameter.
$               ICE Ice concentrations.
$               ISI Icebergs and sea ice.
$               LEV Water levels.
$               WND Winds.
$               WNS Winds (including air-sea temp. dif.)
$               CUR Currents.
$               DAT Data for assimilation.
$
$ Format types : AI Transfer field 'as is'. (ITYPE 1)
$               LL Field defined on regular longitude-latitude
$               or Cartesian grid. (ITYPE 2)
$ Format types : AT Transfer field 'as is', performs tidal
$               analysis on the time series (ITYPE 6)
$               When using AT, another line should be added
$               with the choice of tidal constituents:
$               ALL or FAST or VFAST or a list: e.g. 'M2 S2'
$
$ - Format type not used for field type 'DAT'.

```

```

$
$ Time flag      : If true, time is included in file.
$ Header flag   : If true, header is added to file.
$                (necessary for reading, FALSE is used only for
$                incremental generation of a data file.)
$
$ 'WND' 'LL' T T
$
$ Name of spatial dimensions----- $
$ NB: time dimension is expected to be called 'time' and must respect
$     Julian or Gregorian calendar with leap day.
$
$ longitude latitude
$
$ Variables to use ----- $
$
$ U V
$
$ Additional time input ----- $
$ If time flag is .FALSE., give time of field in yyyyymmdd hhmmss format.
$
$ 19680606 053000
$
$ Define data files ----- $
$ The input line identifies the filename using for the forcing field.
$
$ 'wind.nc'
$
$ ----- $
$ End of input file $
$ ----- $

```

end of example input file (traditional form)

See note at the end of the previous section (4.4.6) for tools that can be used to pack input files in custom programs.

4.4.8 The tide prediction program

Program : ww3_prtide (W3TIDE)
 Code : ww3_prtide.ftn
 Input : ww3_prtide.inp (10) Formatted input file for program.
 mod_def.ww3 (20) Model definition file.
 current.ww3_tide (user) File with tidal constituents.
 or level.ww3_tide
 Output : standard out (6) Formatted output of program.
 current.ww3 or (33) Level or current forcing.
 level.ww3

start of example input file (traditional form)

```

$ ----- $
$ WAVEWATCH III Field preprocessor input file $
$ ----- $
$ types of field
$   Field types : LEV   Water levels.
$                 CUR   Currents.
$   'CUR'
$
$ List of tidal constituents----- $
$
$ Z0 M2
$
$ Maximum allowed values ----- $
$ First line: name of tidal constituents for which the max. are defined
$             these should be chosen among the ones available in the
$             tidal analysis.
$             If analysis was performed with ww3_prcn, the default list
$             is Z0 SSA MSM MSF MF 2N2 MU2 N2 NU2 M2 S2 K2 MSN2 MN4 M4
$             MS4 S4 M6 2MS6 M8
$ Second line: values of maximum magnitude of the amplitude
$ at points where not values are defined or where these maxima are
$ exceeded, the constituents are extrapolated from neighbors
$ (e.g. tidal flats ...)
$   Z0  SSA MSF
$   1.0  0.5 0.5
$
$ Start time  step          end time
$   19680606 000000 1800 19680607 120000
$
$ Define data files ----- $

```

```

$ The input line identifies the filename using for the forcing field.
$
  'ww3_tide'
$ ----- $
$ End of input file                               $
$ ----- $

```

end of example input file (traditional form)

The user-provided file `current.ww3_tide` or `level.ww3_tide` is a binary file that can be obtained by running `ww3_prc` with the 'AT' option and then renaming the resulting file `current.ww3` or `level.ww3` into `current.ww3_tide` or `level.ww3_tide`. The choice of tidal constituents used for the tidal prediction can be a subset of the ones present in these files or all of them.

Because of wetting and drying or grid mismatches, the tidal constituents may be erroneous or absent for some of the WAVEWATCH III nodes. The erroneous ones can be detected using a maximum amplitude on particular components. When the amplitudes exceeds these maxima, then the tidal constituents are extrapolated from the nearest nodes. This feature has only been tested on triangular meshes.

4.4.9 The generic shell

Program	:	ww3_shel		(W3SHEL)
Code	:	ww3_shel.ftn		
Input	:	ww3_shel.inp	(10)	Formatted input file for program.
		mod_def.ww3	(30)	Model definition file.
		restart.ww3	(30)	Restart file.
		nest.ww3*	(33)	Boundary conditions file.
		level.ww3*	(11)	Water levels file.
		current.ww3*	(12)	Current fields file.
		wind.ww3*	(13)	Wind fields file.
		ice.ww3*	(14)	Ice fields file.
		data0.ww3*	(15)	Assimilation data.
		data1.ww3*	(16)	Assimilation data.
		data2.ww3*	(17)	Assimilation data.
		track.i.ww3*	(22)	Output track information.
Output	:	standard out	(6)	Formatted output of program.
		log.ww3	(20)	Output log of wave model (see Section 4.2).
		test.ww3*	(6/21)	Test output of wave model.
		restartn.ww3*	(30)	Restart file(s).
		nestn.ww3*	(34-42)	Nesting file(s).
		out_grd.ww3*	(31)	Raw output of gridded fields.
		out_pnt.ww3*	(32)	Raw output of spectra.
		track_o.ww3*	(23)	Raw output of spectra along tracks.
Scratch	:	ww3_shel.scratch	(90)	Formatted scratch file.

start of example input file (traditional form)

```

$ ----- $
$ WAVEWATCH III shell input file $
$ ----- $
$ Define input to be used with F/T/C flag for use or nor or coupling and
$ T/F flag for definition as a homogeneous field.
$
$ Include ice and mud parameters only if IC1/2/3/4 used :
  F F    Ice parameter 1
  F F    Ice parameter 2

```



```

F F    Ice parameter 3
F F    Ice parameter 4
F F    Ice parameter 5
F F    Mud parameter 1
F F    Mud parameter 2
F F    Mud parameter 3
F F    Water levels
F F    Currents
T T    Winds
T      Ice concentrations
F      Assimilation data : Mean parameters
F      Assimilation data : 1-D spectra
F      Assimilation data : 2-D spectra
$
$ Time frame of calculations ----- $
$ - Starting time in yyyyymmdd hhmmss format.
$ - Ending time in yyyyymmdd hhmmss format.
$
    19680606 000000
    19680606 060000
$
$ Define output data ----- $
$
$ Define output server mode. This is used only in the parallel version
$ of the model. To keep the input file consistent, it is always needed.
$ IOSTYP = 1 is generally recommended. IOSTYP > 2 may be more efficient
$ for massively parallel computations. Only IOSTYP = 0 requires a true
$ parallel file system like GPFS.
$
$   IOSTYP = 0 : No data server processes, direct access output from
$                 each process (requires true parallel file system).
$   1 : No data server process. All output for each type
$         performed by process that performs computations too.
$   2 : Last process is reserved for all output, and does no
$         computing.
$   3 : Multiple dedicated output processes.
$
    2
$
$ Five output types are available (see below). All output types share
$ a similar format for the first input line:
$ - first time in yyyyymmdd hhmmss format, output interval (s), and
$   last time in yyyyymmdd hhmmss format (all integers).
$ Output is disabled by setting the output interval to 0.
$

```

```

$ ----- $
$
$ Type 1 : Fields of mean wave parameters
$       Standard line and line with logical flags to activate output
$       fields as defined in section 2.4 of the manual. The logical
$       flags are not supplied if no output is requested. The logical
$       flags can be placed on multiple consecutive lines. However,
$       the total number and order of the logical flags is fixed.
$
$               The raw data file is out_grd.wv3,
$               see w3iogo.ftn for additional doc.
$
$       19680606 000000   3600  19680608 000000
$-----
$ Output request flags identifying fields.
$
$ The table below provides a full definition of field output parameters
$ as well as flags indicating if they are available in different field
$ output output file types (ASCII, grib, NetCDF).
$ Further definitions are found in section 2.4 of the manual.
$
$ Selection of field outputs may be made in two ways:
$   F/T flags: first flag is set to F, requests made per group (1st line)
$               followed by parameter flags (total of 10 groups).
$   Namelists: first line is set to N, next line contains parameter
$               symbol as per table below.
$
$   Example of F/T flag use is given in this sample ww3_shel.inp, below.
$   For namelist usage, see the sample ww3_ounf.inp for an example.
$
$ -----
$ Output field parameter definitions table
$ -----
$
$ All parameters listed below are available in output file of the types
$ ASCII and NetCDF. If selected output file types are grads or grib,
$ some parameters may not be available. The first two columns in the
$ table below identify such cases by flags, cols 1 (GRB) and 2 (GXO)
$ refer to grib (ww3_grib) and grads (gx_outf), respectively.
$
$ Columns 3 and 4 provide group and parameter numbers per group.
$ Columns 5, 6 and 7 provide:
$   5 - code name (internal)
$   6 - output tags (names used is ASCII file extensions, NetCDF
$       variable names and namelist-based selection (see ww3_ounf.inp)
$   7 - Long parameter name/definition

```

```

$
$ G G
$ R X Grp Param Code Output Parameter/Group
$ B O Numb Numbr Name Tag Definition
$ -----
$ 1 Forcing Fields
$ -----
$ T T 1 1 DW DPT Water depth.
$ T T 1 2 C[X,Y] CUR Current velocity.
$ T T 1 3 UA WND Wind speed.
$ T T 1 4 AS AST Air-sea temperature difference.
$ T T 1 5 WLV WLV Water levels.
$ T T 1 6 ICE ICE Ice concentration.
$ T T 1 7 IBG IBG Iceberg-induced damping.
$ T T 1 8 D50 D50 Median sediment grain size.
$ T T 1 9 IC1 IC1 Ice thickness.
$ T T 1 10 IC5 IC5 Ice flow diameter.
$ -----
$ 2 Standard mean wave Parameters
$ -----
$ T T 2 1 HS HS Wave height.
$ T T 2 2 WLM LM Mean wave length.
$ T T 2 3 TO2 TO2 Mean wave period (Tm02).
$ T T 2 4 TOM1 TOM1 Mean wave period (Tm0,-1).
$ T T 2 5 TO1 TO1 Mean wave period (Tm01).
$ T T 2 6 FPO FP Peak frequency.
$ T T 2 7 THM DIR Mean wave direction.
$ T T 2 8 THS SPR Mean directional spread.
$ T T 2 9 THPO DP Peak direction.
$ T T 2 10 HIG HIG Infragravity height
$ T T 2 11 STMAXE MXE Max surface elev (STE)
$ T T 2 12 STMAXD MXES St Dev of max surface elev (STE)
$ T T 2 13 HMAXE MXH Max wave height (STE)
$ T T 2 14 HCMAXE MXHC Max wave height from crest (STE)
$ T T 2 15 HMAXD SDMH St Dev of MXC (STE)
$ T T 2 16 HCMAXD SDMHC St Dev of MXHC (STE)
$ -----
$ 3 Spectral Parameters (first 5)
$ -----
$ F F 3 1 EF EF Wave frequency spectrum
$ F F 3 2 TH1M TH1M Mean wave direction from a1,b2
$ F F 3 3 STH1M STH1M Directional spreading from a1,b2
$ F F 3 4 TH2M TH2M Mean wave direction from a2,b2
$ F F 3 5 STH2M STH2M Directional spreading from a2,b2
$ F F 3 6 WN WN Wavenumber array

```

\$						
\$						
4						
Spectral Partition Parameters						

\$	T	T	4	1	PHS	PHS Partitioned wave heights.
\$	T	T	4	2	PTP	PTP Partitioned peak period.
\$	T	T	4	3	PLP	PLP Partitioned peak wave length.
\$	T	T	4	4	PDIR	PDIR Partitioned mean direction.
\$	T	T	4	5	PSI	PSPR Partitioned mean directional spread.
\$	T	T	4	6	PWS	PWS Partitioned wind sea fraction.
\$	T	T	4	7	PWST	TWS Total wind sea fraction.
\$	T	T	4	8	PNR	PNR Number of partitions.

\$						
\$						
5						
Atmosphere-waves layer						

\$	T	T	5	1	UST	UST Friction velocity.
\$	F	T	5	2	CHARN	CHA Charnock parameter
\$	F	T	5	3	CGE	CGE Energy flux
\$	F	T	5	4	PHIAW	FAW Air-sea energy flux
\$	F	T	5	5	TAUWI[X,Y]	TAW Net wave-supported stress
\$	F	T	5	6	TAUWN[X,Y]	TWA Negative part of the wave-supported stress
\$	F	F	5	7	WHITECAP	WCC Whitecap coverage
\$	F	F	5	8	WHITECAP	WCF Whitecap thickness
\$	F	F	5	9	WHITECAP	WCH Mean breaking height
\$	F	F	5	10	WHITECAP	WCM Whitecap moment

\$						
\$						
6						
Wave-ocean layer						

\$	F	F	6	1	S[XX,YY,XY]	SXY Radiation stresses.
\$	F	F	6	2	TAUO[X,Y]	TWO Wave to ocean momentum flux
\$	F	F	6	3	BHD	BHD Bernoulli head (J term)
\$	F	F	6	4	PHIOC	FOC Wave to ocean energy flux
\$	F	F	6	5	TUS[X,Y]	TUS Stokes transport
\$	F	F	6	6	USS[X,Y]	USS Surface Stokes drift
\$	F	F	6	7	[PR,TP]MS	P2S Second-order sum pressure
\$	F	F	6	8	US3D	USF Spectrum of surface Stokes drift
\$	F	F	6	9	P2SMS	P2L Micro seism source term
\$	F	F	6	10	TAUCE	TWI Wave to sea ice stress
\$	F	F	6	11	PHICE	FIC Wave to sea ice energy flux

\$						
\$						
7						
Wave-bottom layer						

\$	F	F	7	1	ABA	ABR Near bottom rms amplitudes.
\$	F	F	7	2	UBA	UBR Near bottom rms velocities.
\$	F	F	7	3	BEDFORMS	BED Bedforms
\$	F	F	7	4	PHIBBL	FBB Energy flux due to bottom friction

```

$ F F 7 5 TAUBBL TBB Momentum flux due to bottom friction
$ -----
$ 8 Spectrum parameters
$ -----
$ F F 8 1 MSS[X,Y] MSS Mean square slopes
$ F F 8 2 MSC[X,Y] MSC Spectral level at high frequency tail
$ F F 8 3 WLO2[X,Y] WLO2 East/X North/Y mean wavelength compon
$ F F 8 4 ALPXT AXT Correl sea surface gradients (x,t)
$ F F 8 5 ALPYT AYT Correl sea surface gradients (y,t)
$ F F 8 6 ALPXY AXY Correl sea surface gradients (x,y)
$ -----
$ 9 Numerical diagnostics
$ -----
$ T T 9 1 DTDYN DTD Average time step in integration.
$ T T 9 2 FCUT FC Cut-off frequency.
$ T T 9 3 CFLXYMAX CFX Max. CFL number for spatial advection.
$ T T 9 4 CFLTHMAX CFD Max. CFL number for theta-advection.
$ F F 9 5 CFLKMAX CFK Max. CFL number for k-advection.
$ -----
$ 10 User defined
$ -----
$ F F 10 1 U1 User defined #1. (requires coding ...)
$ F F 10 2 U2 User defined #1. (requires coding ...)
$ -----
$
$ Section 4 consist of a set of fields, index 0 = wind sea, index
$ 1:NOSWLL are first NOSWLL swell fields.
$
$ Actual active parameter selection section
$
$ (1) Forcing Fields
T
$ DPT CUR WND AST WLW ICE IBG D50 IC1 IC5
T T T T T F F F F F
$ (2) Standard mean wave Parameters
T
$ HS LM T02 TOM1 T01 FP DIR SPR DP
T T T T T T T T T
$ (3) Frequency-dependent parameters
T
$ EF TH1M STH1M TH2M STH2M WN
T T T F F F
$ (4) Spectral Partition Parameters
T
$ PHS PTP PLP PDIR PSPR PWS TWS PNR

```

```

T T T T T T T T
$ (5) Atmosphere-waves layer
T
$ UST CHA CGE FAW TAW TWA WCC WCF WCH WCM
T T T T T T T T T T
$ (6) Wave-Ocean layer
T
$ SXY TWO BHD FOC TUS USS P2S USF P2L TWI FIC
T T T T T T T F F F F
$ (7) Wave-bottom layer
T
$ ABR UBR BED FBB TBB
T T T T T
$ (8) Spectrum parameters
T
$ MSS MSC WLO2 AXT AYT AXZ
T T T T T T
$ (9) Numerical diagnostics
T
$ DTD FC CFX CFD CFK
T T T T T
$ (10) User defined (NOEXTR flags needed)
F
$ U1 U2
$ T T
$
$-----
$
$ Type 2 : Point output
$ Standard line and a number of lines identifying the
$ longitude, latitude and name (C*10) of output points.
$ The list is closed by defining a point with the name
$ 'STOPSTRING'. No point info read if no point output is
$ requested (i.e., no 'STOPSTRING' needed).
$ Example for spherical grid.
$ The raw data file is out_pnt.wv3,
$ see w3iogo.ftn for additional doc.
$
$ NOTE : Spaces may be included in the name, but this is not
$ advised, because it will break the GrADS utility to
$ plots spectra and source terms, and will make it more
$ difficult to use point names in data files.
$
19680606 000000 900 19680608 000000
$

```

```

-0.25 -0.25 'Land      '
 0.0  0.0  'Point_1  '
 2.0  1.0  'Point_2  '
 1.8  2.2  'Point_3  '
 2.1  0.9  'Point_4  '
 5.0  5.0  'Outside  '
$
 0.0  0.0  'STOPSTRING'
$
$ Type 3 : Output along track.
$       Flag for formatted input file.
$               The data files are track_i.ww3 and
$               track_o.ww3, see w3iotr.ftn for ad. doc.
$
19680606 000000  1800  19680606 013000
  T
$
$ Type 4 : Restart files (no additional data required).
$               The data file is restartN.ww3, see
$               w3iors.ftn for additional doc.
$
19680606 030000  3600  19680607 030000
$
$ Type 5 : Boundary data (no additional data required).
$               The data file is nestN.ww3, see
$               w3iobcmd.ftn for additional doc.
$
19680606 000000  3600  20010102 000000
$
$ Type 6 : Separated wave field data (dummy for now).
$       First, last step IX and IY, flag for formatted file
$
19680606 000000  3600  20010102 000000
 0 999 1 0 999 1 T
$
$ Type 7 : Coupling. (must be fully commented if not used with switch COU)
$       Namelist type selection is used here.
$       Diagnostic fields to exchange. (see namcouple for more information)
$
19680606 000000  3600  20010102 000000
$ N
$
$ - Sent fields by ww3:
$   - Ocean model : TOM1 OHS DIR BHD TWO UBR FOC TAW TUS USS LM DRY
$   - Atmospheric model : CHA AHS TP (or FP)

```

```

$
$ CHA
$
$ - Received fields by ww3:
$   - Ocean model : SSH CUR
$   - Atmospheric model : WND
$
$ WND
$
$ Homogeneous field data ----- $
$ Homogeneous fields can be defined by a list of lines containing an ID
$ string 'LEV' 'CUR' 'WND', date and time information (yyyymmdd
$ hhhmss), value (S.I. units), direction (current and wind, oceanogr.
$ convention degrees) and air-sea temperature difference (degrees C).
$ 'STP' is mandatory stop string.
$ Also defined here are the speed with which the grid is moved
$ continuously, ID string 'MOV', parameters as for 'CUR'.
$
$   'LEV' 19680606 010000    1.00
$   'CUR' 19680606 073125    2.0   25.
$   'WND' 19680606 000000   20.   145.   2.0
$   'MOV' 19680606 013000    4.0   25.
$   'STP'
$
$ ----- $
$ End of input file                               $
$ ----- $

```

end of example input file (traditional form)

4.4.10 Automated grid splitting for ww3_multi (ww3_gspl)

Program	:	ww3_gspl		(W3GSPL)
Code	:	ww3_gspl.ftn		
Input	:	ww3_gspl.inp	(10)	Formatted input file for program.
		mod_def. <i>xxx</i>	(11)	Model definition file of grid to be split.
Output	:	standard out	(6)	Formatted output of program.
		<i>xxx</i> .bot	(11)	File with bathymetry for sub-grid.
		<i>xxx</i> .obst	(11)	File with obstructions for sub-grid.
		<i>xxx</i> .mask	(11)	File with mask for sub-grid.
		<i>xxx</i> .tmpl	(11)	ww3_grid.inp for sub-grid.
		ww3_multi. <i>xxx.n</i>	(11)	Template for part of ww3_multi.inp that needs to be modified.
		ww3.ww3_gspl	(35)	GrADS file with map of sub-grids (with switch O16).
		ww3.ctl	(35)	GrADS map control file (O16).

start of example input file (traditional form)

```

$ ----- $
$ WAVEWATCH III Grid splitting input file $
$ ----- $
$ Grid identifier (file extension for mod_def file of grid to be split)
$
$ 'glo_2d'
$
$ Number of sub-grids to be created, maximum number of iterations,
$ target grid point count std in percent. user defined halo extension
$ (default should be 2, used because of inconsistencies between halo
$ computation in this code and in the main wave model code). Increase
$ the latter number if ww3_multi fails on halo overlaps between
$ equally ranked grids.
$
12 250 0.75 2
$
$ IDLA, IDFM, scale and RFORM for bottom, obstruction and mask files.
$ Note that the third file is integers. Suggest IDFM = 1 and IDLA = 1
$
3 2 1.0 '(12F11.3)'
3 2 1.0 '(26F5.2)'
3 2 1 '(66I2)'

```

```
$  
$ lowest and highest fraction of communicator to be used for grid.  
$ and flag for running grids side-by-side inside fraction  
$ F: for test purposes only, defeats most reasons for splitting  
$ T: normal operations  
$  
  0.4  1.  F  
$ ----- $  
$ End of input file $  
$ ----- $
```

end of example input file (traditional form)

To further automate the splitting of the grid, a script `ww3_gspl.sh` is provided. This script runs `ww3_gspl`, and subsequently generated the `mod_def` files for all sub-grids. If a file `ww3_multi.inp` is provided, then this file is updated too. The workings of the script are shown with the `-h` command line flag, which results in the output of the script as shown in Fig. 4.3.

Figure 4.3: Options for `ww3_gspl.sh`, as obtained by running it with the `-h` command line option.

4.4.11 The multi-grid shell

Program	:	ww3_multi		(W3MLTI)
Code	:	ww3_multi.ftn		
Input	:	ww3_multi.nml	(8)	Input file for multi-grid wave model: alternative namelist form.
Input	:	ww3_multi.inp	(8)	Input file for multi-grid wave model: traditional format.
Output	:	standard out	(6)	Formatted output of program.
		log.mww3	(9)	Output log of wave model driver.
		test.mww3*	(auto)	Test output of wave model.

This wave model program requires and produces a plethora of input and output files consistent with those of `ww3_shel` in Section 4.4.9, where file extensions `.ww3` are replaced by an identifier for a specific grid. Note that all files are opened by name, and that the unit number assignment is dynamic and automatic.

In order to make all existing features available there is a new version of the input file that uses namelists. This is the version that will be supported in the future as it allows a more flexible addition of new features. **Please note that the namelist form is not supported by GCC compilers before version 4.8.2.**

start of example input file (namelist form)

```

! ----- !
! Define top-level model parameters via domain_def_nml namelist
! * namelist must be terminated with /
! * definitions & defaults:
!   domain%nrinp = 0 ! Number of grids defining input fields.
!   domain%nrgrd = 1 ! Number of wave model grids.
!   domain%nmmove = 1 ! Number of moving grid inputs.
!   domain%unipts = f ! Flag for using unified point output file.
!   domain%iostyp = 1 ! Output server type as in ww3_shel.nml
!   domain%upproc = f ! Flag for dedicated process for unified point output.
!   domain%pshare = f ! Flag for grids sharing dedicated output processes.
!   domain%flghg1 = f ! Flag for masking computation in two-way nesting
!   domain%flghg2 = f ! Flag for masking at printout time
!   domain%start = '19680606 000000' ! Start date for the entire model
!   domain%stop = '19680607 000000' ! Stop date for the entire model
! ----- !
&domain_def_nml

```

```

domain%nrinp = 3
domain%nrgrd = 5
domain%unipts = t
domain%start = '20100101 120000'
domain%stop  = '20101231 000000'
/

! ----- !
! Define each input grid via the input_grid_nml namelist
! * namelist must be terminated with /
! * input(i)%name must be set for each active input grid i
! * definitions & defaults:
!   input(i)%name           = 'unset'
!   input(i)%forcing%water_levels = f
!   input(i)%forcing%currents   = f
!   input(i)%forcing%winds      = f
!   input(i)%forcing%ice_conc   = f
!   input(i)%forcing%ice_param1 = f
!   input(i)%forcing%ice_param2 = f
!   input(i)%forcing%ice_param3 = f
!   input(i)%forcing%ice_param4 = f
!   input(i)%forcing%ice_param5 = f
!   input(i)%forcing%mud_density = f
!   input(i)%forcing%mud_thickness = f
!   input(i)%forcing%mud_viscosity = f
!   input(i)%assim%mean         = f
!   input(i)%assim%spec1d       = f
!   input(i)%assim%spec2d       = f
! ----- !
&input_grid_nml

  input(1)%name           = 'atm'
  input(1)%forcing%winds  = t
  input(1)%forcing%mud_viscosity = t
  input(1)%assim%mean     = t

  input(2)%name           = 'ocn'
  input(2)%forcing%water_levels = t
  input(2)%forcing%currents   = t

  input(3)%name           = 'ice'
  input(3)%forcing%ice_conc   = t
  input(3)%forcing%ice_param1 = t

```

```

input(3)%forcing%ice_param2    = t

/

! ----- !
! Define each model grid via the model_grid_nml namelist
! * namelist must be terminated with /
! * model(i)%name must be set for each active model grid i
! * definitions & defaults:
!   model(i)%name                = 'unset'
!   model(i)%forcing%water_levels = 'no'
!   model(i)%forcing%currents    = 'no'
!   model(i)%forcing%winds       = 'no'
!   model(i)%forcing%ice_conc    = 'no'
!   model(i)%forcing%ice_param1  = 'no'
!   model(i)%forcing%ice_param2  = 'no'
!   model(i)%forcing%ice_param3  = 'no'
!   model(i)%forcing%ice_param4  = 'no'
!   model(i)%forcing%ice_param5  = 'no'
!   model(i)%forcing%mud_density = 'no'
!   model(i)%forcing%mud_thickness = 'no'
!   model(i)%forcing%mud_viscosity = 'no'
!   model(i)%assim%mean          = 'no'
!   model(i)%assim%spec1d        = 'no'
!   model(i)%assim%spec2d        = 'no'
!   model(i)%resource%rank_id    = i
!   model(i)%resource%group_id   = 1
!   model(i)%resource%sibling_id = 0
!   model(i)%resource%comm_frac  = 0.00,1.00
!   model(i)%resource%bound_flag = f
!
!   model(4)%forcing = 'no' 'no' 'no' 'no' 'no' 'no'
!
!   model(2)%resource = 1 1 0 0.00 1.00 f
! ----- !
&model_grid_nml

model(1)%name                = 'grd1'
model(1)%forcing%winds       = 'atm'
model(1)%forcing%currents    = 'ocn'
model(1)%forcing%water_levels = 'ocn'

model(2)%name                = 'grd2'

```

```

model(2)%forcing%winds      = 'atm'
model(2)%forcing%currents   = 'ocn'
model(2)%forcing%water_levels = 'ocn'
model(2)%forcing%ice_conc   = 'ice'

model(3)%name               = 'grd3'
model(3)%forcing%winds      = 'atm'
model(3)%forcing%currents   = 'ocn'
model(3)%forcing%water_levels = 'ocn'
model(3)%forcing%ice_conc   = 'ice'

model(4)%name = 'grd4'
model(5)%name = 'grd5'

model(4)%forcing = 'ocn' 'ocn' 'atm' 'ice' 'ice' 'ice'
model(5)%forcing = 'ocn' 'ocn' 'atm' 'ice' 'ice' 'ice'

model(1)%resource = 1 1 0 0.00 0.50 t
model(2)%resource = 2 1 0 0.25 0.75 f
model(3)%resource = 3 1 0 0.50 1.00 f
model(4)%resource = 4 1 0 0.00 1.00 f
model(5)%resource = 4 1 0 0.00 1.00 f

model(5)%resource%bound_flag = t

/

! ----- !
! Define the output types point parameters via output_type_nml namelist
! * namelist must be terminated with /
! * alltype will apply the output types for all the model grids
! * type(i) will apply the output types for the model grid number i
! * need domain%unipts equal true to use a unified point output file
! * the point file is a space separated values per line : lon lat 'name'
! * the full list of field names is :
! DPT CUR WND AST WLV ICE IBG D50 IC1 IC5 HS LM T02 TOM1 T01 FP DIR SPR
! DP HIG EF TH1M STH1M TH2M STH2M WN PHS PTP PLP PDIR PSPR PWS TWS PNR
! UST CHA CGE FAW TAW TWA WCC WCF WCH WCM SXY TWO BHD FOC TUS USS P2S
! USF P2L TWI FIC ABR UBR BED FBB TBB MSS MSC DTD FC CFX CFD CFK U1 U2
! * output track file formatted (t) or unformatted (f)
! * definitions & defaults:
!     alltype%point%name      = 'unset'
!     alltype%point%file      = 'unset'

```

```

!      alltype%field%list      = 'unset'
!      alltype%track%format    = t
!      alltype%partition%x0    = 0
!      alltype%partition%xn    = 0
!      alltype%partition%nx    = 0
!      alltype%partition%y0    = 0
!      alltype%partition%yn    = 0
!      alltype%partition%ny    = 0
!      alltype%partition%format = t
!
!      type(3)%track%format    = f
! ----- !
&output_type_nml
  alltype%point%name      = 'points'
  alltype%point%file      = 'points.list'
  alltype%field%list      = 'HS DIR SPR'

  type(3)%field%list      = 'HS DIR SPR WND ICE CUR LEV'
/

! ----- !
! Define output dates via output_date_nml namelist
! * namelist must be terminated with /
! * alldate will apply the output dates for all the model grids
! * date(i) will apply the output dates for the model grid number i
! * start and stop times are with format 'yyyymmdd hhmmss'
! * if time stride is equal '0', then output is disabled
! * time stride is given in seconds
! * it is possible to overwrite a global output date for a given grid
! * definitions & defaults:
!      alldate%field%start    = '19680606 000000'
!      alldate%field%stride   = '0'
!      alldate%field%stop     = '19680607 000000'
!      alldate%point%start    = '19680606 000000'
!      alldate%point%stride   = '0'
!      alldate%point%stop     = '19680607 000000'
!      alldate%track%start    = '19680606 000000'
!      alldate%track%stride   = '0'
!      alldate%track%stop     = '19680607 000000'
!      alldate%restart%start  = '19680606 000000'
!      alldate%restart%stride = '0'
!      alldate%restart%stop   = '19680607 000000'
!      alldate%boundary%start = '19680606 000000'

```



```

!   alldate%boundary%stride      = '0'
!   alldate%boundary%stop        = '19680607 000000'
!   alldate%partition%start      = '19680606 000000'
!   alldate%partition%stride     = '0'
!   alldate%partition%stop       = '19680607 000000'
!
!   alldate%restart               = '19680606 000000' '0' '19680607 000000'
!
!   date(3)%partition%startdate = '19680606 000000'
! ----- !
&output_date_nml
  alldate%field%start = '20100101 000000'
  alldate%field%stride = '3600'
  alldate%field%stop   = '20101231 000000'
  alldate%point%start  = '20100101 000000'
  alldate%point%stride = '3600'
  alldate%point%stop   = '20101231 000000'

  alldate%restart      = '20101231 000000' '43200' '20501231 000000'

  date(5)%partition%start = '20100601 000000'
  date(5)%partition%stride = '3600'
  date(5)%partition%start = '20101201 000000'
/

! ----- !
! Define homogeneous input via homonegenous_input_nml namelist
! * namelist must be terminated with /
! * the number of moving grid inputs is defined by domain_def%nmove
! * each homogeneous input must start from index 1 to nmove
! * if speed is equal 0, then the moving grid is deactivated
! * definitions & defaults:
!   homogeneous%n_moving          = 0
!   homogeneous(1)%moving%start   = '19680606 000000'
!   homogeneous(1)%moving%speed   = 0
!   homogeneous(1)%moving%direction = 0
!   homogeneous(1)%moving%gradient = 0
!   ...
!   homogeneous(3)%moving%start   = '19680606 000000'
! ----- !
&homogeneous_input_nml
  homogeneous(1)%moving%start = '20100610 000000'

```

210

```
homogeneous(1)%moving%speed      = 5.  
homogeneous(1)%moving%direction = 90.  
/
```

end of example input file (namelist form)

start of example input file (traditional form)

```

$ ----- $
$ WAVEWATCH III multi-grid model driver input file $
$ ----- $
$
$ *****
$ *** NOTE : This is an example file from the mww3_test_05 script ***
$ ***           Unlike other input example files this one CANNOT           ***
$ ***           be run as an independent interactive run                       ***
$ *****
$
$ The first input line sets up the general multi-grid model definition
$ by defining the following six parameters :
$
$ 1) Number of wave model grids. ( NGRD )
$ 2) Number of grids defining input fields. ( NRINP )
$ 3) Flag for using unified point output file. ( UNIPPTS )
$ 4) Output server type as in ww3_shel.inp
$ 5) Flag for dedicated process for unified point output.
$ 6) Flag for grids sharing dedicated output processes.
$
$ 3 1 T 1 T T
$
$ ----- $
$ If there are input data grids defined ( NRINP > 0 ), then these
$ grids are defined first. These grids are defined as if they are wave
$ model grids using the file mod_def.MODID. Each grid is defined on
$ a separate input line with MODID, and eight input flags identifying
$ the presence of 1) water levels 2) currents 3) winds 4) ice and
$ 5-7) assimilation data as in the file ww3_shel.inp.
$
$ 'input' F F T F F F F
$
$ In this example, we need the file mod_def.input to define the grid
$ and the file wind.input to provide the corresponding wind data.
$
$ ----- $
$ If all point output is gathered in a unified point output file
$ ( UNIPPTS = .TRUE. ), then the output spectral grid needs to be
$ defined. This information is taken from a wave model grid, and only
$ the spectral definitions from this grid are relevant. Define the
$ name of this grid here
$
$ 'points'
$

```

```

$ In this example, we need the file mod_def.points to define the
$ spectral output grid, and the point output will be written to the
$ file out_pnt.points
$
$ ----- $
$ Now each actual wave model grid is defined using 13 parameters to be
$ read from a single line in the file. Each line contains the following
$ parameters
$   1) Define the grid with the extension of the mod_def file.
$   2-8) Define the inputs used by the grids with 8 keywords
$        corresponding to the 8 flags defining the input in the
$        input files. Valid keywords are:
$         'no'      : This input is not used.
$         'native'  : This grid has its own input files, e.g. grid
$                   grdX (mod_def.grdX) uses ice.grdX.
$         'MODID'   : Take input from the grid identified by
$                   MODID. In the example below, all grids get
$                   their wind from wind.input (mod_def.input).
$   9) Rank number of grid (internally sorted and reassigned).
$   10) Group number (internally reassigned so that different
$        ranks result in different group numbers.
$   11-12) Define fraction of communicator (processes) used for this
$         grid.
$   13) Flag identifying dumping of boundary data used by this
$        grid. If true, the file nest.MODID is generated.
$
$ 'grd1' 'no' 'no' 'input' 'no' 'no' 'no' 'no'  1  1  0.00 1.00  F
$ 'grd2' 'no' 'no' 'input' 'no' 'no' 'no' 'no'  2  1  0.00 1.00  F
$ 'grd3' 'no' 'no' 'input' 'no' 'no' 'no' 'no'  3  1  0.00 1.00  F
$ 'grd1' 'no' 'no' 'input' 'no' 'no' 'no' 'no'  1  1  0.00 0.50  F
$ 'grd2' 'no' 'no' 'input' 'no' 'no' 'no' 'no'  2  1  0.25 0.75  F
$ 'grd3' 'no' 'no' 'input' 'no' 'no' 'no' 'no'  3  1  0.50 1.00  F
$
$ In this example three grids are used requiring the files
$ mod_def.grdN. All files get their winds from the grid 'input'
$ defined by mod_def.input, and no other inputs are used. In the lines
$ that are commented out, each grid runs on a part of the pool of
$ processes assigned to the computation.
$
$ ----- $
$ Starting and ending times for the entire model run
$
$   19680606 000000   19680607 000000
$
$ ----- $

```

```

$ Specific multi-scale model settings (single line).
$   Flag for masking computation in two-way nesting (except at
$                                     output times).
$   Flag for masking at printout time.
$
  F F
$
$ ----- $
$ Conventional output requests as in ww3_shel.inp. Will be applied
$ to all grids.
$
  19680606 000000   3600  19680607 000000
$-----
$
$ Output request flags identifying fields as in ww3_shel.inp. See that
$ file for a full documentation of field output options. Namelist type
$ selection is used here (for alternative F/T flags, see ww3_shel.inp).
$
  N
  DPT CUR WND HS TOM1 FP DP PHS PTP PDIR
$
$-----
$
$ NOTE: If UNIPITS = .TRUE. then the point output needs to be defined
$       here and cannot be redefined below.
$
  19680606 000000   3600  19680608 000000
    0.E3    0.E3   'eye      '
    0.E3   50.E3   'mN       '
   -35.E3   35.E3   'mNW      '
   -50.E3    0.E3   'mW       '
   -35.E3  -35.E3   'mSW      '
    0.E3   -50.E3   'mS       '
    35.E3  -35.E3   'mSE      '
    50.E3    0.E3   'mE       '
    35.E3   35.E3   'mNE      '
    0.E3   100.E3   'aN       '
   -70.E3   70.E3   'aNW      '
  -100.E3    0.E3   'aW       '
   -70.E3  -70.E3   'aSW      '
    0.E3  -100.E3   'aS       '
    70.E3  -70.E3   'aSE      '
   100.E3    0.E3   'aE       '
    70.E3   70.E3   'aNE      '
    0.E3   210.E3   'bN       '

```

```

-150.E3  150.E3  'bNW      '
-210.E3   0.E3  'bW       '
-150.E3 -150.E3  'bSW      '
  0.E3  -210.E3  'bS       '
 150.E3 -150.E3  'bSE     '
 210.E3   0.E3  'bE       '
 150.E3  150.E3  'bNE     '
  0.E3   800.E3  'cN       '
-550.E3  550.E3  'cNW      '
-800.E3   0.E3  'cW       '
-550.E3 -550.E3  'cSW     '
  0.E3  -800.E3  'cS       '
 550.E3 -550.E3  'cSE     '
 800.E3   0.E3  'cE       '
 550.E3  550.E3  'cNE     '
  0.E3   0.E3  'STOPSTRING'

$
$ Four additional output types: see ww3_shel.inp for documentation.
$
$ track output
19680606 000000      0 19680608 000000
$
$ restart files
19680606 000000      0 19680608 000000
$
$ boundary output
19680606 000000      0 19680608 000000
$
$ separated wave field data
19680606 000000      0 19680608 000000
$
$ ----- $
$ Output requests per grid and type to overwrite general setup
$ as defined above. First record per set is the grid name MODID
$ and the output type number. Then follows the standard time string,
$ and conventional data as per output type. In mww3_test_05 this is
$ not used. Below, one example generating partitioning output for
$ the inner grid is included but commented out.
$
$ 'grd3' 6
$ 19680606 000000      900 19680608 000000
$   0 999 1 0 999 1 T
$
$ ----- $
$ Mandatory end of output requests per grid, identified by output

```

```
$ type set to 0.  
$  
  'the_end'  0  
$  
$ ----- $  
$ Moving grid data as in ww3_shel.inp. All grids will use same data.  
$  
  'MOV' 19680606 000000  5.  90.  
  'STP'  
$  
$ ----- $  
$ End of input file $  
$ ----- $
```

end of example input file (traditional form)

4.4.12 Grid Integration

Program	:	ww3_gint		(W3GINT)
Code	:	ww3_gint.ftn		
Input	:	ww3_gint.inp	(10)	Formatted input file for program.
		mod_def.*	(20)	Model definition files in WAVE-WATCH III format for base and target grids
		out_grd.*	(30+)	Gridded field files in WAVE-WATCH III format for base grids
Output	:	standard out	(6)	Formatted output of program.
		out_grd.*	(30+)	Gridded field files in WAVE-WATCH III format for target grid

This post processor program takes field data from several overlapping grids and produces a unified output file. The different model definition and field output files are identified by the unique identifier associated with each specific grid. At this moment the program works with curvilinear and rectilinear grids.

start of example input file (traditional form)

```

$ ----- $
$ WAVEWATCH III Grid integration input file $
$ ----- $
$ Time, time increment and number of outputs
$
19680606 060000 10800. 1
$
$ Total number of grids (NGR). The code assumes that the first NGR-1
$ grids are the input grids and the last grid is the target grid in
$ which the output fields are to be interpolated. It also assumes
$ that all the grids have the same output fields switched on
$
$ NGR
$
4
$
$ Grid Ids
$
'grd1'
```



```

'grd2'
'grd3'
'grd4'
$
$ In this example grd1, grd2 and grd3 are the input grids. For each
$ of these grids a mod_def.grdN and an out_grd.grdN are available.
$ The target grid is grd4, and a mod_def.grd4 is also made available.
$ Upon execution of the code an out_grd.grd4 is generated via
$ interpolation of output fields from the various out_grd.grdN
$ (N varying from 1 to 3) files.
$
$ ----- $
$ End of input file                               $
$ ----- $

```

end of example input file (traditional form)

Note that this program can be used in concert with the grid splitting program `ww3_gspl`, and that `ww3_gspl.sh` has an option to produce a template input file for his program (see Section 4.4.10).

4.4.13 Gridded output post-processor

Program	:	ww3_outf		(W3OUTF)
Code	:	ww3_outf.ftn		
Input	:	ww3_outf.inp	(10)	Input file for gridded output post-processor.
		mod_def.ww3	(20)	Model definition file.
		out_grd.ww3	(20)	Raw gridded output data.
Output	:	standard out	(6)	Formatted output of program.
		...*	(50)	Transfer file.

start of example input file (traditional form)

```

$ ----- $
$ WAVEWATCH III Grid output post-processing $
$ ----- $
$ Time, time increment and number of outputs
$
19680606 060000 10800. 1
$
$ Output request flags identifying fields as in ww3_shel.inp. See this
$ file for a full documentation of the field output options.
$
N
DPT HS FP T01 WL02 ALPXT ALPYT ALPHY
$
$ Output type ITYPE [0,1,2,3], and IPART [ 0,...,NOSWLL ]
$
1 0
$ ----- $
$ ITYPE = 0, inventory of file.
$       No additional input, the above time range is ignored.
$
$ ----- $
$ ITYPE = 1, print plots.
$       IX,IY range and stride, flag for automatic scaling to
$       maximum value (otherwise fixed scaling),
$       vector component flag (dummy for scalar quantities),
$
1 12 1 1 12 1 F T
$
$ ----- $
$ ITYPE = 2, field statistics.
$       IX,IY range.

```

```

$
$ 1 12 1 12
$
$ ----- $
$ ITYPE = 3, transfer files.
$       IX, IY range, IDLA and IDFM as in ww3_grid.inp.
$       The additional option IDLA=5 gives longitude, latitude
$       and parameter value(s) per record (defined points only),
$
$ 2 11 2 11 1 2
$
$ For each field and time a new file is generated with the file name
$ ww3.yymmddhh.xxx, where yymmddhh is a conventional time indicator,
$ and xxx is a field identifier. The first record of the file contains
$ a file ID (C*13), the time in yyyyymmdd hhmmss format, the lowest,
$ highest and number of longitudes (2R,I), id. latitudes, the file
$ extension name (C*$), a scale factor (R), a unit identifier (C*10),
$ IDLA, IDFM, a format (C*11) and a number identifying undefined or
$ missing values (land, ice, etc.). The field follows as defined by
$ IDFM and IDLA, defined as in the grid preprocessor. IDLA=5 is added
$ and gives a set of records containing the longitude, latitude and
$ parameter value. Note that the actual data is written as an integers.
$
$ ----- $
$ End of input file                                     $
$ ----- $

```

end of example input file (traditional form)

The extension of the file name of transfer files for `ITYPE = 3` identifies the content of the file. The file extension for each data type is given in Table 4.1 on page 240.

4.4.14 Gridded NetCDF output post-processor

Program	:	ww3_ounf		(w3OUNF)
Code	:	ww3_ounf.ftn		
Input	:	ww3_ounf.inp	(10)	Input file for gridded output post-processor.
		mod_def.ww3	(20)	Model definition file.
		out_grd.ww3	(20)	Raw gridded output data.
		NC_globatt.inp	(994)	Additional global attributes.
Output	:	standard out	(6)	Formatted output of program.
		*.nc	()	NetCDF file

start of example input file (traditional form)

```

$ ----- $
$ WAVEWATCH III Grid output post-processing $
$ ----- $
$ First output time (yyyymmdd hhmmss), increment of output (s),
$ and number of output times.
$
19850101 000000 3600. 1000
$
$ Fields requested ----- $
$
$ Output request flags identifying fields as in ww3_shel.inp. See that
$ file for a full documentation of field output options. Namelist type
$ selection is used here (for alternative F/T flags, see ww3_shel.inp).
$
$ DPT CUR WND AST WLW ICE IBG D50 IC1 IC5 HS LM T02 TOM1 T01 FP DIR SPR
$ DP HIG EF TH1M STH1M TH2M STH2M WN PHS PTP PLP PDIR PSPR PWS TWS PNR
$ UST CHA CGE FAW TAW TWA WCC WCF WCH WCM SXY TWO BHD FOC TUS USS P2S
$ USF P2L TWI FIC ABR UBR BED FBB TBB MSS MSC DTD FC CFX CFD CFK U1 U2
$
N
DPT HS FP T01
$
$----- $
$ netCDF version [3,4]
$ and variable type 4 [2 = SHORT, 3 = it depends , 4 = REAL]
$ swell partitions [0 1 2 3 4 5]
$ variables in same file [T] or not [F]
$
3 4

```

```

0 1 2
T
$
$ ----- $
$ File prefix
$ number of characters in date [4(yearly),6(monthly),8(daily),10(hourly)]
$ IX and IY ranges [regular:IX NX IY NY, unstructured:IP NP 1 1]
$
ww3.
6
1 1000000 1 1000000
$
$ For each field and time a new file is generated with the file name
$ ww3.date_XXX.nc , where date is a conventional time indicator with S3
$ characters, and XXX is a field identifier.
$
$ ----- $
$ End of input file $
$ ----- $

```

end of example input file (traditional form)

When a single field is put in the file, the abbreviated field name (file extensions from `ww3_outf`) for each data type is given in Table 4.1 on page 240.

4.4.15 Gridded output post-processor for GrADS

Program	:	gx_outf		(GXOUTF)
Code	:	gx_outf.ftn		
Input	:	gx_outf.inp	(10)	Input file for gridded output post-processor.
		mod_def.ww3	(20)	Model definition file.
		out_grd.ww3	(20)	Raw gridded output data.
Output	:	standard out	(6)	Formatted output of program.
		ww3.grads	(50)	GrADS data file.
		ww3.ctf	(51)	GrADS control file.

start of example input file (traditional form)

```

$ ----- $
$ WAVEWATCH III Grid output post-processing ( GrADS ) $
$ ----- $
$ Time, time increment and number of outputs.
$
19680606 000000 3600. 25
$
$ Output request flags identifying fields as in ww3_shel.inp. See that
$ file for a full documentation of field output options. Namelist type
$ selection is used here (for alternative F/T flags, see ww3_shel.inp).
$
N
DPT HS FP T01
$
$ -----
$ Grid range in discrete counters IXmin,max, IYmin,max, flags for
$ including sea and boundary points in map
$
0 999 0 999 T T
$
$ NOTE : In the Cartesian grid version of the code, X and Y are
$ converted to longitude and latitude assuming that 1 degree
$ equals 100 km if the maximum of X or Y is larger than 1000km.
$ For maxima between 100 and 1000km 1 degree is assumed to be
$ 10km etc. Adjust labels in GrADS scripts accordingly.
$
$ ----- $
$ End of input file $
$ ----- $

```

end of example input file (traditional form)

This post-processor generates input files with gridded model parameters for the Grid Analysis and Display System (GrADS, [Doty, 1995](#)). Although GrADS can also work with GRIB files, the present preprocessor is preferable, as the data file also gives access to a land-sea-ice map.

4.4.16 Gridded GRIB output post-processor

Program	:	ww3_grib		(w3GRIB)
Code	:	ww3_grib.ftn		
Input	:	ww3_grib.inp	(10)	Input file for gridded output post-processor.
		mod_def.ww3	(20)	Model definition file.
		out_grd.ww3	(20)	Raw gridded output data.
Output	:	standard out	(6)	Formatted output of program.
		gribfile	(50)	GRIB file.

start of example input file (traditional form)

```

$ ----- $
$ WAVEWATCH III Grid output post-processing ( GRIB ) $
$----- $
$ Time, time increment and number of outputs.
$
19680606 000000 3600. 3
$
$ Output request flags identifying fields as in ww3_shel.inp. See that
$ file for a full documentation of field output options. Namelist type
$ selection is used here (for alternative F/T flags, see ww3_shel.inp).
$
N
DPT HS FP T01
$
$ Additional info needed for grib file
$ Forecast time, center ID, generating process ID, grid definition
$ and GDS/BMS flag
$
19680606 010000 7 10 255 192
$
$ ----- $
$ End of input file $
$----- $

```

end of example input file (traditional form)

This post-processor packs fields of mean wave parameters in GRIB format, using GRIB version II and NCEP's w3 and bacio library routines, or in

GRIB2, using NCEPS's operational package. Additional packing data can be found in Table 4.1 on page 240.

The GRIB packing is performed using the NCEP's GRIB tables as described in NCEP (1998). Because the w3 and bacio routine are not fully portable, they are not supplied with the code. The user will have to provide corresponding routines. It is suggested that such routines are activated with additional WAVEWATCH III switches in the mandatory switch group containing the 'NOGRB' switch, as if presently the case with the NCEP routines. The GRIB2 packing is performed according to WMO (2001), and is performed with NCEP's standard operational packages.

Table 4.1 shows the KPDS(5) data values for GRIB packing. For the partitioned data, the first number identifies the wind sea, the second number identifies swell. Most data are packed as surface data (KPDS(6) = 0). For the partitioned swell fields, however, consecutive fields are packed at consecutive levels, with the level type indicator set to (KPDS(6) = 241). KPDS(7) identifies the actual level or swell field number.

Table 4.1 shows several KPDS data values for GRIB2 packing. The first number in the table represents LISTSEC0(2), which identifies the discipline type (e.g., oceanography, meteorology, etc.) The second number represents KPDS(1), which identifies the parameter category (e.g., waves, circulation, ice, etc.) within the discipline type. The third number represents KPDS(2), which identifies the actual parameter. For the partitioned data, A/B means A for wind sea and B for swell. Additionally KPDS(10) = 0 for surface data, and KPDS(10) = 241 to pack consecutive swell fields at consecutive levels. KPDS(12) identifies the actual level or swell field number.

Although the above input file contains flags for all 31 output fields of WAVEWATCH III, not all fields can be packed in GRIB. If a parameter is chosen for which GRIB packing is not available, a message will be printed to standard output. Table 4.1 shows which parameter can be packed in GRIB. Note that at NCEP the conversions from GRIB to GRIB2 coincided with the introduction of partitioned wave model output. This required some duplicate definitions in GRIB and some apparent inconsistencies between GRIB and GRIB2 packing.

4.4.17 Point output post-processor

Program	:	ww3_outp		(W3OUTP)
Code	:	ww3_outp.ftn		
Input	:	ww3_outp.inp	(10)	Input file for point output post-processor.
		mod_def.ww3	(20)	Model definition file.
		out_pnt.ww3	(20)	Raw point output data.
		NC_globatt.inp	(994)	Additional global attributes.
Output	:	standard out	(6)	Formatted output of program.
		tabnn.ww3 *	(nn)	Table of mean parameters where <i>nn</i> is a two-digit integer.
		... *	(user)	Transfer file.

start of example input file (traditional form)

```

$ ----- $
$ WAVEWATCH III Point output post-processing $
$ ----- $
$ First output time (yyyymmdd hhmmss), increment of output (s),
$ and number of output times.
$
$ 19680606 060000 3600. 7
$
$ Points requested ----- $
$ Define points for which output is to be generated.
$
$ 1
$ 2
$ 3
$ 4
$
$ mandatory end of list
-1
$
$ Output type ITYPE [0,1,2,3,4]
$
$ 1
$ ----- $
$ ITYPE = 0, inventory of file.
$ No additional input, the above time range is ignored.
$
$ ----- $

```

```

$ ITYPE = 1, Spectra.
$   - Sub-type OTYPE :  1 : Print plots.
$                       2 : Table of 1-D spectra
$                       3 : Transfer file.
$   - Scaling factors for 1-D and 2-D spectra Negative factor
$     disables, output, factor = 0. gives normalized spectrum.
$   - Unit number for transfer file, also used in table file
$     name.
$   - Flag for unformatted transfer file.
$
$  1  0.  0.  33  F
$
$ The transfer file contains records with the following contents.
$
$ - File ID in quotes, number of frequencies, directions and points.
$   grid name in quotes (for unformatted file C*21,3I,C*30).
$ - Bin frequencies in Hz for all bins.
$ - Bin directions in radians for all bins (Oceanographic conv.).
$
$                                     -+
$ - Time in yyymmdd hhmmss format                                     | loop
$                                     -+                               |
$ - Point name (C*10), lat, lon, d, U10 and                          | loop   | over
$   direction, current speed and direction                          | over  |
$ - E(f,theta)                                                         | points | times
$                                     -+                               -+
$
$ The formatted file is readable using free format throughout.
$ This data set can be used as input for the bulletin generator
$ w3split.
$
$ ----- $
$ ITYPE = 2, Tables of (mean) parameter
$   - Sub-type OTYPE :  1 : Depth, current, wind
$                       2 : Mean wave pars.
$                       3 : Nondimensional pars. (U*)
$                       4 : Nondimensional pars. (U10)
$                       5 : 'Validation table'
$                       6 : WMO standard output
$   - Unit number for file, also used in file name.
$
$  6  66
$
$ If output for one point is requested, a time series table is made,
$ otherwise the file contains a separate tables for each output time.
$

```

```

$ ----- $
$ ITYPE = 3, Source terms
$   - Sub-type OTYPE :  1 : Print plots.
$                       2 : Table of 1-D S(f).
$                       3 : Table of 1-D inverse time scales
$                         (1/T = S/F).
$                       4 : Transfer file
$   - Scaling factors for 1-D and 2-D source terms. Negative
$     factor disables print plots, factor = 0. gives normalized
$     print plots.
$   - Unit number for transfer file, also used in table file
$     name.
$   - Flags for spectrum, input, interactions, dissipation,
$     bottom, ice and total source term.
$   - scale ISCALE for OTYPE=2,3
$       0 : Dimensional.
$       1 : Nondimensional in terms of U10
$       2 : Nondimensional in terms of U*
$       3-5: like 0-2 with f normalized with fp.
$   - Flag for unformatted transfer file.
$
$ 1 0. 0. 50  T T T T T T T 0  F
$
$ The transfer file contains records with the following contents.
$
$ - File ID in quotes, number of frequencies, directions and points,
$   flags for spectrum and source terms (C*21, 3I, 6L)
$ - Bin frequencies in Hz for all bins.
$ - Bin directions in radians for all bins (Oceanographic conv.).
$
$ - Time in yyymmdd hhmmss format
$
$ - Point name (C*10), depth, wind speed and
$   direction, current speed and direction
$ - E(f,theta) if requested
$ - Sin(f,theta) if requested
$ - Snl(f,theta) if requested
$ - Sds(f,theta) if requested
$ - Sbt(f,theta) if requested
$ - Sice(f,theta) if requested
$ - Stot(f,theta) if requested
$
$
$ ----- $
$ ITYPE = 4, Spectral partitions and bulletins
$   - Sub-type OTYPE :  1 : Spectral partitions

```

```

$           2 : Bulletins ASCII format
$           3 : Bulletins CSV format
$           4 : Bulletins ASCII and CSV formats
$ - Unit number for transfer file, also used in table file
$   name.
$ - Reference date/time in YYYYMMDD HHMMSS format, used for
$   including in bulletin legend, and computing forecast time
$   in CSV type output (if the first field is negative, the
$   reference time becomes the first simulation time slice)
$ - Three-character code indicating time zone (UTC, EST etc)
$
$ 4 2 19680606 060000 'UTC'
$
$ The transfer file contains records with the following contents.
$
$ - File ID in quotes, number of frequencies, directions and points.
$   grid name in quotes (for unformatted file C*21,3I,C*30).
$ - Bin frequencies in Hz for all bins.
$ - Bin directions in radians for all bins (Oceanographic conv.).
$
$ - Time in yyymmdd hhmss format
$
$ - Point name (C*10), lat, lon, d, U10 and
$   direction, current speed and direction
$ - E(f,theta)
$
$           -+
$           | loop
$           |
$           -+
$           | loop
$           | over
$           |
$           | over
$           |
$           | points
$           | times
$           -+
$           -+
$
$ ----- $
$ End of input file
$ ----- $

```

end of example input file (traditional form)

In previous releases of WAVEWATCH III spectral bulletins were generated using spectral data transfer file generated with `ITYPE = 1` and `OTYPE = 3` and the `w3split` program (see section 5.2). This is an obsolescent code that is produced here for backward compatibility only. This program reads the following five records from standard input (no comment lines allowed) :

- Name of output location.
- Identifier for run to be used in table.

- Name of input file.
- Logical identifying UNFORMATTED input file.
- Name of output file.

All above strings are read as characters using free format, and therefore need to be enclosed in quotes.

4.4.18 Point output NetCDF post-processor

Program	:	ww3_ounp		(W3OUNP)
Code	:	ww3_ounp.ftn		
Input	:	ww3_ounp.inp	(10)	Input file for point output post-processor.
		mod_def.ww3	(20)	Model definition file.
		out_pnt.ww3	(20)	Raw point output data.
Output	:	standard out	(6)	Formatted output of program.
		...*	(user)	Transfer file.

start of example input file (traditional form)

```

$ ----- $
$ WAVEWATCH III NETCDF Point output post-processing $
$ ----- $
$ First output time (yyyymmdd hhmmss), increment of output (s),
$ and number of output times.
$
19850101 000000 3600. 1000
$
$ Points requested ----- $
$
$ Define points index for which output is to be generated.
$ If no one defined, all points are selected
$ One index number per line, negative number identifies end of list.
$ 1
$ 2
$ mandatory end of list
-1
$
$ ----- $
$ file prefix
$ number of characters in date [4(yearly),6(monthly),8(daily),10(hourly)]
$ netCDF version [3,4]
$ points in same file [T] or not [F]
$ and max number of points to be processed in one pass
$ output type ITYPE [0,1,2,3]
$ flag for global attributes WW3 [0] or variable version [1-2-3-4]
$ flag for dimensions order time,station [T] or station,time [F]
$
ww3.
6
4

```

```

T 150
1
0
T
$
$ ----- $
$ ITYPE = 0, inventory of file.
$       No additional input, the above time range is ignored.
$
$ ----- $
$ ITYPE = 1, netCDF Spectra.
$       - Sub-type OTYPE :  1 : Print plots.
$                           2 : Table of 1-D spectra
$                           3 : Transfer file.
$                           4 : Spectral partitioning.
$       - Scaling factors for 1-D and 2-D spectra Negative factor
$         disables, output, factor = 0. gives normalized spectrum.
$
3 1 0
$
$ The transfer file contains records with the following contents.
$
$ - File ID in quotes, number of frequencies, directions and points.
$   grid name in quotes (for unformatted file C*21,3I,C*30).
$ - Bin frequencies in Hz for all bins.
$ - Bin directions in radians for all bins (Oceanographic conv.).
$
$                                     +-
$ - Time in yyymmdd hhmmss format      | loop
$                                     +- |
$ - Point name (C*10), lat, lon, d, U10 and | loop | over
$   direction, current speed and direction | over |
$ - E(f,theta)                            | points | times
$                                     +-   +-
$
$ ----- $
$ ITYPE = 2, netCDF Tables of (mean) parameter
$       - Sub-type OTYPE :  1 : Depth, current, wind
$                           2 : Mean wave pars.
$                           3 : Nondimensional pars. (U*)
$                           4 : Nondimensional pars. (U10)
$                           5 : 'Validation table'
$                           6 : WMO standard output
$
4
$
$ ----- $

```



```

$ ITYPE = 3, netCDF Source terms
$   - Sub-type OTYPE :  1 : Print plots.
$                       2 : Table of 1-D S(f).
$                       3 : Table of 1-D inverse time scales
$                         (1/T = S/F).
$                       4 : Transfer file
$   - Scaling factors for 1-D and 2-D source terms. Negative
$     factor disables print plots, factor = 0. gives normalized
$     print plots.
$   - Flags for spectrum, input, interactions, dissipation,
$     bottom, ice and total source term.
$   - scale ISCALE for OTYPE=2,3
$       0 : Dimensional.
$       1 : Nondimensional in terms of U10
$       2 : Nondimensional in terms of U*
$       3-5: like 0-2 with f normalized with fp.
$
$ 4 0 0 T T T T T T 0
$
$ The transfer file contains records with the following contents.
$
$ - File ID in quotes, number of frequencies, directions and points,
$   flags for spectrum and source terms (C*21, 3I, 6L)
$ - Bin frequencies in Hz for all bins.
$ - Bin directions in radians for all bins (Oceanographic conv.).
$
$ - Time in yyymmdd hhmmss format
$
$ - Point name (C*10), depth, wind speed and
$   direction, current speed and direction
$ - E(f,theta) if requested
$ - Sin(f,theta) if requested
$ - Snl(f,theta) if requested
$ - Sds(f,theta) if requested
$ - Sbt(f,theta) if requested
$ - Sice(f,theta) if requested
$ - Stot(f,theta) if requested
$
$
$ ----- $
$ End of input file $
$ ----- $

```

end of example input file (traditional form)

4.4.19 Point output post-processor for GrADS

Program :	gx_outp	(GXOUTP)	
Code :	gx_outp.ftn		
Input :	gx_outp.inp	(10)	Input file for point output post-processor.
	mod_def.ww3	(20)	Model definition file.
	out_pnt.ww3	(20)	Raw point output data.
Output :	standard out	(6)	Formatted output of program.
	ww3.spec.grads	(30)	GrADS data file with spectra and source terms.
	ww3.mean.grads	(31)	File with mean wave parameters.
	ww3.spec.ctl	(32)	GrADS control file.

start of example input file (traditional form)

```

$ ----- $
$ WAVEWATCH III Point output post-processing ( GrADS ) $
$ ----- $
$ First output time (yyyymmdd hhmmss), increment of output (s),
$ and number of output times.
$
19680606 000000 3600. 7
$
$ Points requested ----- $
$ Define points for which output is to be generated.
$
$ 1
$ 2
3
$ 4
$ mandatory end of list
-1
$
$ ----- $
$ Flags for plotting F, Sin, Snl, Sds, Sbt, Sice, Stot
$
T T T T T T
$
$ NOTE : In the Cartesian grid version of the code, X and Y are
$ converted to km. Use source_xy.gs instead of source.gs
$
$ ----- $

```

```

$ End of input file                                     $
$ -----                                             $

```

end of example input file (traditional form)

This post-processor is intended to generate data files with which GrADS (see previous section) can plot polar plots of spectra and source terms. To achieve this, spectra and source terms are stored as "longitude-latitude" grids. For each output point a different name is generated for the data, typically *LOCnnn*. When the data file is loaded in GrADS, the variable *LOC001* will contain a spectral grid for the first requested output point at level 1, the input source term at level 2, etc. For the second output point the data is stored in *LOC002* etc. The actual output point names are passed to GrADS through the control file *ww3.specctl*. Wave heights and environmental data are obtained from *ww3.mean.grads*. The user, however, need not be aware of the details of the GrADS data files and data storage. The GrADS scripts *spec.gs*, *source.gs* and *1source.gs* are provided to automatically generate spectral plots from the output files of this post-processor.

Note: for the GrADS scripts to work properly, the names of the output points should not contain spaces.

4.4.20 Track output post-processor

```

Program : ww3_trck           (W3TRCK)
Code    : ww3_trck.ftn
Input   : track_o.ww3       (11)   Raw track output data.
Output  : standard out      (6)    Formatted output of program.
         : track.ww3         (51)   Formatted data file.

```

This post-processor does not require a formatted input file with program commands. It will simply convert the entire unformatted file to an integer compressed formatted file. The file contains the following header records :

- File identifier (character string of length 34).
- Number of frequencies and directions, first direction and directional increment (radians, oceanographic convention).
- Radian frequencies of each frequency bin.
- Corresponding directional bin size times frequency bin size to obtain discrete energy per bin.

For each output point the following records are printed :

- Date and time in `yyyymmdd hhmmss` format, longitude and latitude in degrees, and a status identifier 'ICE', 'LND' or 'SEA'. The following two records are written only for sea points.
- Water depth in meters, current and wind u and v components in meters per second, friction velocity in meters per second, air-sea temperature difference in degrees centigrade and scale factor for spectrum.
- The entire spectrum in integer packed format (can be read using free format).

4.4.21 Spatial and temporal tracking of wave systems

Program	:	ww3_systrk		(W3SYSTRK)
Code	:	ww3_systrk.ftn		
Input	:	ww3_systrk.inp	(10)	Formatted input file for program.
		partition.ww3	(11)	Spectral partition file.
		sys_restart.ww3*	(12)	Restart file with system memory.
		sys_mask.ww3*	(13)	Mask file.
Output	:	sys_log.ww3	(20)	Output log (appended with processor number in parallel run).
		sys_coord.ww3	(21)	Lat/lon coordinates of fields.
		sys_hs.ww3	(22)	Significant wave height fields of individual wave systems.
		sys_tp.ww3	(23)	Peak period fields of individual wave systems.
		sys_dir.ww3	(24)	Peak direction fields of individual wave systems
		sys_dspr.ww3	(25)	Direction spread fields of individual wave systems.
		sys_pnt.ww3	(26)	Point output file for significant wave height, peak period, and peak direction.
		sys_restart1.ww3	(27)	Restart file.
		*.nc	()	NetCDF file.

start of example input file (traditional form)

```

$ ----- $
$ WAVEWATCH III Spatial and temporal tracking of wave systems $
$ ----- $
$ File name for raw partition data
$
$ 'partition.ww3'
$
$ First time level (yyyymmdd hhmmss), time increment and number of
$ time levels to process.
$
$ 20091122 000000 3600 4
$
$ Output type [1,3,4] [text file, netCDF version 3, netCDF version 4]
$ Note for NetCDF version 3 the TRKNC switch is needed and

```

```

$ for NetCDF version 4 the TRKNC and NC4 switches are needed.
  1
$
$ Wave tracking domain. First line: longitude limits, longitude intervals
$ (NX-1); second line: latitude limits, latitude intervals (NY-1).
$
  100. 275. 175
    0. 55. 55
$
$ Parameters of tracking algorithm ----- $
$ - dirKnob (deg), perKnob (s), hsKnob (m), wetPts (frac),
$   dirTimeKnob (deg), tpTimeKnob (s)
$ - seedLat, seedLon
$
  10. 1. 0.25 0.1 10. 1.
    0. 0.
$
$ Output points ----- $
$ Longitude, latitude. End with 0. 0. string on last line.
$
  222.54 40.75
  199.42 19.02
  205.94 23.55
  290.35 31.98
  347.60 48.70
  337.00 21.00
  197.94 24.32
  206.10 23.56
    0. 0.
$ ----- $
$ End of input file $
$ ----- $

```

end of example input file (traditional form)

Program currently implemented for regular grids only. The spatial and temporal tracking is performed on the basis of the spectral partition data file. Both the time interval and geographic domain over which wave systems are tracked can be subsets of the data contained in the partition file. The combining parameters `dirKnob` and `perKnob` are used to influence the strictness of the system combining algorithm in geographic space, and `dirTimeKnob` and `perTimeKnob` are the corresponding parameters in temporal space. Lower

values imply stricter criteria, which results in smaller, more numerous systems. This also typically increases the processing time. Recommended values are given above. These values can be influenced locally, for example around an island, by defining a mask file `sys_mask.wv3`. Parameters `hsKnob` and `wetPts` are a low-energy and small system filters—all wave systems with an average H_{m0} below `hsKnob` or with a size of less than `wetPts*100%` of the overall domain size are purged. Parameters `seedLat` and `seedLon` influence the origin of the wave system search spiral, with default at the center of model domain (indicated by 0. 0.). At the end of a tracking run, the end state of system memory is stored in `sys_restart1.wv3`. This file, renamed as `sys_restart.wv3`, can be used to restart a tracking sequence from this previous system memory state.

group	field	description extension	file data	GRIB1 data	GRIB2
1	1	depth	.dpt	–	–
1	2	mean current components	.cur	–	–
1	3	wind speed	.wnd	32	0,2,1
		wind direction		31	0,2,0
		wind u		33	0,2,2
		wind v		34	0,2,3
1	4	air-sea temp. dif.	.dt	–	–
1	5	water level	.wlv	–	10,3,1
1	6	ice coverage	.ice	91	10,2,0
2	1	wave height H_s	.hs	100	10,0,3
2	2	mean wave length	.l	–	–
2	3	mean wave period $T_{m0,2}$.t02	–	–
2	4	mean wave period $T_{m0,1}$.t	103	10,0,15
2	5	mean wave period $T_{m0,-1}$.tm1	–	–
2	6	peak frequency f_p	.fp	108	10,0,11
2	7	mean wave direction θ_m	.dir	101	–
2	8	directional spread σ	.spr	–	–
2	9	peak direction θ_p	.dp	107	10,0,10
4	1	H_s of partition	.phs	102,105	10,0,5/8
4	2	T_p of partition	.ptp	110,106	10,0,6/9
4	3	L_p of partition	.plp	–	–
4	4	θ_m of partition	.pdir	109,104	10,0,4/7
4	5	σ of partition	.psi	–	–
4	6	wind sea fraction of part.	.pws	–	–
4	7	total wind sea fraction	.wsf	–	–
4	8	number of partitions	.pnr	–	–
5	1	friction velocity comp.	.ust	–	–
5	2	Charnock parameter for air side	.cha	–	–
5	3	Energy flux $\int C_g E(f) df$.CgE	–	–
5	4	Wind to wave energy flux	.faw	–	–
5	5	Wave-supported stress	.taw	–	–
5	6	Upward wave-supported stress	.twa	–	–
5	7	Whitecap coeverage	.wcc	–	–
5	8	Average whitecap foam thickness	.wcf	–	–
5	9	Significant breaking wave height	.wch	–	–
5	10	Whitecap moment	.wcm	–	–

Table 4.1: Field output post processors ancillary data.

group	field	description extension	file data	GRIB1 data	GRIB2
6	1	radiation stress	.Sxy	—	—
6	2	Breaking wave momentum flux	.two	—	—
6	3	Bernoulli head	.J	—	—
6	4	Breaking wave energy flux	.foc	—	—
6	5	Stokes transport	.tus	—	—
6	6	Surface Stokes drift	.uss	—	—
6	7	Second order pressure at $k = 0$.p2s	—	—
7	1	near-bottom amplitude	.cfb	—	—
7	2	near-bottom velocity	.ubr	—	—
7	3	bedform parameters	.bed	—	—
7	4	Energy flux to bot. boundary layer	.fbb	—	—
7	5	Momentum flux to bot. boundary layer	.tbb	—	—
8	1	mean square slopes	.mss	—	—
8	2	Phillips constant	.msc	—	—
9	1	average time step	.dtd	—	—
9	2	cut-off frequency f_c	.fc	—	—
9	3	cut-off frequency f_c	.fc	—	—
9	4	maximum CFL for X-Y advection	.cfx	—	—
9	5	maximum CFL for θ advection	.cfd	—	—
9	6	maximum CFL for k advection	.cfk	—	—
10	1	user defined #1	.us1	—	—
10	2	user defined #2	.us2	—	—

Table 4.1, continued.

5 Installing, Compiling and Running the wave model

5.1 Introduction

WAVEWATCH III is written in ANSI standard FORTRAN-90, with no machine-dependent elements, so that WAVEWATCH III can be installed without modifications on most platforms. WAVEWATCH III utilizes its own preprocessor to select model options at the compile level, and to switch test output on or off. This approach proved to be efficient during the development of WAVEWATCH III, but complicates its installation. To minimize complications, a set of UNIX/Linux scripts is provided to automate the installation in general and the use of the preprocessor in particular. This option is not supported for other operation systems like MS products. If the code is to be compiled on one of the latter platforms, it is suggested to extract a working code in a UNIX/Linux environment using the utility `w3_source` (see below), and then to port this clean code to the platform of choice.

WARNING

If version 5.16 is implemented as an upgrade to previous versions of WAVEWATCH III, please note that this version may not be compatible with previous model versions. It is therefore prudent *NOT* to install the new version of WAVEWATCH III on top of the old version. See Appendix A for suggestions on managing multiple model version.

WARNING

5.2 Installing files

In its packaged public version (tar file distribution), WAVEWATCH III is contained in several files:

- `install_wwatch3_tar` The WAVEWATCH III install program.
- `wwatch3.[VERTAG].model.tar` Archive file containing source codes (ftn directory), programs and scripts controlling the compiling and linking of and code management of WAVEWATCH III(aux and bin directories), and sample input files (inp directory).
- `wwatch3.[VERTAG].regtests.tar` Archive file containing several regression test cases.
- `wwatch3.[VERTAG].cases.tar` Archive file containing several large tests involving real case scenarios.

The label [VERTAG] is typically a version number for the model package, which may be followed or preceded by alpha-numeric tags describing other characteristics of the distribution package (e.g., v4.18.beta for the beta version 4.18 etc).

As the first step of installing WAVEWATCH III, these files have to be copied to a work directory on the machine on which WAVEWATCH III will be installed. Because this directory will be the ‘home’ directory of WAVEWATCH III, it is suggested that a new directory is created (see also warning in previous section). Furthermore `install_wwatch3_tar` has to be made executable by typing

```
chmod 700 install_wwatch3_tar
```

after which the installation of the files is started by typing

```
install_wwatch3_tar
```

at your Linux/Unix prompt.

WARNING

The install program will ask for a compiler to compile some auxiliary FORTRAN codes. Unlike the actual WAVEWATCH III source code, these programs are still written in FORTRAN-77. It is therefore sufficient to point toward the generic FORTRAN-77 compiler on the system. The `install_ww3_tar` script allows the user to set pre-defined choices that will point the FORTRAN-77 to a generic executable `f77`. This may not be available on your system, so make sure that an appropriate choice is made during the installation process.

WARNING

When `install_wwatch3_tar` is executed for the first time, it will ask the user to identify the directory in which WAVEWATCH III will be installed. This has to confirm that the installation directory is the current directory. Next, the script jumps to the most crucial option, which determines if a local or generic install is to be performed.

The type of install deals with where to save the traditional `wwatch3.env` file, containing the general user-dependent directory and basic FORTRAN and C compiler choices. The local install will save this at the same location as the package is being installed, which is the main WAVEWATCH III directory. This results in a standalone version that allows multiple installations (or other branches or the trunk) to co-exist without interference. The general install means `wwatch3.env` will be save in the user's home directory in the form `$HOME/.wwatch3.env`, and that this will be the main or central installation in that work area. The existence of a general install does not preclude the existence of multiple local installs, but the user has to be mindful of which code is being invoked when using the general install (things can get very confusing if not kept explicitly on track).

After a choice is made for local or generic install, the script will search for existing config files. If none is found, it will print a message that it cannot find the setup file, and ask some questions. The same questions are asked if a setup file is found, except that the intention there is to confirm the existing options have not changed. In any case, having a pre-existing setup or not, the script will give the user an opportunity to revise defaults/existing and change if needed. The script will echo the existing options, and the default/existing answers or options are shown in square brackets.

Other than the generic or local `wwatch3.env` files, a third alternate setup file may be specified prior to running `install_wwatch3_tar` by setting `WWATCH3_ENV` in the user environment. The setup can be modified by rerunning the install program, or by manually editing the setup file. The 'home' directory of WAVEWATCH III can only be changed by editing or removing the local or generic `wwatch3.env` or by changing `WWATCH3_ENV` in the user environment.

WARNING

In case you decide to use the generic installation, you have to make sure that the model installation directory is either `$HOME/wwatch3` or if it has a different name, it is linked to `$HOME/wwatch3`. If this is not the case the generic install may fail or compromise other pre-existing installations.

WARNING

After the setup file is processed, the install program asks if the user wants to continue with the installation. If the user chooses to continue, the program will look for the archive files. If no files are found, the archive files do not reside in the home directory, or the home directory is erroneously defined, the installation will exit. Check the location of the archive files, and the 'home' directory of WAVEWATCH III (see previous paragraphs).

After files to be unpacked have been identified, the program will ask if old files should be overwritten automatically. If the user chooses 'n', the program will ask permission to overwrite each file that already exists. Files that contain user specific information, such as compile and link options, will never be replaced by the install program.

As the first step of the actual installation, the install program checks if the following directories exist in the 'home' directory of WAVEWATCH III.

arc	Archive directory.
aux	Raw auxiliary programs (source codes etc.).
bin	Executables and shell scripts for compiling and linking.
exe	WAVEWATCH III executables.
ftn	Source code and makefile.
inp	Input files.
mod	Module files.
obj	Object files.
test	Scripts with test cases.
work	Auxiliary work directory.

All these directories are generated by the install program `install_wwatch3`, except for the archive directory, which is generated by `arc_wwatch3` (see below).

Unlike previous version, where the user could choose which parts of the package were to be installed, the current `install_ww3_tar` script installs the entire updated package without prompting.

Installation of the auxiliary programs will first process source codes of auxiliary programs, using the compiler as defined by the user in the setup file. Note that these codes are still in fixed format FORTRAN-77.

w3adc.f	WAVEWATCH III FORTRAN preprocessor.
w3prnt.f	Print files (source codes) including page and line numbers.

<code>w3list.f</code>	Generate a generic source code listing.
<code>w3split.f</code>	Generate spectral bulletin identifying individual wave fields within a spectrum from the spectral output of the point output post-processor (see Section 4.4.17). This is a legacy code superseded by generating bulletins directly from <code>ww3_outp</code> . It is retained here for historical reasons only.

The above source codes are stored in the directory `aux` and the executables are stored in the directory `bin`. A more detailed description of these programs (including instructions on running the executables) can be found in the documentation included in the above source code files. After the compilation of these programs, several UNIX shell scripts and auxiliary files are installed in the `bin` directory.

<code>ad3</code>	Script to run the preprocessor <code>w3adc</code> and the compile script <code>comp</code> for a given source code file.
<code>ad3_test</code>	Test version of <code>ad3</code> , showing modifications to original source file. This script does not compile code.
<code>all_switches</code>	Generates a list of all <code>w3adc</code> switches present in the source code files.
<code>arc_wwatch3</code>	Program to archive versions of WAVEWATCH III in the directory <code>arc</code> .
<code>comp.gen</code>	Generic compiler script. The actual compiler script <code>comp</code> will be copied from this script if it does not exist.
<code>comp.xxx</code>	The compiler script <code>comp</code> for a specific hardware-compiler combination.
<code>find_switch</code>	Script to find WAVEWATCH III source code files containing compiler switches (or arbitrary strings).
<code>install_ww3_svn</code>	Script to install WAVEWATCH III from the svn repository.
<code>install_ww3_tar</code>	Script to install WAVEWATCH III from tar files.
<code>link.gen</code>	Generic linker script. Actual script is <code>link</code> .
<code>link.xxx</code>	The link script <code>comp</code> for a specific hardware-compiler combination.
<code>list</code>	Script to print source code listing using <code>w3prnt</code> .
<code>ln3</code>	Script to make symbolic link of source code file to work directory.

<code>make_MPI</code>	Script to separately compile MPI and non-MPI programs.
<code>make_OMP</code>	Script to separately compile OpenMP and single threaded programs.
<code>make_HYB</code>	Script to separately compile hybrid MPI-OpenMP and single threaded programs.
<code>make_makefile.sh</code>	Script to generate the of the makefile based on selections in the file <code>switch</code>).
<code>switch.gen</code>	Generic file with preprocessor switches (Section 5.4).
<code>switch.xxx</code>	Examples of preprocessor switches provided by users or developers.
<code>w3_clean</code>	Script to clean up work and scratch directories by removing files generated during compilation or test runs.
<code>w3_make</code>	Script to compile and link components of WAVEWATCH III using a makefile.
<code>w3_new</code>	Script to touch correct source code files to account for changes in compiler switches in combination with the makefile.
<code>w3_setup</code>	Script for creating/editing the WAVEWATCH III environment setup file. The default setup file is <code>\${HOME}/.wwatch3.env</code> . An alternate setup file can be specified with the <code>WWATCH3_ENV</code> environment variable.
<code>w3_source</code>	Script to generate a true FORTRAN source code for any of he WAVEWATCH III program elements.
<code>ww3_gspl.sh</code>	Script to automate use of <code>ww3_gspl</code> program (see Section 4.4.10).

The use of these scripts is explained in Section 5.3. Note that the above scripts acquire setup information from the WAVEWATCH III environment setup file defined by `WWATCH3_ENV`, or, if that is not defined, from the generic setup file `.wwatch3.env` in the home directory of the user, or the local setup file `wwatch3.env` in the directory where the wave model package is being installed.

After installation in the `bin` directory, several GrADS scripts are installed in the `aux` directory.

<code>cbarn.gs</code>	Semi-standard GrADS script for displaying color bars.
<code>colorset.gs</code>	Script to define colors used in shading.
<code>profile.gs</code>	Script to display profiling data generated by <code>ww3_multi</code> .
<code>source.gs</code>	Script for composite plot of spectra and source terms (2-D polar or Cartesian plots in color or in black and white).
<code>1source.gs</code>	Script to plot single source term.
<code>spec.gs</code>	Script to plot spectra.
<code>spec_ids.gen</code>	Data file used by spectral / source scripts.

This directory also has various additional tools in and documentations, see the actual directory for its contents. These include contributed *Matlab* scripts, IDL scripts and tools, and a manual on using **SMG** type grids.

As the final step of `aux` processing, some links between directories are established.

Finally, the `install` program lists manual modifications required by or suggested to the user. These messages are printed only if the `compile` and `link` system are installed. An example of an installation session using the script `install_ww3_tar` is provided below for a case where local install was chosen.


```
GUIDE >> tar zxvf wwatch3.beta.v4.18.tar.gz
install_ww3_tar
guide.beta.v4.18.pdf
manual.beta.v4.18.pdf
wwatch3.beta.v4.18.model.tar
wwatch3.beta.v4.18.regtests.tar
```

```
GUIDE >> ls -l
total 354836
-rw-----. 1 wd20ha wd2    197909 Jan 14 10:11 guide.beta.v4.18.pdf
-rwx-----. 1 wd20ha wd2     38670 Jan 14 10:12 install_ww3_tar
-rw-----. 1 wd20ha wd2   3545855 Jan 14 10:12 manual.beta.v4.18.pdf
-rw-----. 1 wd20ha wd2 135690240 Jan 14 10:12 wwatch3.beta.v4.18.model.tar
-rw-----. 1 wd20ha wd2 123136000 Jan 14 10:12 wwatch3.beta.v4.18.regtests.tar
-rw-----. 1 wd20ha wd2 100731957 Mar 13 15:05 wwatch3.beta.v4.18.tar.gz
```

```
GUIDE >> ./install_ww3_tar
```

```
=====
----- Installing WAVEWATCH III v.4 -----
=====
```

```
Script for installing package from tar files.
Requires files in same directory as script.
```

```
Continue? [y|n] y
```

```
=====
----- Installing WAVEWATCH III v.4 -----
=====
                        from tar source
```

```
This installation requires a configuration file (wwatch3.env).
The current version allows two types of env files:
- A local [L] wwatch3.env (Allowing multiple independent installations).
- A generic [G] dot-file .wwatch3.env (Old-fashioned option).
[L] Installs new, uses existing or updates env file in current directory.
[G] Installs new, uses existing or updates env file in home directory,
    (home is presumably /export/emc-lw-jhalves/wd20ha}).
```

```
Type your choice now: G
```

```
Installing in
/export/emc-lw-jhalves/wd20ha/WW3_GUIDE
```

```
OK ? [y/n] y
```

Setting up environment variables.

Previous setup file not found. Variables will be set to defaults.

(User must check to see if these setting are appropriate.)

Creating wwatch3.env locally (also in home if G option chosen).

```
Printer (listings)      : printer
FORTRAN comp. (aux only) : f77
C Compiler (aux only)   : cc
Scratch directory      : /export/emc-lw-jhalves/wd20ha/WW3_GUIDE/tmp
Save source code       : yes
Save listings          : yes
```

Update settings ? [y/n] y

Modifying set-up

Type n new settings, or press ENTER to keep [current ones]:

```
Printer for listings [printer] :
Compiler for aux. [f77] : gfortran
Compiler for aux. [cc] : gcc
Scratch space [/export/emc-lw-jhalves/wd20ha/WW3_GUIDE/tmp] :
Save source code files (*.f) [yes] :
Save listing files [yes] :
```

Modified settings:

```
Printer (listings)      : printer
FORTRAN comp. (aux only) : gfortran
C Compiler (aux only)   : gcc
Scratch directory      : /export/emc-lw-jhalves/wd20ha/WW3_GUIDE/tmp
Save sources           : yes
Save listings          : yes
```

New settings OK ? [y/n] y

Continue with actual implementation ? [y/n] y

[=====SCREEN OUTPUT OMMITTED=====]

```
=====
--- Final remarks ---
=====
```

To run the WAVEWATCH III executables and the scripts to generate and update these executables from arbitrary directories, add the following directories to the path of your interactive shell :

```
/export/emc-lw-jhalves/wd20ha/WW3_GUIDE/bin
/export/emc-lw-jhalves/wd20ha/WW3_GUIDE/exe
```

Note that 'comp' and 'link' and 'switch' are user/machine specific.

Several comp and link files for known compilers are found in:
/export/emc-lw-jhalves/wd20ha/WW3_GUIDE/bin

If you cannot find one that suits your machine/preferences, create custom scripts based on the existing ones and add to bin.

```
=====
--- End of program ---
=====
```

```
GUIDE >> ls -l
total 3708
drwx-----. 2 wd20ha wd2 4096 Mar 13 15:45 arc
drwx-----. 6 wd20ha wd2 4096 Mar 13 15:45 aux
drwx-----. 2 wd20ha wd2 4096 Mar 13 15:45 bin
drwx-----. 2 wd20ha wd2 4096 Mar 13 15:45 exe
drwx-----. 3 wd20ha wd2 4096 Mar 13 15:45 ftn
-rw-----. 1 wd20ha wd2 197909 Jan 14 10:11 guide.beta.v4.18.pdf
drwx-----. 2 wd20ha wd2 4096 Mar 13 15:45 inp
lrwxrwxrwx. 1 wd20ha wd2 21 Mar 13 15:45 install_ww3_tar -> ./bin/install_ww3_tar
-rw-----. 1 wd20ha wd2 3545855 Jan 14 10:12 manual.beta.v4.18.pdf
drwx-----. 2 wd20ha wd2 4096 Mar 13 15:45 mod
drwx-----. 2 wd20ha wd2 4096 Mar 13 15:45 obj
drwx-----. 40 wd20ha wd2 4096 Mar 13 15:45 regtests
drwx-----. 2 wd20ha wd2 4096 Mar 13 15:45 tmp
drwx-----. 2 wd20ha wd2 4096 Mar 13 15:45 work
-rw-----. 1 wd20ha wd2 324 Mar 13 15:44 wwatch3.env
```

5.3 Compiling and linking

Compilation of WAVEWATCH III is performed using the script `w3_make` in the `bin` directory⁹. If this script is used without parameters, all basic programs of WAVEWATCH III are compiled. Optionally, names of programs to be compiled can be given as part of the compile command. For instance

```
w3_make ww3_grid ww3_strt
```

will compile the grid preprocessor and the initial conditions program only. `w3_make` uses several of the scripts described in the previous section. A graphical representation is given in Fig. 5.1. If necessary, the script `w3_make` uses the scripts `make_makefile.sh` to generate a makefile. `make_makefile.sh` generates a list of modules to be linked, based on the program switches in the file `switch` (see Section 5.4), and checks all needed sources for module dependencies. If switches have been changed since the last call to `w3_make`, `w3_new` is used to ‘touch’ relevant source code or to delete relevant object files. After the makefile has been completed, the standard UNIX make utility is used to compile and link the programs. Instead of directly using the FORTRAN compiler, the makefile invokes the preprocessor and compile scripts `ad3` and `comp`, and the link script `link`. The script `ad3` uses the extension of the file name to determine the necessary action. Files with extension `.ftn` are processed by `w3adc`, files with extension `.f` or `.f90` are sent to the script `comp` directly. Although a user could try out several of these scripts interactively, he or she generally needs to run `w3_make` only.

Before a first attempt is made at compiling, user intervention is required in three scripts/files. For convenience of debugging and development, links to these three files are made in the work directory `work`. The files in the work directory are

<code>comp</code>	Compiler script. This script requires the correct definition of the compiler and its options. Linked to <code>../bin/comp</code>
<code>link</code>	Linker script. This script requires the correct definition of the linker and its options. Linked to <code>../bin/link</code>

⁹ Note that before running `w3_make` several user interventions are needed as described in the remainder of this section.

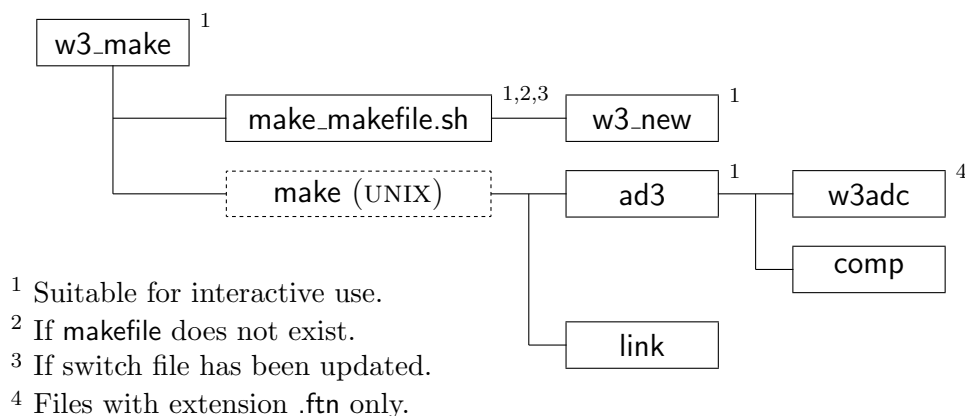


Figure 5.1: General layout of the compiler program w3.make.

switch File containing a list of switches as recognized by the preprocessor w3adc. Linked to ../bin/switch. The file provided with WAVEWATCH III should result in a hardware independent code.

WARNING

The auxiliary scripts w3.make etc. use the switch, comp and link files from the ./bin directory under the WAVEWATCH III home directory, *NOT* from the local directory.

WARNING

After the appropriate changes have been made, or the appropriate example scripts have been copied in, (parts of) WAVEWATCH III can be compiled and linked. When the program is compiled for the first time, it is suggested to compile program parts one-by-one to avoid lengthy errors messages, and to set up error capturing in comp. A good place to start is compilation of the simple test code CTEST. First go to the directory work and make a link to the source code of this routine by typing

```
ln3 ctest
```

This link is made to facilitate later inclusion of errors to test or set-up error capturing in the script `comp`. The inner workings of the preprocessor `w3adc` can be seen by typing the command

```
ad3_test ctest
```

which will show how the actual source code is constructed from `ctest.ftn`, include files and program switches. Next, the compilation of this subroutine can be tested by typing

```
ad3 ctest 1
```

which invokes both the preprocessor `w3adc` and the compile script `comp`. The 1 at the end of this line activates test output. If it is omitted, this command should result in a single line of output, identifying that the routine is being processed. If `ad3` works as expected, an object file `obj/ctest.o` is generated. If requested during the initial set up, a source code and listing file (`ctest.f` and `ctest.l`) can be found in the scratch directory. The listing file is also retained if compilation errors are detected by `comp`. At this time, it is prudent to test error capturing in the script `comp` by adding errors and warnings to `ctest.ftn` in the work directory. The error capturing is discussed in some detail in the documentation of `comp`. After `comp` has been tested, and the errors in `ctest.ftn` have been removed, the link to the work directory and the file `obj/ctest.o` can be deleted.

After a single routine has been compiled successfully, the next step is to try to compile and link an entire program. The grid preprocessor can be compiled by typing

```
w3_make ww3_grid
```

If the compilation appears successful, and if the input files have been installed (see above), the grid preprocessor can be tested by typing

```
ww3_grid
```

in the work directory. If the input files have been installed, a link to the input file `ww3_grid.inp` will be present in the work directory, and the grid preprocessor will run and send its output to the screen. Output files of the grid preprocessor will appear in the work directory. When a program is compiled for the first time, the operating system might not be able to find the executable. If this occurs, try to type

`rehash`

or open a new shell to work from. In this way all separate programs can be compiled and tested. To clean up all temporarily files (such as listings) and data files of the test runs, type

`w3_clean`

Note that `w3_make` only checks the switch file for changes. If the user changes the compile options in the compile and link scripts `comp` and `link`, it is advised to force the recompilation of the entire program. This can be achieved by typing

`w3_new all` or `w3_new`

before invoking `w3_make`. This might also be useful if the compilation is unsuccessful for no apparent reason.

Compilation of the WAVEWATCH III NetCDF enabled programs requires the environment variable `WWATCH3_NETCDF` be set to either `NC3` (compile with NetCDF version 3.x) or `NC4` (compile with NetCDF version 4.x). If the script variable is set to `WWATCH3_NETCDF = NC3`, then the following environment variables are required

`NETCDF_LIBDIR` Path to where the NetCDF-3 libraries are installed.

`NETCDF_INCDIR` Path to where the NetCDF-3 include files are installed.

If `WWATCH3_NETCDF = NC4`, then the following environment variable is required.

`NETCDF_CONFIG` Path to the NetCDF-4 `nc-config` utility program.

The `nc-config` utility program (part of the NetCDF-4 install) is used to determine the appropriate compile and link flags for the `WWATCH3_NETCDF = NC4` compile. The NetCDF-4 compile requires NetCDF version 4.1.1 or higher. Use the command

`nc-config --version`

to check the version of the installed NetCDF. Compiling with the `NC4` switch requires `WWATCH3_NETCDF = NC4` and the NetCDF-4 installation compiled with the NetCDF-4 API enabled. Use

```
nc-config --has-nc4
```

to check if the installed NetCDF has the NetCDF-4 API enabled.

Two additional remarks need to be made regarding parallel versions of the model (OpenMP and MPI versions). First, complications may occur when preparing executables for running in an MPI environment. Such complications are discussed in Appendix D. Secondly, the OpenMP code should be compiled using directives only, i.e., do not use compiler options that automatically thread the code.

5.4 Selecting model options

The file `switch` in the `bin` directory contains a set of strings identifying model options to be selected. Many options are available. Of several groups of options it is mandatory to select exactly one. These mandatory switches are described in Section 5.4.1. Other switches are optional, and are described in Section 5.4.2. Default model settings are identified in Section 5.4.3. The order in which the switches appear in `switch` is arbitrary. How these switches are included in the source code files is described in Section 6.2.

5.4.1 Mandatory switches

Of each of the below groups of switches exactly one has to be selected. The first group of switches controls the selection of machine-dependent code. With the introduction of FORTRAN-90 this set of switches should have become obsolete. Problems with some compilers have prompted the retention of the second switch.

- | | |
|-----|--|
| F90 | FORTRAN-90 style date and time capturing and program abort. |
| DUM | Dummy to be used if WAVEWATCH III is to be installed on previously untried hardware. |

Hardware model (first group) and message passing protocol (second group). Note that these two groups share a switch. This implies that the MPI switch can only be used in combination with the DIST switch.

SHRD	Shared memory model.
DIST	Distributed memory model.
SHRD	Shared memory model, no message passing.
MPI	Message Passing Interface (MPI).

Word length used to determine record length in direct access files

LRB4	4 byte words.
LRB8	8 byte words.

Compilation as a subroutine (called by a coupled model system using PALM) or a stand-alone program.

NOPA	Compilation as a stand-alone program
PALM	Compilation as a subroutine

Selection of propagation schemes and GSE alleviation method. These represent two sets of switches with some shared switches between the groups. Note that the second set of switches is secondary to the selection of program modules in the first set of switches, and therefore, does not have a user-defined option.

PR0	No propagation scheme / GSE alleviation used.
PR1	First order propagation scheme, no GSE alleviation.
PR2	Higher-order schemes with Booij and Holthuijsen (1987) dispersion correction.
PR3	Higher-order schemes with Tolman (2002a) averaging technique.
PRX	Experimental (user supplied).
PR0	No propagation scheme used.
PR1	First-order propagation scheme.
UNO	Second-order (UNO) propagation scheme.
UQ	Third-order (UQ) propagation scheme.

Selection of flux computation:

FLX0	No routine used; flux computation included in source terms,
FLX1	Friction velocity according to Eq. (2.56).
FLX2	Friction velocity from Tolman and Chalikov input.

FLX3	Idem, with cap of Eq. (2.78) or (2.79).
FLX4	Friction velocity according to Eq. (2.136).
FLXX	Experimental (user supplied).

Selection of linear input:

LN0	No linear input.
SEED	Spectral seeding of Eq. (3.70).
LN1	Cavaleri and Malanotte-Rizzoli with filter.
LNx	Experimental (user supplied).

Selection of input and dissipation. STAB n switches are optional and additional to corresponding ST n switch:

ST0	No input and dissipation used.
ST1	WAM3 source term package.
ST2	Tolman and Chalikov (1996) source term package. See also the optional STAB2 switch.
STAB2	Enable stability correction (2.95) - (2.98) for ST2.
ST3	WAM4 and variants source term package.
STAB3	Enable stability correction from Abdalla and Bidlot (2002) for ST4.
ST4	Ardhuin et al. (2010) source term package.
ST6	BYDRZ source term package.
STX	Experimental (user supplied).

Selection of nonlinear interactions:

NL0	No nonlinear interactions used.
NL1	Discrete interaction approximation (DIA).
NL2	Exact interaction approximation (WRT).
NL3	Generalized Multiple DIA (GMD).
NL4	Two-scale approximation (TSA).
NLx	Experimental (user supplied).

Selection of bottom friction:

BT0	No bottom friction used.
BT1	JONSWAP bottom friction formulation.
BT4	SHOWEX bottom friction formulation.
BT8	Dalrymple and Liu formulation (fluid mud seafloor).

BT9 Ng formulation (fluid mud seafloor).
 BTX Experimental (user supplied).

Selection of term for damping by sea ice:

IC0 No damping by sea ice.
 IC1 Simple formulation.
 IC2 Liu et al. formulation.
 IC3 Wang and Shen formulation.
 IC4 Frequency-dependent damping by sea ice.

Selection of term for scattering by sea ice:

IS0 No scattering by sea ice.
 IS1 Diffusive scattering by sea ice (simple).
 IS2 Floe-size dependent scattering and dissipation.

Selection of term for reflection:

REF0 No reflection.
 REF1 Enables reflection of shorelines and icebergs

Selection depth-induced breaking of :

DB0 No depth-induced breaking used.
 DB1 Battjes-Janssen.
 DBX Experimental (user supplied).

Selection of triad interactions:

TR0 No triad interactions used.
 TR1 Lumped Triad Interaction (LTA) method.
 TRX Experimental (user supplied).

Selection of bottom scattering:

BS0 No bottom scattering used.
 BS1 Magne and Arduin.
 BSX Experimental (user supplied).

Selection of supplemental source term:

xx0 No supplemental source term used.

xxx Experimental (user supplied).

Selection of method of wind interpolation (time):

WNT0 No interpolation.
 WNT1 Linear interpolation.
 WNT2 Approximately quadratic interpolation.

Selection of method of wind interpolation (space):

WNX0 Vector interpolation.
 WNX1 Approximately linear speed interpolation.
 WNX2 Approximately quadratic speed interpolation.

Selection of method of current interpolation (time):

CRT0 No interpolation.
 CRT1 Linear interpolation.
 CRT2 Approximately quadratic interpolation.

Selection of method of current interpolation (space):

CRX0 Vector interpolation
 CRX1 Approximate linear speed interpolation.
 CRX2 Approximate quadratic speed interpolation.

Switch for user supplied GRIB package.

NOGRB No package included.
 NCEP1 NCEP GRIB1 package for IBM SP.
 NCEP2 NCEP GRIB2 package for IBM SP.

5.4.2 Optional switches

All switches below activate model behavior if selected, but do not require particular combinations. The following switches control optional output for WAVEWATCH III programs.

o0 Output of namelists in grid preprocessor.
 o1 Output of boundary points in grid preprocessor.

- o2 Output of the grid point status map in grid preprocessor.
- o2a Generation of land-sea mask file `mask.ww3` in grid preprocessor.
- o2b Output of obstruction map in grid preprocessor.
- o2c Print status map in format as read by `ww3_grid`.
- o3 Additional output in loop over fields in field preprocessor.
- o4 Print plot of normalized one-dimensional energy spectrum in initial conditions program.
- o5 Id. two-dimensional energy spectrum.
- o6 Id. spatial distribution of wave heights (not adapted for distributed memory).
- o7 Echo input data for homogeneous fields in generic shell.
- o7a Diagnostic output for output points.
- o7b Idem in `ww3_multi`.
- o8 Filter field output for extremely small wave heights in wave model (useful for some propagation tests).
- o9 Assign a negative wave height to negative energy in wave model. Used in testing phase of new propagation schemes.
- o10 Identify main elements of multi-grid model extensions in standard output.
- o11 Additional log output on management algorithm in `log.mww3`.
- o12 Identify removed boundary points in overlapping grids (center).
- o13 Identify removed boundary points in overlapping grids (edge).
- o14 Generate log file with buoy data `buoy_log.ww3` for output type `ITYPE = 0` in `ww3_outp`.
- o15 Generate log file with time stamps of input data file `times.XXX` in `ww3_prep`.
- o16 Generate GrADS output of grid partitioning in `ww3_gspl`.

The following switches enable parallelization of the model using OpenMP directives, also known as ‘threading’. Before model version 5.01, threading and parallelization using the MPI switch could no be used simultaneously. With version 5.01, pure MPI, pure OMP and hybrid MPI-OMP approaches became available. Switches used in version 5.01 and higher are not compatible with switches used in previous model versions.

- OMPG General loop parallelization directives used for both exclusive OpenMP parallelization and hybrid MPI-OpenMP

	parallelization.
OMPX	Idem, but for directives used only for exclusive OpenMP parallelization.
OMPH	Idem, but for directives used only for hybrid MPI-OpenMP parallelization.

Note that these switches can only be used in certain combinations, as enforced in the model installation scripts (particularly `make_makefile.sh`). A pure MPI approach requires the `DIST` and `MPI` switches. A pure OpenMP approach requires the `SHRD`, `OMPG` and `OMPX` switches, and the hybrid approach requires the `DIST`, `MPI`, `OMPG`, and `OMPH` switches.

The following switches are associated with the continuously moving grid options. The first switch activates the option, the other two are optional additions.

MGP	Activate propagation correction in Eq. (3.45).
MGW	Apply wind correction in moving grid approach.
MGG	Activate GSE alleviation correction in Eq. (3.48).

The following compiler dependent switches are available. They may not have been maintained for recent compiler versions.

C90	Compiler directives for Cray C90 (vectorization).
NEC	Compiler directives for NEC SX6/SX8 (vectorization).

Furthermore the following miscellaneous switches are available:

ARC	Arctic grid option for SMC grid ¹⁰ .
COU	Activates the calculation of variables required for coupling
DSS0	Switch off frequency dispersion in diffusive dispersion correction.
FLD1	Sea-state dependent τ Reichl et al. (2014) (Section 2.5.2).
FLD2	Sea-state dependent τ Donelan et al. (2012) (Section 2.5.3).
IG1	Second-order spectrum and free infragravity waves (Section 2.4.8).
MLIM	Use Miche-style shallow water limiter of Eq. (3.71).
MPIBDI	Experimental parallelization of multi-grid model initialization.

¹⁰ Not yet fully tested according to author.

MPIT	Test output for MPI initializations.
MPRF	Profiling of individual models and nesting in <code>ww3_multi</code> .
NC4	Activates the NetCDF-4 API in the NetCDF pre- and post-processing programs.
NCC	NCEP coupler.
NCO	Code modifications for operational implementation at NCO (NCEP Central Operations). Mostly changes unit numbers and file names. Not recommended for general use.
NLS	Activate nonlinear smoother (Section 2.3.6).
NNT	Generate file <code>test_data_nnn.ww3</code> with spectra and nonlinear interactions for training and testing of NNIA.
OASIS	Initializes OASIS Coupler (App. F.3).
OASACM	OASIS atmospheric model coupling fields(App. F.3).
OASOCM	OASIS oceanic model coupling fields (App. F.3).
REFRX	Enables refraction based on spatial gradients in phase velocity (Section 2.4.3)
REFT	Test output for shoreline reflection (which is activated with REF1).
RTD	Rotated grid option.
RWND	Correct wind speed for current velocity.
S	Enable subroutine tracing in the main WAVEWATCH III subroutines by activating calls to the subroutine STRACE.
SCRIP	Enable SCRIP remapping routines (App. E.3)
SCRIPNC	Enable storage of remapping weights in NetCDF files (App. E.3)
SEC1	Enable the use of global time steps less than 1 s, but does not allow output at time steps less than 1 s.
SMC	Activate SMC grid.
T	Enable test output throughout the program(s).
Tn	Id.
TDYN	Dynamic increment of swell age in diffusive dispersion correction (test cases only).
TIDE	Enables tidal analysis: used for pre-processing of input files, run-time tidal prediction in <code>ww3_shel</code> or tidal prediction with <code>ww3_prtide</code> .
TIDET	test output for tidal analysis.
TRKNC	Activates the NetCDF API in the wave system tracking post-processing program. Selecting TRKNC alone will gen-

erate NetCDF-3 files. Selecting both TRKNC and NC4 will generate NetCDF-4 files.

xw0	Swell diffusion only in ULTIMATE QUICKEST scheme.
xw1	Id. wave growth diffusion only.

5.4.3 Default model settings

Up to model version 3.14, the NCEP operational model setup was considered as the default model setup. However, with subsequent versions of WAVEWATCH III, the model has evolved into a modeling framework rather than a single model. With this, WAVEWATCH III is run differently at various centers, and a clear “default” model version can no longer be identified. Nevertheless, in order to be able to concisely identify in publications exactly which model setup is used, “default” configurations of various centers are now provided in the `bin` directory. These configurations are provided in example switch files and README files, such as `switch_NCEP_st2` and `README.NCEP`. Note that these files are provided to simplify referring to model version, but do not imply an endorsement of the specific model configuration.; in this context, it should be noted that by nature, model versions at operational centers are in a continuous state of development.

5.5 Modifying the source code

Source code can obviously be modified by editing the source code files in the `ftn` directory. However, it is usually more convenient to modify source code files from the work directory `work`. This can be done by generating a link between the `ftn` and `work` directories. Such a link can be generated by typing

```
ln3 filename
```

where `filename` is the name of a source code or include file, with or without its proper extension. Working from the work directory is recommended for several reasons. First, the program can be tested from the same directory, because of similar links to the input files. Secondly, links to the relevant switch, compile and link programs are also available in this directory. Third,

it makes it easy to keep track of files which have been changed (i.e., only those files to which links have been created might have been changed), and finally, source codes will not disappear if files (links) are accidentally removed from the work directory.

Modifying source codes is straightforward. Adding new switches to existing subroutines, or adding new modules requires modification of the automated compilation scripts. If a new subroutine is added to an existing module, no modifications are necessary. If a new module is added to WAVEWATCH III, the following steps are required to include it in the automatic compilation:

- 1) Add the file name to sections 2.b and c of `make_makefile.sh` to assure that the file is included in the makefile under the correct conditions.
- 2) Modify section 3.b of this script accordingly to assure that the proper module dependency is checked. Note that the dependency with the object code is checked, allowing for multiple or inconsistent module names in the file.
- 3) Run script interactively to assure that makefile is updated.

For details of inclusion, see the actual scripts. Adding a new switch to the compilation systems requires the following actions:

- 1) Put switch in required source code files.
- 2) If the switch is part of a new group of switches, add a new 'keyword' to `w3_new`.
- 3) Update files to be touched in `w3_new` if necessary.
- 4) Update `make_makefile.sh` with the switch and/or keyword.

These modifications need only be made if the switch selects program parts. For test output etc., it is sufficient to simply add the switch to the source code. Finally, adding an old switch to an additional subroutine requires these actions:

- 1) Update files to be touched in `w3_new`.

If WAVEWATCH III is modified, it is convenient to maintain copies of previous versions of the code and of the compilation scripts. To simplify this, an archive script (`arc_wwatch3`) is provided. This script generates `tar` files that

can be reinstalled by the install program `install_wwatch3`. The archive files are gathered in the directory `arc`. The names of the archive files can contain user defined identifiers (if no identifier is used, the name will be identical to the original WAVEWATCH III files). The archive program is invoked by typing

```
arc_wwatch3
```

The interactive input to this script is self-explanatory. An archive file can be re-installed by copying the corresponding `tar` files to the WAVEWATCH III home directory, renaming them to the file names expected by the install program, and running the install program.

For co-developers using the NCEP svn repository, changes in the code should be made using the best practices as outlined in (Tolman, 2014c).

5.6 Running test cases

If WAVEWATCH III is installed and compiled successfully, it can be tested by running different program elements interactively from the `work` directory. The switch settings in the generic switch file correspond to the activated inputs in the example input files. It should therefore be possible to run all model elements by typing

```
ww3_grid | more
ww3_strt | more
ww3_bound | more
ww3_prep | more
ww3_shel | more
ww3_outf | more
ww3_outp | more
ww3_ounf | more
ww3_ounp | more
ww3_trck | more
ww3_grib | more
gx_outf | more
gx_outp | more
```

where the `more` command is added to allow for on-screen inspection of the output. This `| more` can be replaced by redirection to an output file, e.g.

```
ww3_grid > ww3_grid.out
```

Note that `ww3_grib` will only provide GRIB output if a user-supplied packing routine is linked in. Note furthermore that no simple interactive test case for `ww3_multi` is provided. GrADS can then be run from the work directory to generate graphical output for these calculations. All intermediate output files are placed in the `work` directory, and can be removed conveniently by typing

```
w3_clean
```

Up to version 3.14, WAVEWATCH III was provided with a set of simple tests to established assess the proper behavior of the basic functionality of the model. In the early development of the next release of the model, Erick Rogers and Tim Campbell converted these in regression tests that could be run more easily in an automated version. Up to model version 4.06, these modified tests were gathered in the `nrtest` directory, while keeping the old tests in the `test` directory. In model version 4.07, the `nrtest` were adopted as the new test cases for WAVEWATCH III in a new `regtests` directory, while eventually the remaining real-world test cases in `test` were moved to the `cases` directory, while discontinuing the `test` directory completely. The following regression tests are available in the `regtests` directory.

<code>ww3_tp1.1</code>	1D propagation around the world along the equator (no land).
<code>ww3_tp1.2</code>	1D propagation, along meridian (no land).
<code>ww3_tp1.3</code>	1D propagation, shoaling test.
<code>ww3_tp1.4</code>	1D propagation, spectral refraction (x).
<code>ww3_tp1.5</code>	1D propagation, spectral refraction (y).
<code>ww3_tp1.6</code>	1D propagation, wave blocking by current.
<code>ww3_tp1.7</code>	1D propagation, IG wave generation.
<code>ww3_tp1.8</code>	1D propagation, wave breaking on a beach.
<code>ww3_tp1.9</code>	1D propagation, Beji and Battjes (1993) barred flume case.
<code>ww3_tp2.1</code>	2D propagation under angle with grid.
<code>ww3_tp2.2</code>	2D propagation over half the globe without land (with directional spread).

ww3_tp2.3	2D propagation, GSE test.
ww3_tp2.4	2D propagation, East Pacific curvilinear grid test.
ww3_tp2.5	2D propagation, Arctic Grid, curvilinear grid test.
ww3_tp2.6	2D propagation, Limon Harbor unstructured grid test.
ww3_tp2.7	Reflection on a 2D unstructured grid.
ww3_tp2.8	Tidal constituents on a 2D regular grid.
ww3_tp2.9	Tests for obstruction grids.
ww3_tp2.10	Tests for SMC grid.
ww3_tp2.11	Tests for rotated grid.
ww3_tp2.12	Test for system tracking.
ww3_tp2.13	Test for propagation under angle with grid (tripole)
ww3_tp2.14	Test for toy-model using OASIS coupler.
ww3_tp2.15	Test for space-time extremes parameters.
ww3_ts1	Source term test, time limited growth.
ww3_ts2	Source term test, fetch limited growth.
ww3_ts3	Source term test, hurricane with single moving grid.
ww3_tic1.1	Wave-ice interaction, 1D test of S_{ice} .
ww3_tic1.2	Wave-ice interaction, 1D test of “shoaling” effect.
ww3_tic1.3	Wave-ice interaction, 1D test of refraction effect.
ww3_tic1.4	Wave-ice interaction, 1D test with ice floes and ice thickness.
ww3_tic2.1	Wave-ice interaction, 2D test of S_{ice} .
ww3_tic2.2	Wave-ice interaction, 2D test with non-uniform ice.
ww3_tic2.3	Wave-ice interaction, 2D test with uniform ice with increasing thickness.
ww3_tbt1.1	Wave-mud interaction, 1D test of S_{mud} .
ww3_tbt2.1	Wave-mud interaction, 2D test of S_{mud} .
mww3_test_01	Test for expanded grid mask with wetting and drying, etc.
mww3_test_02	Two-way nesting test with single inner grid.
mww3_test_03	Overlapping grids and two-way nesting tests (6-grid version with beach in high-resolution grids.)
mww3_test_04	Current or sea-mount test for two-way nesting with stationary swell conditions.
mww3_test_05	Three nested hurricane grids with moving grids test.
mww3_test_06	Tests for irregular grid(s) w/ <code>ww3_multi</code> .
mww3_test_07	Tests for unstructured grid(s) w/ <code>ww3_multi</code> .

`mww3_test_08` Tests with wind and ice input.

These regression tests are now run using the `run_test` script in the `regtests/bin` directory (primary author: Tim Campbell). How to run this script, including options, is shown by running

```
run_test -h
```

The output of running this command is shown here in Fig. 5.2. The test cases are stored in directories under the `regtests` directory, e.g. `regtests/ww3_tp1.1`. For example, the contents of `/ww3_tp1.1` might be

<code>info</code>	A file containing information about the test case.
<code>input</code>	A permanent directory containing input files for the test case.
<code>work_PR3</code>	A scratch directory for model output (in this example, filename is such because the user had specified “ <code>run_test -w work_PR3 ...</code> ”).

Also provided now is a matrix of regression tests, used by the code developers to assure that new model versions do not break older model versions. The core of this matrix is the file `regtests/bin/matrix.base`. An example of how to run this is given in `regtests/bin/matrix_zeus_HLT`, which is Hendrik’s driver for the matrix at the NCEP Zeus R&D computer¹¹. To run this, make a link to it in the `regtests` directory and execute after setting the desired option flags in the script. This will make a file `matrix` in `regtests`, which can then be run interactively or in batch mode as desired. The file can also be manually edited further if so desired. The `bin` directory under `regtests` contains the following tools.

<code>cleanup</code>	Cleanup work directories.
<code>comp_switch</code>	Compare switches inside and across test cases. <code>comp_switch -h</code> provides documentation.
<code>matrix.base</code>	Core script to generate matrix of test cases.
<code>matrix.comp</code>	Script to compare output of matrix of test cases between separately checked out model versions.
<code>matrix_zeus_HLT</code>	Example of driver for <code>matrix.base</code> .

¹¹ Please build your own driver for your own setup using this as a blueprint, rather than editing this file.

`run_test` Basic test script as described above.

Note that efficient running of the matrix of regression tests requires a minimization of the need to recompile code between regression tests. This is achieved by the ordering of the regression tests in `matrix.base`. A way to assure that identical switch files are identified as such is to systematically sort them. This can be done with the script `sort_switch` in the main `bin` directory. This script will add default values of missing switches and can also be used to remove or add switches from the file. Run

```
comp_switch -h
```

for documentation of the script.

Finally, the `cases` directory hold the real-world test cases as described below.

`mww3_case_01` Atlantic case with five grids focusing on Trondheim.
`mww3_case_02` Pacific case with three grids focusing on Alaska.
`mww3_case_03` Original multi-grid case used as global model at NCEP.

Each of these cases is a single script executing the entire model run. Before executing the script, compile the model with the switches indicated in the documentation at the head of the script. Additional data used by these scripts is contained in the directories

`mww3_data_00` Wind fields and ice data used by all example cases.
`mww3_data_nn` Specific data needed for script `mww3_case_nn`.

These examples can be used as blueprints for setting up other real model applications.

```

Usage: run_test [options] source_dir test_name
Required:
  source_dir : path to top-level of WW3 source
  test_name  : name of test case (directory)
Options:
  -a ww3_env      : use WW3 environment setup file <ww3_env>
                  :   *default is <source_dir>/wwatch3.env
                  :   *file will be created if it does not already exist
  -c cmplr       : setup comp & link files for specified cmplr
  -C             : enable coupling using OASIS3-mct
  -d             : invoke main program using gdb (non-parallel)
  -e             : prompt for changes to existing WW3 environment
  -f             : force pre- and post-processing programs to be compiled
                  : non-MPI (i.e., with SHRD switch); default is all programs
                  : compiled with unmodified switch settings
  -g grid_string : use ww3_grid_<grid_string>.inp
  -G             : create GrADS data files using gx_outX.inp
  -h             : print usage and exit
  -i inpdир     : use inputs in test_name/<inpdир> (default test_name/input)
  -m grid_set    : execute multi-model test
                  :   *grid names are obtained from input/<grid_set>
                  :   *ww3_multi_<grid_set> will execute instead of ww3_shel
                  :   *to execute a single model test case with ww3_multi use
                  :   grid_set = none
  -n nproc       : specify <nproc> processors for parallel run
                  :   *some <runcmd> programs do not require <nproc>
                  :   *ignored if -p <runcmd> or -O is not specified
  -o outopt      : limit output post-processing based on <outopt>
                  :   native : post-process only native output
                  :   netcdf : post-process only NetCDF output
                  :   both  : post-process both native and NetCDF output
                  :   * default is native
                  :   * note that required input files must be present for
                  :   selected output post-processing to occur
  -O             : parallel run using OpenMP paradigm and OMP_NUM_THREADS
                  : environment variable and number of processors defined with
                  : the -n np option
  -p runcmd      : run in parallel using <runcmd> to start program
                  :   *MPICH or OpenMPI: mpirun or mpiexec (default <nproc> = 1)
                  :   *IBM with Loadleveler: poe (no <nproc> required)
                  :   *LSF: mpirun.lsf (no <nproc> required)
  -q program     : exit script after program <program> executes
  -r program     : only execute program <program>
  -s switch_string : use switch_<switch_string>
  -S             : create stub file <finished>. with end data and time.
                  : tests not executed if file is found.
  -t nthrd       : Threading option. (this is system dependant and can be used
                  : only for the hybrid option)
  -w work_dir    : run test case in test_name/work_dir (default test_name/work)

```

Figure 5.2: Options for run_test, as obtained by running it with the -h command line option.

6 System documentation

6.1 Introduction

In this chapter a brief system documentation is presented. Discussed are the custom preprocessor used by WAVEWATCH III (Section 6.2), the contents of the different source code files (Section 6.3), optimization (Section 6.4), and the internal data storage (Section 6.5). For a more elaborate documentation, reference is made to the source code itself, which is fully documented.

6.2 The preprocessor

The WAVEWATCH III source code files are not ready to use FORTRAN files; mandatory and optional program options still have to be selected, and test output may be activated¹². Compile level options are activated using 'switches'. The arbitrary switch 'SWT' is included in the WAVEWATCH III files as comment of the form `!/SWT`, where the switch name SWT is followed by a space or by a `'/'`. If a switch is selected, the preprocessor removes the comment characters, thus activating the corresponding source code line. If `'/'` follows the switch, it is also removed, thus allowing the selective inclusion of hardware-dependent compiler directives etc. The switches are case sensitive, and available switches are presented in Section 5.4. Files which contain the switch `C/SWT` can be found by typing

```
find_switch '!/SWT'
```

A list of all switches included in the WAVEWATCH III files can be obtained by typing

```
all_switches
```

¹² Exceptions are some modules that are not originally part of WAVEWATCH III, like the exact interaction modules. Such modules with the extension `.f` or `.f90` bypass the preprocessor and get copied to the work directory with the `.f` extension.


```

0 1
constants.ftn' constants.f'
'F90 NOGRB LRB4 SHRD NOPA PR3 UQ FLX2 LN1 ST2 STAB2
  NL1 BT1 DB1 MLIM TRO BSO XXO WNX1 WNT1 CRX1 CRT1
  00 01 02 03 04 05 06 07 011 014'

```

Figure 6.1: Example input for w3ADC.

Pre-processing is performed by the program `w3adc`. This program is found in the file `w3adc.f`, which contains a ready to compile FORTRAN source code and a full documentation¹³. Various properties of `w3adc` are set in PARAMETER statements in `w3adc.f`, i.e., the maximum length of switches, the maximum number of include files, the maximum number of lines in an include file and the line length. `w3adc` reads its ‘commands’ from standard input. An example input file for `w3adc` is given in Fig. 6.1. Line-by-line, the input consists of

- Test indicator and compress indicator.
- File names of the input and output code.
- Switches to be turned on in a single string (see Section 5.4).
- Additional lines with include files can be given, but these are no longer used in the automated compile system.

A test indicator 0 disables test output, and increasing values increase the detail of the test output. A compress indicator 0 leaves the file as is. A compress indicator 1 results in the removal of all comment lines indicated by ‘!’, except for empty switches, i.e., lines starting with ‘!/’. A compress indicator 2 results in the subsequent removal of all comments. Comment lines are not allowed in this input file. The above input for `w3ADC` is read using free format. Therefore quotes are needed around strings. Echo and test output is send to the standard output device. To facilitate the use of the preprocessor, several UNIX scripts are provided with WAVEWATCH III

¹³ Presently still in fixed-format FORTRAN-77.

as discussed in Section 5.3. Note that compiler directives are protected from file compression by defining them using a switch.

6.3 Program files

The WAVEWATCH III source code files are stored in files with the extension `ftn`¹⁴. Starting with version 2.00, the code has been organized in modules. Only the main programs are not packaged in modules. Originally, variables were bundled with the code modules, resulting in a single static data structure. In model version 3.06, a separate dynamical data structure was introduced, allow for the presence of multiple wave grids in a single program, as a preparation for the development of the the multi-grid model driver.

The subroutines contained in the modules are described in some detail below. The relation between the various subroutines is graphically depicted in Figs. 6.2 and 6.3. Three groups of codes are considered. The first are the main wave model subroutine modules, which are generally identified by the file name structure `w3xxxxmd.ftn`. These modules are described in Section 6.3.1. The second group consists of modules specific to the multi-grid wave model driver, which are generally identified by the file name structure `wmxxxxmd.ftn`. These modules are described in Section 6.3.2. The final group consists of auxiliary programs and wave model drivers, and is described in Section 6.3.4. Section 6.3.3 briefly describes the data assimilation module.

6.3.1 Wave model modules

At the core of the wave model are the wave model initialization module and the wave model module.

Main wave model initialization module w3initmd.ftn

<code>w3init</code>	The initialization routine <code>W3INIT</code> , which prepares the wave model for computations (internal).
<code>w3mpii</code>	MPI initialization (internal).
<code>w3mpio</code>	MPI initialization for I/O (internal).

¹⁴ with the exception of some modules provided by others.

w3mpip MPI initialization for I/O (internal, point output only).

Main wave model module w3wavemd.ftn

w3wave The actual wave model W3WAVE.
w3gath Data transpose to gather data for spatial propagation in a single array (internal).
w3scat Corresponding scatter operation (internal).
w3nmin Calculate minimum number of sea points per processor (internal).

The main wave model routines and all other subroutines require a data structure to exist. The data structure is contained in the following modules.

Define model grids and parameter settings w3gdatmd.ftn

w3nmod Set number of grids to be considered.
w3dimx Set dimensions for spatial grid and allocate storage.
w3dims Set dimensions for spectral grid and allocate storage.
w3setg Set pointers to selected grid.
w3dimug Set dimensions for arrays specific to the triangle-based grids (grid connectivity ...).
w3gntx Develop unstructured grid structures.

Dynamic wave data describing sea state w3wdatmd.ftn

w3ndat Set number of grids to be considered.
w3dimw Set dimensions and allocate storage.
w3setw Set pointers to selected grid.

Auxiliary storage w3adatmd.ftn

w3naux Set number of grids to be considered.
w3dim_a, w3xd_{ma}, w3dm_{nl} Set dimensions and allocate storage.
w3set_a, w3xeta Set pointers to selected grid.

Model output w3odatmd.ftn

w3nout Set number of grids to be considered.
w3dmo2, w3dmo3, w3dmo5
 Set dimensions and allocate storage.
w3seto Set pointers to selected grid.

Model input w3idatmd.ftn

w3ninp Set number of grids to be considered.
w3dimi Set dimensions and allocate storage.
w3seti Set pointers to selected grid.

The input fields such as winds and currents are transferred to the model through the parameter list of W3WAVE. The information is processed within W3WAVE by the routines in the following module.

Input update module w3updtmd.ftn

w3ucur Interpolation in time of current fields.
w3uwnd Interpolation in time of wind fields.
w3uini Generate initial conditions from the initial wind field.
w3ubpt Updating of boundary conditions in nested runs.
w3uice Updating of the ice coverage.
w3ulev Updating of water levels.
w3utrnr Updating grid box transparencies.
w3ddxy Calculation of spatial derivatives of the water depth.
w3dcxy Calculation of spatial derivatives of the currents.

There are seven types of WAVEWATCH III data files (other than the pre-processed input fields, which are part of the program shall rather than the actual wave model). The corresponding routines are gathered in six modules.

I/O module (mod_def.ww3) w3iogrmd.ftn

w3iogr Reading and writing of mod_def.ww3.

I/O module (out_grd.ww3) w3iogomd.ftn

w3outg Calculation of gridded output parameters.

w3iogo	Reading and writing of out_grd.ww3.	
I/O module (out_pnt.ww3)		w3iopomd.ftn
w3iopp	Processing of requests for point output.	
w3iope	Calculating point output data.	
w3iopo	Reading and writing of out_pnt.ww3.	
I/O module (track_o.ww3)		w3iotrmd.ftn
w3iotr	Generate track output in track_o.ww3.	
I/O module (restart.ww3)		w3iorsmd.ftn
w3iors	Reading and writing of restartn.ww3.	
I/O module (nest.ww3)		w3iobcmd.ftn
w3iobc	Reading and writing of nestn.ww3.	
I/O module (partition.ww3)		w3iofsmd.ftn
w3iofs	Writing of partition.ww3.	
<p>There are presently several propagation schemes and GSE alleviation techniques available for rectangular and curvilinear grids, as well as a 'slot' for a user supplied propagation routine, and there are four schemes for triangle-based grids. The propagation schemes are packaged in the following modules.</p>		
Propagation module (first order, no GSE alleviation)		w3pro1md.ftn
w3map1	Generation of auxiliary maps.	
w3xyp1	Propagation in physical space.	
w3ktp1	Propagation in spectral space.	
Propagation module (higher order scheme with GSE diffusion)		w3pro2md.ftn
w3map2	Generation of auxiliary maps.	
w3xyp2	Propagation in physical space.	
w3ktp2	Propagation in spectral space.	

Propagation module (higher order scheme with GSE averaging) `w3pro3md.ftn`

`w3map3` Generation of auxiliary maps.
`w3mapt` Generation of transparency maps.
`w3xyp3` Propagation in physical space.
`w3ktp3` Propagation in spectral space.

Propagation module (slot for user supplied routines) `w3proxmd.ftn`

`w3xypx` Propagation in physical space.
`w3ktpx` Propagation in spectral space.

Propagation module (generic UQ) `w3uqckmd.ftn`

`w3qckn` Routines performing ULTIMATE QUICKEST scheme
in arbitrary spaces (1: regular grid. 2: irregular grid
3: regular grid with obstructions).

Propagation module (generic UNO) `w3uqckmd.ftn`

`w3uno`, `w3unor` `w3unos`
Like UQ schemes above.

SMC grid routines `w3psmcmd.ftn`

`W3PSMC` Spatial propagation on SMC grid.
`W3KSMC` Spectral modification by GCT and refraction.
`SMCxUNO2/3` Irregular grid mid-flux on U-faces by UNO2/3.
`SMCyUNO2/3` Irregular grid mid-flux on V-faces by UNO2/3.
`SMCxUNO2r/3r` Regular grid mid-flux on U-faces by UNO2/3.
`SMCyUNO2r/3r` Regular grid mid-flux on V-faces by UNO2/3.
`SMCkUNO2` Shift in k-space due to refraction by UNO2.
`SMCGradn` Evaluate field gradient at cell centre.
`SMCAverg` 1-2-1 weighted average for centre field.
`SMCGtCrfr` Refraction and GCT rotation in theta.
`SMCDHXY` Evaluate depth gradient and refraction limiter.
`SMCDCXY` Evaluate current velocity gradient.
`W3GATHSMC` `W3SCATSMC`
Gather and scatter spectral components.

Triangle-based propagation schemes	w3profsmd.ftn
w3xypug	Interface to the unstructured propagation schemes.
w3cflug	Computes the maximum CFL number for spatial propagation.
w3xypfsn2	N-scheme.
w3xypfpsi2	PSI-scheme.
w3xypfsnimp	Implicit version of the N-scheme.
w3xypfsfct2	FCT-scheme.
bcgstab	Part of the iterative SPARSKIT solver, used for the implicit scheme.

The source term calculation and integration is contained in several modules. The module `w3srcemd.ftn` manages the general calculation and integration. Additional modules contain the actual source term options.

Source term integration module	w3srcemd.ftn
w3srce	Integration of source terms.
Flux (stress) module (Wu, 1980)	w3flx1md.ftn
w3flx1	Calculation of stresses.
Flux (stress) module (Tolman and Chalikov)	w3flx2md.ftn
w3flx2	Calculation of stresses.
Flux (stress) module (Tolman and Chalikov, capped)	w3flx3md.ftn
w3flx3	Calculation of stresses.
Flux (stress) module (slot for user supplied routines)	w3flxxmd.ftn
w3flxx	Calculation of stresses.
inflxx	Initialization routine.
Linear input (Cavaleri and Malanotte Rizzoli)	w3sln1md.ftn
w3sln1	Calculation S_{lin} .

Linear input (slot for user supplied routines)		w3slnxmd.ftn
w3slnx	Calculation S_{lin} .	
inslrx	Corresponding initialization routine.	
Input and dissipation module (dummy version)		w3src0md.ftn
w3spr0	Calculation of mean wave parameters (single grid point).	
Input and dissipation module (WAM-3)		w3src1md.ftn
w3spr1	Calculation of mean wave parameters (single grid point).	
w3sin1	Calculation of S_{in} .	
w3sds1	Calculation of S_{ds} .	
Input and dissipation module Tolman and Chalikov 1996		w3src2md.ftn
w3spr2	Calculation of mean wave parameters (single grid point).	
w3sin2	Calculation of S_{in} .	
w3sds2	Calculation of S_{ds} .	
inptab	Generation of the interpolation table for β .	
w3beta	Function to calculate β (internal).	
Input and dissipation module WAM-4 and ECWAM.		w3src3md.ftn
w3spr3	Calculation of mean wave parameters (single grid point).	
w3sin3	Calculation of S_{in} .	
w3sds3	Calculation of S_{ds} .	
tabu_stress	Tabulation of wind stress as a function of U_{10} and τ_w	
tabu_tauhf	Tabulation of the short waves-supported stress	
calc_ustar	Computes friction velocity using stress table	
Input and dissipation module Ardhuin et al. 2010		w3src4md.ftn
w3spr4	Calculation of mean wave parameters (single grid point).	
w3sin4	Calculation of S_{in} .	
w3sds4	Calculation of S_{ds} .	
tabu_stress	Tabulation of wind stress as a function of U_{10} and τ_w	
tabu_tauhf	Tabulation of the short waves-supported stress	

tabu_tauhf2	Tabulation of the short waves-supported stress with sheltering	
tabu_swellft	Tabulation of oscillatory friction factor for negative part of S_{in} .	
calc_ustar	Computes friction velocity using stress table	
Input and dissipation module BYDRZ		w3src6md.ftn
w3spr6	Integral parameter calculation following ST1.	
w3sin6	Observation-based wind input.	
w3sds6	Observation-based dissipation.	
irange	Generate a sequence of integer values.	
lfactor	Calculate reduction factor for S_{in} .	
tauwinds	Normal stress calculation for S_{in} .	
polyfit2	Quadratic fit using least-squares.	
Input and dissipation module (slot for user supplied routines)		w3srcxmd.ftn
w3sinx	Calculation of S_{in} .	
w3sdsx	Calculation of S_{ds} .	
Swell dissipation module		w3swldmd.ftn
w3swl4	Ardhuin et al (2010+) swell dissipation.	
w3swl6	Babanin (2011) swell dissipation.	
irange	Generate a sequence of integer values.	
Nonlinear interaction module (DIA)		w3snl1md.ftn
w3snl1	Calculation of S_{nl} .	
insnl1	Initialization for S_{nl} .	
Nonlinear interaction module (WRT)		w3snl2md.ftn
w3snl2	Interface routine for S_{nl} .	
insnl2	Initialization for S_{nl} .	
<p>These routines provide the interface to the WRT routines. The WRT routines are provided in the files <code>mod_constants.f90</code>, <code>mod_fileio.f90</code>, <code>mod_xnl4v4.f90</code>, and <code>serv_xnl4v4.f90</code>. For details on these files, see Van Vledder (2002b).</p>		
Nonlinear interaction module (GMD)		w3snl3md.ftn

w3snl3	Calculation of S_{nl} .
expand	Expand spectral space.
expan2	Map form expanded to original spectral space.
insnl3	Initialization for S_{nl} .

Nonlinear interaction module (slot for user supplied routines) w3snlxmd.ftn

w3snlx	Calculation of S_{nl} .
insnlx	Initialization for S_{nl} .

Nonlinear high-frequency filter w3snlsmd.ftn

w3snls	Calculation of filter.
expand	Expand spectral space.
insnls	Initialization for filter.

Bottom friction module (JONSWAP) w3sbt1md.ftn

w3bt1	Calculation of S_{bot} .
-------	----------------------------

Bottom friction module (SHOWEX) w3sbt4md.ftn

insbt4	Initialization of S_{bot}
tabu_erf	Table or error function.
w3sbt4	Calculation of S_{bot} , and energy and momentum fluxes to the bottom boundary layer.

Fluid mud dissipation (Dalrymple and Liu, 1978) w3sbt8md.ftn

w3sbt8	Source term.
--------	--------------

Fluid mud dissipation (Ng, 2000)		w3sbt9md.ftn
w3sbt9	Source term.	
Bottom friction module (slot for user supplied routines)		w3sbtxmd.ftn
w3sbtx	Calculation of S_{bot} .	
insbtx	Initialization of S_{bot} .	
Depth induced breaking module (Battjes-Janssen)		w3sdb1md.ftn
w3sdb1	Calculation of S_{db} .	
Depth induced breaking module (slot for user supplied routines)		w3sdbxmd.ftn
w3sdbx	Calculation of S_{db} .	
insdbx	Initialization of S_{db} .	
Triad interactions module (LTA)		w3str1md.ftn
w3str1	Calculation of S_{tr} .	
Triad interactions module (slot for user supplied routines)		w3strxmd.ftn
w3strx	Calculation of S_{tr} .	
instrx	Initialization of S_{tr} .	
Bottom scattering module		w3sbs1md.ftn
w3sbs1	Calculation of S_{bs} and associated momentum flux to the bottom.	
insbs1	Initialization of S_{bs} .	
Bottom scattering module (slot for user supplied routines)		w3sbsxmd.ftn
w3sbsx	Calculation of S_{bs} .	
insbsx	Initialization of S_{bs} .	

Wave-ice interactions (simple)		w3sic1md.ftn
w3sic1	Calculation of S_{id} .	
Wave-ice interactions (Liu et al.)		w3sic2md.ftn
w3sic2	Calculation of S_{id} . Interpolation tables.	
Wave-ice interactions Wang and Shen (2010)		w3sic3md.ftn
w3sic3	Calculation of S_{id} .	
bsdet	Calculate the determinant for the dispersion relation.	
wn_complex	Calculate complex wavenumber in ice.	
cmplx_root_muller	Find root for complex numbers.	
fun_zhao	Wrapper for functions below.	
func0_zhao, func1_zhao		
w3sis2	Calculation of S_{is} .	
Waves scattering in ice and ice break-up		w3sis2md.ftn
Shoreline reflection		w3ref1md.ftn
w3ref1	Calculation of S_{ref} .	
Module for unclassified source term (slot for user supplied routines)		w3sxxxmd.ftn
w3sxxx	Calculation of S_{xx} .	
insxxx	Initialization of S_{xx} .	

To complete the basic wave model, several additional modules are needed. For the actual contents of the service modules see the documentation in the source code files.

constants.ftn	Physical and mathematical constants and Kelvin functions.
w3arrymd.ftn	Array manipulation routines including 'print plot' routines.
w3bullmd.ftn	Perform bulletin style output for output points.
w3cspcmd.ftn	Conversion of spectral discretization.

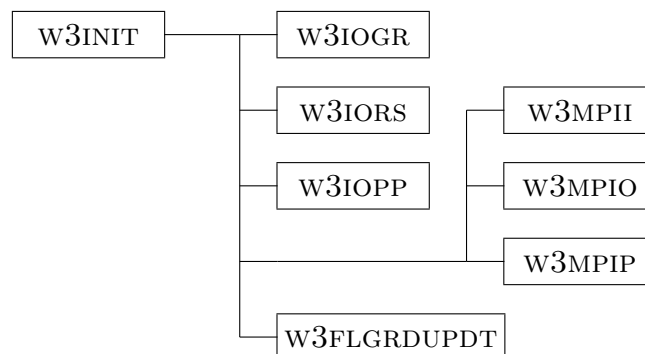


Figure 6.2: Subroutine structure for wave model initialization routine without service routines, data base management routines and MPI calls. Note that W3IOGR on reading data in calls all necessary initialization routines for interpolation tables and physics parameterizations.

- w3dispmd.ftn Routines to solve the Laplace dispersion relation (linear waves, flat bottom, no ice), including interpolation tables. Includes also ice corrections in `liu_forward_dispersion` and `liu_inverse_dispersion`.
- w3gsrumd.ftn Regridding utilities.
- w3partmd.ftn Perform spectral partitioning for a single spectrum.
- w3servmd.ftn General service routines.
- w3timemd.ftn Time management routines.
- w3triamd.ftn Basic routines for triangle-based grids: reading, interpolation, definition of miscellaneous arrays, determination of boundary points.

This completes the description of the basic wave model routines. The relation between the initialization routine and other routines is illustrated in Fig. 6.2. A similar relational diagram for the wave model routine is presented in Fig. 6.3.

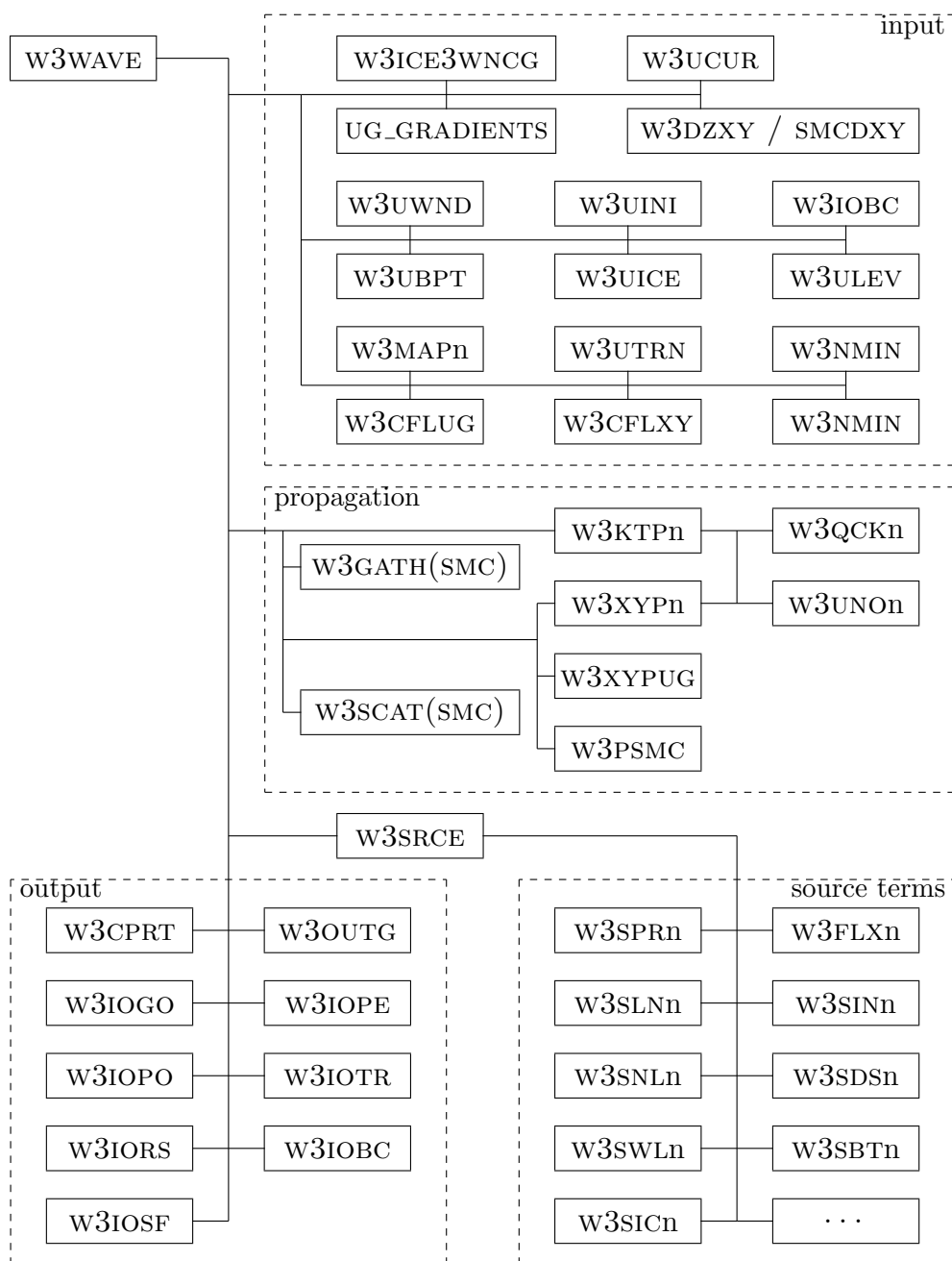


Figure 6.3: Subroutine structure for wave model routine without service routines, routines managing the data structures, and MPI routines. ‘...’ identifies additional source term routines.

6.3.2 Multi-grid modules

The multi-grid wave model shell `ww3_multi` provides a shell around the basic wave model as described in the previous section. This shell manages the side-by-side running of multiple wave model grids, and all communication between the grids. To achieve this various additional modules have been developed. At the core are the initialization, multi-grid model and finalization routines.

Initialization of multi-grid model `wmunitmd.ftn`

`wmunit` Multi-grid model initialization.

Running of multi-grid model `wmwavemd.ftn`

`wmwave` Multi-grid model execution.

`wmprnt` Printing to log file.

`wmbcst` Non-blocking MPI broadcast.

`wmwout` Idem.

Finalizing of multi-grid model `wmfinlmd.ftn`

`wmfinl` Multi-grid model finalization.

These routines are designed to become part of a coupled model. For the structure of the actual wave model routine, reference is made to [Tolman \(2007\)](#). The resulting wave model driver `ww3_multi` consequently becomes extremely simple; it initializes the MPI environment, and then calls the above three modules consecutively.

The main multi-grid wave model routines require an expansion of the data structure used by WAVEWATCH III. Furthermore, main activities are gathered in subroutines in various modules.

Data storage `wmmdatmd.ftn`

`wmndat` Set number of grids to be considered.

`wmdimd, wmdimm`

Set dimensions and allocate storage.

`wmsetm` Set pointers to selected grid.

Determine grid relations wmgridmd.ftn

wmglow	Relations to lower ranked grids.
wmghgh	Relations to higher ranked grids.
wmgeql	Relations between equal ranked grids.
wmrspc	Determine need for spectral conversion between grids.

Update model input wmupdtmd.ftn

wmupdt	General input update routine.
wmupd1	Update input from native files using w3fldsmd.ftn from Section 6.3.4.
wmupd2	Update input from pore-defined input grids.
wmupdv	Update vector fields.
wmupds	Update scalar fields.

Perform internal communications wminiomd.ftn

wmiobs	Stage internal boundary data.
wmiobg	Gather internal boundary data.
wmiobf	Finalize WMIOBS (MPI only).
wmiohs	Stage internal high to low rank data.
wmiohg	Gather internal high to low rank data.
wmiohf	Finalize WMIOHS (MPI only).
wmioes	Stage internal data between equal ranked grids.
wmioeg	Gather internal data between equal ranked grids.
wmioef	Finalize WMIOES (MPI only).

Unify point output to single file wmiopomd.ftn

wmiopp	Initialization routine.
wmiopo	Data gather and write routine (using w3iopo in w3iopomd.ftn).

To complete the multi-grid wave model, one additional service module is needed. For the actual contents of the service module see the documentation in the source code files.

wmunitmd.ftn	Dynamic unit number assignment
wmscrpmd.ftn	SCRIP utilities.

6.3.3 Data assimilation module

WAVEWATCH III[®] includes a data assimilation module that can work in conjunction with the main wave model routine, and is integrated in the generic program shell. The module is intended as an interface to a data assimilation package to be provided by the user.

Data assimilation module w3wdasmd.ftn

w3wdas Data assimilation interface.

6.3.4 Auxiliary programs

WAVEWATCH III[®] has several auxiliary pre- and post-processors, and two wave model shells (see Section 4.4). These auxiliary programs and some additional routines are stored in the following files. Generally, subroutines used only by the programs are stored as internal subroutines with the main program. There is no need for using the module structure in this case. The exception is an additional module `w3fldsmd.ftn` which deals with the data flow of input fields for the wave model between the field pre-processor and the stand-alone model shell. The latter module does not have any explicit WAVEWATCH III dependencies, and can therefore be integrated in any custom data pre-processor.

Input data file management module w3fldsmd.ftn

w3fldo	Opening and checking of data files for W3SHEL.
w3fldg	Reading and writing of data files for W3SHEL (model input).
w3fldd	Reading and writing of data files for W3SHEL (data assimilation).
w3fldp	Prepare interpolation of input fields from arbitrary grids.
w3fldh	Management of homogeneous input fields in W3SHEL.
w3fldm	Process moving grid data in W3SHEL.

Grid pre-processing program		ww3_grid.ftn
w3grid	The grid preprocessor.	
readnl	Reading NAMELIST input (internal).	
Initial conditions program		ww3_strt.ftn
w3strt	The initial conditions program.	
Boundary conditions program		ww3_bound.ftn
Boundary conditions program (NetCDF)		ww3_bound.ftn
w3bound	The boundary conditions program (NetCDF).	
Input field pre-processing program		ww3_prep.ftn
Input field pre-processing program from NetCDF files		ww3_prnc.ftn
w3prep	Pre-processor for the input fields for the generic shell.	
Tide pre-processing program		ww3_ptide.ftn
w3ptide	Pre-processor for tides.	
Generic wave model program		ww3_shel.ftn
w3shel	The generic program shell.	
Grid splitting for ww3_multi		ww3_gspl.ftn
w3gspl	The grid splitting program.	
grinfo, grtrim, grfill, grlost, grsqrq, grsnql, grsepa, grfsml, grfrlg, gr1grd	Routines to incrementally adjust individual grids.	
Generic wave model program		ww3_multi.ftn
w3mlti	The multi-grid program shell.	
Grid output integration for ww3_multi		ww3_gint.ftn
w3gint	The post-processing program for integrating gridded fields of mean wave parameters.	
w3exgi	Actual output routine (internal).	
Gridded data post-processing program		ww3_outf.ftn
w3outf	The post-processing program for gridded fields of mean wave parameters.	
w3exgo	Actual output routine (internal).	

Gridded data post-processing program (NetCDF)		ww3_ounf.ftn
w3ounf	The post-processing program for gridded fields of mean wave parameters, using NetCDF3 or NetCDF4 libraries for Fortran90.	
w3crnc	Creation of NetCDF files, definition of dimensions and header data.	
w3exnc	Actual output routine (internal).	
Gridded data post-processing program (GrADS)		gx_outf.ftn
gxoutf	The post-processing program for converting gridded fields of mean wave parameters to input files for GrADS.	
gxexgo	Actual output routine (internal).	
Gridded data post-processing program (GRIB)		ww3_grib.ftn
w3grib	The post-processing program for generating GRIB files.	
w3exgb	Actual output routine (internal).	
Point post-processing program		ww3_outp.ftn
w3outp	The post-processing program output at selected locations.	
w3expo	Actual output routine (internal).	
Point post-processing program		ww3_ounp.ftn
w3ounp	The post-processing program output at selected locations using NetCDF.	
w3crnc	Creation of NetCDF files, definition of dimensions and header data.	
w3exnc	Actual output routine (internal).	
Point post-processing program (GrADS)		gx_outp.ftn
gxoutp	The post-processing program for converting output at selected locations to input files for GrADS.	
gxexpo	Actual output routine (internal).	

Track output post-processing program	ww3_trck.ftn
w3trck	Converting unformatted direct access track output file to integer-packed formatted file.
Wave field tracking post-processing program	ww3_systrk.ftn
w3systrk	Tracking wave fields in space and time.

6.4 Optimization

The source code of WAVEWATCH III is written in ANSI standard FORTRAN 90, and has been compiled and run on a variety of platforms ranging from PC's to supercomputers.

Optimization for vector computers has been performed by structuring the code in long vector loops where possible. Optimization was originally performed for the Cray YMP and C90. Note that some compiler directives for vectorization have been used. Note also that the vector optimization has not been updated since about 1997, and therefore needs to be revisited if the model is implemented on a vector machine. Vectorization directives are activated by the corresponding preprocessor switch (C90).

Parallelization for shared memory machines using threading has been implemented using standard OpenMP directives. Such parallelization takes place mainly in the loop calling the source term routine W3SRCE and the different propagation routines. OpenMP directives are activated by the corresponding preprocessor switches (OMP*n*).

Parallelization for distributed memory machines is discussed in some detail in section 6.5.2.

Note that an important part of the optimization is the use of interpolation tables for the solution of the dispersion relation and for the calculation of the wind-wave interaction parameter.

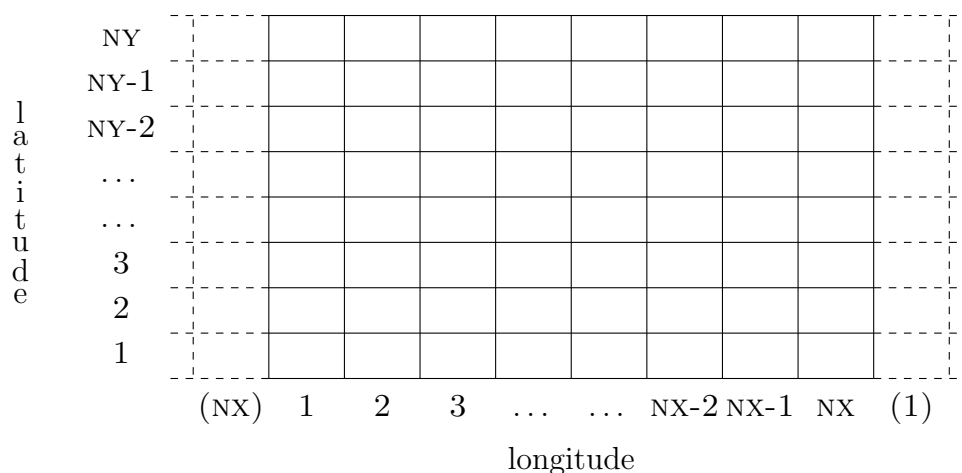


Figure 6.4: Layout of the spatial grid. Grid points are denoted as boxes, dotted boxes denoted repeated columns for global model applications.

6.5 Internal data storage

The remainder of this chapter will deal with the internal data storage used by WAVEWATCH III. In Section 6.5.1 the layout of a single wave model grid as used in `ww3_shel` is discussed. In Section 6.5.2 the parallelization approaches for a single grid are discussed. In Section 6.5.3 the simultaneous storage of multiple wave grids is discussed. Finally, the actual wave model variables are described in Section 6.6. Note that the code is fully documented, including the variables defining the data storage.

6.5.1 Grids

For convenience and economy of programming, spatial and spectral grids are considered separately. This approach is inspired by the splitting technique described in chapter 3. For spatial propagation, a simple ‘rectangular’ spatial grid is used, as is illustrated in Fig. 6.4. The grid can either be a Cartesian ‘ (x, y) ’ grid, a spherical grid (with regular steps on latitude and longitude), a curvilinear grid, or a triangle-based grid. In a spherical grid, the longitudes

are denoted throughout the program by the counter IX , and latitudes by the counter IY , and the corresponding grid dimensions (NX,NY) . All spatial field arrays are dynamically allocated within the code, corresponding work arrays are usually automatic, to allow for thread-safe code. The closure of the grid in case of a global applications is handled within the model, and does not require user intervention. To simplify the calculation of derivatives of in particular the current, the outer grid points $(IX=1,NX)$, unless the grid is global) and $(IY=1,NY)$ will be considered as land points, inactive points or active boundary points. The minimum grid size therefore is $NX=3$, $NY=3$, except for triangle-based grids. In that latter case, all the nodes are listed as a long vector of dimension NX , while $NY=1$, allowing to keep the same code structure. Input arrays are typically assumed to be of the form

$$\text{ARRAY}(NX,NY) ,$$

and are read row by row (see also chapter 4). Within the program, however, they are typically stored with rotated indices

$$\text{ARRAY}(NY,NX) .$$

This makes it easier to provide global closure, which typically requires extension of the x axis. Furthermore, such two-dimensional array are usually treated as one-dimensional arrays, to increase vector lengths. The array ARRAY , its one-dimensional equivalent VARRAY and IXY are defined as

$$\begin{aligned} \text{ARRAY}(MY,MX) , \text{VARRAY}(MY*MX) , \\ \text{IXY} = IY + (IX-1)*MY . \end{aligned}$$

Note that this representation of the grid is used *internally* within the model only.

The spectral grid for a given spatial grid point (IX,IY) is defined similarly, using a directional counter ITH and a wavenumber counter IK (Fig. 6.5). The size of the spectral grid is set using dynamic allocation. As with the spatial grid, the internal description of the spectrum A is defined as

$$A(NTH,NK) ,$$

and equivalent one-dimensional arrays are used throughout the program.

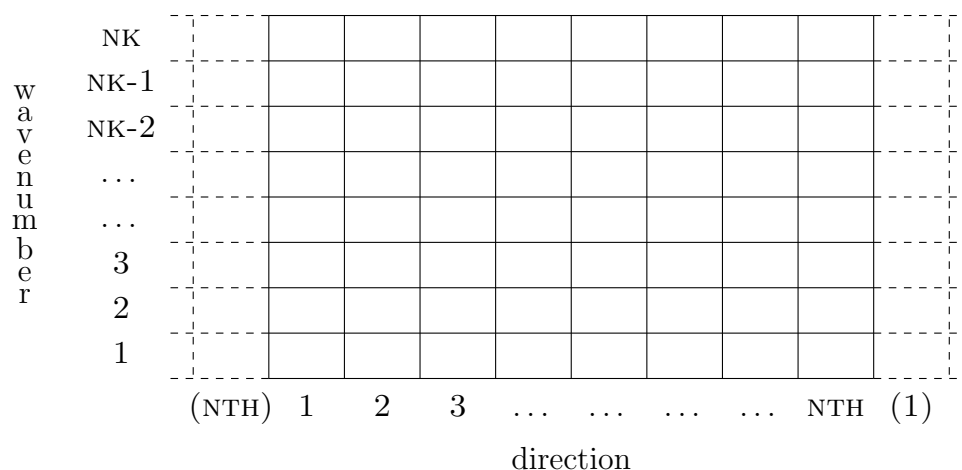


Figure 6.5: Layout of the spectral grid. Dotted boxes denoted repeated columns for directional closure.

Inside the model, directions are always Cartesian, $\theta = 0^\circ$ corresponds to propagation from west to east (positive x or IX direction), and $\theta = 90^\circ$ corresponds to propagation from south to north (positive y or IY direction). Output directions use other conventions, as is discussed in Chapter 4.

The storage of the wave spectra accounts for the majority of the memory required by the model, because the splitting technique used assures that any part of the model operates on a small subset of the entire wave field. To minimize the amount of memory needed, only spectra for actual sea points are stored. Sea points are here defined as points where spectra are potentially needed. This includes active boundary points, and sea points covered by ice. For archiving purposes, a one-dimensional sea point grid is defined using the counter ISEA. Spectra are then stored as

$$A(\text{ITH}, \text{IK}, \text{ISEA}) .$$

An example of the layout of this storage grid in relation to the full grid of Fig. 6.4 is given in Fig. 6.6. Obviously, the relation between the storage grid and the full spatial grid requires some bookkeeping. For this purpose, two ‘maps’ MAPFS and MAPSF are defined.

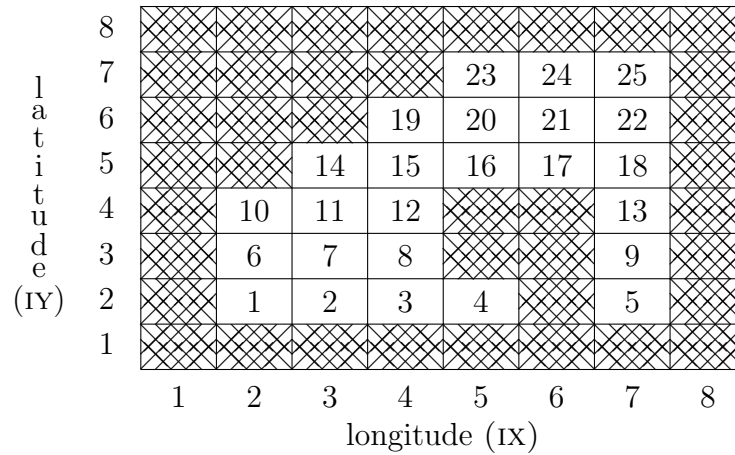


Figure 6.6: An example of the one-dimensional storage grid for spectra. Hatched grid boxes denote land points. Numbers within the grid boxes show the grid counter ISEA of the storage grid.

$$\begin{aligned}
 \text{MAPSF}(\text{ISEA},1) &= \text{IX} , \\
 \text{MAPSF}(\text{ISEA},2) &= \text{IY} , \\
 \text{MAPSF}(\text{ISEA},3) &= \text{IXY} , \\
 \text{MAPFS}(\text{IY},\text{IX}) &= \text{VMAPFS}(\text{IXY}) = \text{ISEA} ,
 \end{aligned}$$

where $\text{MAPFS}(\text{IY},\text{IX}) = 0$ for land points. Finally, status maps $\text{MAPSTA}(\text{IY},\text{IX})$ and $\text{MAPST2}(\text{IY},\text{IX})$ are maintained to identify sea, land, active boundary and ice points. MAPSTA represents the main status map for the grid;

$$\begin{aligned}
 \text{MAPSTA}(\text{IY},\text{IX}) &= 0 && \text{for excluded points,} \\
 \text{MAPSTA}(\text{IY},\text{IX}) &= 1 && \text{for sea points,} \\
 \text{MAPSTA}(\text{IY},\text{IX}) &= 2 && \text{for active boundary points.}
 \end{aligned}$$

Sea points and active boundary point which are not considered in the wave model due to the presence of ice are marked by their corresponding negative status indicator (-1 or -2). MAPST2 contains secondary information. For excluded points $\text{MAPSTA}(\text{IY},\text{IX}) = 0$, this map distinguished between land points $\text{MAPST2}(\text{IY},\text{IX}) = 0$ and otherwise excluded points $\text{MAPST2}(\text{IY},\text{IX})$

= 1. For sea points that are disabled $MAPSTA(IY,IX) < 0$, consecutive bits in MAPST2 identify the reason for deactivation (bit value 1 indicating deactivation).

bit	identifies
1	Ice coverage
2	Point dried out
3	Land in moving grid or inferred in nesting
4	Masked in two-way nesting

Two additional considerations have been made. First, the two status maps can be collapsed into a single map for storage. To assure that the storage is backward compatible with the previous mode version, the two maps are combined into a single map MAPTMP

$$MAPTMP = MAPSTA + 8 * MAPST2$$

considering that only the first few bits of MAPSTA contain data. It is this map MAPTMP that is saved in NetCDF files. The original maps can be recovered as

$$MAPSTA = MOD (MAPTMP + 2 , 8) - 2$$

$$MAPST2 = MAPTMP - MAPSTA$$

Second, a single map is used in the graphics output program, to simplify the plotting of the status of grid points. In the graphics files, the map is defined as

map	implies
2	Active boundary point
1	Active sea point
0	Land point (including as identified in MAPST2)
-1	Point covered by ice, but wet
-2	Dry point, not covered by ice
-3	Dry point covered by ice
-4	Point masked in the two-way nesting scheme
-5	Other disabled point

Similarly, a single map can be used to simplify processing in the grid preparation program `ww3_grid`. In this map a distinction is made between points as follows:

map	implies
3	Excluded points
2	Active boundary point
1	Active sea point
0	Land point

6.5.2 Distributed memory concepts.

The general grid structure described in the previous paragraph is used for both shared and distributed memory versions of the model, with some minor differences. For the distributed memory version of the model, not all data is kept at each processor. Instead, each spectrum is kept at a single processor only. The spectra on the storage grid are distributed over the available processors with a constant stride. Because only part of the spectra are stored locally on a given processor, a distinction needs to be made between the above global sea point counter `ISEA`, and the local sea point counter `JSEA`. If the actual number of processors used in the computation is `NAPROC`, and if `IAPROC` is the processor number ranging from 1 to `NAPROC`, these parameters are related in the following way

$$\begin{aligned} ISEA &= IAPROC + (JSEA-1) NAPROC , \\ JSEA &= 1 + (ISEA-1) / NAPROC , \\ IAPROC &= 1 + \text{MOD}(ISEA-1, NAPROC) . \end{aligned}$$

In model version 3.10, a further refinement was introduced. The actual number of processors `NAPROC` can be smaller than the total number of processors used by the program (`NTPROC`). Processors where $NAPROC < IAPROC \leq NTPROC$ are reserved for output processing only.

With this data distribution, source terms and intra-spectral propagation can be calculated at the each given processor without the need for communication between processors. For spatial propagation, however, a data transpose is required where the spectral components (`ITH,IK`) for all spatial grid points have to be gathered at a single processor. After propagation has

been performed, the modified data have to be scattered back to their ‘home’ processor. Individual spectral components are assigned to specific processors in such a way that the number of partial propagation steps to be performed by each processor is roughly identical. This makes a good load balance possible. The actual algorithm can be found in section 4.d of the subroutine `W3INIT` (`w3initmd.ftn`).

The data transpose for the gather operation is implemented in two steps using the Message Passing Interface (MPI) standard (e.g. [Gropp et al., 1997](#)). First, values for each spatial grid point for a given spectral bin (`ITH,IK`) are gathered in a single target processor in a one-dimensional array `STORE(ISEA)`, which then is converted to the full two-dimensional field of spectral components. After propagation has been performed, the transpose for the scatter operation reverses this process, using the same one-dimensional array `STORE`. Whereas the algorithm for distributing spatial propagation over individual processors assures a global (per time step) load balance, it does not assure that communication is synchronized, because not each calculation at each processor will take the same effort. To avoid that this results in a load imbalance, non-blocking communication has been used. Furthermore, the one-dimensional array `STORE(ISEA)` is replaced by `STORE(ISEA,IBUF)`, where the added dimension of the array supplies an actively managed buffer space (see `W3GATH` and `W3SCAT` in `w3wavemd.ftn`). These buffers allow that spare clock cycles as may occur during communication can be used for calculation, and that hiding of communication behind calculation will occur if the hardware is capable of doing this. To avoid problems with incompatibilities between FORTRAN and MPI, separate gather and scatter data arrays are used. The buffered data transposes are graphically depicted in [Fig. 6.7](#). More details can be found in [Tolman \(2002b\)](#).

In principle only the storage array `A(ITH,IK,JSEA)` is influenced by the data distribution. Input fields, maps and output fields of mean wave parameters in principle are retained at full resolution at each grid point. Full maps are available at each processor at each phase of the calculation. Input and output fields generally contain pertinent data at the stride `NAPROC` only.

Distributed memory also requires modifications to the I/O. Input files are read completely by each separate processor. The type of file output is determined by the I/O type indicator `IOSTYP`.

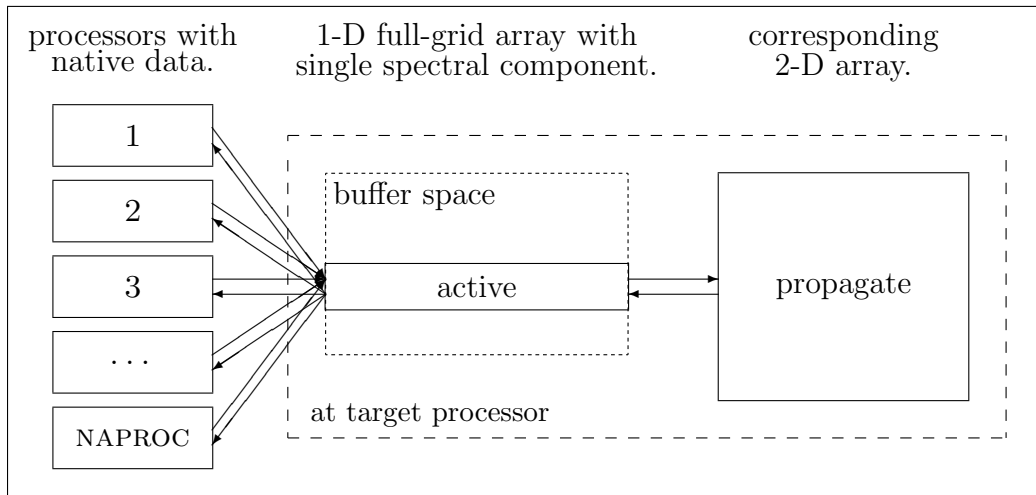


Figure 6.7: Data transpose in distributed memory model version. First, the data is moved from left to right in the figure during the gather operation. After the calculation is performed, the data is moved from right to left in the scatter operation.

IOSTYP	implies
0	Restart file written from each individual process.
1	Each file written from assigned process.
2	Each file written from a single dedicated output process.
3	Dedicated output processes for each output type.

Note that the restart file is a direct access file, so that each processor can efficiently gather only the locally stored spectra, without the need of reading through the entire file. The restart file is either written by each individual process directly, or all data is funneled through a dedicated processor. The first method requires a parallel file system, the second method is generally applicable.

The present algorithm for data distribution has been chosen for several reasons. First, it results in an automatic and efficient load balancing with respect to the (dynamic) integration of source terms, the exclusion of ice covered grid points, and of intra-spectral propagation. Secondly, the communication by definition becomes independent of the numerical propagation scheme, unlike for the more conventional domain decomposition. In the latter case, only a so-called ‘halo’ of boundary data needs to be converted

to neighboring ‘blocks’ of grid points. The size of the halo depends on the propagation scheme selected. The main disadvantage of the present data distribution scheme is that the amount of data to be communicated each time step is much larger than for a more conventional domain decomposition, particularly when relatively small numbers of processors are used. On an IBM RS6000 SP, on which the distributed memory version of WAVEWATCH III was tested, the relatively large amount of communication did not constitute a significant part of the overall time of computation, and the model shows excellent scaling behavior for up to $O(100)$ processors (Tolman, 2002b).

More recently, hybrid parallelization techniques have been developed using a combination of a course scale domain decomposition and a local data transpose, using approaches already available in `ww3_multi`. To accommodate this, the file `ww3_gspl(.sh)` tools were introduced in model version 4.10. Although this approach still needs some work with respect to the model memory footprint in the initialization in `ww3_multi`, initial scaling results obtained with this approach are encouraging (see Tolman, 2013b).

6.5.3 Multiple grids

So far, only a single wave model grid has been considered. To make it possible to run several model grids in a single program, a data structure needs to be devised in which all different model grids and internal work arrays for all models are retained simultaneously, with a simple mechanism to choose the actual wave model grid to work on. In order to achieve this, some FORTRAN 90 features (e.g., Metcalf and Reid, 1999) are used in the following way:

- 1) Define one or more data structures in the model code that contain the model setup and relevant work arrays, using a TYPE declaration.
- 2) Construct arrays of these data structures, with each element of the array defining a separate model grid.
- 3) Redefine the basic parameters describing the model such as the number of grid points `NX` and `NY` as pointers, and point these to the proper element of the proper data structures to generate instantaneous aliases.

```

!/
!/ Data structures
!/
      TYPE GRID
            INTEGER                :: NX, NY, NSEA
            REAL, POINTER           :: ZB(:)
      END TYPE GRID
!/
!/ Data storage
!/
      TYPE(GRID), TARGET, ALLOCATABLE :: GRIDS(:)
!/
!/ Data aliases
!/
      INTEGER, POINTER              :: NX, NY, NSEA
      REAL, POINTER                 :: ZB(:):
!/

```

Figure 6.8: Example of the data structure declarations used in `w3gdatmd.ftn` to define multiple spatial grids in the wave model. For simplicity, the example considers only the grid dimensions `NX`, `NY` and `NSEA`, and the bottom depth array `ZB`.

In this way it is possible to define a multi-model data structure, while keeping the layout of all original variables describing the model unchanged inside the model subroutines. Such a structure and its usage are illustrated in Figs. 6.8 and 6.9 with an example from the actual source code. Note that the pointer arrays like `ZB` inside the structures are assigned memory as

$$\text{ALLOCATE GRIDS(IMOD)\%ZB(NSEA)}$$

After this statement, the alias pointer `ZB` again needs to be pointed to the proper element of the structure for this alias to properly point to the newly allocated space. For this reason, the subroutine `W3DIMX`, which allocates the arrays in this structure, includes at the end a call to the subroutine `W3SETX`,

```

!
    NX      => GRIDS(IMOD)%NX
    NY      => GRIDS(IMOD)%NY
    NSEA    => GRIDS(IMOD)%NSEA
!
    ZB      => GRIDS(IMOD)%ZB
!

```

Figure 6.9: Example of the source code used to activate the pointer aliases in Fig. 6.8 for the model number IMOD.

which in turn sets all pointer aliases for the selected grid. The same is true for other subroutines setting array sizes in other structures.

6.6 Variables in modules

In the documentation of model versions up to version 3.14, all PUBLIC and PRIVATE variables in modules were described in the present and following sections. All these parameters are also documented in the source code of the model. Keeping two separate unlinked copies of the documentations is becoming a daunting task with little benefit to the model user and developer. Hence, from model version 5.16 on, the main documentation of the variables in the code is kept up to date in the source code itself, and second full documentation in the manual is no longer maintained. In this manual, we now only describe PARAMETER definitions, as they may influence model behavior, and identify critical versions of I/O elements of the code. The file name of the module is given at the right margin of the start of each list. The second column of each list identifies the type of the variable. I, R, L and C represent integer, real, logical and character, A identifies an array, and P identifies a PARAMETER declaration. All variables are public, unless marked with *. The following sections account for parameter settings in modules (and programs), and give a top level description of what is stored in the data structures, and where these data structures are located in the code.

6.6.1 Parameter settings in modules

Several modules have internally used parameter settings. Here only parameter settings that are generally usable or impact model behavior are presented.

Physical and mathematical constants : constants.ftn

GRAV	RP	Acceleration of gravity g .	(m s^{-2})
DWAT	RP	Density of water.	(kg m^{-3})
DAIR	RP	Density of air.	(kg m^{-3})
NU_AIR	RP	Kinematic viscosity of air	$(\text{m}^2 \text{s}^{-1})$
NU_WATER	RP	Kinematic viscosity of water	$(\text{m}^2 \text{s}^{-1})$
SED_SD	RP	Specific gravity of sediment	$(-)$
KAPPA	RP	Von Karman's constants	$(-)$
PI	RP	π .	
TPI	RP	2π .	
HPI	RP	0.5π .	
TPIINV	RP	$(2\pi)^{-1}$.	
HPIINV	RP	$(0.5\pi)^{-1}$.	
RADE	RP	Conversion factor from radians to degrees.	
DERA	RP	Conversion factor from degrees to radians.	
RADIUS	RP	Radius of the earth.	(m)
G2PI3I	RP	$g^{-2}(2\pi)^{-3}$.	
G1PI1I	RP	$g^{-1}(2\pi)^{-1}$.	

Wave model initialization module : w3initmd.ftn

CRITOS	RP	Critical fraction of resources used for output only (triggers warning output).
WWVER	CP	Version number of the main program.
SWITCHES	CP	Switches taken from bin/switch.

I/O module (mod_def.ww3) : w3iogrmd.ftn

VERGRD	CP*	Version number of file mod_def.ww3.
IDSTR	CP*	ID string for file.

I/O module (out_grd.ww3) : w3iogomd.ftn

VEROGR	CP*	Version number of file out_grd.ww3.
--------	-----	-------------------------------------

IDSTR	CP*	ID string for file.	
I/O module (out_pnt.ww3) :			w3iopmd.ftn
VEROPT	CP*	Version number of file out_pnt.ww3.	
IDSTR	CP*	ID string for file.	
ACC	CP	Relative offset below which output point is moved to grid point.	
I/O module (track_o.ww3) :			w3iotrmd.ftn
VERTRK	CP*	Version number of file track_o.ww3.	
IDSTR	CP*	ID string for file track_i.ww3.	
OTYPE	CP	Array dimension.	
I/O module (restart.ww3) :			w3iorsmd.ftn
VERINI	CP*	Version number of file restart.ww3.	
IDSTR	CP*	ID string for file.	
LRB	CP	Word length set with LRB <i>n</i> switch.	
I/O module (nest.ww3) :			w3iobcmd.ftn
VERBPT	CP*	Version number of file nest.ww3.	
IDSTR	CP*	ID string for file.	
I/O module (partition.ww3) :			w3iosfmd.ftn
VERTRT	CP*	Version number of file partition.ww3.	
IDSTR	CP*	ID string for file.	
Multi-grid model input update :			wmupdtmd.ftn
SWPMAX	IP	Maximum number of extrapolation sweeps allowed to make maps match in conversion from input from input grid to wave model grid.	

Several routines contain interpolation tables that are set up with parameter statements, including

Solving the dispersion relation :	w3dispmd.ftn
-----------------------------------	--------------

NAR1D	IP	Dimension of interpolation tables.
DFAC	RP	Maximum nondimensional water depth kd .
ECG1	RA	Table for calculating group velocities from the frequency and the depth.
EWN1	RA	Id. wavenumbers.
N1MAX	I	Largest index in tables.
DSIE	R	Nondimensional frequency increment.

Shallow water quadruplet lookup table for GMD : w3snl3md.ftn

NKD	IP	Number of nondimensional depths in storage array.
KDMIN	RP	Minimum relative depth in table.
KDMAX	RP	Maximum relative depth in table.
LAMMAX	RP	Maximum value for λ or μ .
DELTHM	RP	Maximum angle gap θ_{12} ($^\circ$).

Shallow water lookup table for nonlinear filter : w3snlsmf.ftn

NKD	IP	Number of nondimensional depths in storage array.
KDMIN	RP	Minimum relative depth in table.
KDMAX	RP	Maximum relative depth in table.
ABMAX	RP	Maximum value for a_{34} .

Lookup table for β in Tolman and Chalikov 1996 : w3src2md.ftn

NRSIGA	IP	Array dimension (σ_a).
NRDRAG	IP	Array dimension (C_d).
SIGAMX	RP	Maximum nondimensional frequency $\tilde{\sigma}_a$.
DRAGMX	RP	Maximum drag coefficient C_d

Lookup table for ... in WAM-4 / ECWAM : w3src3md.ftn

KAPPA	RP	von Kármán's constant.
NU_AIR	RP	air viscosity.
ITAUMAX	IP	size of stress dimension.
JUMAX	IP	size of wind dimension.
IUSTAR	IP	size of ustar dimension.
IALPHA	IP	size of Charnock dimension.
ILEVTAIL	IP	size of tail level dimension.
UMAX	RP	Maximum wind speed in table.
TAUWMAX	RP	Maximum ustar in table.

EPS1	RP	Small number for stress convergence.
EPS2	RP	Small number for stress convergence.
NITER	IP	Number of iterations in stress table.
XM	IP	power of TAUW/TAU in roughness parameterization.
JTOT	IP	Number of points in discretization of tail.

Lookup tables Ardhuin et al. 2010 : w3src3md.ftn
 Combination of previous two sets of parameters.

Table of error functions in bottom friction : w3sbt4md.ftn

SIZEERFTABLE	IP	Size of table for erf function.
XERFMAX	RP	Maximum value of x in table of erf(x).
WSUB	RPA	Weights for 3-point Gauss-Hermitte quadrature.
XSUB	RPA	x values for 3-point Gauss-Hermitte quadrature.

Some model parameters are set using parameter statements.

Source term computation and integration : w3srcemd.ftn

OFFSET	RP*	Offset ϵ in Eq. (3.61).
--------	-----	----------------------------------

Auxiliary data storage : w3adatmd.ftn

MPIBUF	IP	Number of buffers used in MPI data transpose.
--------	----	---

Some service routines contain parameters that can be used to influence, for instance, the model output.

Array I/O including text outputs : w3arrymd.ftn

ICOL	IP*	Set maximum columns on output (now set to 80).
NFRMAX	IP*	Set maximum number of frequency in spectral print plots (now set to 50).

Automatic unit number assignment : wmunitmd.ftn

UNITLW	IP	Lowest unit number to be considered.
UNITHG	IP	Highest unit number to be considered.
INPLow, INPHGH	IP	Range of input file unit numbers.

OUTLOW, OUTHGH

IP Range of output file unit numbers.

SCRLOW, SCRHGH

IP Range of scratch file unit numbers.

Creating spectral bulletins :

w3bullmd.ftn

NPTAB, NFLD, NPMAX, BHSMIN, BHSDROP, DHSMAX,

DPTMX, DDMMAX, DDWMAX, AGEMIN

I/RP Setting of size of bulletin as well as various filter values.

6.6.2 Data structures

As outlined in Section 6.5.3, the core of the wave model consists of a set of data structures allowing for the consecutive storage of data for multiple grids. The individual storage structures are contained in the following modules:

w3gdatmd.ftn Information for spatial and spectral grids, and all physical and numerical model parameters.

w3wdatmd.ftn The actual wave data, consisting of spectra and the fields like u_* that are needed to hot-start the model.

w3adatmd.ftn Auxiliary fields and parameters.

w3odatmd.ftn Output data.

w3idatmd.ftn Input data.

wmmdatmd.ftn Data specific to the multi-grid model.

The data structures are fully documented in the above files, and the documentation is no longer reproduced here in the manual.

This page is intentionally left blank.

References

- Abdalla, S. and J. R. Bidlot, 2002: Wind gustiness and air density effects and other key changes to wave model in CY25R1. Tech. Rep. Memorandum R60.9/SA/0273, Research Department, ECMWF, Reading, U. K.
- Ardhuin, F. and A. Boyer, 2006: Numerical modelling of sea states: validation of spectral shapes (in French). *Navigation*, **54**, 55–71.
- Ardhuin, F., B. Chapron and F. Collard, 2009a: Ocean swell evolution from distant storms. *Geophys. Res. Lett.*, **36**.
- Ardhuin, F., F. Collard, B. Chapron, F. Girard-Ardhuin, G. Guitton, A. Mouche and J. Stopa, 2015: Estimates of ocean wave heights and attenuation in sea ice using the SAR wave mode on Sentinel-1A. *Geophys. Res. Lett.*, **42**, 2,317–2,325.
- Ardhuin, F., J. Hanafin, Y. Quilfen, B. Chapron, P. Queffeuou, M. Obrebski, J. Sienkiewicz and D. Vandermark, 2011a: Calibration of the IOWAGA global wave hindcast (1991-2011) using ECMWF and CFSR winds. in *Proc. 12th Int. Workshop on Wave Forecasting and Hindcasting*, pp. 1–13.
- Ardhuin, F. and T. H. C. Herbers, 2002: Bragg scattering of random surface gravity waves by irregular seabed topography. *J. Fluid Mech.*, **451**, 1–33.
- Ardhuin, F. and A. D. Jenkins, 2006: On the interaction of surface waves and upper ocean turbulence. *J. Phys. Oceanogr.*, **36**(3), 551–557.
- Ardhuin, F. and R. Magne, 2007: Scattering of surface gravity waves by bottom topography with a current. *J. Fluid Mech.*, **576**, 235–264.
- Ardhuin, F., L. Marié, N. Rasclé, P. Forget and A. Roland, 2009b: Observation and estimation of Lagrangian, Stokes and Eulerian currents induced by wind and waves at the sea surface. *J. Phys. Oceanogr.*, **39**(11), 2,820–2,838.
- Ardhuin, F., W. C. O’Reilly, T. H. C. Herbers and P. F. Jessen, 2003: Swell transformation across the continental shelf. Part I: Attenuation and directional broadening. *J. Phys. Oceanogr.*, **33**, 1,921–1,939.
- Ardhuin, F., A. Rawat and J. Aucan, 2014: A numerical model for free infragravity waves: definition and validation at regional and global scales. *Ocean Mod.*, **77**, 20–32.
- Ardhuin, F., W. E. Rogers, A. V. Babanin, J. Filipot, R. Magne, A. Roland, A. van der Westhuysen, P. Queffeuou, J. Lefevre, L. Aouf and F. Collard, 2010: Semiempirical dissipation source functions for ocean waves. Part I: Definition, calibration, and validation. *J. Phys. Oceanogr.*, **40**, 1,917–1,941.

- Ardhuin, F. and A. Roland, 2012: Coastal wave reflection, directional spread, and seismoacoustic noise sources. *J. Geophys. Res.*, **117**, C00J20.
- Ardhuin, F., P. Sutherland, M. Doble and P. Wadhams, 2016: Ocean waves across the Arctic: Attenuation due to dissipation dominates over scattering for periods longer than 19 s. *Geophys. Res. Lett.*, **43**(11), 5775–5783.
- Ardhuin, F., J. Tournadre, P. Queffelec and F. Girard-Ardhuin, 2011b: Observation and parameterization of small icebergs: Drifting breakwaters in the Southern Ocean. *Ocean Mod.*, **39**, 405–410.
- Babanin, A. V., 2009: Breaking of ocean surface waves. *Acta Phys. Slovaca*, **59**(4), 305–535.
- Babanin, A. V., 2011: *Breaking and dissipation of ocean surface waves*. Cambridge University Press, 480 pp.
- Babanin, A. V., M. L. Banner, I. R. Young and M. A. Donelan, 2007: Wave-follower field measurements of the wind-input spectral function. Part iii: Parameterization of the wind-input enhancement due to wave breaking. *J. Phys. Oceanogr.*, **37**, 2,764–2,775.
- Babanin, A. V. and Y. P. Soloviev, 1987: Parameterization of width of directional energy distributions of wind-generated waves at limited fetches. *Izvestiya, Atmos. and Oceanic Phys.*, **23**, 645–651.
- Babanin, A. V., K. N. Tsagareli, I. R. Young and D. J. Walker, 2010: Numerical investigation of spectral evolution of wind waves. Part II: Dissipation term and evolution tests. *J. Phys. Oceanogr.*, **40**, 667–683.
- Babanin, A. V. and I. R. Young, 2005: Two-phase behaviour of the spectral dissipation of wind waves. in *Proc. Fifth Int. Symp. Ocean Waves Measurement and Analysis*.
- Babanin, A. V., I. R. Young and M. L. Banner, 2001: Breaking probabilities for dominant surface waves on water of finite constant depth. *J. Geophys. Res.*, **106**, 11,659–11,676.
- Banner, M. L., A. V. Babanin and I. R. Young, 2000: Breaking probability for dominant waves on the sea surface. *J. Phys. Oceanogr.*, **30**, 3,145–3,160.
- Banner, M. L. and W. L. Peirson, 1998: Tangential stress beneath wind-driven air–water interfaces. *J. Fluid Mech.*, **364**, 115–145.
- Barbariol, F., J.-H. G. M. Alves, A. Benetazzo, F. Bergamasco, L. Bertotti, S. Carniel, L. Cavaleri, Y. Y. Chao, A. Chawla, A. Ricchi, M. Sclavo and H. L. Tolman, 2016: Numerical modeling of space-time wave extremes using WAVEWATCH III. *Ocean Dynamics*, **Under rev.**
- Barbariol, F., A. Benetazzo, S. Carniel and M. Sclavo, 2015: Space-time wave extremes: The role of metocean forcings. *J. Phys. Oceanogr.*, **45**(7),

- 1,897–1,916.
- Battjes, J. A. and J. P. F. M. Janssen, 1978: Energy loss and set-up due to breaking of random waves. in *Proc. 16th Int. Conf. Coastal Eng.*, pp. 569–587. ASCE.
- Benetazzo, A., F. Barbariol, F. Bergamasco, A. Torsello, S. Carniel and M. Sclavo, 2015: Observation of extreme sea waves in a space-time ensemble. *J. Phys. Oceanogr.*, **45**(9), 2,261–2,275.
- Bidlot, J.-R., 2012: Present status of wave forecasting at E.C.M.W.F. in *Proceedings of ECMWF workshop on ocean wave forecasting, June*.
- Bidlot, J. R., S. Abdalla and P. A. E. M. Janssen, 2005: A revised formulation for ocean wave dissipation in CY25R1. Tech. Rep. Memorandum R60.9/JB/0516, Research Department, ECMWF, Reading, U. K.
- Bidlot, J. R., P. A. E. M. Janssen and S. Abdalla, 2007: A revised formulation of ocean wave dissipation and its model impact. Tech. Rep. Memorandum 509, ECMWF, Reading, U. K.
- Booij, N. and L. H. Holthuijsen, 1987: Propagation of ocean waves in discrete spectral wave models. *J. Comput. Physics*, **68**, 307–326.
- Booij, N., R. C. Ris and L. H. Holthuijsen, 1999: A third-generation wave model for coastal regions, 1. Model description and validation. *J. Geophys. Res.*, **104**, 7,649–7,666.
- Bouws, E. and G. J. Komen, 1983: On the balance between growth and dissipation in an extreme depth-limited wind-sea in the southern North Sea. *J. Phys. Oceanogr.*, **13**, 1,653–1,658.
- Bretherton, F. P. and C. J. R. Garrett, 1968: Wave trains in inhomogeneous moving media. *Proc. Roy. Soc. London*, **A 302**, 529–554.
- Cahyono, 1994: *Three-dimensional numerical modelling of sediment transport processes in non-stratified estuarine and coastal waters*. Ph.D. Thesis, University of Bradford, 315 pp.
- Cavaleri, L. and P. Malanotte-Rizzoli, 1981: Wind-wave prediction in shallow water: Theory and applications. *J. Geophys. Res.*, **86**, 10,961–10,973.
- Chalikov, D. V., 1995: The parameterization of the wave boundary layer. *J. Phys. Oceanogr.*, **25**, 1,333–1,349.
- Chalikov, D. V. and M. Y. Belevich, 1993: One-dimensional theory of the wave boundary layer. *Bound. Layer Meteor.*, **63**, 65–96.
- Charnock, H., 1955: Wind stress on a water surface. *Quart. J. Roy. Meteor. Soc.*, **81**, 639–640.
- Chawla, A. and H. L. Tolman, 2007: Automated grid generation for WAVE-WATCH III. Tech. Note 254, NOAA/NWS/NCEP/MMAB, 71 pp.

- Chawla, A. and H. L. Tolman, 2008: Obstruction grids for spectral wave models. *Ocean Mod.*, **22**, 12–25.
- Christoffersen, J. B., 1982: Current depth refraction of dissipative water waves. Series Paper 30, Institute of Hydrodynamics and Hydraulic Engineering, Techn. Univ. Denmark.
- Cole, D., R. Johnson and G. Durell, 1998: Cyclic loading and creep response of aligned first-year sea ice. *J. Geophys. Res.*, **103**(C10), 21,751–21,758.
- Dalrymple, R. A. and P. L. F. Liu, 1978: Waves over soft muds: A two-layer fluid model. *J. Phys. Oceanogr.*, **986**, 1,121–1,131.
- Davis, R. W. and E. F. More, 1982: A numerical study of vortex shedding from rectangles. *J. Fluid Mech.*, **116**, 475–506.
- Devaliere, E. M., J. L. Hanson and R. Luettich, 2009: Spatial tracking of numerical wave model output using a spiral search algorithm. in *2009 WRI World Congress on Computer Science and Information Engineering, Los Angeles, CA*, Vol. 2, pp. 404–408.
- Donelan, M. A., 1999: Wind-induced growth and attenuation of laboratory waves. in *Wind-over-wave couplings: Perspectives and prospects*, pp. 183–194. Clarendon Press.
- Donelan, M. A., 2001: A nonlinear dissipation function due to wave breaking. in *Proc. ECMWF Workshop on Ocean Wave Forecasting*, pp. 87–94.
- Donelan, M. A., A. V. Babanin, I. R. Young and M. L. Banner, 2006: Wave follower measurements of the wind-input spectral function. Part II. Parameterization of the wind input. *J. Phys. Oceanogr.*, **36**, 1,672–1,689.
- Donelan, M. A., M. Curcic, S. S. Chen and A. K. Magnusson, 2012: Modeling waves and wind stress. *J. Geophys. Res.*, **117**, 1–26.
- Dore, B. D., 1978: Some effects of the air-water interface on gravity waves. *Geophys. Astrophys. Fluid. Dyn.*, **10**, 215–230.
- Doty, B., 1995: *The grid analysis and display system GrADS*. COLA, <http://www.iges.org/grads>.
- Dumont, D., A. Kohout and L. Bertino, 2011: A wave-based model for the marginal ice zone including a floe breaking parameterization. *J. Geophys. Res.*, **116**(C4), C04001.
- Eldeberky, Y., 1995: Personal communication with R. Ris. Tech. rep.
- Eldeberky, Y., 1996: *Nonlinear transformations of wave spectra in the nearshore zone*. Ph.D. thesis, Delft University of Technology, Delft, The Netherlands.
- Eldeberky, Y. and J. A. Battjes, 1996: Spectral modelling of wave breaking: Application to boussinesq equations. *J. Geophys. Res.*, **101**, 1,253–1,264.

- Elgar, S., T. H. C. Herbers and R. T. Guza, 1994: Reflection of ocean surface gravity waves from a natural beach. *J. Phys. Oceanogr.*, **24**, 1,503–1,511.
- Falconer, R. A. and Cayhono, 1993: Water quality modelling in well mixed estuaries using higher order accurate differencing schemes. in S. S. Y. Wang, editor, *Advances in Hydro- Science and Engineering*, pp. 81–92. CCHE, University of Mississippi.
- Fedele, F., 2012: Space–time extremes in short-crested storm seas. *J. Phys. Oceanogr.*, **42**(9), 1,601–1,615.
- Fedele, F., A. Benetazzo, G. Gallego, P.-C. Shih, A. Yezzi, F. Barbariol and F. Ardhuin, 2013: Space-time measurements of oceanic sea states. *Ocean Mod.*, **70**, 103–115.
- Fedele, F., G. Gallego, A. Yezzi, A. Benetazzo, L. Cavaleri, M. Sclavo and M. Bastianini, 2012: Euler characteristics of oceanic sea states. *Mathematics and Computers in Simulation*, **82**(6), 1,102–1,111.
- Filipot, J.-F. and F. Ardhuin, 2012: A unified spectral parameterization for wave breaking: From the deep ocean to the surf zone. *J. Geophys. Res.*, **117**(C11).
- Filipot, J.-F., F. Ardhuin and A. Babanin, 2010: A unified deep-to-shallow-water wave-breaking probability parameterization. *J. Geophys. Res.*, **115**(C4).
- Fletcher, C. A. J., 1988: *Computational techniques for fluid dynamics, part I and II*. Springer, 484 pp.
- Foreman, M. G. G., J. Y. Cherniawsky and V. A. Ballantyne, 2009: Versatile harmonic tidal analysis: Improvements and applications. *J. Atmos. Oceanic Techn.*, **26**, 806–817.
- Grant, W. D. and O. S. Madsen, 1979: Combined wave and current interaction with a rough bottom. *J. Geophys. Res.*, **84**, 1,797–1,808.
- Gropp, W., E. Lusk and A. Skjellum, 1997: *Using MPI: Portable parallel programming with the message-passing interface*. MIT Press, 299 pp.
- Hanson, J. L. and R. E. Jensen, 2004: Wave system diagnostics for numerical wave models. in *8th international workshop on wave hindcasting and forecasting*, *JCOMM Tech. Rep. 29*, WMO/TD-No. 1319.
- Hanson, J. L. and O. M. Phillips, 2001: Automated analysis of ocean surface directional wave spectra. *J. Atmos. Oceanic Techn.*, **18**, 177–293.
- Hanson, J. L., B. A. Tracy, H. L. Tolman and D. Scott, 2006: Pacific hindcast performance evaluation of three numerical wave models. in *9th international workshop on wave hindcasting and forecasting*, *JCOMM Tech. Rep. 34*. Paper A2.

- Hara, T. and S. Belcher, 2004: Wind profile and drag coefficient over mature ocean surface wave spectra. *J. Phys. Oceanogr.*, **34**, 2345–2358.
- Hardy, T. A., L. B. Mason and J. D. McConochie, 2000: A wave model for the Great Barrier Reef. *Ocean Eng.*, **28**, 45–70.
- Hardy, T. A. and I. R. Young, 1996: Field study of wave attenuation on an offshore coral reef. *J. Geophys. Res.*, **101**, 14,311–14,326.
- Hargreaves, J. C. and J. D. Annan, 1998: Integration of source terms in WAM. in *Proceedings of the 5th International Workshop on Wave Forecasting and Hindcasting*, pp. 128–133.
- Hargreaves, J. C. and J. D. Annan, 2001: Comments on “Improvement of the short fetch behavior in the ocean wave model (WAM)”. *J. Atmos. Oceanic Techn.*, **18**, 711–715.
- Hasselmann, K., 1962: On the non-linear energy transfer in a gravity wave spectrum, Part 1. General theory. *J. Fluid Mech.*, **12**, 481–500.
- Hasselmann, K., 1963a: On the non-linear transfer in a gravity wave spectrum, Part 2, Conservation theory, wave-particle correspondence, irreversibility. *J. Fluid Mech.*, **15**, 273–281.
- Hasselmann, K., 1963b: On the non-linear transfer in a gravity wave spectrum, Part 3. Evaluation of energy flux and sea-swell interactions for a Neuman spectrum. *J. Fluid Mech.*, **15**, 385–398.
- Hasselmann, K., T. P. Barnett, E. Bouws, H. Carlson, D. E. Cartwright, K. Enke, J. A. Ewing, H. Gienapp, D. E. Hasselmann, P. Kruseman, A. Meerburg, P. Müller, D. J. Olbers, K. Richter, W. Sell and H. Walden, 1973: Measurements of wind-wave growth and swell decay during the Joint North Sea Wave Project (JONSWAP). *Ergänzungsheft zur Deutschen Hydrographischen Zeitschrift, Reihe A(8)*, **12**, 95 pp.
- Hasselmann, S. and K. Hasselmann, 1985: Computations and parameterizations of the nonlinear energy transfer in a gravity-wave spectrum, Part I: A new method for efficient computations of the exact nonlinear transfer integral. *J. Phys. Oceanogr.*, **15**, 1,369–1,377.
- Hasselmann, S., K. Hasselmann, J. H. Allender and T. P. Barnett, 1985: Computations and parameterizations of the nonlinear energy transfer in a gravity-wave spectrum, Part II: Parameterizations of the nonlinear energy transfer for application in wave models. *J. Phys. Oceanogr.*, **15**, 1,378–1,391.
- Herbers, T. H. C. and M. C. Burton, 1997: Nonlinear shoaling of directionally spread waves on a beach. *J. Geophys. Res.*, **102**(C9), 21,101–21,114.
- Hersbach, H. and P. A. E. M. Janssen, 1999: Improvement of the short fetch

- behavior in the wave ocean model (WAM). *J. Atmos. Oceanic Techn.*, **16**, 884–892.
- Hersbach, H. and P. A. E. M. Janssen, 2001: Reply to comments on “Improvement of the short fetch behavior in the wave ocean model (WAM)”. *J. Atmos. Oceanic Techn.*, **18**, 716–721.
- Herterich, K. and K. Hasselmann, 1980: A similarity relation for the non-linear energy transfer in a finite-depth gravity-wave spectrum. *J. Fluid Mech.*, **97**, 215–224.
- Hino, M., 1968: Equilibrium-range spectra of sand waves formed by flowing water. *J. Fluid Mech.*, **34**(3), 565–573.
- Holthuijsen, L. H., N. Booij, R. C. Ris, I. G. Haagsma, A. T. M. M. Kieftenburg and E. E. Kriez, 2001: *SWAN Cycle III version 40.11 user manual*. Delft University of Technology, Department of Civil Engineering, P.O. Box 5048, 2600 GA Delft, The Netherlands, see <http://swan.ct.tudelft.nl>.
- Horvat, C. and E. Tziperman, 2015: A prognostic model of sea-ice floe size and thickness distribution. *The Cryosphere*, **9**, 2,119–2,134.
- Hwang, P. A., 2001: A note on the ocean surface roughness spectrum. *J. Atmos. Oceanic Techn.*, **28**, 436–443.
- J. Larson, R. Jacob, E. O., 2005: The model coupling toolkit: A new fortran90 toolkit for building multiphysics parallel coupled models. *Int. J. High Perf. Comp. App.*, **19**(3), 277–292.
- Janssen, P. A. E. M., 1982: Quasilinear approximation for the spectrum of wind-generated water waves. *J. Fluid Mech.*, **117**, 493–506.
- Janssen, P. A. E. M., 1989: Wind-induced stress and the drag of air-flow over sea waves. *J. Phys. Oceanogr.*, **19**, 745–754.
- Janssen, P. A. E. M., 1991: Quasi-linear theory of of wind wave generation applied to wave forecasting. *J. Phys. Oceanogr.*, **21**, 1,631–1,642.
- Janssen, P. A. E. M., 2004: *The interaction of ocean waves and wind*. Cambridge University Press.
- Janssen, P. A. E. M., 2009: On some consequences of the canonical transformation in the Hamiltonian theory of water waves. *J. Fluid Mech.*, **637**, 1–44.
- Jones, P. W., 1998: *A User’s Guide for SCRIP: A Spherical Coordinate Remapping and Interpolation Package, Version 1.5*. 29 pp.
- Jones, P. W., 1999: First- and second-order conservative remapping schemes for grids in spherical coordinates. *Mon. Wea. Rev.*, **127**, 2,204–2,210.
- Kahma, K. K. and C. J. Calkoen, 1992: Reconciling discrepancies in the observed growth rates of wind waves. *J. Phys. Oceanogr.*, **22**, 1,389–1,405.

- Kahma, K. K. and C. J. Calkoen, 1994: *Dynamics and modelling of ocean waves*. Chap. II.8 Growth curve observations, pp. 174–182. Cambridge Univ. Press.
- Kohout, A., M. Williams, S. Dean and M. Meylan, 2014: Storm-induced sea-ice breakup and the implications for ice extent. *Nature*, **509**, 604–607.
- Kohout, A. L. and M. H. Meylan, 2008: An elastic plate model for wave attenuation and ice floe breaking in the marginal ice zone. *J. Geophys. Res.*, **113**(C9).
- Komen, G. J., L. Cavaleri, M. Donelan, K. Hasselmann, S. Hasselmann and P. A. E. M. Janssen, 1994: *Dynamics and modelling of ocean waves*. Cambridge University Press, 532 pp.
- Komen, G. J., S. Hasselmann and K. Hasselmann, 1984: On the existence of a fully developed wind-sea spectrum. *J. Phys. Oceanogr.*, **14**, 1,271–1,285.
- Krasitskii, V. P., 1994: On reduced equations in the Hamiltonian theory of weakly nonlinear surface waves. *J. Fluid Mech.*, **272**, 1–20.
- Kreisel, G., 1949: Surface waves. *Quart. Journ. Appl. Math.*, pp. 21–44.
- Kuik, A. J., G. P. Van Vledder and L. Holthuijsen, 1988: A method for the routine analysis of pitch-and-roll buoy wave data. *J. Phys. Oceanogr.*, **18**, 1,020–1,034.
- Leckler, F., 2013: *Observation and modelling of wave breaking*. Ph.D. thesis, Université de Bretagne Occidentale, Brest, France.
- Leonard, B. P., 1979: A stable and accurate convective modelling procedure based on quadratic upstream interpolation. *Comput. Methods Appl. Mech. Engng.*, **18**, 59–98.
- Leonard, B. P., 1991: The ULTIMATE conservative difference scheme applied to unsteady one-dimensional advection. *Comput. Methods Appl. Mech. Engng.*, **88**, 17–74.
- Leonard, B. P., A. P. Lock and M. K. MacVean, 1996: Conservative explicit unrestricted-time-step multidimensional constancy-preserving advection schemes. *Mon. Wea. Rev.*, **124**, 2,588–2,606.
- Li, J. G., 2003: A multiple-cell flat-level model for atmospheric tracer dispersion over complex terrain. *Bound. Layer Meteor.*, **107**, 289–322.
- Li, J. G., 2008: Upstream nonoscillatory advection schemes. *Mon. Wea. Rev.*, **136**, 4,709–4,729.
- Li, J. G., 2011: Global transport on a spherical multiple-cell grid. *Mon. Wea. Rev.*, **139**, 1,536–1,555.
- Li, J. G., 2012: Propagation of ocean surface waves on a spherical multiple-cell grid. *J. Comput. Physics*, **231**(24), 8,262–8,277.

- Li, J. G., 2016: Ocean surface waves in an ice-free Arctic Ocean. *Ocean Dynamics*, **66**(8), 989–1,004.
- Liu, A. K., B. Holt and P. W. Vachon, 1991: Wave propagation in the marginal ice zone: model predictions and comparisons with buoy and synthetic aperture radar data. *J. Geophys. Res.*, **96**(C3), 4,605–4,621.
- Liu, A. K. and E. Mollo-Christensen, 1988: Wave propagation in a solid ice pack. *J. Phys. Oceanogr.*, **18**, 1,702–1,712.
- Longuet-Higgins, M. S. and R. W. Stewart, 1961: The changes in amplitude of short gravity waves on steady non-uniform currents. *J. Fluid Mech.*, **10**, 529–549.
- Longuet-Higgins, M. S. and R. W. Stewart, 1962: Radiation stress and mass transport in gravity waves, with application to 'surf-beats'. *J. Fluid Mech.*, **10**, 529–549.
- Madsen, P. and O. Sorensen, 1993: Bound waves and triad interactions in shallow water. *J. Ocean Engng.*, **20**(4), 359–388.
- Magne, R., F. Ardhuin and A. Roland, 2010: Waves forecast and hindcast from global ocean to the beach. *Eur. J. of Environ. and Civil Eng.*, **14**(2), 149–162.
- Magne, R., K. Belibassakis, T. H. C. Herbers, F. Ardhuin, W. C. O'Reilly and V. Rey, 2007: Evolution of surface gravity waves over a submarine canyon. *J. Geophys. Res.*, **112**(C1).
- McCowan, J., 1894: On the highest wave of permanent type. *Philosophical Magazine*, **38**, 351–358.
- Mei, C. C., 1983: *The applied dynamics of ocean surface waves*. Wiley, New York, 740 pp.
- Mellor, M., 1986: Mechanical behavior of sea ice. in N. Untersteiner, editor, *The Geophysics of Sea Ice*, NATO ASI Series, pp. 165–281. Springer US, DOI: 10.1007/978-1-4899-5352-0.3.
- Metcalf, M. and J. Reid, 1999: *FORTTRAN 90/95 explained, second edition*. Oxford University Press, 341 pp.
- Metzger, E. J., O. M. Smedstad, P. G. Thoppil, H. E. Hurlburt, J. A. Cummings, A. J. Wallcraft, L. Zamudio, D. S. Franklin, P. G. Posey, M. W. Phelps, P. J. Hogan, F. L. Bub and C. J. Dehaan, 2014: US Navy operational global ocean and Arctic ice prediction systems. *Oceanogr.*, **27**(3), 32–43.
- Meylan, M., L. Bennets and A. Kohout, 2014: In situ measurements and analysis of ocean waves in the Antarctic marginal ice zone. *Geophys. Res. Lett.*, **41**(C14), 5,046–5,051.

- Meylan, M. H. and D. Masson, 2006: Physics-based parameterization of air-sea momentum flux at high wind speeds and its impact on hurricane intensity predictions. *Ocean Mod.*, **11**, 417–427.
- Miche, A., 1944: Mouvements ondulatoire de la mer en profondeur croissante ou décroissante. Forme limite de la houle lors de son déferlement. Application aux digues maritimes. Deuxième partie. Mouvements ondulatoires périodiques en profondeur régulièrement décroissante. *Annales des Ponts et Chaussées*, **114**, 25–78, 131–164, 270–292, 369–406.
- Miles, J. W., 1957: On the generation of surface waves by shear flows. *J. Fluid Mech.*, **3**.
- Moon, I. J., I. Ginnis, T. Hara and B. Thomas, 2006: Physics-based parameterization of air-sea momentum flux at high wind speeds and its impact on hurricane intensity predictions. *Mon. Wea. Rev.*, **135**, 2,869–2,878.
- Murray, R. J., 1996: Explicit generation of orthogonal grids for ocean models. *J. Comput. Physics*, **126**(2), 251–273.
- NCEP, 1998: GRIB. Office Note 388, NOAA/NWS/NCEP, Available by anonymous ftp from ftp://nic.fb4.noaa.gov.
- Nelson, R. C., 1994: Depth limited wave heights in very flat regions. *Coastal Eng.*, **23**, 43–59.
- Nelson, R. C., 1997: Height limits in top down and bottom up wave environments. *Coastal Eng.*, **32**, 247–254.
- Ng, C., 2000: Water waves over a muddy bed: a two-layer Stokes' boundary layer model. *Coastal Eng.*, **40**(3), 221–242.
- O'Reilly, W. C., R. T. Guza and R. J. Seymour, 1999: Wave prediction in the Santa Barbara Channel. in *5th California Islands Symposium, March 29-31*. Mineral Management Service, Santa Barbara CA.
- Perrie, W. and D. T. Resio, 2009: A two-scale approximation for efficient representation of nonlinear energy transfers in a wind wave spectrum. Part II: Application to observed wave spectra. *J. Phys. Oceanogr.*, **39**(10), 2,451–2,476.
- Perrie, W., B. Toulany, D. T. Resio, A. Roland and J.-P. Auclair, 2013: A two-scale approximation for wave-wave interactions in an operational wave model. *Ocean Mod.*, **70**, 38 – 51.
- Phillips, O. M., 1977: *The dynamics of the upper ocean, second edition*. Cambridge Univ. Press, 336 pp.
- Phillips, O. M., 1984: On the response of short ocean wave components at a fixed wavenumber to ocean current variations. *J. Phys. Oceanogr.*, **14**, 1,425–1,433.

- Phillips, O. M., 1985: Spectral and statistical properties of the equilibrium range in wind-generated gravity waves. *J. Fluid Mech.*, **156**, 505–531.
- Pierson, W. J. and L. Moskowitz, 1964: A proposed spectral form for fully developed wind seas based on the similarity theory of S. A. Kitaigorodskii. *J. Geophys. Res.*, **69**, 5,181–5,190.
- Polnikov, V. G. and I. V. Lavrenov, 2007: Calculation of the nonlinear energy transfer through the wave spectrum at the sea surface covered with broken ice. *Oceanol.*, **47**, 334–343.
- R. Jacob, J. Larson, E. O., 2005: M×N communication and parallel interpolation in CCSM3 using the model coupling toolkit. *Int. J. High Perf. Comp. App.*, **19**(3), 293–307.
- Rasch, P. J., 1994: Conservative shape-preserving two-dimensional transport on a spherical reduced grid. *Mon. Wea. Rev.*, **122**, 1,337–1,350.
- Rascle, N. and F. Ardhuin, 2013: A global wave parameter database for geophysical applications. Part 2: Model validation with improved source term parameterization. *Ocean Mod.*, **70**, 174–188.
- Reichl, B. G., T. Hara and I. Ginis, 2014: Sea state dependence of the wind stress over the ocean under hurricane winds. *J. Geophys. Res.*, **119**(1), 30–51.
- Resio, D. T., C. E. Long and W. Perrie, 2011: The role of nonlinear momentum fluxes on the evolution of directional wind-wave spectra. *J. Phys. Oceanogr.*, **41**(4), 781–801.
- Resio, D. T. and W. Perrie, 1991: A numerical study of nonlinear energy fluxes due to wave–wave interactions. Part 1: Methodology and basic results. *J. Fluid Mech.*, **223**, 603–629.
- Resio, D. T. and W. Perrie, 2008: A two-scale approximation for efficient representation of nonlinear energy transfers in a wind wave spectrum. Part I: Theoretical development. *J. Phys. Oceanogr.*, **38**(12), 2,801–2,816.
- Roe, P. L., 1986: Characteristic-based schemes for the Euler equations. *Ann. Rev. Fluid Mech.*, **18**, 337–365.
- Rogers, W. E., A. V. Babanin and D. W. Wang, 2012: Observation-consistent input and whitecapping dissipation in a model for wind-generated surface waves: Description and simple calculations. *J. Atmos. Oceanic Techn.*, **29**, 1,329–1,346.
- Rogers, W. E. and T. J. Campbell, 2009: Implementation of curvilinear coordinate system in the WAVEWATCH III model. report NRL/MR/7320–09-9193, Naval Research Laboratory, Stennis Space Center, MS.
- Rogers, W. E. and K. Holland, 2009: A study of dissipation of wind-waves

- by mud at Cassino Beach, Brazil: Prediction and inversion. *Cont. Shelf Res.*, **29**, 676–690.
- Roland, A., 2009: *Development of WWM II: Spectral wave modelling on unstructured meshes*. Ph.D. thesis, Technische Universität Darmstadt, Institute of Hydraulic and Water Resources Engineering.
- Roland, A., 2012: Application of residual distribution (RD) schemes to the geographical part of the wave action equation. in *Proceedings of ECMWF workshop on ocean wave forecasting, June*.
- Saha, S., S. Moorthi, H. Pan, X. Wu, J. Wang, S. Nadiga, P. Tripp, R. Kistler, J. Woollen, D. Behringer, H. Liu, D. Stokes, R. Grumbine, G. Gayno, J. Wang, Y. Hou, H. Chuang, H. Juang, J. Sela, M. Iredell, R. Treadon, D. Kleist, P. V. Delst, D. Keyser, J. Derber, M. Ek, J. Meng, H. Wei, R. Yang, S. Lord, H. van den Dool, A. Kumar, W. Wang, C. Long, M. Chelliah, Y. Xue, B. Huang, J. Schemm, W. Ebisuzaki, R. Lin, P. Xie, M. Chen, S. Zhou, W. Higgins, C. Zou, Q. Liu, Y. Chen, Y. Han, L. Cucurull, R. Reynolds, G. Rutledge and M. Goldberg, 2010: The NCEP climate forecast system reanalysis. *Bull. Am. Meteor. Soc.*, **91**, 1,015–1,057.
- Shemdin, O., K. Hasselmann, S. V. Hsiao and K. Heterich, 1978: Nonlinear and linear bottom interaction effects in shallow water. in *Turbulent fluxes through the sea surface, wave dynamics and prediction*, pp. 347–365. NATO Conf. Ser. V, Vol 1.
- Snyder, R. L., F. W. Dobson, J. A. Elliott and R. B. Long, 1981: Array measurements of atmospheric pressure fluctuations above surface gravity waves. *J. Fluid Mech.*, **102**, 1–59.
- Soulsby, R., 1997: *Dynamics of marine sands, a manual for practical applications*. Thomas Telford Publications, London.
- Teixeira, M. A. C. and S. E. Belcher, 2002: On the distortion of turbulence by a progressive surface wave. *J. Fluid Mech.*, **458**, 229–267.
- Thornton, E. B. and R. T. Guza, 1983: Transformation of wave height distribution. *J. Geophys. Res.*, **88**, 5,925–5,938.
- Tolman, H. L., 1990: The influence of unsteady depths and currents of tides on wind wave propagation in shelf seas. *J. Phys. Oceanogr.*, **20**, 1,166–1,174.
- Tolman, H. L., 1991: A third-generation model for wind waves on slowly varying, unsteady and inhomogeneous depths and currents. *J. Phys. Oceanogr.*, **21**, 782–797.
- Tolman, H. L., 1992: Effects of numerics on the physics in a third-generation wind-wave model. *J. Phys. Oceanogr.*, **22**, 1,095–1,111.

- Tolman, H. L., 1994: Wind-waves and moveable-bed bottom-friction. *J. Phys. Oceanogr.*, **24**, 994–1,009.
- Tolman, H. L., 1995a: On the selection of propagation schemes for a spectral wind wave model. Office Note 411, NWS/NCEP, 30 pp + figures.
- Tolman, H. L., 1995b: Sub-grid modeling of moveable-bed bottom-friction in wind-wave models. *Coastal Eng.*, **26**, 57–75.
- Tolman, H. L., 2001: Improving propagation in ocean wave models. in B. L. Edge and J. M. Hemsley, editors, *4th International Symposium on Ocean Wave Measurement and Analysis*, pp. 507–516. ASCE.
- Tolman, H. L., 2002a: Alleviating the garden sprinkler effect in wind wave models. *Ocean Mod.*, **4**, 269–289.
- Tolman, H. L., 2002b: Distributed memory concepts in the wave model WAVEWATCH III. *Parallel Computing*, **28**, 35–52.
- Tolman, H. L., 2002c: Limiters in third-generation wind wave models. *The Global Atmosphere and Ocean System*, **8**, 67–83.
- Tolman, H. L., 2002d: Testing of WAVEWATCH III version 2.22 in NCEP’s NWW3 ocean wave model suite. Tech. Note 214, NOAA/NWS/NCEP/OMB, 99 pp.
- Tolman, H. L., 2002e: User manual and system documentation of WAVEWATCH III version 2.22. Tech. Note 222, NOAA/NWS/NCEP/MMAB, 133 pp.
- Tolman, H. L., 2002f: Validation of WAVEWATCH III version 1.15 for a global domain. Tech. Note 213, NOAA/NWS/NCEP/OMB, 33 pp.
- Tolman, H. L., 2003a: Optimum Discrete Interaction Approximations for wind waves. Part 1: Mapping using inverse modeling. Tech. Note 227, NOAA/NWS/NCEP/MMAB, 57 pp. + Appendices.
- Tolman, H. L., 2003b: Treatment of unresolved islands and ice in wind wave models. *Ocean Mod.*, **5**, 219–231.
- Tolman, H. L., 2004: Inverse modeling of Discrete Interaction Approximations for nonlinear interactions in wind waves. *Ocean Mod.*, **6**, 405–422.
- Tolman, H. L., 2005: Optimum Discrete Interaction Approximations for wind waves. Part 2: Convergence of model integration. Tech. Note 247, NOAA/NWS/NCEP/MMAB, 74 pp. + Appendices.
- Tolman, H. L., 2006: Toward a third release of WAVEWATCH III; a multi-grid model version. in *9th international workshop on wave hindcasting and forecasting*, *JCOMM Tech. Rep. 34*. Paper L1.
- Tolman, H. L., 2007: Development of a multi-grid version of WAVEWATCH III. Tech. Note 256, NOAA/NWS/NCEP/MMAB, 194 pp. + Appendices.

- Tolman, H. L., 2008a: A mosaic approach to wind wave modeling. *Ocean Mod.*, **25**, 35–47.
- Tolman, H. L., 2008b: Optimum Discrete Interaction Approximations for wind waves. Part 3: Generalized multiple DIAs. Tech. Note 269, NOAA/NWS/NCEP/MMAB, 117 pp.
- Tolman, H. L., 2009a: Practical nonlinear interaction algorithms. in *11th international workshop on wave hindcasting and forecasting & coastal hazards symposium*, *JCOMM Tech. Rep. 52, WMO/TD-No. 1533*. Paper J2.
- Tolman, H. L., 2009b: User manual and system documentation of WAVEWATCH III[™] version 3.14. Tech. Note 276, NOAA/NWS/NCEP/MMAB, 194 pp. + Appendices.
- Tolman, H. L., 2010a: A genetic optimization package for the Generalized Multiple DIA in WAVEWATCH III[®]. Tech. Note 289, Ver. 1.0, NOAA/NWS/NCEP/MMAB, 21 pp.
- Tolman, H. L., 2010b: Optimum Discrete Interaction Approximations for wind waves. Part 4: Parameter optimization. Tech. Note 288, NOAA/NWS/NCEP/MMAB, 175 pp.
- Tolman, H. L., 2010c: WAVEWATCH III[®] development best practices. Tech. Note 286, Ver. 0.1, NOAA/NWS/NCEP/MMAB, 19 pp.
- Tolman, H. L., 2011a: A conservative nonlinear filter for the high-frequency range of wind wave spectra. *Ocean Mod.*, **39**, 291–300.
- Tolman, H. L., 2011b: On the impact of nonlinear interaction parameterizations in practical wave models. in *12th international workshop on wave hindcasting and forecasting & 3^d coastal hazards symposium*. Paper I15, 10 pp.
- Tolman, H. L., 2013a: A Generalized Multiple Discrete Interaction Approximation for resonant four-wave nonlinear interactions in wind wave models with arbitrary depth. *Ocean Mod.*, **70**, 11–24.
- Tolman, H. L., 2013b: Scaling of WAVEWATCH III[®] on massively-parallel computer architectures. Part I: hybrid parallelization. Tech. note, NOAA/NWS/NCEP/MMAB, In Preparation.
- Tolman, H. L., 2014a: A genetic optimization package for the Generalized Multiple DIA in WAVEWATCH III[®]. Tech. Note 289, Ver. 1.4, NOAA/NWS/NCEP/MMAB, 21 pp. + Appendix.
- Tolman, H. L., 2014b: WAVEWATCH III[®] development best practices. Tech. Note 286, Ver. 1.1, NOAA/NWS/NCEP/MMAB, 23 pp.
- Tolman, H. L., 2014c: WAVEWATCH III[®] development best practices. Tech. Note 286, Ver. 1.1, NOAA/NWS/NCEP/MMAB, 23 pp.

- Tolman, H. L. and J. H. G. M. Alves, 2005: Numerical modeling of wind waves generated by tropical cyclones using moving grids. *Ocean Mod.*, **9**, 305–323.
- Tolman, H. L., B. Balasubramanian, L. D. Burroughs, D. V. Chalikov, Y. Y. Chao, H. S. Chen and V. M. Gerald, 2002: Development and implementation of wind generated ocean surface wave models at NCEP. *Wea. Forecasting*, **17**, 311–333.
- Tolman, H. L. and N. Booij, 1998: Modeling wind waves using wavenumber-direction spectra and a variable wavenumber grid. *The Global Atmosphere and Ocean System*, **6**, 295–309.
- Tolman, H. L. and D. V. Chalikov, 1996: Source terms in a third-generation wind-wave model. *J. Phys. Oceanogr.*, **26**, 2,497–2,518.
- Tolman, H. L. and R. W. Grumbine, 2013: Holistic genetic optimization of a Generalized Multiple Discrete Interaction Approximation for wind waves. *Ocean Mod.*, **70**, 25–37.
- Tolman, H. L. and V. M. Krasnopolsky, 2004: Nonlinear interactions in practical wind wave models. in *8th international workshop on wave hindcasting and forecasting*, *JCOMM Tech. Rep. 29*, WMO/TD-No. 1319. Paper E1.
- Tracy, B., E.-M. Devaliere, T. Nicolini, H. L. Tolman and J. L. Hanson, 2007: Wind sea and swell delineation for numerical wave modeling. in *10th international workshop on wave hindcasting and forecasting & coastal hazards symposium*, *JCOMM Tech. Rep. 41*, WMO/TD-No. 1442. Paper P12.
- Tracy, B. and D. T. Resio, 1982: Theory and calculation of the nonlinear energy transfer between sea waves in deep water. WES Report 11, US Army Corps of Engineers.
- Tracy, F. T., B. Tracy and D. T. Resio, 2006: ERDC MSRC Resource. Tech. Rep. Fall 2006, US Army Corps of Engineers.
- Tsagareli, K. N., A. V. Babanin, D. J. Walker and I. R. Young, 2010: Numerical investigation of spectral evolution of wind waves. Part I: Wind-input source function. *J. Phys. Oceanogr.*, **40**, 656–666.
- Valcke, S., 2013: The OASIS3 coupler: a European climate modelling community software. *Geosci. Model Dev.*, **6**, 373–388.
- Van der Westhuysen, A. J., J. L. Hanson and E. M. Devaliere, 2016: Spatial and temporal tracking of wave systems. *J. Atmos. Oceanic Techn.*, ‘In prep.
- Van Vledder, G. P., 2000: Improved method for obtaining the integration space for the computation of nonlinear quadruplet wave-wave interaction.

- in *Proceedings of the 6th International Workshop on Wave Forecasting and Hindcasting*, pp. 418–431.
- Van Vledder, G. P., 2002a: Improved parameterizations of nonlinear four wave interactions for application in operational wave prediction models. Report 151a, Alkyon, The Netherlands.
- Van Vledder, G. P., 2002b: A subroutine version of the Webb/Resio/Tracy method for the computation of nonlinear quadruplet interactions in a wind-wave spectrum. Report 151b, Alkyon, The Netherlands.
- Vincent, L. and P. Soille, 1991: Watersheds in digital spaces: An efficient algorithm based on immersion simulations. *IEEE Transactions of Pattern Analysis and Machine Intelligence*, **13**, 583–598.
- Voorrips, A. C., V. K. Makin and S. Hasselmann, 1997: Assimilation of wave spectra from pitch-and-roll buoys in a North Sea wave model. *J. Geophys. Res.*, **102**, 5,829–5,849.
- Wadhams, P., 1973: Attenuation of swell by sea ice. *J. Geophys. Res.*, **78**(18), 3,552–3,563.
- Wadhams, P., 1975: Airborne laser profiling of swell in an open ice field. *J. Geophys. Res.*, **80**(33), 4,520–4,528.
- Wadhams, P., V. Squire, D. Goodman, A. Cowan and S. Moore, 1988: The attenuation rates of ocean waves in the marginal ice zone. *J. Geophys. Res.*, **93**, 6,799–6,818.
- WAMDIG, 1988: The WAM model – A third generation ocean wave prediction model. *J. Phys. Oceanogr.*, **18**, 1,775–1,810.
- Wang, R. and H. H. Shen, 2010: Gravity waves propagating into an ice-covered ocean: A viscoelastic model. *J. Geophys. Res.*, **115**(C6).
- Webb, D. J., 1978: Non-linear transfers between sea waves. *Deep-Sea Res.*, **25**, 279–298.
- Wessel, P. and W. Smith, 1996: A global self-consistent hierarchical high resolution shoreline database. *J. Geophys. Res.*, **101**, 8,741–8,743.
- Whitham, G. B., 1965: A general approach to linear and non-linear dispersive waves using a Lagrangian. *J. Fluid Mech.*, **22**, 273–283.
- Williams, T. D., L. G. Bennetts, V. A. Squire, D. Dumont and L. Bertino, 2013: Wave-ice interactions in the marginal ice zone. Part 1: Theoretical foundations. *Ocean Mod.*, **70**(1), 81–91.
- WISE Group, 2007: Wave modelling - the state of the art. *Progress in Oceanography*, **75**, 603–674.
- WMO, 2001: WMO MANUAL ON CODES VOLUME I - International codes; part B - binary codes. Publication Number 306, WMO.

- Wu, J., 1982: Wind-stress coefficients over sea surface from breeze to hurricane. *J. Geophys. Res.*, **87**, 9,704–9,706.
- Young, I. R. and A. V. Babanin, 2006: Spectral distribution of energy dissipation of wind-generated waves due to dominant wave breaking. *J. Phys. Oceanogr.*, **36**, 376–394.
- Zieger, S., A. V. Babanin, W. E. Rogers and I. R. Young, 2015: Observation-based source terms in the third-generation wave model WAVEWATCH. *Ocean Mod.*, **96**, 2–25.
- Zijlema, M., 2010: Computation of wind-wave spectra in coastal waters with SWAN on unstructured grids. *Coastal Eng.*, **57**(3), 267 – 277.

APPENDICES

This page is intentionally left blank.

A Managing multiple model versions

WARNING

If version 5.16 is implemented as an upgrade to previous versions of WAVEWATCH III, please note that this version may not be compatible with previous model versions. It is therefore prudent *NOT* to install the new version of WAVEWATCH III on top of the old version.

WARNING

When WAVEWATCH III is first installed, the user needs to define a ‘home’ directory for WAVEWATCH III. This information is stored in `.wwatch3.env` in the users home directory, or locally with the implementation (option selected in installation script), and is used by virtually all WAVEWATCH III utility scripts. If a new model version is developed or installed, it is prudent to do this in a new directory, to avoid loss of previous work or issues of possible incompatibility of model versions. In order to have the proper scripts work with the proper model version, the user has several basic options.

- Dynamically update the environment file `.wwatch3.env` to point to the proper directory in which the present work is done.
- Use an environment file stored locally with the implementation (option introduced in model version 5.16).
- Point the environment file `.wwatch3.env` to a generic directory name like `wwatch3`, and store various model versions in directories with specific names like `wwatch3_3.14` or `wwatch3_dev`. Then make the generic name `wwatch3` a symbolic link to the specific directory to select that directory to work with.

At NCEP, the second and third method are used, depending on the preferences of the team member.

This page is intentionally left blank.

B Setting model time steps

Model time steps are set on a grid-by-grid basis and are considered as a part of the model setup in the model definition file `mod_def.ww3`. This implies that in a multi-grid model set-up (using the model driver `ww3_multi`) each grid is associated with its own time step setting. In this section some guidance is given for setting time steps for individual grids, and for grids in a mosaic approach. Examples of practical time step setting for practical grids can be found in the individual grids used in the test cases `mww3_case_01` through `mww3_case_03`.

B.1 Individual grids

A basic wave model grid requires the definition of four time steps as is described in Section 3.2 on page 101 of this manual. Typically, the first step to consider is the CFL time step for spatial propagation, that is, the second of the four time steps defined in `ww3_grid.inp` for the grid considered. The critical CFL number C_c that identifies stability of the numerical scheme is defined as [compare Eq. (3.16)]

$$C_c = \frac{c_{g,\max}\Delta t}{\min(\Delta x, \Delta y)} \quad , \quad (\text{B.1})$$

where $c_{g,\max}$ is the maximum group velocity, and Δt , Δx , and Δy are time and space increments. The maximum group velocity is the group velocity for the lowest discrete model frequency. Noting that for a given frequency the largest group velocity occurs in intermediate water depth, this maximum velocity is approximately 1.15 times the deep water group velocity for the lowest discrete spectral frequency. Note that the CFL number formally includes affects of currents [Eq. (2.9)] and grid movement [Eq. (3.45)]. The latter two effects are accounted for internally in the model by adjusting the corresponding minimum time step dynamically depending on the current velocity and the grid movement speed. Hence, the user can define this minimum propagation time step ignoring currents and grid movement. For the schemes used here the critical CFL number is 1.

The second time step to consider is the overall time step (the first time step identified in `ww3_grid.inp`). For maximum numerical accuracy, this time

B.2

step should be set smaller than or equal to the above CFL time step. However, particularly in spherical grids, the critical CFL condition occurs only in a few grid points. In most grid points, CFL numbers will be much smaller. In such grids, accuracy does not suffer significantly if the overall time step is taken as 2 to 4 times the critical CFL time steps. Such a setting generally has a major positive impact on model economy. The key to numerical accuracy is the interpretation of the CFL number. This number represents the normalized distance over which information propagates in a single time step. Inaccuracy occurs if information propagates over several grid boxes before source terms are applied. With $\text{CFL} \approx 1$ and the overall time step four times the CFL time step, information will propagate over four grid boxes before source terms are applied. This may lead to model inaccuracies. If, however, the maximum CFL number is 1, but the average CFL number is only 0.25, as is the case even for the lowest frequency in many spherical grids, information only propagates over one grid box in a single overall time step, and no issues with accuracy develop.

An effective overall time step also considers requested time intervals at which model forcing is available, and at which model output is requested. If input and output time steps are multiple integer times the overall time step, a balanced and consistent numerical integration scheme exists, although the model does not require this. Most important in this consideration is reproducibility of results. If input or output time steps are modified so that they are no longer an integer multiple of the overall model time step, then the actual discrete time stepping in the model will be modified by these input and output time steps, and hence an impact on actual model results may be expected. Such an impact may be notable, but is generally very minor.

The third time step to consider is the maximum refraction (and wavenumber shift) time step. For maximum model economy, this time step should be set equal to (or larger than) the overall time step. However, this will alternate the order of spatial and refraction computations for consecutive model time steps, which in cases of strong refraction may lead to a minor oscillation of wave parameter with a period of $2\Delta t$. Such oscillations can be avoided altogether by setting the maximum refraction time step to half the overall time step. Considering the minor cost of the refraction term in the model, this generally has a negligible impact on model economy. The preferred refraction time step is therefore half the overall model time step.

One note of caution is appropriate with setting this time step. To assure numerical stability, the characteristic refraction velocities are filtered as in

Eq. (3.51). This filtering suppresses refraction in cases with rapidly changing bottom topography. The impact of this filtering is reduced when the refraction time step is reduced. It is therefore prudent to test a model grid with much smaller intra-spectral model time steps to assess the impact of this filtering.

The final time step to set is the minimum time step for the dynamical source term integration in Section 3.6. This is a safety valve to avoid prohibitively small time steps in the source term integration. Depending on the grid increment size this is typically set to 5 to 15s. Note that increasing this time step does not necessarily improve model economy; a larger minimum source term integration time step will increase the spectral noise in the integration, which in turn may *reduce* the average source term integration time step!

B.2 Mosaics of grids

Considerations for time step settings for individual grids making up a mosaic model using `ww3_multi` are in principle identical to those for individual grids as discussed in the previous section. Additional considerations are:

- Overall time steps for individual grids do not need to ‘match’ in any way for the management algorithm for the mosaic approach to work properly. However, if identically ranked grids share overall time steps, and if integer ratios between time steps of grids with different ranks are employed, then it will be much easier to follow and predict the working of the management algorithm,
- If two grids with identical rank overlap, then the required width of the overlap area will be defined by the stencil width of the numerical scheme, and the number of times this scheme is called for the longest wave component (ratio of overall time step to maximum CFL time step). Thus, model economy for individual grids will improve with increased overall model time step, but the required overlap of equally ranked grids will then increase, reducing the economy of the mosaic approach.

This page is intentionally left blank.

C Setting up nested runs

C.1 Using `ww3_shel`

The mechanics of running nested models using the single-grid wave model program `ww3_shel` in principle is simple. A large scale model produces a file with boundary data, for instance `nest1.ww3`. This file is then renamed to `nest.ww3` and put in the directory in which the nested (small scale) model is run. The small scale model then will automatically process the file and update the boundary conditions as required and available. Setting up the nesting consistently is more involved. A simple step-by-step method is presented here. Another possibility, described in the next subsection is to assemble the `nest.ww3` file from spectral output using `ww3_bound`.

- 1) The first step is to set up the large scale model completely, but without generating boundary data for the nested model(s). Include the proper wind fields, graphical outputs etc. Test this model until you are satisfied that it works properly.
- 2) Set up the small scale model, for the moment ignoring the boundary conditions. Take into consideration that the boundary conditions ideally should coincide with grid lines in the large scale model to minimize the file size of the boundary data files. Set up this model in the same way as the large scale model, and test it thoroughly.
- 3) When the small scale model is set up satisfactorily in the above way, the boundary conditions need to be defined. Go into the file `ww3_grid.inp` for the small scale model, and mark all the intended input boundaries as outlined in the documentation in section 4.4.2. Make sure that the model switch `!/O1` is selected in the `switch` file, and recompile if necessary. Run `ww3_grid` and save the screen output. The output of this program now includes a list of all points that are marked as input boundary points. Also make sure that stored copies of `mod_def.ww3` for the small scale model (if any) are properly updated.
- 4) The next step is to include all the input boundary points in the above list as output boundary points in the large scale model. Keep

C.2

the list handy, and go to the file `ww3_grid.inp` for the large scale model. Add all points of the above list as output boundary points as indicated in the documentation in section 4.4.2. Make sure that all data (and no other data) is sent to a single file, and run `ww3_grid` with the proper input file. This should now give a list of output boundary points that should be consistent with the above list of input boundary points. Note that the order in which the points occur in the list is inconsequential. Again make sure that stored copies of `mod_def.ww3` for the large scale model (if any) are properly updated.

- 5) If there are discrepancies between the two lists of points, iterate between the two previous steps until the lists are consistent.
- 6) The next step is to start generating the boundary data from the large scale model. This requires the nesting output to be activated in the large scale model. The output is already set up and included in the model definition file (`mod_def.ww3`) of the large scale model in the above steps. It now needs to be activated by setting the beginning time, time increment and ending time in the input file `ww3_shel.inp` for the actual model run of the large scale model. This step does not need to be performed if a second or consecutive nest is added. The large scale model will now produce the file with boundary data. If this is the first nest included the output file will be `nest1.ww3`. This file needs to be saved for use in the small scale model.
- 7) To include the nesting data in the small scale model, the above boundary data file needs to be renamed to `nest.ww3` and needs to be put in the directory from which `ww3_shel` for the small scale model is run. If the small scale model has properly defined the input boundary points in its definition file `mod_def.ww3`, it will automatically process the file `nest.ww3` and update the boundary data as available. At this point, two additional tests are recommended.
 - When first running the small scale model with the file `nest.ww3` present, pay close attention to the output of `ww3_shel` to assure that (i) the program reports that the file `nest.ww3` has been processed and has been found OK, and (ii) that no additional

warnings are present regarding incompatible or missing boundary data. Also check the log file `log.ww3` to assure that the boundary data are updated at the expected times.

- When all data apparently are processed, it is illustrative and prudent to make a model run of the small scale model where the wind fields are switched off in `ww3_shel.inp`, and where no restart file `restart.ww3` is made available. In such a model run, wave energy can only enter the domain from the boundaries. This is a good test to assure that the boundary data is passed from the large scale model to the small scale model as expected.

Additional nested models can be added in the same way. Adding a second level nest from the small scale model is also done in the same way. The model is presently set up for producing up to 9 files with boundary data per model run. There are no limitations on the number of consecutive (‘telescoping’) nests.

C.2 Using `ww3_bound` and/or unstructured grids

In some circumstances it is difficult or impossible to know in advance the position of the forcing points for small scale model when running the large scale model. This is the case if one wants to run a coastal zoom using boundary condition from an on-line or third-party database.

In this case, it is possible to generate `nest.ww3` file from spectral output using `ww3_bound`. This is particularly handy also for unstructured grids due to the irregular spacing of points on the boundary. `ww3_bound` takes a list of spectra files, which should have the same spectral grid, and generates a `nest.ww3`. The interpolation coefficients are determined from the positions of the nearest available spectra and the positions of the active boundary points in the small scale model.

C.4

C.3 Using `ww3_multi`

Performing two-way nesting in the wave model driver `ww3_multi` is greatly simplified compared to using the wave model driver `ww3_shel`, because all data transfer needed is performed internally in the multi-grid wave model routines. A mosaic model system is set up by iteratively going through the following steps.

- 1) Set up a grid using the `ww3_grid` utility. Define the grid, its active boundary points and all other model information such as time steps, but *do not* attempt to generate output nesting data for other grids. This will be assessed automatically by the multi-grid wave model routines in `ww3_multi`. Note that the lowest ranked grid can optionally use active boundary data, either as read from file or to be kept constant during computation. Higher ranked grids will require active boundary point in order to be valid in the mosaic approach,
- 2) Add this grid as an extra grid to the input file `ww3_multi.inp` with the appropriate rank number. Running `ww3_multi` will identify discrepancies between grids and requested boundary data points that can be resolved iteratively, and other discrepancies between grids. It can be tedious to remove such discrepancies by hand. The grid generation package of [Chawla and Tolman \(2007, 2008\)](#) checks for such discrepancies automatically, and is therefore recommended for grid generation for this version of WAVEWATCH III.

Note that grid on which input data fields are defined can be added in a similar way. Note that the use of land-sea masks in oceanic input fields (current, water level and ice) is recommended to assure realistic input values at coastal points.

Generally, lower ranked grids are developed first, although grid of any rank could be added at any time.

D Setting up for distributed machines (MPI)

D.1 Model setup

In order to run WAVEWATCH III on a distributed memory machine using MPI, two requirements need to be met. First, all executables need to be compiled properly. This implies that the codes are compiled with the proper WAVEWATCH III options (switches), and with the proper compiler options. Second, the parallel version of the model needs to be run in a proper parallel environment. This implies that the parallel codes are run on a multi-processor machine, invoking the proper parallel environment on that machine. These two issues are discussed in some detail below.

Of all the WAVEWATCH III programs described in section 4, only three benefit from a parallel implementation with MPI: the actual models `ww3_shel` and `ww3_multi`, and the initial conditions program `ww3_strt`. `ww3_strt` is typically not used in operational environments, and can generally be run in single processor mode. The main reason for running `ww3_strt` in multi-processor mode is to reduce its memory requirements. These three codes are the only codes that manipulate all spectra for all grid points simultaneously, and hence require much more memory than all other WAVEWATCH III programs. An added benefit (other than reduced run times) of running these programs in parallel is that the parallel versions of these programs require less memory per processor if the number of processors is increased.

Considering the above, it is sufficient for most implementations on parallel machines to compile only the main programs `ww3_shel` and `ww3_multi` with the MPI options. All other WAVEWATCH III programs with the exception of `ww3_strt` are designed for single-processor use. The latter programs should not be run in a parallel environment, because this will lead to I/O errors in output files. Furthermore, there is no possible gain in run time for these codes in a parallel environment due to their design. Because all programs share subroutines, it is important to assure that this compilation is done correctly, that is, that the subroutines and main programs are compiled with compatible compiler settings. This implies that subroutines that are shared between parallel and non-parallel programs should be compiled individually for each application.

The first step for compiling the MPI version of programs is to assure that

D.2

the proper compiler and compiler options are used. Examples of this for an IBM system using the xlf compiler, and a Linux system using the Portland compiler can be found in the example `comp` and `link` scripts provided with the distribution of WAVEWATCH III.

The second step is to invoke the proper compile options (switches) in compiling all parts of WAVEWATCH III. Most programs will be compiled for single-processor use. To assure that all subroutines are consistent with the main programs to which they are linked, the compile procedure should be divided into two parts. A simple script that will properly compile all WAVEWATCH III programs is given in Fig. D.1. An expanded version of this example is now available as

```
make MPI
```

Alternatively, the commands in the script can be run interactively, while directly editing the `switch` file when appropriate.

An alternative way of consistently compiling the code is to first extract all necessary subroutines per code using `w3_source`, then put the sources and the makefile in individual directories, and compile using the `make` command. In this case the code for `ww3_shel` and `ww3_multi` are extracted using the appropriate MPI switches, whereas all other codes are extracted using the switches for the shared memory architecture.

After all codes have been compiled properly, the actual wave models `ww3_shell` and `ww3_multi` needs to be run in the proper parallel environment. The actual parallel environment depends largely on the computer system used. For instance, on NCEP's IBM systems, the number of processors and the proper environment is set in 'job cards' at the beginning of the script. The code is then directed to the parallel environment by invoking it as

```
poe ww3_shel
```

Conversely, on many Linux types systems, the MPI implementation includes the `mpirun` command which is typically used in the form

```
mpirun -np $NP ww3_shel
```

where the `-np $NP` option typically requests a number of processes from a resource file (`$NP` is a shell script variable with a numerical value). For details of running parallel codes on your system, please refer to the manual or user support (if available).

```

#!/bin/sh

# Generate appropriate switch file for shared and
# distributed computational environments

cp switch switch.hold
sed -e 's/DIST/SHRD/g' \
    -e 's/MPI //g'      switch.hold > switch.shrd
sed 's/SHRD/DIST MPI/g' switch.hold > switch.MPI

# Make all single processor codes

cp switch.shrd switch
w3_make ww3_grid ww3_strt ww3_prep ww3_outf ww3_outp \
        ww3_trck ww3_grib gx_outf gx_outp

# Make all parallel codes

cp switch.MPI switch
w3_make ww3_shel ww3_multi

# Go back to a selected switch file

cp switch.shrd switch
# cp switch.hold switch

# Clean up

rm -f switch.hold switch.shrd switch.MPI
w3_clean

# end of script

```

Figure D.1: Simple script to assure proper compilation of all WAVE-WATCH III codes in a distributed (MPI) environment. This script assumes that the SHRD switch is selected in the switch file before the script is run.

D.4

Note that the as a part of the parallel model setup, I/O options are available to select between parallel and non-parallel file systems (see also [Tolman, 2003a](#)).

D.2 Common errors

Some of the most common errors made in attempting to run `ww3_shel` and `ww3_multi` under MPI are:

- Running in a parallel environment with a serial code (no MPI in compilation).

This will result in corrupted data files, because all processes are attempting to write to the same file. This can be identified by the standard output of `ww3_shel`. The proper parallel version of the code will produce each output line only once. The non-parallel version will produce one copy of each output line for each individual process started.

- You are running in a parallel environment with a serial code (programs other than intended MPI codes).

This will result in corrupted data files, because all processes are attempting to write to the same file. This can be identified by the standard output of the programs, which will produce multiple copies of each output line.

- `ww3_shel` or `ww3_multi` are compiled properly, but not run in a parallel environment.

On some systems, this will result in automatic failure of the execution of `ww3_shel`. If this does not occur, this can only be traced by using system tools for tracking when and where the code is running.

- During compilation serial and parallel compiled subroutines are mixed.

This is the most common source of compiling, linking and run time errors of the code. Follow the steps outlined in the previous section to avoid this.

D.3 MPI point-to-point communication errors

Running `ww3_multi` in parallel with several large overlapping grids involves a large number of concurrently active MPI point-to-point communications (MPI send/recv pairs). For correct execution, each active MPI message must have a unique envelope (send id, recv id, tag, communicator) with an allowed tag value. In this context two types of MPI point-to-point communication errors may occur: (1) the MPI message tag value exceeds an upper-bound or (2) two or more MPI messages have the same envelope. The first error may result in `ww3_multi` crashing with a MPI “invalid tag” error or an internal tag upper-bound exceeded error. The second error may result in spectra sent from one MPI task to another being delivered to the wrong location. The second error is more difficult to detect in that it is not trapped by MPI and may only be manifested as strange results in model output.

To address these possible errors the allowed ranges of MPI tags for the different sets of point-to-point communication in `ww3_multi` are controlled by the `MTAGB`, `MTAG0`, `MTAG1`, `MTAG2`, and `MTAG_UB` parameters defined in `WMMDATMD`. These parameters must satisfy $MTAGB \geq 0$ and $7 * NRGRD - 1 \leq MTAG0 < MTAG1 < MTAG2 < MTAG_UB \leq MPI_TAG_UB$, where `MPI_TAG_UB` is the tag upper-bound for the MPI implementation.

The value of `MPI_TAG_UB` for a specific MPI implementation can be obtained at run-time using the `MPI_COMM_GET_ATTR` routine. An MPI implementation is free to set the value of `MPI_TAG_UB` larger than the minimum set by the MPI standard ($32767 = 2^{15} - 1$). In the current release version of OpenMPI, the value of `MPI_TAG_UB` is 2147483647 ($2^{31} - 1$). On the Cray XC40 with Cray MPICH, the value of `MPI_TAG_UB` is much smaller, that is, 2097151 ($2^{21} - 1$). As the currently known lowest value of `MPI_TAG_UB` amongst available parallel platforms, the Cray XC40 value is used to set `MTAG_UB` in `WMMDATMD`.

If an MPI tag value exceeds the upper-bound (`MPI_TAG_UB`) imposed by the MPI implementation, `ww3_multi` may crash with a MPI “invalid tag” error. If an MPI tag value exceeds one of the internal tag upper-bounds, `ww3_multi` will crash with error code 1001 and a report of which tag upper-bound was exceeded. What follows is a description of the allowed MPI tag ranges and how they are set.

The `MTAGB` parameter is only used as the tag lower-bound for blocking

D.6

communication that does not overlap with other point-to-point communication. Hence it is sufficient to set $MTAGB$ to the lowest allowed MPI tag value of 0.

In addition to being the tag lower-bound for communication of internal boundary data in `WMINIOMD`, the $MTAG0$ parameter is used in `WMIOPOMD` as the tag upper-bound for the unified point output communication. To ensure that the unified point output communication tag values are ≥ 0 , $MTAG0$ must be at least $7 * NRGRD - 1$. A generous setting of $MTAG0 = 1000$ is used in `WMMDATMD`.

The allowed tag range for point-to-point communication of internal boundary data (`WMINIOMD:WMIOBS`) is $(MTAG0, MTAG1]$. Given that this communication involves only the boundary points of the model grids a generous setting of $MTAG1 = 10000$ is used in `WMMDATMD`.

The allowed tag range for point-to-point communication from high rank to low rank grids (`WMINIOMD:WMIOHS`) is $(MTAG1, MTAG2]$. The allowed tag range for point-to-point communication between equal rank model grids (`WMINIOMD:WMIOES`) is $(MTAG2, MTAG_UB]$. The high-rank-to-low-rank and equal-rank communications involve both boundary and interior points of model grids. Hence, the allowed tag ranges for these two communication sets should be larger than the allowed range for the communication of internal boundary data. In nested grid applications (e.g., a single global grid with several regional nests) the required tag range for high-rank-to-low-rank communications will be larger than the required tag range for the equal-rank communications. The setting of $MTAG2 = 1500000$ is used in `WMMDATMD` to give a larger portion of the total allowed range of tags for the high-rank-to-low-rank communications. Other multiple grid applications may require adjusting $MTAG2$.

E Mosaic approach with non-regular grids

E.1 Introduction

WAVEWATCH III version 3.14 (Tolman, 2009b) introduced multi-grid capability. This capability is described above (Section 3.14.2). With model version 4, there is an option to use irregular grids or unstructured grids, as described in Section 3.4.3 and Section 3.4.4, respectively. Unfortunately, the methods described in Section 3.14.2 are not general, as they are intended for regular grids only. Some new capabilities are implemented in 5.16 to accommodate irregular and unstructured grids within the multi-grid approach.

The core component for communication from lower rank grids to higher rank grids of Tolman (2008a) is an interpolation in space to provide boundary data at the higher spatial resolution. For version 5.16 the technique was generalized by making calls to the grid-search-utility (GSU) implemented in WAVEWATCH III version 4 by T. Campbell. Other generalizations were made to ancillary components of this routine.

The core component for communication from higher rank grids to lower rank grids of Tolman (2008a) is a conservative remapping operation: the spectral density of a larger (low rank) grid cell is updated based on the spectral densities of the overlapping smaller (high rank) grid cells, weighted according to the fraction of the larger cell that is covered by each smaller cell, keeping in mind that a smaller cell may be overlapping with more than one larger cell. For version 5.16 the technique was generalized by making calls to an external software package, SCRIP-WW3, which is described below. The remapping weights are stored in a FORTRAN “derived data type” array. Generalizations were also made to ancillary components of the remapping routine, for example to the logic used to calculate distances to the boundaries, to deal with masked points and land points, etc.

E.2 SCRIP-WW3

The SCRIP-WW3 software package is adapted from the SCRIP (Spherical Coordinate Remapping and Interpolation Package) software package of

E.2

Jones (1998), which we refer to here as SCRIP-LANL. SCRIP-WW3 is based on SCRIP-LANL v1.5. The primary difference between SCRIP-LANL and SCRIP-WW3 is that the former is a standalone code using NetCDF files for user interface, and the latter is modified to run within WAVEWATCH III with communication via system memory. Further, SCRIP-WW3 only utilizes the conservative remapping feature, whereas SCRIP-LANL has a number of other optional uses, such as bi-linear remapping.

The conservative remapping used in SCRIP is based on Jones (1999). In this method, for each source/destination grid pair, line integrals are computed around all cells in each grid while keeping track of intersections with the other grid, resulting in area of overlap between grids. The method is designed for use with a spherical coordinate system (as opposed to treating latitudes and longitudes as if they are x- any y-axes in a Cartesian system) and includes special logic for handling longitude wrapping (the so-called “branch cut”) and cells that include a pole. It also allows for unstructured grids, with arbitrary number of cell corners. The grid corner coordinates must be given in an order which traces the outside of a grid cell in a counterclockwise direction. The software allows either first- or second-order remapping; weights for both are calculated in SCRIP-WW3. At present, only the first-order remapping is implemented in WAVEWATCH III : Jones (1999) points out that there is virtually no advantage to using the second-order method when mapping from a fine grid to a coarse grid.

E.3 SCRIP Operation

SCRIP-WW3 is activated by including SCRIP in the file `switch`. If the user attempts to use irregular or unstructured grids within `ww3_multi` without this switch, this will result in an error message and program termination. SCRIP-WW3 is not required for `ww3_shel` (traditional one-way nesting), and is not required for `ww3_multi` with only regular grids, since original methods for remapping are retained in the code for this purpose. SCRIP-WW3 source files are kept in a separate directory `/ftn/SCRIP/`, since it is modified 3rd party software. With the SCRIP switch, the build system (`ww3.make`) will automatically compile files from this directory and link them into `ww3_multi`.

A user may also optionally include the switch `SCRIPNC` along with SCRIP. This feature requires NetCDF. Instructions for using NetCDF in

WAVEWATCH III are found in Section 5.3 and in the file `w3_make`. With SCRIPNC activated, for each source/destination grid pair, a NetCDF file will be created, e.g. `rmp_src_to_dst_conserv_002_001.nc`, with 002 and 001 referring to the source and destination grid respectively; the numbering of grids is assigned by `ww3_multi` and is indicated in screen output of that program. This `.nc` file contains all information required by WAVEWATCH III for remapping. Additional diagnostic information about the remapping can be included in the `.nc` file by adding the switch `T38`. Note: switch should include either ‘SCRIP SCRIPNC’ or ‘SCRIP’; using SCRIPNC without SCRIP will result in a compile error.

Though it is not required, SCRIP-WW3 may be utilized for remapping between regular grids. In the case of spherical (lat/lon) grids, there may be slight differences using SCRIP-WW3, since SCRIP-WW3 calculates areas based on real distances, and the non-SCRIP approach uses degrees lat/lon.

E.4 Optimization and common problems

SCRIP-WW3 routines are not parallelized. Therefore, if `ww3_multi` is run with many processes, each process will perform identical calculations of all weights. For remapping between grids with large numbers of points, this can make the preparations for `ww3_multi` time-consuming, e.g. 3 to 10 minutes, which can be prohibitively expensive for routine, operational use. To deal with this problem, SCRIP-WW3 has been adapted to allow use of remapping weights that were computed in a prior application of `ww3_multi`. If the appropriate `.nc` files are found by `ww3_multi`, it will simply read the remapping data from these files, and SCRIP will not be called. Of course, if any grids have been changed since the prior run, or if moving grids are used, pre-computed weights should not be used.

An additional feature is provided for user convenience: if a file named `SCRIP_STOP` is found in the run directory, `ww3_multi` will terminate after the `.nc` files are created. The content of `SCRIP_STOP` is unimportant; it may be an empty file. When this feature is used, remapping operations will be distributed among processes: `rmp_src_to_dst_conserv_002_001.nc` is created by process 1, `rmp_src_to_dst_conserv_003_001.nc` is created by process 2, etc., which will dramatically improve performance in cases where a significant number of grids are used. To clarify, there are two modes of operation

E.4

that are targetted with this feature: Mode A) Precalculate weights, where `SCRIP_STOP` exists and `.nc` files do not exist. Mode B) Use precalculated weights, where `SCRIP_STOP` does not exist and `.nc` files do exist. If both files types exist (through accident) in the work directory, `ww3_multi` will fail with an error. In a hypothetical operational context, Mode A is used for the first run and Mode B is used for all subsequent runs with the same grid set. The scalability is limited by the most expensive remapping pair, i.e. load balancing is an issue. For a case where 12 remapping pairs are calculated and each pair requires 1/12th of the computation time, speed-up will be by factor twelve. For another case with 12 remapping pairs, where one remapping pair takes 50% of computation time, speed-up will be by factor two only. Note that resources are maximized by using a number of processes equal to the number of remapping pairs: extra processes will not be used.

To further explain the options available to users, take an example of a multi-grid system with 9 grids and 12 remapping pairs, with many sea points, run twice a day for several months, for a total of 1000 forecasts. The user may handle this in different ways:

- 1) Using `SCRIP`, `SCRIPNC`, and `MPI`, and using the `SCRIP_STOP` feature, the calculation of weights will be done in parallel. The first time the model is applied, this may take 5 to 10 minutes to calculate remapping weights (Mode A above) and 20 minutes to perform the model forecast (Mode B above). For forecasts 2 to 1000, only the 20 minutes to perform the model forecast (Mode B) is needed.
- 2) Using `SCRIP`, `SCRIPNC` and the `SCRIP_STOP` feature, but creating the `.nc` files running in serial mode and running the forecast with `MPI`, the first time the model is applied, this may take 20 minutes to calculate remapping weights and 20 minutes to perform the model forecast. For forecasts 2 to 1000, only the 20 minutes to perform the model forecast is needed.
- 3) Using `SCRIP`, `SCRIPNC`, and `MPI`, without using the `SCRIP_STOP` feature, the calculation of weights will not be done in parallel, and will even be slower than if run in serial, because of communications. The first time the model is applied, this may take 40 minutes to calculate remapping weights and 20 minutes to perform the model forecast. For forecasts 2 to 1000, only the 20 minutes to perform the model forecast is needed.

- 4) Using SCRIP and MPI, running on 12 processors, the calculation of weights will not be done in parallel, will be slow, and will need to be computed each time. For all forecasts 1 to 1000, this may take 40 minutes to calculate remapping weights and 20 minutes to perform the model forecast.

In some cases, SCRIP-WW3 will return suspicious values for some points, which will result in warning message(s) in the screen output. When this occurs for a small fraction of grid points, our experience (from analysis of the diagnostic output in the .nc files) is that the remapping weights are valid, since the problem points are at edges where WAVEWATCH III does not use the weights. However, when this occurs for a large fraction of grid points, it is likely that SCRIP-WW3 has truly failed. In this case, WAVEWATCH III stops with an error message. Our experience is that this occurs most often for overlapping regular grids with a large number of coincident line segments. A workaround exists: it can be remedied by adding an artificial offset to one of the grids. It was already possible to specify an offset in `ww3_grid.inp` in the grid description, but since that offset is intended as a real quantity, this other, artificial offset is implemented separately as a namelist option. It is `GSHIFT` under namelist group `MISC`. An example namelist would be: `MISC GSHIFT = 1.0D-6`. A smaller number will result in less regridding error, though the number must be sufficient large to actually have the intended beneficial effect. We recommend to determine this by trial-and-error, varying by factor 10 each time.

E.5 Limitations

Two features are not yet addressed, and will be addressed in a later version:

- 1) Communication between equal rank grids is still limited to regular grids. If one of the grids is irregular or unstructured, `ww3_multi` will terminate with an error message. It is possible to have non-regular grids as part of a multi-grid system which includes equal rank grids, as long as the overlapping equal-ranked grids are all regular.
- 2) The “input grid” (or “F modid”) option for defining input fields (e.g. winds) is not implemented yet for irregular or unstructured

E.6

grids. If this is attempted, `ww3_multi` will terminate with an error message. The “native” input grid option should be used instead.

Attribution statement: This section was written by E. Rogers. The coding and testing for this effort was performed by E. Rogers, M. Dutour, A. Roland, F. Arduin, and K. Lind. Technical advice was given by H. Tolman and T. Campbell.

F Ocean-Waves-Atmosphere coupling with OASIS

F.1 Introduction

WAVEWATCH III has been interfaced with OASIS3-MCT to allow coupling simulations with atmosphere and/or ocean models. OASIS (Ocean Atmosphere Sea Ice Soil)¹ – note that waves are missing in that acronym – is a coupling software developed by the CERFACS and CNRS (Valcke, 2013). The current OASIS3-MCT version is interfaced with MCT, the Model Coupling Toolkit (J. Larson, 2005; R. Jacob, 2005). developed by the Argonne National Laboratory. The OASIS coupler is also interfaced with the SCRIP library developed by Los Alamos National Laboratory. All the information on how to use the OASIS coupler is present in the oasis user guide. Here we will just add the information about the use of OASIS in WAVEWATCH III.

In a nutshell, OASIS3-MCT ...

- ... is totally parallelized
- ... doesn't have an executable (we don't need to give it processes when we launch a coupling simulation)
- ... is able to exchange 2D and 3D fields
- ... is able to exchange fields in parallel
- ... support unstructured grids
- ... uses an input file called *namcouple* that allows changes to the coupling characteristics (exchange time, interpolation type, number of exchange fields) without recompiling the code...

¹<https://verc.enes.org/oasis/>

F.2

F.2 Interfacing with OASIS3-MCT

To communicate with another model, a component model (ocean, wave or atmosphere) needs to include a few specific calls to the OASIS3-MCT coupling library. To use these OASIS's functions in WAVEWATCH III we created 3 new modules:

- `w3oacpmd.ftn`, module containing common functions for atmosphere and ocean coupling. These functions are called before the temporal loop, in the `ww3_shel` program.
- `w3ogcmmd.ftn` and `w3agcmmd.ftn`, modules containing specific functions for, respectively, waves-ocean coupling and waves-atmosphere coupling. These functions are called in the temporal loop.

F.3 Compiling with OASIS3-MCT

To use or not these coupling functions 4 switches were created:

- switch `COU`, to perform the coupling : reading the `ww3_shel.inp` input file and define the number of variable exchanged and the time exchange.
- switch `OASIS`, to initialize the coupler OASIS `w3oacpmd.ftn`
- switch `OASACM` and/or `OASOCM`, to send/receive the coupling fields to/from the atmospheric model `w3agcmmd.ftn` and/or the oceanic model `w3ogcmmd.ftn`

To allow the use of OASIS, WAVEWATCH III[®] should be compiled with the following switches. For a coupling with an atmospheric circulation model

`COU OASIS OASACM`

and with an ocean circulation model

`COU OASIS OASOCM`

and both ocean and atmosphere circulation models

COU OASIS OASACM OASOCM

Only the program `ww3_shel` is compiled with the OASIS library, all the other programs can be used as usual.

The switches for interpolation in time of the wind and current forcing fields must not be used regarding the fact that coupling mechanisms cannot provided the future value of the forcing field. Depending on the type of coupling, the switch `WNT0` must be set for atmospheric coupling and the switch `CRT0` must be set for oceanic coupling.

F.4 Launch a coupling simulation

To launch a coupling simulation, for example with Intel Mpi, we need the:

- input files for WW3 : `ww3_shel.inp`, and the usual `*.ww3` files.
- input file for OASIS : `namcouple`
- input files for ocean/atmosphere models : files depends on the model

To launch a coupling simulation, the `mpirun` command should be used as follows

```
mpirun -np $nbre_cores_WW3 exe_WW3 : -np $nbre_cores_OA exe_OA
```

F.5 Limitations

A few limitations are not yet addressed, and will be addressed in a later version:

- the coupling with OASIS is only coding for `ww3_shel` program, not yet for the `ww3_multi`
- in the WW3 suite, there are 2 versions of SCRIP, one for OASIS and one for the `ww3_multi`
- ...